IJEST

ISSN: 0973-6255
Vol. 6 No. 1&2
January - December 2012

Indian Journal of Engineering, Science, and Technology

A Refereed Research Journal

Published by

BANNARI AMMAN INSTITUTE OF TECHNOLOGY

(Autonomous Institution Affiliated to Anna University of Technology, Coimbatore -
Approved by AICTE - Accredited by NBA and NAAC with "A" Grade)
Sathyamangalam - 638 401 Erode District Tamil Nadu India
Ph: 04295-226340 - 44 Fax: 04295-226666
www.bitsathy.ac.in E-mail: ijest@bitsathy.ac.in

Indian Journal of Engineering, Science, and Technology

IJEST is a refereed research journal published half-yearly by Bannari Amman Institute of Technology. Responsibility for the contents rests upon the authors and not upon the IJEST. For copying or reprint permission, write to Copyright Department, IJEST, Bannari Amman Institute of Technology, Sathyamanagalam, Erode District - 638 401, Tamil Nadu, India.

Economic Analysis of 10kw Roof-mounted Grid Connected Photovoltaic System

R.Vijay Kumar[1], Yuva Raju Anand[2] and R. Rudramoorthy[3]
[1,2&3]PSG College of Technology, Coimbatore - 641 004, Tamil Nadu
E-mail: Vijaykumar.R@in.bosch.com, yuvaraj1.psg@gmail.com

Abstract

This paper reports the investigation results of the energy payback time (EPBT) and greenhouse-gas payback time (GPBT) of a roof mounted grid-connected PV system in Coimbatore and cost of PV power system component to measure its sustainability. EPBT is a function of competing energy sources with which electricity from solar PV is compared, and the amount of electricity generated from the solar PV system which varies with local irradiation and ambient conditions. Therefore, it is more appropriate to use site-specific EPBT for major decision-making in power generation planning. The annual power output of 10kWp PV array is facing south with inclined angle of 45o was found to be 14400kWh. The embodied energy for the whole system in the lifespan was 105,816 kWh, including 71% from PV modules and 29% from balance of system (BOS). The percentage of embodied energy for silicon purification and processing reached 44%. The EPBT of the PV system was 7.3 years, and the GPBT was estimated to be 4.1 years considering fuel of local power stations. This paper also discusses the EPBTs for different orientations, ranging from 7.3 years (optimal orientation) to 20.0 years (west-facing vertical PV façade). The results show that the 'sustainability' of a PV system is affected by its installation orientation and location Based on life cycle cost (LCC) analysis, capital cost (US$/kWP) and unit cost of electricity (US$/kWh) were determined for the roof mounted grid-connected PV system. The mitigation of CO2emission, carbon of PV system is presented in this paper. Effect of carbon credit on the economics of PV system showed reduction in unit cost of electricity by 17–19% for grid connected pv systems. This methodology was illustrated using actual case study on 10 kWP PV system located in PSG College, Coimbatore (India).

Keywords: *EPBT, GPBT, BOS, LCC, PV*

1. INTRODUCTION

The operation of solar PV system is free from fossil fuel use but a considerable amount of energy is consumed in the manufacturing of solar PV modules. Global warming caused by greenhouse gas (GHG) emissions from combustion of fossil fuels has become an important environmental issue in the global arena. As a result, non-fossil energy sources are explored, and thus the power generation from solar photovoltaic (PV) systems plays a prominent role. Generally, PV technology, generating electricity from solar energy, is considered 'sustainable'. However, PV system operation is free from energy consumption; it consumes a lot of energy during PV manufacturing processes, balance of system (BOS) production, transport, system installation, system retrofitting, and system disposal or recycling in its life cycle. For BOS, it comprises system wiring, electronic and electrical components, foundation, support structure, battery (stand-alone system), and system installation.

There are other researches which provide us a wide range of EPBT values for different PV systems in different locations. As the EPBT is defined by the embodied energy consumption of a PV system and its BOS divided by its annual energy output of the system, the EPBT calculation of a PV system is affected by many factors. It is important to investigate the percentage of energy used in some major processes and focus on the main sectors because they have great impacts on the results for calculating the embodied energy and hence the EPBT. However, it is impossible to gather all the data and understand each step in creating each single component in a PV system, and some simplified assumptions have to be made [7].

Greenhouse-gas payback time (GPBT) is also used to measure the system or technology sustainability especially when the whole world is tackling the global warming problems by reducing emission of greenhouse gases (GHG) for environmental protection. Using PV is always recommended as one of the best solutions because it does not generate CO2 during the operation.

However, it does generate CO2 and other gases during its entire lifecycle such as extraction, production and disposal processes. Therefore, it is important to study the payback period based on the GHG emission to determine the sustainability and 'greenness' of the PV system. The GHG payback time (GPBT) is given by the embodied GHG of the system (PV modules) and BOS divided by the GHG produced by a local power plant for the power generated by the PV system [7]. Similar to embodied energy estimation, estimating the embodied GHG is also a great challenge and will have significant impact on the GPBT calculation. The most common way to express the GHG emission is using the unit of kg CO2 equivalent, kg CO2eq.

The cost of PV system components were determined based on the size of PV system components. The life cycle cost analysis for the PV system was presented for estimation of unit cost of electricity generated from the roof mounted grid connected PV systems. The environmental benefits such as carbon credit earned from the PV systems were determined based on the mitigation of CO2 emissions. The effect of carbon credit on the economics of PV system was presented as a policy issue which was rarely reported in the present literature. The practical case study on 10 kWP roof mounted PV system located in PSG College; Coimbatore (India) [11N, 77.28E] was conducted and presented in this paper.

2. METHODOLOGY

In this study, the conventional LCA procedure viz. goal and scope definition, life cycle inventory, impact assessment, is used. The aim of this LCA study is to quantify the non-renewable primary energy use and GHG emissions from electricity generation from the solar PV system. All indicators of the study such as energy use, emissions are indexed based on the functional unit which is defined as 1 kWh of AC electricity. Manufacturing of solar PV modules and balance of the system (BOS) such as inverters, supporting structures and their accessories, are included in the system boundary. Figure 1 shows the LCA boundary.

The roof-mounted PV system (10 kWp) is installed on the roof of Electrical Block of The PSG College of Technology, Coimbatore. This is a grid-connected PV system and all the PV modules face no shading. The orientation of all the PV modules is facing south with an inclined angle of 45^{o}, as demonstrated in Figure 2. Forty Eight mono-crystalline PV modules (Titan Energy S5-60) are installed in the system. There are four parallel strings are connected. Each parallel string is connected with twelve PV modules in series. The rated peak power of each PV module is 235Wp, and other key characteristics of the mono-crystalline PV module (Titan Energy S5-60) are summarized in Table 1.

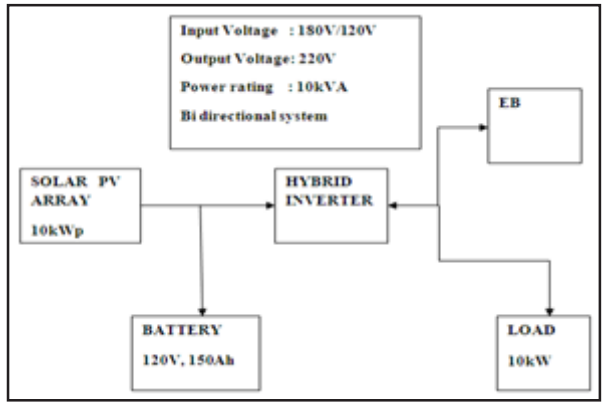

Fig.1 Schematic diagram of PV system at PSG College of Technology

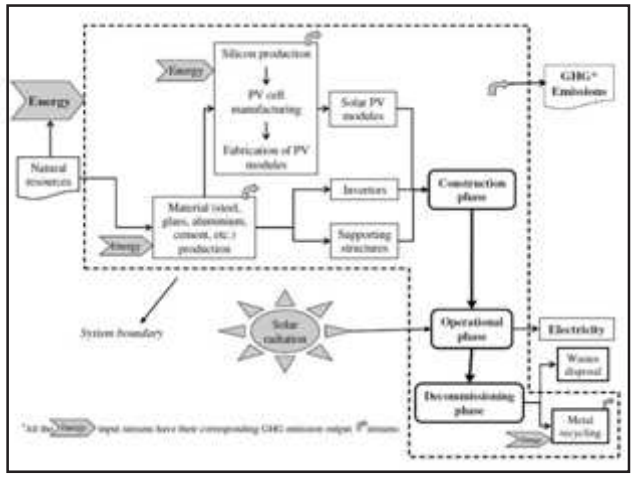

Fig. 2 LCA Boundary of solar PV system

Fig. 3 The 10kWp roof-mounted PV system

2.1 Energy Payback Time (Epbt) Estimation

Energy payback time (EPBT) is calculated by:

$$EPBT = \frac{E_{S,E} + E_{BOS,E}}{E_{output}} \quad (1)$$

where E_{SE}, is the embodied energy of the system (PVmodules), kWh; EBOS,E is the embodied energy of the BOS, kWh; and EOUTPUT is the annual energy output of the system, kWh.

Table 1Main Characteristics of the PV Module (Titan Energy S5-60)

Maximum Rated Power Pmp(W)	235
Maximum Power Voltage Vmp(V)	29.48
Maximum Power Current Imp (A)	8
Open Circuit Voltage Voc (V)	37.44
Short Circuit Current Isc (A)	8.52
Number of Cells (Mono Crystalline)	10 X 6=60
Cell Size	156X156 =0.0243m2
Module Dimensions	0.987X1.657 =1.635m2

2.2 Embodied Energy Estimation

Embodied energy refers to the energy used within the whole lifecycle from the extraction of primary resources to the deployment including manufacturing processes, transportation and installation. Here, the embodied energy is divided into two categories, i.e., embodied energy of the system (PV modules) and embodied energy of BOS. The embodied energy of the system (PV modules) is defined by:

$$E_{S,E} = E_P + E_S + E_F + E_T + E_D \quad (2)$$

where EP is embodied energy of silicon purification and processing, kWh; ES is embodied energy of silicon ingot slicing, kWh; EF is embodied energy of PV module fabrication, kWh; ET is energy to transport PV modules from factory to installation site, kWh; and ED is decommissioning and disposal or other end-of-life energy requirements of PV modules kWh.

The balance of system (BOS) is a factor that affecting the embodied energy calculation. When the embodied energy of a PV system is analyzed, the PV module itself is not the only item to be considered even though it contributes to the largest amount of energy. Others components are called the BOS, including electrical BOS components and mechanical BOS components.

The electrical BOS components include inverters, electrical wirings and electronic control devices while mechanical BOS components include mounting materials and structures. The embodied energy of the BOS is calculated by:

$$E_{BOS,E} = E_{EBOS} + E_{MBOS} \quad (3)$$

where EEBOS is embodied energy of the electrical BOS components, kWh; and EMBOS is embodied energy of the mechanical BOS components, kWh.

2.3 Annual Energy Output Estimation

The annual energy output of a PV system depends on local weather conditions (such as hourly solar irradiance and ambient temperature), operating performance of the PV modules and PV system, system design (such as orientations, grid-connected or stand-alone).

The data monitoring and recording system was set up along with the PV system when it was installed. Incident hourly solar irradiance on the module plane and hourly ambient temperatures are used to analyze the power output of PV modules from weather data monitoring stations. As the system is a grid connected one, no storage is considered.

2.4 Greenhouse-gas Payback Time (GPBT) Estimation

The GHG payback time (GPBT) is given by:

$$GPBT = \frac{GHG_S + GHG_{BOS}}{GHG_{OUTPUT}} \quad (4)$$

where GHGS is the embodied GHG of system (PV modules), kg CO2eq; GHGBOS is embodied GHG of BOS, kg CO2eq; and GHG output is annual GHG produced by the local power plant for the power generated by the PV system, kg CO2eq.

2.5 Life Cycle Cost Analysis

The life cycle cost analysis was carried out to estimate the cost per unit of electricity generated using PV system. The life cycle cost analysis was carried out for the existing

PV system assuming useful life of 30 years for PV array system and 5 years life for battery bank. Let n is the life of the PV system (30 years) and i is the interest rate. The initial investment or capital cost (Pi) for PV system is obtained assuming the battery bank replacement cost remains uniform throughout the life of PV system (i.e. 30 years) then the replacement cost for the battery bank (CB) can be estimated as follows:

Replacement cost of battery bank (CB) = 0.93 x cost of battery bank.

The present cost of battery bank for future investments at every five years interval can be determined as follows.

Present battery bank cost (PB) =

$$\left[\frac{C_B}{(1+i)^5}\right]+\left[\frac{C_B}{(1+i)^{10}}\right]+\left[\frac{C_B}{(1+i)^{15}}\right]+\left[\frac{C_B}{(1+i)^{20}}\right]+\left[\frac{C_B}{(1+i)^{25}}\right] \quad (5)$$

The salvage value is assumed equal to the present cost of balance of system.

Salvage value of PV system after 30 years = Present cost of Balance of system.

Present salvage value of PV system (PS) =

$$\left[\frac{S}{(1+i)^{30}}\right] \quad (6)$$

Net present cost of PV system (PNet) is determined as summation of capital investment (Pi), all other cost components converted into present cost and subtracted by present salvage value.

PNet=Pi+PB-PS (7)

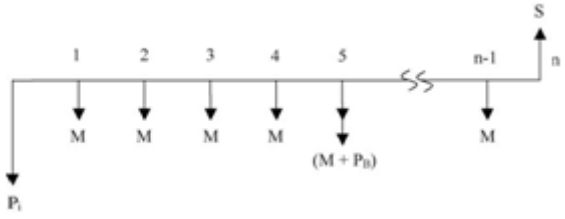

Fig 4.Cash flow diagram of Life cycle cost of PV system

The uniform annualized cost of PV power system (CA) over the 30 years lifetime is expressed mathematically as follows:

$$C_A = P_{Net}\, X \left[\frac{(i\, X\, (1+i)^{30})}{((1+i)^{30}-1)}\right] \quad (8)$$

If M is the annual maintenance cost, generally considered as 2% of uniform annualized cost (CA). The annualized life cycle cost (ALCC) of PV system can be determined as follows:
Annualized life cycle cost (ALCC) / year = 1.05 x CA

The total annual electrical energy units consumed (E) by the specified electrical load is determined as

E(kWh / year) = Daily electrical load (kWh / day) x Number of days of operation / year.
The cost per unit of electricity generated (U) by PV system is

$$U\left(\frac{Rs}{kWh}\right) = \left[\frac{1.1\, X\, C_A}{E}\right] \quad (9)$$

The LCC analysis was carried out for different interest rate to estimate the cost of electricity produced by PV system with capital investment.

The suitable annual interest rates considered are in the range of 4–16% and the reasons for this are as follows:

- 4% is the subsidized interest rate normally offered by government sectors in India to promote the use of renewable energy applications.
- 7-8 % is the interest rate normally offered by government banks.
- 10-12 % is the interest rate offered by private banking sectors.
- 12-16% is the interest rate for any other private source.

2.6 Mitigation of CO2 Emissions From PV System and its Carbon Credit Potential

The carbon credit potential of PV system was determined on the basis of total amount of CO2 emissions mitigation from the system in its life time.

Mitigation of CO2 emissions from PV system:

Energy conversion through photovoltaic (PV) system is one of the more reliable and environmental friendly renewable energy technologies which have the potential to contribute significantly to the development of sustainable energy systems for power generation. It also plays an important role to mitigate CO2 emissions. The numerical computation was carried out to estimate the amount of CO2 emissions mitigated due to the existing PV system. As discussed in the literature survey that

average intensity of CO2 emission from Diesel Plant is 0.9 kg/kWh [11, 17]. The total mitigation of CO2 emissions from the existing PV system for 30 years life can be calculated using Eq. (10) as follows:

CO2 emission mitigated (kg/life) = 1.57 (kg/kWh) x E (kWh/year) x n (year) (10)

A PV power system does not dissipate enormous amount of heat energy into the surrounding environment and saves huge amount of CO2 emissions. Hence, PV system is an environment friendly option for power generation and should be preferred where there is no electricity or extension of grid power is costlier option.

Carbon credit potential of PV system:

The amount of carbon credit earned by PV system can be calculated from the following Eq. (11) as follows: Carbon credit earned = Rs 500/ton x CO2 emission mitigated by PV system (tons/life). (11)

The factor considered in Eq. (11) is Rs 500 /ton of CO2 mitigation represents the monetary value of one carbon credit for mitigation of 1 ton of CO2 emission [18].

3. RESULTS AND DISCUSSIONS

3.1 EPBT Calculations

For the embodied energy of the PV system, it was mainly referred to the previous research studies considering the similarity. In this paper, the main focus on the energy output of the PV system as it can affect the EPBT value significantly if the PV system is installed at different places with different orientations.

3.1.1 Embodied Energy of the PV System

Silica is melted, and manufactured into MG-Si and then into EG-Si. Finally, after the Czochralski or other production process, silicon is produced for the solar cell production. Accordingly to the previous researches, the energy required to produce 1 kg MG-Si is 20 kWh [27-29]. The energy to create 1 kg EG-Si is 100 kWh, and there is 90% loss of silicon during this process. In addition, the required energy to make mono-crystalline silicon for the Czochralski process is 290kWh/kg, and there is a 72% mass loss. 1.448 kg mono-crystalline silicon is needed for 1 m2 solar cells, so the required embodied energy for silicon purification and processing for 1m2 solar cells (or 1.448 kg mono-crystalline silicon) is calculated by:

$$E_p = 290 \times 1.448 + 100 \times \frac{1.448}{72\%} + 20 \times \left(\frac{1.448}{72\% \times 90\%}\right) = 666 kwh/m^2 \quad (12)$$

The silicon ingot is needed to be sliced into wafer. According to the manufacture data, the required energy, ES, to conduct this slicing process is 120 kWh for 1 m2 solar cells [30]. The solar cells are then tested, packed and interconnected with other components to create PV modules. The required energy, EF, to produce 1 m2 PV module is 190 kWh [31]. The transportation energy ET to transport the PV modules to installation site is estimated to be 95.68 kWh per module. ED is ignored due to its insignificance and it is not possible to determine. For the rooftop integrated PV system, the energy requirement is 200kWh/m2 for making its supporting structure [33]. Besides the supporting structure, 33kWh/m2 is taken for the embodied energy used in the production of inverters, and 125kWh/m2 is chosen for all other energy used in system operation and maintenance, electronic components, cables and miscellaneous, etc.

Therefore, the total embodied energy of the 10kWP grid-connected PV system is 105,816kWh, including 31,256kWh (29.53%) from BOS, and 74,560kWh from PV modules (71%). The pie chart of the embodied energy distribution in the case PV system is demonstrated in Figure 3. The percentage of the embodied energy for silicon purification and processing is the highest, 44%, and the BOS is 29.53%.

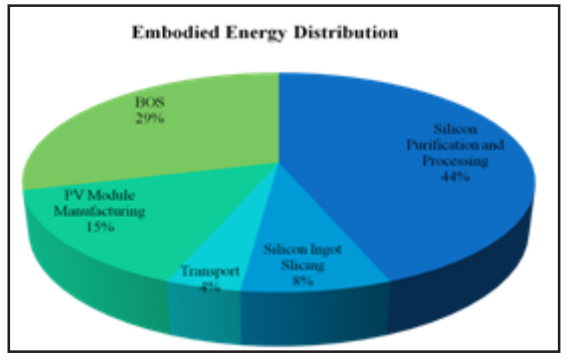

Fig.4 Pie chart of embodied energy used in the rooftop grid connected PV system

3.1.2 Energy Output of the PV System

For the 10kWP roof-mounted PV system, facing south with a tilted angle of 45o, the annual solar radiation received by the PV array is 266,174 kWh using the weather data from 2006 to 2010, and the annual energy output (AC electricity) is 14400kWh. The energy output

of the PV system could be significantly affected by the orientations of the PV modules. Therefore, different orientations of PV arrays and the corresponding annual energy output are investigated for a similar size PV system. Obviously, for the same size PV system, the energy output could be totally different if the PV modules are installed with different orientations or inclined angles. If the 10kWP PV system is installed on vertical south-facing facade, the system power output is decreased by 45.1%.

3.1.3 Energy Payback Time of the PV System

For the 10kWP roof-mounted PV system, facing south with the tilted angle of 45°, the EPBT of the system is estimated to be 7.348 years, which is obviously much shorter than the lifespan of PV modules which is usually 20–30 years. However, when the PV system is installed with different orientations, the estimation results of the EPBT could be totally different, ranging from 7.1 years to 20 years. The results show that the EPBT varies greatly with the PV panel orientations and installation locations. For vertical PV façade, the EPBT is much longer, which means less sustainable and should be avoided. In general, choosing good sun exposure places or locations and choosing optimal orientations are the keys to use the PV technology economically and sustainably.

3.2 GPBT Calculations

3.2.1 Greenhuse-gas Payback Time of the PV System

The greenhouse gases produced for power generation depends greatly on fuel type. Based on the data provided by diesel power stations in Coimbatore, the greenhouse gas emission rate is about 768.57 g CO2eq/kWhe.

The annual energy output (AC electricity) of the PV system was estimated to be 14400 kWh. The equivalent saved CO2 emissions generated from the power station is 14400kWh × 768.57 g CO2eq/ kWhe = 11,067.42 kg of CO2eq. Regarding the embodied greenhouse gases produced during the cell fabrication processes, 463 kg CO2eq/m2 [4] was chosen for the production of PV modules. For the BOS for rooftop installation, 7.1 kg CO2eq/m2 was estimated for array support and cabling [15], and 225 kg CO2eq/m2 was found for inverters [6]. Greenhouse gas emissions during transportation and disposal are not considered here. The greenhouse gases emitted during the PV system manufacturing and installation is estimated to be 45,655 kg CO2eq. Therefore, the GPBT of the PV system is estimated to be 4.125 years. If the PV system is installed with other orientations, the GPBT will change with the same trend as the EPBT.

3.3 Capital Cost Estimation

The cost of PV system components were determined based on their specifications. The specifications of PV system components were obtained and the cost of each component was determined as follows:

3.3.1 Cost of PV Array

The cost of PV module is determined based on the actual PV array size that can be obtained using Eq. (13)
Cost of mono- crystalline pv module – Rs 85/Wp

Cost of PV Array = N x PV module wattpeak (Wp) x cost/Wp

= 48 x 235 x 70 = Rs 7, 89,600 (13)

The cost of PV module is taken in the range from Rs 70/Wp to Rs 85/ Wp depending on the type of PV module e.g. Mono/Multi crystalline or Thin film module. In June 2012, the cost of mono-crystalline PV module is Rs 70 / Wp as reported by website [14].

3.3.2 Cost of Battery Bank

The cost of battery bank is determined based on the actual battery bank size using Eq. (14) .Cost of battery bank /Ah is Rs 47/ Ah. Cost of charge controller is Rs 276 /A & Cost of inverter is Rs 34/VA.

Battery bank cost = Number of Batteries x Each battery capacity (Ah)x cost/Ah

Battery bank cost = 10 x 200 Ah x Rs 215/Ah
= Rs 4, 30,000. (14)

3.3.3 Cost of Solar Power Conditioning Unit (Spcu)

The cost of solar charge controller and inverter can be obtained from Eqs. (15) and (16), respectively.

Cost of charge controller = charge controller capacity (A)cost/Ampere
Cost of charge controller = 40 A x Rs 276/A
= Rs 11040 (15)

Cost of inverter = Inverter capacity (VA) x cost/VA
Cost of inverter = 10000 VA x Rs 34/VA
= Rs 3, 40,000 (16)
Solar power conditioning unit (PCU) = charge controller cost + inverter cost.
Solar power conditioning unit (PCU) = 11040+3, 40,000 = Rs 351040.

The cost of charge controller in October 2011 is Rs 40/ A while the cost of inverter is Rs 34/VA as reported by website [14].

3.3.4 Cost of Balance of System

The balance of system or structure cost is approximately 20% of the total PV system component cost which is widely assumed all over the world as reported by SECO [6, 16]. Based on these assumptions, the capital cost (Pi) for the PV system is determined using Equation (17). The balance of system or structure cost is 20% of the total PV system cost.
Capital cost (Pi) = cost of array + cost of battery bank + cost of PCU+ BOS cost (17)

The Cost of PV array is Rs 7, 89,600 and the Battery bank cost is Rs 430000. Cost of charge controller is obtained as Rs 11040 And the Cost of Inverter can obtain as Rs 3, 51,040. Capital cost Pi is calculated from Eq. (17) which is the sum of cost of array. Cost of battery bank and cost of PCU along with the BOS cost as 18, 84,768. Replacement cost of Battery bank (CB) is Rs 399900.

The Present battery cost (PB) is Rs 11, 53,415 with Salvage value of Rs 1, 43,363. The Net Capital cost (PNET) is Rs 17, 99,651. The Uniform Annualized Cost (CA) is calculated by PNET is Rs 1, 06,155.5. Finally the Annualized Life cycle cost /year is obtained as Rs 1, 11,463.3. With this the Cost / unit of Electricity is obtained as Rs 7.74 /kWh.

3.3.5 Cost Distribution of PV System

The cost distribution is shown by using the pie chart. The cost of PV system components is represented in percentage of total cost of PV system.

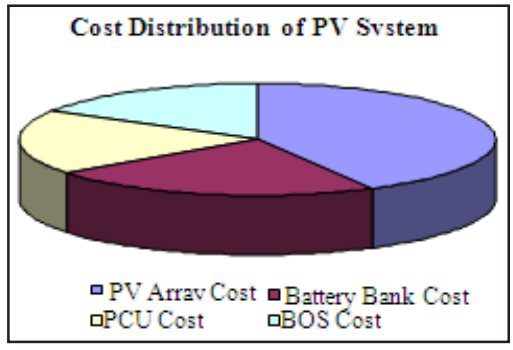

Fig. 5 Pie chart of cost distribution in PV system used in the rooftop Grid Connected PV system

3.3.6 Cost per Unit of Generated Electricity by PV System

The Cost analysis was carried out for different interest rate to estimate the cost of electricity produced by PV system with capital investment. The suitable annual interest rates considered are in the range of 4–16%. When the interest rate is varying from 4% to 16%, per unit cost of electricity is changing from Rs 7.74 to Rs 13.58.

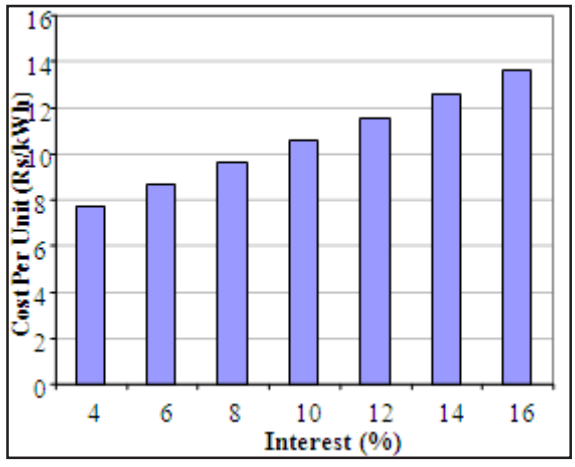

Fig.6 Cost per unit of electricity generated from the rooftop grid Connected PV system

4. CONCLUSION

To study the sustainability of a roof-mounted 10kWP Grid Connected PV system in Coimbatore, this paper investigated the EPBT and GPBT of the Grid Connected PV system in Coimbatore by comparing its EPBT and GPBT with its lifespan by using local weather data from 2006 to 2010. The embodied energy for the whole system in the lifespan was estimated to be 105,816 kWh with 71% from the embodied energy of PV modules and 29% from the embodied energy of BOS. Nearly half of the embodied energy is for the silicon purification and

processing. The EPBT of the PV system is calculated to be 7.34 years which is much shorter than its lifespan of 20-30 years. The GPBT is estimated to be 4.1 years. However, with the rapid development of PV technologies and other industries, the calculation results could vary with the changing input data. In conclusion, the roof-mounted 10kW Grid Connected PV system is truly sustainable and green with a lifespan of 20–30 years. However, if the same capacity PV system is installed at different orientations or other cities, the results could be totally different. Choosing locations and orientations with higher incident solar irradiance is the key for PV technology applications. Local energy mix (power stations) also affects the estimation of GPBT, which should be taken into account. The cost per unit of Electricity is Rs.7.74.

REFERENCES

[1] Solarbuzz™. Marketbuzz™ 2008: Annual World Solar Photovoltaic Industry Report; 2008. <http://www.solarbuzz.com/Marketbuzz2008-intro.htm>.

[2] R.Wilson and A.Young, "The Embodied Energy Payback Period of Photovoltaic Installations Applied to Buildings in the Uk", Build Environ, Vol.31, No.4, 1996, pp.299-305.

[3] K. Knapp and T.Jester, "Empirical Investigation of the Energy Payback Time For Photovoltaic Modules", Sol Energy, Vol.71, No.3, 2001, pp.165-72.

[4] R.Battisti and A.Corrado, "Evaluation of Technical Improvements of Photovoltaic Systems Through Life Cycle Assessment Methodology", Energy, Vol.30, No.7,2005, pp.952-67.

[5] RH. Crawford, GJ.Treloar, RJ. Fuller and M. Bazilian, "Life-Cycle Energy Analysis Of Building Integrated Photovoltaic Systems (Bipvs) With Heat Recovery Unit", Renew Sets Energy Rev,Vol.10, No.6, 2006, pp.559-75.

[6] I. Nawaz and GN.Tiwari, "Embodied Energy Analysis of Photovoltaic (PV) System Based On Macro- And Micro-Level", Energy Policy, Vol.34, No.17, 2006, pp.3144-52.

[7] KP.Cheng, "Energy Payback Time And Greenhouse Gas Emission Analysis Of A Roof-Mounted BIPV In Hong Kong", Meng. Dissertation. The Hong Kong Polytechnic University; 2008.

[8] GA. Keoleian, " Lewis GMcD. Application of Life-Cycle Energy Analysis to Photovoltaic Module Design. Prog Photovolta: Res Appl., Vol.5, No.4, 1997, pp.287-300.

[9] L. Lu and HX. Yang, "A Study on Simulation of Power Output And Practical Models For Building-Integrated Photovoltaic Systems", J Sol Energy-Trans ASME, Vol.126, No.3,2004,pp.929-35.

[10] L. Lu and HX. Yang, "The Optimum Tilt Angles And Orientations of PV Claddings For Building Integrated Photovoltaic (Bipv) Applications", J Sol Energy-Trans ASME, Vol.129, No.2, 2007, pp.253-5.

[11] M. Watt, A.Johnson, M.Ellis and N. Quthred, "Life Cycle Air Emission From PV Power Systems", Prog Photovolta: Res Appl., Vol.6, No.2, 1998, pp.127-36.

[12] J.Mason, VM. Fthenakis, T.Hansen and HC.Kim, "Energy Payback And Life Cycle CO2 Emissions of the Bos in An Optimized 3.5 MWPV Installation", Prog Photovolta:Res Appl., Vol.14, No.2,2006, pp.179-90.

[13] VM. Fthenakis and HC. Kim, "Greenhouse-Gas Emissions From Solar Electric- And Nuclear Power: A Life-Cycle Study", Energy Policy, Vol.35, No.4, 2007, pp.2549-57.

[14] M. Raugei, S.Bargigli and S.Ulgiati, "Life Cycle Assessment and Energy Pay-Back Time of Advanced Photovoltaic Modules: Cdte and Cis Compared to Poly-Si", Energy, Vol.32, No.8, 2007, pp.1310-8.

[15] EA. Alsema and MJ. de Wild-Scholten", Environmental Impact of Crystalline Silicon Photovoltaic Module Production", In: Material research society symposium proceedings, 0895-G03-03; 2006.

[16] S . Krauter and R.Ruther, "Considerations For the Calculation of Greenhouse Gas Reduction by Photovoltaic Solar Energy", Renew Energy,Vol.35, No.29, 2004, pp.345-55.

[17] TT.Chow, ALS.Chan, KF.Fong, Z.Lin, W.He and J. Ji, "Annual Performance of Building Integrated Photovoltaic/Water-Heating System For Warm Climate Application", Appl. Energy, Vol.86, No.5, 2009, pp.686-9.

[18] HW.Li Danny, NT. Lam Tony, WH. Chan Wilco and HL. Mak Ada, "Energy and Cost Analysis of Semi-Transparent Photovoltaic in Office Buildings", Appl. Energy, Vol.8, No.5, 2009.

Experimental Research on Improving the Concrete Property by Using Nanosilica Flyash

Yuvaraj Shanmuga Sundaram, Dinesh Nagarajan, Karthic Ramachandran and SatishBabu
Department of Civil Engineering, Karpagam University, Coimbatore - 641 021, Tamil Nadu
E-mail: sanyuvayad@gmail.com, dinukanch@gmail.com, karthiccivil@yahoo.co.in,

Abstract

This paper deals with the study of Nano Technology in Civil Engineering field as the influence of NanoSilica in concrete increases their strength and their sustainability for rapid development with the adoption of Nano Concreting and their new methodologies. In order to reduce the carbon emission due to the cement manufacturing the fly ash is partially replaced in ordinary Portland cement and termed as Portland pozzolana cement (PPC) it not only reduces the environmental impact, improves the workability, corrosion strength and long term strength of concrete but this replacement of fly ash in the ordinary Portland cement deviating its strength consequently. Hence here we added Nano silica as an additive to fill up the deviation, and it is possible because the silica(S) in the sand reacts with calcium hydrate in (CH) the cement at Nano scale to form C-S-H bond and its improve the strengthening factor of concrete, which are in turn helpful in the achieving high compressive strength even in early days. This process which has proved to increase the strength may have a possibility of turning the concrete less alkaline because as the concentration of CH crystals is reduced the alkalinity of concrete will be reduced. This can induce corrosion in reinforcement bars. Hence we study the corrosion resistance property of nano silica added concrete. Also measuring permeability helps detect durability problems and allows timely and cost-effective protection of the concrete structure. Hence the recent progress and advancement in Nano-engineering and Nano modification in cement concrete is presented

Keywords: *Calcium silica hydrate, Corrosion, Fly ash, Nano concrete,Nano silica,Permeability.*

1. INTRODUCTION

Concrete is at something of a crossroads: there are many opportunities and some threats. For those opportunities to change into beneficial practice, engineers, material scientists, architects manufacturers and suppliers must focus on the changes that are required to champion concrete and maintain its dominance within the global construction industry. Recent research has shown that a state-of-the-art process for high-performance cement adds a new dimension to 'classical' cement technology; similarly this is the time to work on "NANO TECHNOLOGY" for development of construction industry by innovations in concrete techniques and also some new materials for the concrete technology. As concrete is most usable material in construction industry it's been requiring to improve its quality. The main objective of this paper is to outline promising research areas.

2. WHAT IS NANO TECHNOLOGY?

"Nanotechnology is defined as fabrication of devices or materials with atomic or molecular scale precision" Nanotechnology is usually associated with study of materials of micro size i.e. one billionth of a meter (a Nanometer).

3. DEFINITION OF NANO-CONCRETE

For discussions presented in this paper, Nano-concrete is defined as "A concrete made with Portland cement particles that are less than 500 Nano-meters as the cementing agent. Currently cement particle sizes ranges from a few Nano-meters to a maximum of about100 micro meters. In the case of micro-cement the average particle size is reduced to 5 micro meters. An order of magnitude reduction is needed to produce Nano-cement. The SEM image of the Nano silica we had taken for our investigation is shown in Figure 1.

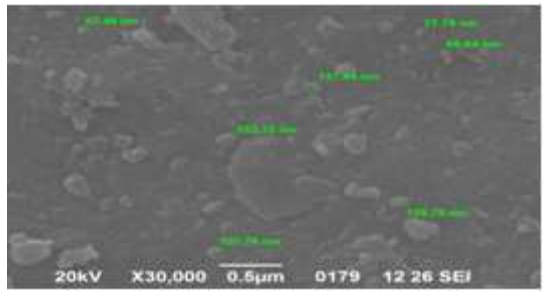

Fig. 1 The SEM image of nano silica

4. NANOSCALE CONCRETE

i. Fundamental research into the interactions between fly ash and the Nanostructure of Portland cement gel is under way, using neutron scattering technology

ii. Nanotechnology is providing a close-up look at the hydration of cement grains and the Nanostructure of cement reactivity as hydrated surfaces develop on individual cement grains.

iii. The feasibility of Cyberliths, or Smart Aggregates, as wireless sensors embedded in concrete or soil is under examination.

Concrete ills such as alkali-silica reactivity (ASR) and delayed stringier formation, the bane of concrete highways and bridges, are being explored at the molecular level using neutron-scattering technology and other processes.

4.1 Cement Reactivity at Nano Scale

We need to better know how to control the timing of concrete setting. The evolution of the hydrogen profile shows the timing of the surface layer's breakdown. This information can be used to Study the concrete setting process as a function of time, temperature, cement chemistry, and other factors. For example, researchers used NRRA (Nuclear Resonance Reaction Analysis) to determine that in cement hydrating at 30°C, the breakdown occurs at 1.5 hours. The surface disintegration then releases accumulated silicate into the surrounding solution, where it reacts with calcium ions to form a calcium-silicate hydrate gel, which binds cement grains together and sets the concrete. "This resolves a scientific debate that has been going on for more than a century." The 20-Nanometer-thick surface layer acts as a semi permeable barrier that allows water to enter the cement grain and calcium ions to leach out. However, the larger silicate ions in the cement are trapped behind this layer. As the reaction continues, a silicate gel forms there, causing swelling within the cement.

5. OBJECTIVES OF THIS INVESTIGATION

To determine the Improvement of Compression Strength, Corrosion resistance and Permeability strength of Concrete by Nano technology.
The Objective of this Investigations are:

i. Studies on compressive strength, corrosion resistance and permeability strength of concrete were made separately by partially replacing of cement with fly ash and find out the optimum replacement percentage of fly ash to the weight of cement.

ii. Different proportions of replacing of fly ash with cement for studies are 0%, 10%, 20%, 30%, 40%, 50%, 60%, 70%, and 80% .

iii. Same proportions of replacing of cement with fly ash with addition of Nano silica at a rate 2.5% to the weight of cement are done and their results are studied.

iv. Then a comparative analysis of compressive strength, Corrosion resistance and Permeability factor of Partially Replaced Fly ash Concrete with the Nano concrete.

6. MATERIALS AND METHODS

6.1 An Investigation of Nano Silica in Cement Hydration Process

With the advent of nano technology, materials have been developed that can be applied to high performance concrete mix designs. Nano silica reacts with calcium hydroxide (CH) to develop more of the strength carrying structure of cement: calcium silica hydrate (CSH). In this paper, relationships have been developed to distinguish the benefits when using different sizes of nano silica in cement paste. An extensive regime of experimental analysis was carried out to determine the effect of nano silica. Through these experiments the heat of hydration of multiple cement mix designs was measured. After that, the concentration of CH was recorded through X-ray diffraction. Then, the grain structures were examined through Scanning Electron Microscopy. Finally, the compressive strength was determined for each cement paste mixture. Through these experiments it was found that as the silica particles decreased in size and their size distribution broadened, the CSHs became more rigid; this increased the compressive strength.

6.2 Specimen Casting and Curing

A laboratory type concrete mixer machine was used to mix the ingredients of concrete. The following procedure was followed in mixing.

i. First cement, fly ash and Nano silica were mixed for one minute and after that the fine aggregate was also included and mixed and coarse aggregate was mixed thoroughly in dry state and cement were mixed for one minute.

ii. Super plasticizer is mixed with water and it being added within two minutes now concrete was allowed to mix for three minutes.
iii. All the specimens were well compacted using table vibrator, and cured for 7, 14 and 28 days respectively.
iv. This specimen and casting is individually done and followed for Compression, Corrosion and Permeability setup

7. COMPRESSION TEST SETUP

The test is carried out on 150 x 150 x 150 mm size cubes, as per **IS: 516-1959**. The test specimens are marked and removed from the mould and unless required for test within 24 hours, immediately submerged clean fresh water and kept there until taken out just prior to test. A 2000kN capacity Compression Testing Machine (CTM) is used to conduct the test. The specimen is placed between the steel plates of CTM and total load is applied at the rate of 140kg/m^3/min and the failure load in kN is observed from the digital gauge.

7.1 Design of Concrete MIX

The concrete mix are designed as per IS 10262-2009, the table below enumerates the summary of design results which fulfill the requirements as per the code standard.

Table 1 According to IS 10262-2009 Concrete Mix Design (M_{40})

Step No.	Parameter		M_{40}
1	Target mean strength(N/mm2)		48.25
2	Water/Cement Ratio		0.45
3	Quantities	Water Content(lit/m^3)	140
		Sand (%)	38
4	Final Water Content(kg/m^3)		140
5	Actual Cement Content(kg/m^3)		350
6	Check for Minimum Cement Content(kg/m^3)		320
7	Aggregate Quantity	Fine aggregate (kg/m^3)	862
		Coarse aggregate (kg/m^3)	1097
8	Mix Proportion		0.45:1: 1.65:2. 92

7.1 Specimen Details

This experimental program consists of casting and testing of 162 concrete cubes of standard size of 150 mm x 150 mm x 150 mm. Number of cubes casted, their id, descriptions and their curing period are summarized below. The results obtained from the above elaborative experiments are discussed. The results of mechanical strength properties such as cube compressive strength have discussed and the compression strength variations for 7, 14 and 28 days cured concrete cubes of only fly ash replacement and fly ash replacement with Nano silica as additive are also analyzed.

Table 2 Table Shows the Specimen Details of Partially Replaced Flyash Concrete

Cube ID	Fly Ash Replacement	No. of Cubes For		
		7 Days Curing	14 Days Curing	28 Days Curing
C	0%	3	3	3
F 1	10%	3	3	3
F 2	20%	3	3	3
F 3	30%	3	3	3
F 4	40%	3	3	3
F 5	50%	3	3	3
F 6	60%	3	3	3
F 7	70%	3	3	3
F8	80%	3	3	3

8. CORROSION TEST SETUP

The test was carried out on 150 x 300 mm size concrete cylinders with a rod of height 450 mm in the center throughout the specimen. The test specimens are marked and removed from the moulds after 24-48 hours from casting depending upon the percentage of fly ash and submerged in clean fresh water for curing. The impressed current technique which is commonly used for accelerating reinforcement corrosion in concrete specimen was used for testing. The specimen was placed in water bath containing calculated quantity of dissolved sodium chloride (table salt) to act as electrolyte. Calculated voltage of current was passed through the concrete specimen till the concrete cracks. The percentage weight loss in rebars and the width of cracks in concrete were studied.

Table 3 Table Shows the Specimen Details of Nano Concrete Cubes

Cube ID	Fly Ash Replacement	Nano Silica As Additive	No. of Cubes For		
			7 Days Curing	14 Days Curing	28 Days Curing
C	0%	2.50%	3	3	3
F 1	10%	2.50%	3	3	3
F 2	20%	2.50%	3	3	3
F 3	30%	2.50%	3	3	3
F 4	40%	2.50%	3	3	3
F 5	50%	2.50%	3	3	3
F 6	60%	2.50%	3	3	3
F 7	70%	2.50%	3	3	3
F8	80%	2.50%	3	3	3

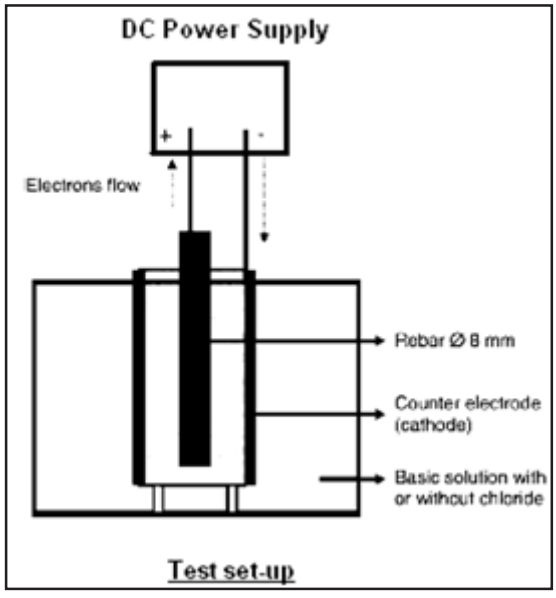

Fig.2 Impressed current test setup

8.1 Results Attained for Corrosion Test

The testing was carried out using the Test Set Up and the graphs for the comparison of Mass of Actual Rust, Degree of Induced Corrosion and Crack Width between the Fly Ash added concrete and nS + Fly ash added concrete are plotted.

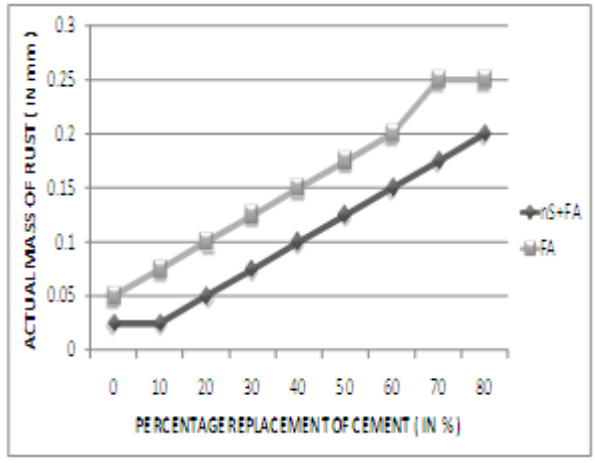

Graph 1 Actual mass of rust comparison result for (M_{40}) 28 days

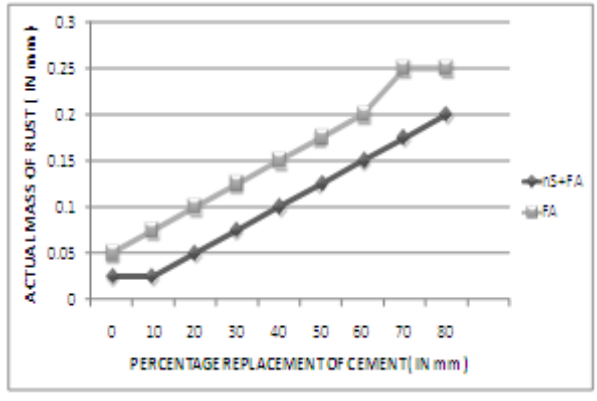

Graph 2 Degree of induced corrosion comparison result for (M_{40}) 28 day

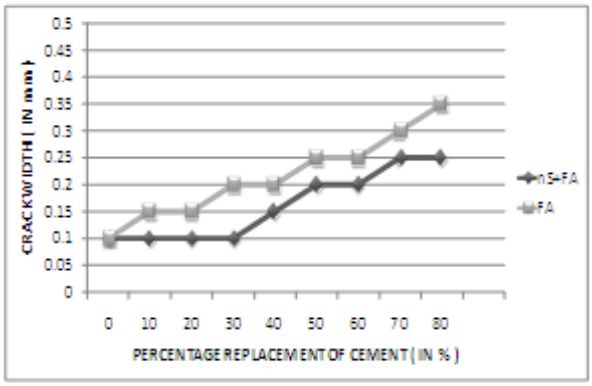

Graph 3 Crack width comparison result for (M_{40}) 28 days

9. PERMEABILITY TEST SETUP

i. The test is carried out on 150 x 150 x 150 mm size cubes, as per **IS: 3085-1965**. The test specimens are marked and removed from the mould and unless required for test within 24 hours, immediately submerged clean fresh water and kept there until taken out just prior to test.

ii. The standard test pressure head to be applied to the water in the reservoir should be 10 kg/cm^2. This may, however, be reduced up to 5 kg/cm^2 in the case of relatively more permeable specimens where steady state of flow is obtained in a reasonable time, and may be increased up to 15 kg/cm^2 for relatively less permeable specimens and whe1.e selling could be ensured to be fully effective.

iii. The quantity of percolate and the gauge-glass readings shall be recorded at periodic intervals. In the beginning, the rate of water intake is larger than the rate of outflow. As the steady state of flow is approached, the two rates tend to become equal and the outflow reaches a maximum and stabilizes. With further passage of time, both the inflow and outflow generally register a gradual drop. Permeability test shall be continued for about 100 hours after the steady state of flow has been reached and the outflow shall be considered as average of all the outflows measured during this period of 100 hours.

9.1 Results Attained

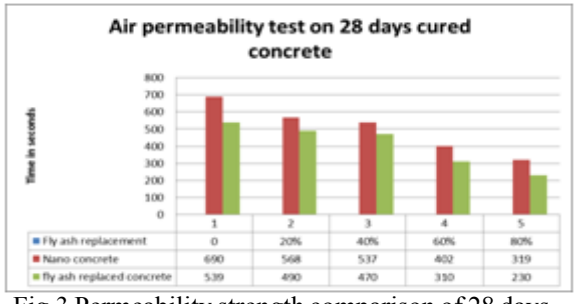

Fig.3 Permeability strength comparison of 28 days

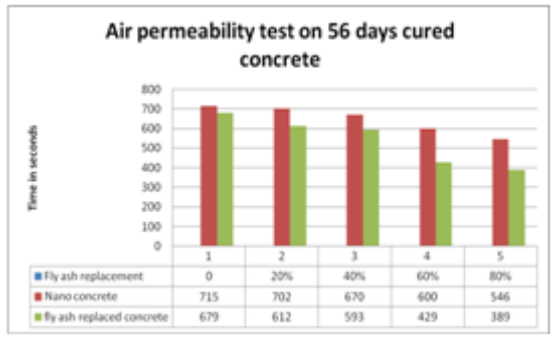

Fig. 4 Permeability strength comparison of 56 days cured specimen

TIME IN SECONDS	INTERPRETATION
<30	Poor
30 - 100	Moderate
100 - 300	Fair
300 - 1000	Good
> 1000	Excellent

Fig.5 Interference of the permeability result

9.2 Discussions

i. The permeability of concrete attain by adding fly ash and Nano silica in the partial replacement of cement possess some significant higher strength.

ii. Nano-silica consumes calcium hydroxide crystals, reduces the size of the crystals at the interface zone and transmute the calcium hydroxide feeble crystals to the C-S-H crystals, and improves the interface zone and cement paste structures.

iii. The water absorption tests indicate that the Nano-silica concrete has better permeability resistance than the normal concretes, Due to the microstructure of the Nano silica concrete is more uniform and denser than that of reference concrete as shown in The SEM test.

iv. Permeable strength of the concrete increases with adding the Nano-silica, especially at early ages. However the early strength of the concrete decreases slightly with adding the fly ash, but decreases at later ages. These results indicate that the Nanosilica may adopt for higher strength green concrete technologies.

10. CONCLUSIONS

From the above experiments and results we safely conclude the points as follow.

i. Nano concrete could control the carbon dioxide emission from the earth which is shown by using fly ash concrete products instead of cement concrete.

ii. Thus the Nano particles which is in the form of silica can easily react with cement particles which are normally in Nano scale initiate the CSH reaction and hence its tend to accelerate the compressive strength of concrete.

iii. Nano-silica consumes calcium hydroxide crystals, reduces the size of the crystals at the interface zone and transmute the calcium hydroxide feeble crystals to the silica may adopt for higher strength green concrete technologies.

iv. C-S-H crystals, and improves the interface zone and cement paste structures.

v. Compressive strength of the concrete increases with adding the Nano-silica, especially at early ages. However the early strength of the concrete decreases slightly with adding the fly ash, but decreases at later ages. These results indicate that the Nano

vi. Corrosion resistance property of the nS added concrete is comparatively higher than ordinary fly ash concrete.

vii. The corrosion resistance of optimum percentage replacement of fly ash is higher in nano concrete than the ordinary fly ash concrete.

viii. The average increases in compressive strength up to 7% than the compressive strength ordinary partially replaced fly ash concrete on 7 days cured concrete

ix. But in the fourteen days cured cubes the increase in compressive strength is incrementally up by 13% percentages compared to the ordinary partially replaced fly ash concrete.

x. Finally the compressive strength of twenty eight days cured Nano concrete possess an incremental strength by 23% than the ordinary fly ash replaced concrete.

xi. The permeability of concrete attain by adding fly ash and Nano silica in the partial replacement of cement possess some significant higher strength.

xii. For any special concrete structures such as petrol tanks, bunkers and silos, oil well we can use this type of special concrete to get more strength and performance.

REFERENCES

[1] P.N.Balaguru, “Nanotechnology and Concrete: Background, Opportunities and Challenges”, Proceedings of the International Conference-Application of Technology in Concrete Design, 2005.

[2] P.Arthur Boresi, P. Chong, Ken and Sunil Saigal, “Approximate Solution Methods in Engineering Mechanics”, John Wiley, New York, 2002, pp.280.

[3] P. Balaguru and S.P. Shah, “Fiber Reinforced Cement Composites”, McGraw-Hill, New York, 1992, pp.530.

[4] D. Srivastava, C.Wei and K. Cho, “Nanomechanics of Carbon Nanotubes and composites”, Applied Mechanics, Review, Vol.56, 2003, pp.215-230.

[5] G. LI, “Properties of High-volume Fly Ash Concrete Incorporating Nano-SiO2”, Cement and Concrete, Research, Vol.34, 2004, pp.1043- 1049.

[6] ‘Concrete Technology’ by M.S.SHETTY

[7] www.aggregateresearch.com

[8] www.Nanoc.info/index.html

Zernike Feature based Pattern Retrieval Using Artificial Neural Network

R. Parivallal[1], B. Nagarajan[2] and R. Sathish Kumar[3]

[1&2] Department of Computer Applications, Bannari Amman Institute of Technology, Sathyamangalam - 638 401, Erode Distrcit, Tamil Nadu

[3]Department of Mathematics, Bannari Amman Institute of Technology, Sathyamangalam - 638 401, Erode Distrcit, Tamil Nadu

E-mail: rpaarivallal@gmail.com, nr_mca@rediffmail.com

Abstract

The difficulties faced in an image retrieval system used for searching and retrieving of image in an image databases cannot be underestimated. This requirement formed the driving force behind the emergence of image retrieval techniques. The Image Retrieval is a technology that is being developed to address different application areas, remote sensing, geographic information systems, and weather forecasting, architectural and engineering design, multimedia documents for digital libraries. The goal of this paper is to build an object classifier that first identifies a knowledge pattern like "aero-plane" from the Caltech101 standard database. The image is divided into sub-blocks of equal size without any pre-processing. The Zernike moment features are extracted from each sub-block. The features of the objects are fed to the back-propagation neural classifier after normalization. The performance is checked by blocking models. Quantitative evaluation shows improved results of 91.38%. A critical evaluation of this approach under the proposed standards is presented.

Keywords: *Blocking models, Neural classifier, Normalization, Zernike moments.*

1. INTRODUCTION

Advances in data storage and image acquisition technologies have enabled the creation of large image datasets. Image searching is one of the most important services that need to be supported by such systems developing effective methods for automated annotation of digital images continues to challenge for computer scientist. Knowledge pattern identification and data classification are necessary components in an artificially intelligent autonomous system. Object classification plays a major role in many applications.

In the artificial intelligent system requires identification and classification of aero-plane objects commonly found in the picture. This paper tries to bring out the importance of the zernike features for object classification. The derived zernike features from various sub-blocks of the images are normalized and fed to the neural classifier. The objects of interest being an aero-plane being and non-aero-plane are classified.

Knowledge pattern identification is a major area where researchers design computational systems that can identify and classify objects automatically. Identification and classification of human has been a focus of investigation over last decades [1-3]. Agarwal et al. [4] proposed a new approach to object detection that makes use of a sparse, part-based representation model. This study gives very promising results in the detection of human from a group of natural scenes. Nagarajan and Balasubramanie [5] have proposed their work based on wavelet features towards object classification with cluttered background. Nagarajan and Balasubramanie [6]-[8] have presented their work based on moment invariant features, statistical features and spectral features to classify the objects with mild occlusion and complex background respectively. Shan Li et. al. [9] proposes an image retrieval system based on shape using zernike moment features. Ye Mei and Dimitrios Androutsos [10] work is to bring a region based shape descriptor using zernike moment concept. Zen Chen and Shu-Kuo Sun [11] implemented a phase-based descriptor using zernike moments for local image representation and matching.

2. ZERNIKE MOMENT FEATURES

Zernike moments [9] are a set of complex polynomials $\{V_{nm}(x,y)\}$ which form a complete orthogonal set over the unit disk of $x^2 + y^2 \leq 1$ in polar coordinates. These polynomials are of the form given in Equation (1).

$V_{nm}(x,y) = V_{nm}(r,\theta) = R_{nm}(r)\exp(jm\theta)$

Where n is positive integer or zero and m is an integer subject to constraints is even and $|m| \le n$. $r = \sqrt{x^2 + y^2}$ is the length of the vector from the origin to the pixel (x,y). $\theta = \arctan(\frac{y}{x})$ is the angle between the vector r and x axis in counter clockwise direction. $R_{nm}(r)$ is a radial polynomial defined in Equation (2).

$$R_{nm}(r) = \sum_{s=0}^{(n-|m|)/2} \frac{(-1)^s (n-s)!}{s!\left[\frac{n+|m|}{2}-s\right]!\left[\frac{n-|m|}{2}-s\right]!} r^{n-2s}$$

The two-dimensional zernike moment of order n with repetition m for function $f(x,y)$ is defined in Equation (3).

$$Z_{nm} = \frac{n+1}{\pi}\iint_{unitdisk} f(x,y)\, V^{*}_{nm}(x,y)\,dxdy$$

Where $V^{*}_{nm}(x,y) = V_{n-m}(x,y)$

To compute the zernike moment of a digital image, It is required to change the integrals with summations as given in the Equation (4).

$$A_{nm} = \frac{n+1}{\pi}\sum_{x}\sum_{y} f(x,y)V^{*}_{nm}(x,y),$$

Where $x^2 + y^2 \le 1$.

The defined features of zernike moments themselves are only invariant to rotation. To achieve scale and translation invariance, the image needs to be normalized first by using the regular zernike moments. The translation invariance is achieved by translating the original image $f(x,y)$ to $f(x+\bar{x}, y+\bar{y})$,

where $\bar{x} = \frac{m_{10}}{m_{00}}$ $\bar{y} = \frac{m_{01}}{m_{00}}$

In other words, the original image's center is moved to the centroid before the zernike moment's calculation. Scale invariant is achieved by enlarging or reducing each shape so that the image's 0th regular moment equals to the total number of shape pixels in the image, for a scaled image $f(\alpha x, \alpha y)$, its regular moments

$m'_{pq} = \alpha^{p+q+2} m_{pq}$ m_{pq} is the regular moments of Since the objective is to make $m'_{00} = \beta$, let $\alpha = \sqrt{\frac{\beta}{m_{00}}}$. Substituting $\alpha = \sqrt{\frac{\beta}{m_{00}}}$ into m'_{00}, $m'_{00} = \alpha^2$, $m_{00} = \beta$ is obtained.

The fundamental feature of the zernike moments is their rotational invariance. If $f(x,y)$ is rotated by an angle α, then the zernike moment of the rotated image is obtained by Equation (5).

$$Z'_{nm} = Z_{nm}\, e^{(-jm\alpha)}$$

Thus, the magnitudes of the zernike moments can be used as rotationally invariant image features. Thirty six zernike features are extracted every block of an image.

3. BUILDING A NEURAL CLASSIFIER

A binary Artificial Neural Network (ANN) classifier is built with back-propagation algorithm [12] [13] that learn to classify an image as a member or non-members of a class. The number of input layer nodes is equal to the dimension of the feature space obtained from the hybrid features. The number of output nodes is usually determined by the application [12] which is 1 (either "Yes/ No") where, a threshold value nearer to 1 represents "Yes" and a value nearer to 0 represents "No". The neural classifier is trained with different choices for the number of hidden layer. The final architecture is chosen with single hidden layer shown in Figure 1 that results with better performance.

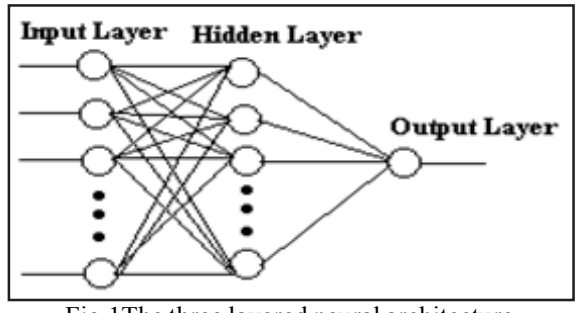

Fig.1The three layered neural architecture

The connections carry the outputs of a layer to the input of the next layer have a weight associated with them. The node outputs are multiplied by these weights before reaching the inputs of the next layer. The output neuron (6) will be representing the existence of a particular class of object.

$$o_j^l(k) = f\left(\sum_{m=0}^{N_l - 1} w_{jm}^l\, o_m^{l-1}\right)$$

4. PROPOSED WORK

This paper addresses the issues to classify objects of aero-plane images containing non-aero-plane amidst

background clutter and mild occlusion. The objects of interest to be classified are aero-plane (positive) and non-aero-plane (negative) images taken from Caltech101 standard database. The image data set consists of 1600 real images for training and testing having 800 in each class. The sizes of the images are uniform with the dimension 360x120 pixels. Thirty zernike features are extracted from each block as mentioned in the previous section using Equation (1) to Equation (5). The zernike features are calculated from each single block of the sub-image. Data normalization is applied for the derived zernike features. Data normalization returns the deviation of each column of D from its mean normalized by its standard deviation. This is known as the Zscore of D. For a column vector V, Z score is calculated from equation (7). This process improves the performance of the neural classifier. $Z = (V - \text{mean}(V)) / \text{std}(V)$

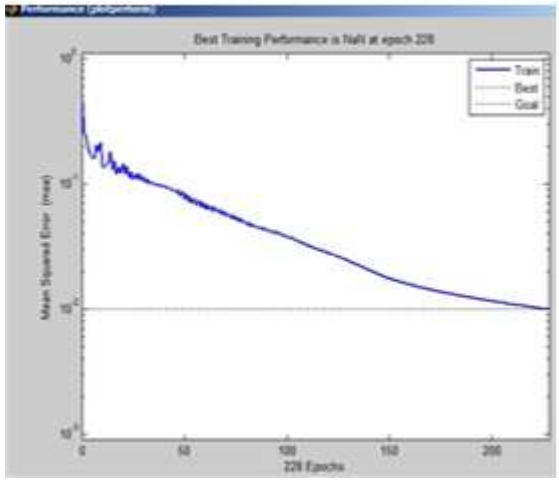

Fig.2 The Performance of neural network training graph

5. IMPLEMENTATION

We trained our methods with different kinds of "aero-plane" objects against a variety of background, partially occluded human objects of positive class. The negative training examples include images of natural scenes, buildings and road views. The training is done with 400 images (200 positive and 200 negative). The testing of images are done with 1600 images (800 positive and 800 negative) taken from the Caltech101 image database [14]. The feed-forward network for learning is done for optimal structure validation is done and the structure given below performs well and leads to better results.

6. DISCUSSION

In object classification problem, the four quantities of results category are given below.

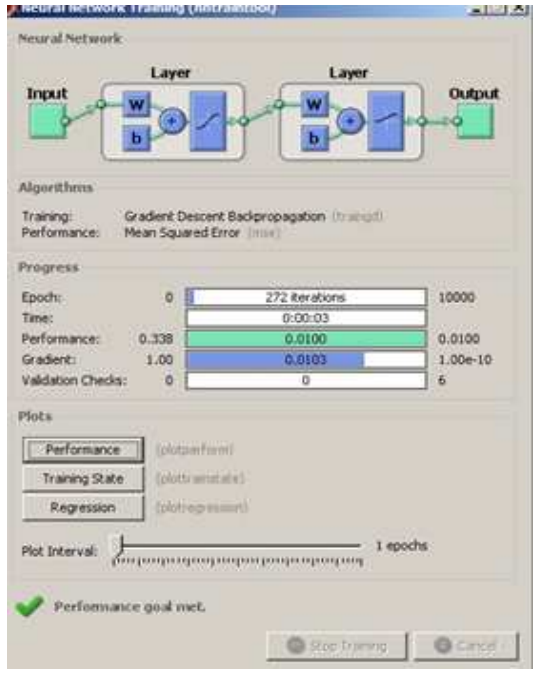

Fig.3 The performance of neural network training: 27 Blocks of size 40x40 each

i. True Positive (TP): Classify a aero-plane image into class of aero-plane images.
ii. True Negative (TN): Misclassify a aero-plane image into class of natural (Non aero-plane images).
iii. False Positive (FP): Classify a natural image into class of none.
iv. False Negative (FN): Misclassify a none image into class of aero-plane.

The objective of any classification is to maximize the number of correct classification denoted by True Positive Rate (TPR) and False Positive Rate (FPR) where by minimizing the wrong classification denoted by True Negative Rate (TNR) and False Negative Rate (FNR).

$$TPR = \frac{\text{Number of true positive (TP)}}{\text{Total no. of positive in data set (nP)}}$$

$$INR = \frac{\text{Number of true negative (TN)}}{\text{Total no. of negative in data set (nN)}}$$

$$FPR = \frac{\text{Number of false positive (FP)}}{\text{Total no. of positive in data set (nP)}}$$

$$FNR = \frac{\text{Number of false negative (FN)}}{\text{Total no. of negative in data set (nF)}}$$

The testing samples are 800 for positive (nP) and 800 for negative (nN) respectively. Most classification algorithm includes a threshold parameter for classification accuracy which can be varied to lie at different trade-off points between correct and false classification. The proposed work gives a significant improvement in classification accuracy. The novelty of the proposed work is that the input images are not pre-processed. The background cluttered or occlusions are not removed using background removal method as found in the literature [6-8].

7. CONCLUSION

Thus an attempt is made to build a system that classifies the objects amidst background clutter and mild occlusion is achieved to certain extent. The novelty of this paper is that the input images are not pre-processed for removing the cluttered background. Thus the goal is to classify objects of real-world images containing "human" images with cluttered background with that of "none" images with natural scenes is presented. The limitation of this method is the object with a high degree of occlusion for classification of images. Further work extension can be made to improve the performance of the classifier system with various feature extraction methods. This paper has presented a brief overview of Knowledge pattern extraction methodology using Zernike features.

REFERENCES

[1] J.W.Hsieh, S. H.Yu, Y. S. Chen and W. F. Hu, "Automatic Traffic Surveillance System for Vehicle Tracking and Classification", IEEE Transansaction on Intelligent Transport System, Vol.7, No.2, 2006, pp.175-187.

[2] Y. Shan, H.S. Sawhney and R. Kumar, "Vehicle Identification Between Non-Overlapping Cameras without Direct Feature Matching", Proceedings of the Tenth IEEE International Conference on Computer Vision (ICCV'05), 2005.

[3] Z. Sun, G.Bebis and R. Miller, "Monocular Precrash Vehicle Detection: Features and Classifiers", IEEE Transaction on Image Processing, Vol.15, 2006, pp.2019-2034.

[4] S. Agarwal, A.Awan and D.Roth, "Learning to Detect Objects in Images Via a Sparse, Part-Based Representation", IEEE Transaction on Pattern Analysis and Machine Intelligent, Vol.26, No.11, 2004, pp.1475-1490.

[5] B. Nagarajan and P. Balasubramanie, "Wavelet Feature Based Neural Classifier system for Object Classification with Complex Background", Proceeding International Conference on Computational Intelligence and Multimedia Applications (ICCIMA'07), IEEE CS Press, Vol.1, 2007, pp.302-307.

[6 Nagarajan B. and P. Balasubramanie, "Neural Classifier System for Object Classification with Cluttered Background Using Invariant Moment Features", International Journal of Soft Computing, 2008, 3(4), 302-307.

[7] B. Nagarajan and P. Balasubramanie, "Object Classification in Static Images with Cluttered Background Using Statistical Feature Based Neural Classifier", Asian Journal of Information Technology, Vol.7, No.4, 2008, pp.162-167.

[8] Shan Li, Moon-Chuen Lee, and Chi-Man Pun, "Complex Zernike Moments Features for Shape-Based Image Retrieval", IEEE Transactions on Systems, Man and Cybernetics, Part A: Systems and Humans, Vol.39, No.1, 2009, pp.227-237.

[9] Ye Mei and Dimitrios Androutsos, "Robust Affine Invariant Region-Based Descriptors: The ICA Zernike Moment Shape Descriptor and the Whitening Zernike Moment Shape Descriptor", IEEE Signal Processing Letters, Vol.16, No.10, 2009, pp.877–880.

[10] Zen Chen and Shu-Kuo Sun, "A Zernike Moment Phase-Based Descriptor for Local Image Representation and Matching", IEEE Transactions on Image Processing, Vol.19, No.1, 2010, pp.205-219.

[11] A. Khotanzand and C. Chung, "Application of MultiLayer Perceptron Neural Networks to Vision Problem", Neural Computing & Applications, Springer-Verlag London Limited, 1998, pp.249-259.

[12] B.Yegnanarayana, "Artificial Neural Networks", 1999, Prentice-Hall of India, New Delhi.

[13] Andreas Opelt and Axel Pinz, "The TU Graz standard database", 2002.

[14] Kavita Choudhary, Manish Pundlik and Dharmendra Choukse **"**An Integrated Approach for Image Retrieval zbased on Content" IJCSI International Journal of Computer Science Issues, Vol. 7, No 7, May 2010, pp.42-47.

Awareness of Natural UV Protection Finish on Garments Among Chennai People

Habeebuniss
National Institute of Fashion Technology, Chennai - 600 113, Tamil Nadu
E-mail: Habeeba2010@rocketmail.com

Abstract

UV protection finish is one of the important finishes and also the most necessary in countries where hot and humid climate is expected. Organic value of eco-friendly product has generated high interest among consumers and they are known for moving towards organic products. Many natural dyes provide various medicinal properties and other benefits, in which UV absorbency by natural dyes is most vital. In this paper an attempt has been made to study the living practices of Chennai people in terms of UV protection as well as their knowledge and awareness on UV protection finished garments.

Keywords: *Natural dyes, UV protection factor, UV finishes for garments*

1. INTRODUCTION

Sunlight is the prime energy source and essential element for survival of human race.[1]UV radiation has the highest quantum energy compared to other radiations. This energy is of order magnitude of organic molecule's bond energy; hence, it has tremendous detrimental effect on human skin.[2] Clothing provides one of the most convenient forms of protection against Ultraviolet radiation, but not all garments offer sufficient sun protection. Nowadays different type of special finish has been given to the fabric /garment to keep humans being safe. UV protection finish is an important such finish that is most necessary in countries where hot and humid climate is expected. By definition, sun-protective clothing is an item of personal apparel (including garments, hats, shoes, and fabric intended to be made into personal apparel) for which a claim of protective advantage against solar ultraviolet radiation is made [3] The textile industry has been condemned as being one of the world's worst offenders in terms of pollution because it requires a great amount of two components: Water and Chemicals. As many as 2,000 different chemicals are used in textile industry.[3] Hence there is a strong need of finishes that are eco-friendly in nature. There are various eco friendly finishes coming up in market for various special finishes. In this paper an attempt had has been made to study the living practices of Chennai people in terms of UV protection as well as their knowledge and awareness on UV protection finished garments. Over-exposure to solar ultraviolet radiation (UV radiation) can cause sunburn, skin damage and an increased risk of developing skin cancer. Clothing provides one of the most convenient forms of protection against UVR but not all garments offer sufficient sun protection, therefore it becomes very important for garments to be finished with UVR absorbers.

Table 1 UPF Rating

UPF Rating	Protection Category
UPF 15 - 24	Good
UPF 25 - 39	Very Good
UPF 40 - 50+	Excellent

According to Table 1, a fabric to give very good protection from UV radiations, it is necessary to have UPF rating above 25. This is in accordance to the ASTM Standard for Sun Protective Clothing and Swimwear which is considered the industry standard in rating sun protective clothing:

1.1 Factors that Contribute to the UPF Rating of a Fabric are:

i. Composition of the yarns (cotton, polyester, etc)
ii. Tightness of the weave or knit (tighter improves the rating)
iii. Colour (darker colours are generally better)
iv. Stretch (more stretch lowers the rating)
v. Moisture (many fabrics have lower ratings when wet)
vi. Condition (worn and faded garments may have reduced ratings)
vii. Finishing (some fabrics are treated with UV absorbing chemicals) [4]

1.2 UV Absorbers

UV absorbers are organic or inorganic colorless compounds with very strong absorption in the UV range

of 290-360nm and block the UV radiation reaching the human skin, when incorporated in the fabric. UV absorbers incorporated in to the fibers convert electronic excitation energy in to thermal energy. They function as radical scavengers and oxygen scavengers. The high energy short wave UVR excites the UV absorber to a high energy absorbed may then be dissipated as longer waveand the UV absorber may then fragment in to non-absorbing isomers. [3] Various attempts have been made to develop UV protective fabric with the help of natural dyes. The results of the studies proved that many fabrics dyed with dyeing plants are characterized with good or very good protection factors.

1.3 UV Protection & Nature of Fibre

Ultraviolet protective factor is strongly dependent on the physical and chemical structure of the fibres. The chemical nature of the fibres influences the UPF, due to variation in ultraviolet transparency [5]. Natural fibres like cotton, silk, and wool have lower degree of absorption of ultraviolet radiation than synthetic fibres. [7, 8]

1.4 UV Protection & Cover Factor

Cover factor is a highly important fabric parameter, because it determines the probability of a UV ray striking a fiber. The greater the probability that UV radiation directed at the fabric surface will strike a fiber and therefore be reflected or absorbed by the surface fiber or other fibers as it continues its journey through the maze of fibers comprising the yarn leads to decreased transmittance (higher UPF). Conversely, the higher the percent porosity of the fabric, the greater the probability that rays directed perpendicular to the fabric surface (as is the case in ransmittance testing) will pass directly through the pores in the fabric (where there is no UV absorbing material. [6]

1.5 UV Protection & Color

The dyes used to colour textiles can have a considerable influence on their permeability to ultraviolet radiations.[3] As a general rule, for the same fabric parameters and dye the darker the shade, the higher the UPF value. A protective effect can be obtained by dyeing and printing, which is better than using heavy weight fabrics which are not suitable for summer conditions. Darker colors such as dark navy blue and blacks, dark reds absorb UV radiation much more strongly than the light pastel colours. [9,10]

1.6 UV Protection & Natural Dyeing

Use of natural dyes are known to man thousands of years ago and only from the 19th century onwards the synthetic dyes were introduced. Natural dyes are mostly nonsubstantive and must be applied on textiles with the help of mordants, usually metallic salts. These metallic mordants after combining with the dye in the fiber, it forms an insoluble precipitation or lake and thus both the dye and mordant gets fixed to become wash fast to a reasonable level.[11,12] Many plants produce substances that have medicinal properties as well, and also plants rich in Tannin are one of the best options of natural mordants Tannin present in the plants help in its own way as anti microbial agents, and also yield darker shades when used with natural dyes. The major drawbacks of natural dyes are they are not colour fast and do no yield darker shades of the color. Various attempts have been made to overcome these drawbacks by use of different types of mordants such as copper sulphate, ferrous sulphate, Alum, Potassium dichromate, Stannous chloride etc.

2. OBJECTIVES OF THE STUDY

The study was undertaken with a view to understand the practices of Chennai people during their outings in summer. Specifically the research was conducted to determine the knowledge about UV protection garments. The study also concentrates on the awareness of usage of such UV treated garments.

3. RESEARCH METHODOLOGY

Descriptive research methodology is used to find the objectives of the study. Both primary and secondary data were collected. The primary data was collected using Questionnaire from the Chennai people (Total no. of respondents:102) who are above the age of 20 years by convenience sampling method. The secondary data was collected from various related websites and journals.

4. DATA ANALYSIS AND INTERPRETATION

Statistical tools like simple percentage method and Chi-square test are used to analyze the data collected through questionnaire. The analysis is done using the SPSS software. Percentage analysis is the method to represent raw streams of data as a percentage for better understanding of collected data. Chi-square test is a statistical hypothesis test between two variables to find their association. In order to obtain the objectives of the

present study, the respondents were divided into three groups i.e., professionals, students and others (people such as those who are self employed, housewives, research scholars, etc.)

4.1 To Understand the Type of Activity People Actively Undertake in Chennai

It is evident from table 2 that maximum no. of people in Chennai prefer Mid Day outing (56.9%) as their activity, whereas 24.5% of them undertake other activities like commuting to office, college, gym, pick up and drop of kids to school etc. apart from the ones listed. About 15.7% of the respondents take up sports activities during day time, whereas only 1% of the respondent prefer to go for swimming in Chennai during the daytime.

4.2 To Understand the Awareness of Various Skin Ailments that Result on Exposure to Sunlight

Table 3 Awareness of Skin Ailments Among Chennai People

Skin Ailment	%
Sun Burn	71.6
Skin Allergy	66.7
Pre Ageing	58.8
Yellow Discoloration of Skin	56.9
Pigmentation	55.9
Wrinkle Formation	60.8
Benign Skin Tumor (Cancer)	55.9

Table 3 gives suggests that all the respondents who participated in the study are aware of all the skin ailments listed in the questionnaire. It is also noted form the above table that sun burn is known to maximum number of respondents whereas benign skin tumor (skin cancer) occurrence due to exposure to UV radiations from direct sunlight is known to only 55.9% of the respondents.

4.3 To Understand the Association between Activity Undertaken by Respondent and Covering the Skin While their Outings in Summer

Inference: Table 4 below indicates the Chi-square value is equals 0.058 at 15 degree of freedom, the significance values is greater than 0.05, suggest that there is no association between covering the skin on exposure to sunlight and the activity undertaken by Chennai people. Hence the null hypothesis is accepted

Ho:- There is no association between activity and the covering of skin on exposure to sunlight.

H1:-There is association between activity and the covering of skin on exposure to sunlight.

4.4 To Understand the Association Between Covering The Skin On Exposure to Sunlight and Occurrence of Skin Ailments among Chennai People

Inference: Table 5 below indicates the Chi-square value is equals 0.215 at 12 degree of freedom, the significance values is greater than 0.05, suggest that there is no association between covering the skin on exposure to sunlight and occurrence of skin ailments among Chennai people. Hence the null hypothesis is accepted .

Ho – There is no association between the covering of skin on exposure to sunlight and the occurrence of skin ailments among Chennai people.

H1 - There is association between the covering of skin on exposure to sunlight and the occurrence of skin ailments among Chennai people.

4.5 To Understand The Preference of Various Fabric Types Among Professionals, Students & Others in Chennai

Table 6 indicates that 65.2% of the professionals prefer to wear cotton medium weight fabric. 50% of the students prefer to wear cotton light weight fabrics, whereas 35% of the other people category people prefer light weight fabrics.

Table 6 Occupation Vs Fabric Colour Preference Among Chennai people

Occupation	Dark Colour	Pastel Colour	No Colour Preference
Professionals	10.90%	50.00%	39.10%
Students	11.10%	52.80%	36.10%
Others	5.00%	25.00%	70.00%

It is evident from table 7 that 97.8% of professionals are aware of Sun protection concept, but none of them are aware of commercially available UV spray or natural UV protection products for garment. But 95.6% of the professionals who participated in the study said they prefer natural dyes for UV protection from direct sunlight.

4.7 To Understand the Awareness of Sun Protection Concepts, Commercial UV Sprays, Natural Dyes Used for UV Protection, Availability of any Such Product and Preference of Natural Dyes for UV Protection Among Professionals, Students & Others in Chennai

Table 7 Awareness of UV Protection Products Among Chennai People

Occupation	Awareness of Sum Protection	Awareness of Commercial UV Sprays	Awareness Of Natural Dyes for UV Protection	Preference of Natural Dyes for UV Protection	Awareness of any Natural UV Protection Product
Professionals	97.8%	0%	30.4%	95.6%	0%
Students	91.6%	0%	41.7%	96.1%	2.8%
Others	90%	0%	20%	100%	0%

5. FINDINGS

i. From the above survey it was found that most of the people from Chennai were active in mid day shopping, which proves that they go out in bright sunlight during the day time.
ii. It was observed that all the respondents were aware of all the skin ailments (above 50%) that result on exposure to sunlight.
iii. There was no association between activity undertaken by respondents and covering their skin while their outings in summer. This means that whatever may be the activity undertaken by the respondents they were not always keen in covering their exposed skin.
iv. It was observed that there was no association between the covering of skin on exposure to FT - 15
v. sunlight and the occurrence of skin ailments among Chennai people. This means that whether the people of
vi. Chennai are covering their head, face and hands or not they are likely to get the mentioned skin ailments.
vii. It was found that the preference of various fabric types among professionals is cotton fabric that is of medium weight, students prefer light weight cotton fabric, while people belonging to the others category prefer mostly light weight & medium weight fabric but some of them belonging to others category also prefer light weight khadi fabric.
viii. It was observed that professionals & students preferred pastel colour fabrics, while people of others category did not have any colour preferences.
ix. It was observed that all the respondents were aware of sun protection concept.
x. None of the respondents were aware of commercial UV sprays.
xi. It was also observed that less than 50% of the respondents were aware of Natural dyes used for UV protection.
xii. It was found that the people of Chennai were not aware of the availability of any natural product for sun Protection through garments.
xiii. It was also found that people of Chennai preferred to wear natural dyed fabrics that provide for UV protection

6. CONCLUSION

From the above study, it was concluded that the people of Chennai were active shoppers during the daytime and they preferred to wear light weight and medium weight cotton fabrics that are of pastel colours. More than half of the respondents were aware of the skin ailments and sun protection concepts. It was also found that Chennai people were always not keen in covering their skin and that they were also more likely to get skin ailments on exposure to sunlight. None of the respondents were aware of neither commercial UV sprays/natural dyes nor any such products as natural UV protectors. Most of the respondents opined that if any such natural UV protective clothing were available, then they would prefer to wear such fabrics. Hence more awareness should be created among the people of Chennai for their skin protection against UV rays through sun protection clothing.

REFERENCES

[1] G. Reinert, F. Fuso, R. Hilfiker and E.Schmidt, "UV-Properties of Textile Fabrics and Their Improvement", ext.Chem.Color.,Vol.29, No.12, , 1997, pp.36-43.

[2] F. Palacin, "Textile Finishes Protects Against Ultraviolet Radiation", Melliand Int., Vol.3, 1997, pp.169.

[3] Biswas Ranjan Das, "UV Radiation Protective Clothing", The Open Tex.Journal, No.3, 2010, pp.14-21.

[4] Fabrics are Treated with UV Absorbing Chemicals. http://www.fabriclink.com/dictionaries/textile.

[5] C. N. Sivaramakrishnan, "UPF Testing Protocol", from www.fibretofashion.com

[6] W.B. Achwal, "Sun Protection Properties of Textile Substrate", Colorage, Vol.44, No.2, 1997, pp.31-32.

[7] M. Djam, C. Rosinskaja, Z. Kizil and A. Weinberg, "Assessment Method for UV Protective Proceedings of the IETSD2012: 3-5 September 2012 FT-16 Properties of Textiles", Melliand Int., Vol.7, No.6, 2001, pp.144-146.

[8] M. Fossel, U. Gassan, B. Koksel, M. Schuicrer, and B. Terrier, "Practical Experience Wih Solartex Products In Finishing of Sun Protection Fabrics", Melliand

[9] Texilber., Vol.78, No.3, 1997, pp.168-169.

[10] "Ultraviolet Absorbers for Sun Protective Cotton", Available at www.inteletex.com.

[11] R. Hunt, "Oppurtunities in UV Protection", Knit. Intl., No.2, 2003, pp.51&53.

[12] M. Srinivasan and B.M. Gatewood, "Relationship Of Dye Characteristics To Uv Protection Provided By Cotton Fabric", Text.Chem. Color. Am. Dyest. Rep.,Vol.32, No.4, 2000, pp.36-43.

[13] S. K. Mallik and T. Arora, "UV Radiation Problems And Remedies", Manmade Text. India, Vol.46, No.5, 2003, pp.164-169.

A Coverage Inference Protocol for Wireless Sensor Networks

Yuguang Fang[1] and P. Dineshkumar[2]
[1]Tsinghua University, China
[2]Department of Computer Science and Engineering, Karpagam University, Coimbatore - 641 021, Tamil Nadu

Abstract

After a wireless sensor network (WSN) is deployed, sensor nodes are usually left unattended for a long period of time.There is an inevitable devolution of the connected coverage of the WSN due to battery exhaustion of sensor nodes, intended physical destruction attacks on sensor nodes, unpredictable node movement by physical means like wind, and so on. It is, therefore, critical that the base station (BS) learns in real time how well the WSN performs the given sensing task (i.e., what is the current connected coverage) under a dynamically changing network topology. In this paper, we propose a coverage inference protocol (CIP), which can provide the BS an accurate and in-time measurement of the current connected coverage in an energy-efficient way. Especially, we show that the scheme called BOND, which our CIP requires to be implemented on each sensor node, enables each node to locally self-detect whether it is a boundary node with the minimal communication and computational overhead. The BOND can also be exploited to seamlessly integrate multiple functionalities with low overhead. Moreover, we devise extensions to CIP that can tolerate location errors and actively predict the change of the connected coverage based on residual energy of sensor nodes.

Keywords: *Connected coverage, Self-monitoring, Wireless sensor network.*

1. INTRODUCTION

A wireless sensor network (WSN) is a large collection of densely deployed, spatially distributed, autonomous devices (or nodes) that communicate via wireless and cooperatively monitor physical or environmental conditions [1], [18]. In such networks, sensor nodes are deployed over a geographic area (called the region of interest or ROI) by aerial scattering or other means. Each sensor node can only detect events within some very limited distance from itself, called the sensing range. In addition, sensor nodes normally have fairly limited transmission and reception capabilities so that sensing data have to be relayed via a multihop path to a distant base station (BS), which is a data collection center with sufficiently powerful processing capabilities and resources. After being deployed, sensor nodes are usually left unattended for a very long period of time so that they may fail over time due to various reasons such as battery exhaustion and physical destructions by attackers. They may also be moved away from where they were deployed by animals, winds, or other environmental means. As a consequence of node failures, node movements, and other unpredictable factors, the network topology may change with time. It is, therefore, critical that the BS learns in real time how well the WSN performs the given sensing task under dynamically changing Network topology. From the BS's (or user's) point of view, a position in the ROI is really under the surveillance of the WSN if and only if this position is within the sensing range of at least one sensor node connected to the BS.

Although much research [2], [9], [10], [12], [16], [20], [21] has been conducted to ensure high network coverage and connectivity for the WSN, none of them addresses how to help the BS infer the coverage boundary when coverage holes emerge. Possible causes leading to coverage holes include energy depletion of sensor nodes, intended attacks on sensor nodes, and so on. In many WSN applications, especially security-sensitive applications, it is a must to accurately detect the coverage boundary. The protocol developed in this paper can affirmatively answer this open challenging issue. On the other hand, problems related to the self-monitoring of a WSN have been studied in the literature for various applications and purposes.

Comparison, in reactive WSNs, packets are sent only when some event of interest occurs and is sensed. Although for proactive WSNs, each node can simply help the BS infer the connected coverage by piggybacking its status information on data traffic, it is well known that proactive WSNs are energy inefficient and not scalable [8], [18]. Therefore, in this paper, we focus on providing coverage inference for the BS in reactive WSNs.

2 PRELIMINARIES

2.1 Network Model

Throughout this paper, we assume that any two sensor nodes can directly communicate via bidirectional wireless links if their euclidean distance is not greater than rc, the communication range; and a position in the plane can be perfectly monitored (or covered) by a sensor node if their euclidean distance is not greater than rs, the sensing range. Similar to [2], [21], [37], we also assume that sensor nodes are homogeneous in the sense that rc and rs are the same for all nodes, and keep constant during each node's lifetime.

For simplicity, we assume that the ROI is a 2D square planar field hereafter. Our results, however, can be easily extended to2D or3DROIs of arbitrary shapes..We examine a large-scale WSN consisting of hundreds or even thousands of stationary sensor nodes,2 and denote the sensor nodes deployed in the ROI to be V ¼ fs1; . . . ; si; . . . ; sng where si represents the position of node I and n is the total number of sensor nodes (or network size).

2.2 Design Goals

In this paper, we intend to design a coverage inference protocol that can provide the BS an accurate and timely measurement of the current connected coverage in an energy-efficient way. Specifically, our design goals include:

2.2.1 Effectiveness and Robustness

The BS should be able to have a timely and accurate view of the connected coverage,regardless of arbitrary network topologies, location errors of sensor nodes, and error-prone wireless channels such that it can instruct necessary and quick actions, e.g., adding new sensor nodes to enlarge the connected coverage.

1. The formal definition of "boundary nodes" and "local algorithms" will be given in Sections 3.1 and 3.6, respectively.

2. Stationary nodes here do not imply that the topology of the WSN is static. Instead, the WSN may have highly dynamic topology changes due to node failures, new node additions, or nodes switching their states between active and sleeping modes to save energy. One advantage of our schemes lies in the efficiency to handle topology changes in WSNs (cf., Section 3.5).

2.2.2 Truly Localized and Distributed Properties

As compared to previous approaches, the coverage inference protocol is intended to be a truly localized and distributed solution in which each sensor node can self-determine whether it is on the area coverage boundary by a few simple computations on information only from one-hop neighbours.

2.2.3 Universal Applicability

Although WSNs are often said to be highly application dependent [1], [18], the coverage inference protocol is designed to work with arbitrary applications and network topologies and to be independent of all the other components of the network protocol stack.

2.2.4 Versatility

For resource-constrained sensor networks, it is highly desirable that some basic protocol operations for implementing one functionality can be reused in providing other necessary functionalities. Otherwise, the protocol stack of sensor nodes will be too complicated to have high operational efficiency [18]. The design of coverage inference protocol will take this requirement into consideration so that many of its basic operations can be highly reused in realizing important functionalities other than network health diagnosis, as we will show soon.

3. BOUNDARY NODE DETECTION SCHEME

This section presents BOND that enables each node to locally self-detect whether it is a boundary node. We begin with several important definitions, followed by the illustration of BOND.

3.1 Boundary Node and its Detection Algorithm

We say that nodes si and sj (I '" j and si; sj • V) are neighbors or there exists a direct wireless link between them if the euclidean distance between them is no larger than rc. We also denote by Neig(si) the neighbours of node si (not including si). In addition, two nodes si and sj are said to be connected if there is at least one path consisting of direct wireless links between them, similarly a set of nodes is called connected if at least one path exists between each pair of nodes in the set. The fundamental connected unit of WSNs is called a cluster:

Definition 1 (cluster): A connected set of nodes is said to be a cluster if the inclusion of any other node not in this set will break the connectedness property.

We write Clust(si) for the cluster containing node si.Based on the sensing model, the sensing disk (or coverage) of node si can be given by

$$Diski=Disk(si,rs)=\{u \bullet IR^2 \ ||u-si||d" rs\} \quad (1)$$

Specifically, let 0 indicate the origin, we have Disk 0 ¼

Disk(0,rs). Then the coverage corresponding to a cluster can be defined as follows:

Definition 2 (coverage of a cluster): Given Clust(si), we refer to the set of all points in the monitored field that are within radius rs from any node of Clust(si) as the set covered by cluster Clust(si). Denoting this set by Cover(si), we have obviously cover(si).

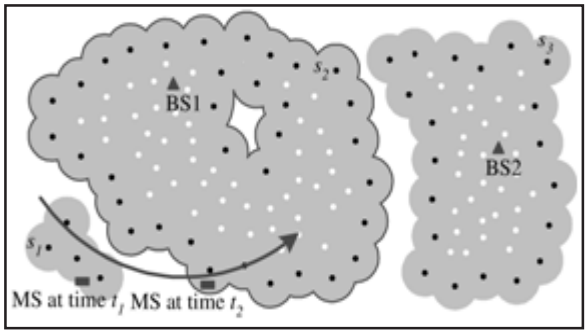

Fig. 1 An exemplary WSNs. There are three sensor clusters: Clust(s1),Clust(s2), and Clust(s3), two static BSs: BS1 and BS2, and one mobile BS: MS. Shaded area, solid dots, and open dots represent the coverage of sensors, boundary nodes, and interior nodes, respectively

3.2 Localized Voronoi Polygons

Our BOND scheme is based on two novel geometric concepts called Localized Voronoi Polygon (LVP) and Tentative LVP (TLVP), which are nontrivial generalization of Voronoi Polygons (VPs) [25] from computational geometry.We must point out that a similar concept called Localized Voronoi Diagrams (LVDs) is introduced as the dual of Localized Delaunay Triangulations (LDTs) in the literature [17], [23]. Moreover, unlike our work, there is no description on how to efficiently construct LVDs given in [17], [23]. Furthermore, the idea of using TLVP to reduce the overhead of the detection algorithm in this paper is completely new. Finally, and most important, our scheme BOND only uses the local information to detect boundary instead of global information commonly used in either VP or DT.

We first define VPs, LVPs, and TLVPs in terms of half planes. For two distinct points si; sj • V , the dominance region of si over sj is defined as the set of points, which is at least as close to si as to sj, i.e.,

Dom(si,sj)={v•IR² ||v-si||d"||v-sj||} (6)

Obviously, Dom(si,sj) is a half plane bounded by the perpendicular bisector of si and sj, which separates all points in the plane closer to si than those closer to sj. Definition 4 (VP, LVP, and TLVP). The VP associated

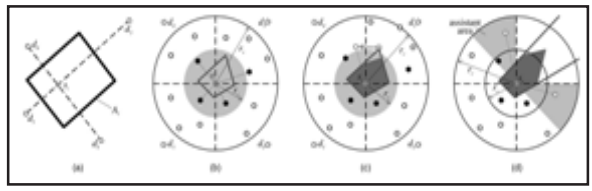

Fig. 2 Illustration of the LVP-based boundary node detection algorithm

3.3 LVP-Based Boundary Node Detection

In this section, we present our BOND scheme for each node to detect whether it is a boundary node based on its own LVP or TLVP by taking node si as an example.

3.3.1 Input

Our BOND is a distributed scheme in that we only need positions of node si's neighbors as the input of our algorithm.We temporally assume that there is no location error and will relax this assumption in Section 6.1. We need to consider twocases based on whether the information about the border of Al, i.e., @Al, is available. In the first case when @Al is unavailable at node si, our detection scheme is based on the construction of LV or(si) (or TLV or(si)); in the second case such that perpendicular bisectors between si and the dummy nodes generate the four border edges of ROI. Then we can calculate LV \ Al by following the same procedure for calculating LV or(si). Therefore, we will only discuss the first case in what follows.

3.3.2 Algorithm

Our goal is to construct the LV or(si) (or TLV or(si), which is sufficient for the boundary node detection with the minimal requirement on the information about si's neighbors. We first divide Disk(si,rc) into four4 quadrants. Then we construct the TLVP of si by using the nearest neighbours (solid nodes in Fig. 2b) in each of the four quadrants. Without lose of generality, we denote these four nearest neighbors as s1, s2, s3, and s4. The first TLVP is calculated by

$$TLV\ or\ (si) \leftarrow \cap 4Dom(si,sj) \quad (3)$$

The new vertices of the new TLVP will be checked to see whether they are covered by Disk(si,rs). This procedure continues until all the vertices of the TLVP are covered by Disk(si,rs) or the LVP of si is calculated and saved.

Note that when §Al is unavailable, LV or(si) may be infinite, which means that it is possible that we cannot find any nodes in one or more quadrants in the first step. See Fig. 2d for an example. If a quadrant contains no neighbors, we define two sectors of angle 45 degree, which are directly adjacent to the quadrant as the assistant area,and add the nodes in this area to SubNeig(si) first. If all the nodes in the assistant area cannot make TLVP finite, we can conclude that LVP must be infinite without need to do further calculation.

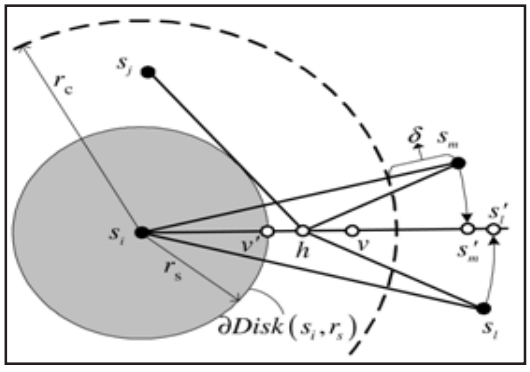

Fig. 3 Illustration of the proof of Theorem 1

3.4 Algorithm Validation

In the VD, the VPs of different nodes are mutually exclusive, but in the LVD, the LVPs of different nodes may overlap This difference makes the validation of our algorithm totally different from that of existing VP-based ones.

Theorem 1. If there is a point v • LV or(si) which is not covered by si, i.e., v 62 Disk(si,rs), there must exist a point h 2 LV or(si) that is not covered by any node, and si must be an area coverage boundary node.

Theorem 2. If there is a point v 2 Al not covered by any sensor node, for every cluster Clust(si), there must exist at least one sensor sj 2 Clust(si) whose LV or(sj) is not completely covered by Disk(sj, rs).

Theorem 3. LV or(si) is fully covered by si if and only if LV or(si) is finite and all the vertices are covered by si.

3.5 Discussions on BOND

Low overhead. It has been shown in [25] that in general, VPs cannot be computed locally. Therefore, the traditional VPbased schemes [9], [11], [36] are not distributed and are very expensive in terms of communication overhead. Our BOND scheme is a truly localized polygon-based solution because computing LV or(si) (or TLV or(si) only needs one-hop information (this can be directly obtained from (8) and (9)) Assuming that the number of neighbors is k, each node can compute its own LV or(si) with complexity smaller than . In addition, the computation of the LV or(si) only involves some simple operations on polygons, which can be efficiently implemented (e.g., PolyBoolean library [22]). Wefurther simplify the detection process by constructing TLVPs first. For a densely deployed WSN, we have LV or(si) or TLV or(si) ! V or(si), and it is well known in computational geometry that under the homogeneous spatial Poisson point process, the average number of vertices of V or(si) is 6 [25].Therefore, when the node density is high, BOND.This unique property will greatly simplify the update of detection results and save precious energy of each sensor node.

3.5.1 Other Applications

We are aware of the following applications of BOND or its basic operations, which are by no means a complete list:

i. Topology control and routing. It has been shown in [17], [23] that the dual of LVP, called LDT, can be used to design distributed topology control and routing protocols for wireless ad hoc networks with energy efficiency and the guarantee of the delivery.From the property of duality, we can directly obtain LVPs if LDTs are determined, or vise versa.
ii. Spatial aggregation. In distributed data processing for WSNs, to reduce the sampling errors in the aggregated spatial data, it is proposed in [31] to first calculate the VP of each sensor. As mentioned before, since the VP cannot be computed locally,the LVP can be used as a good approximation of the VP in spatial aggregation.
iii. Coverage-preserving node sleeping scheduling. Since sensor nodes are usually deployed with redundancy,it is possible to prolong the network lifetime while preserving the connected coverage by scheduling some nodes into the sleeping state [34]. Each node can locally decide whether its own LVP is covered by its neighbors.

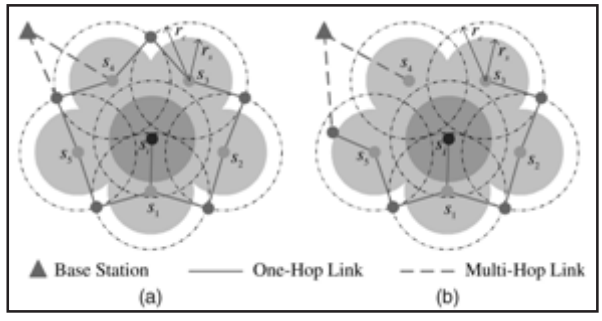

Fig. 4 Nonlocality of the boundary node detection when rc < 2rs

3.6 Locality of Boundary Node Detection

In this section, we investigate further to show that it is impossible to find local algorithms for boundary node detection with arbitrary node distributions when rc=rs < 2.We first define what we mean by local algorithms. This definition is based on a model proposed in [27].

Definition 5 (Local Algorithm). Assume that each computation step takes one unit of time and so does every message to get from one node to its directly connected neighbors. With this model, an algorithm is called local if its computation time is Oð1Þ, in terms of the number of nodes n in the system.

4. COVERAGE INFERENCE PROTOCOL

In this section, we describe how to use BOND to build a practical CIP.

Our design philosophy is that, since the minimum information required to describe the coverage is the positions of boundary nodes (cf., Section 3.1), we just need to detect boundary nodes. In other words, our scheme can ensure that,for the BS to reconstruct the "coverage image" without any distortion, the information transmitted from sensors to the BS is minimized. Also note that our BOND only involves local message exchanges. In a large-scale WSN, the overhead from local broadcast is very small as compared to that from the end-to-end communications from sensor nodes to the BS. Therefore, our approach can save the precious energy of sensor nodes. Fig. 5 illustrates the basic operations of our BOND-based CIP, which consist of the below three steps.

4.1 Neighborhood Monitoring and Self-Detection

After the deployment of the WSN, we assume that localization techniques are available for sensor nodes to decide their positions [18]. Each node then collects the position information of its neighbors by broadcasting its own positions, and executes BOND to detect whether it is a boundary node. If so, it will report its position to the BS. We refer to the neighbors used to construct the LVP or TLVP in the last run of BOND as its consulting neighbors.

In our protocol, both interior and boundary nodes are required to broadcast an Existence Updating Packet (EUP) to their neighbors for a random period of time exponentially distributed with rate TEUP . In addition, each interior node,say, si, maintains a timer C0(si) of expiry value much larger than TEUP for each of its nonconsulting neighbors, say, sj. If si does not overhear any packet (either an EUP or data packet) from sj before C0expires, it will treat sj as a dead neighbor, which can become alive if si overhears any packet from it later. Node si also maintains two timers for each of its consulting neighbors, say, sk: the neighbor monitoring timer C1ðkÞ and the neighbor query timer . If si does not overhear any packet from sk before C1ðkÞ expires, it unicasts a Neighbor Query Packet (NQP) to sk and starts C2. If still alive, sk is required to send back an EUP immediately and wait for an ACK from si. If node si still does not overhear any packet from sk before C2 expires, si will treat sk as a dead neighbor and reexecute BOND with alive neighbors as input. In general, the expiry values of C0 and C1 should be in the same order of TEUP, in order to guarantee that with high probability, each node will receive EUPs from all alive nodes in its neighborhood.The expiry values of C2 should be much smaller than TEUP because we require that the node which receives the NQP needs to send back an EUP immediately.Unlike previous neighbor monitoring schemes employing a single timer [30] or treating neighbors as the same [15], our scheme sets different timers for nonconsulting and consulting neighbors. The major reason for doing so is that data packets and EUP-like broadcast packets are subject to loss due to wireless transmission errors or collisions. As a result, a node may falsely identify an alive neighbor as a dead one. Obviously, for nonconsulting neighbors, we can decrease the false positive rate by setting a larger timer value. However, using a larger timer value for consulting neighbors will increase the response delay, i.e., the delay from when coverage holes emerge to when they are detected by boundary nodes.Therefore,we use two timers for consulting neighbors to ensure both a shorter response delay and a lower false positive rate: although the expiry value of C1ðkÞ is small, we actively query the questionable neighbor before we treat it as the dead neighbor, which may significantly increase the accuracy of our scheme. As mentioned before, if the node distribution follows SPPP, each node only has 4-6 consulting neighbors, on average, which means the high feasibility of our two-timer scheme.

4.2 Self-Reporting of Boundary Nodes

Whenever identifying itself as a boundary node, a sensor node should send its position information to the BS, which can reconstruct the "image of the coverage" based on all the received position information of boundary nodes.

4.3 Explicit ACKs from the BS

Since the packet loss ratio due to collisions or noise is pretty high in the WSN [18], boundary nodes need

some mechanisms to ensure that their reports have been received by the BS. Otherwise, they have to repeatedly resend their reports, which causes energy waste. The issue of reliable sensor-to-BS communication, thus far, has not been addressed thoroughly in WSN research community. The work on reliable communication in WSNs first appears in [35],and then in [32]. However, no guaranteed reliability semantics are provided in these works. In [29], the authors first propose the notion called "event-to-sink" reliability, and study the reliable communication from this perspective.

Their solution is mainly based on adjusting the reporting frequency of source nodes, and is applicable for monitoring a continuously changing event or reporting a huge amount of data. For our case, each sensor node will be on the boundary or not for a relatively long period, and each boundary node only needs to report its location information to the BS. Therefore, the scheme proposed in [29] cannot be applied here. In [26], the authors study the "BS-to-sinks reliability," and argue that the requirement and implementation of reliability in a WSN is firmly dependent upon the specific application, and there is no one-for-all solution.

5. COMPARISON AND SIMULATION

To the best of our knowledge, there is no other coverage inference protocol developed for WSNs, which is as complete as our CIP. We, however, note that many interesting ideas proposed by researchers for WSN coverage and self-monitoring may be adapted to infer WSN coverage. In this section, we exploit these possible alternatives and compare them with our CIP via both theoretical analysis and simulations.

The most important metric used in the comparison is the energy consumption incurred by different coverage inference protocols. In addition, we assume that packet transmissions are subject to noise or collision. Under this assumption, we further define two other performance metrics. The first one is the false alarm probability, defined as the probability that a nonboundary sensor node is falsely diagnosed as a boundary node. This may happen if consecutive EUPs from a sensor node get lost due to collision and/or noise.

The other metric is the response delay, defined as the time from when a sensor node becomes a boundary node to when this event is locally detected. Apparently, the later two metrics are conflicting in essence for a time-out-based coverage inference protocol like our CIP. In particular, to achieve a smaller false alarm probability (i.e., more accurate boundary detection) desires a larger time-out value, which,in turn, would result in a longer response delay, and vice versa. Therefore, we would compare the false alarm probabilities of different coverage inference protocols for a given response delay, or equivalently compare their response delays for a given false alarm probability.The evaluation philosophy and simulation settings are given in the Appendix. To facilitate the presentation, we also classify the possible coverage inference protocols into two categories,namely boundary-node-based approaches and aggregation-based approaches, based on how the coverage information is gathered and reported to the BS.

5.1 Boundary-Node-Based Approaches

Approaches in this category are to find boundary nodes first and then transmit such information to the BS in a way similar to what was described in Section 4. In what follows,we further classify these approaches according to the boundary node identification methods they adopted.

5.1.1 Polygon-Based Schemes

In [9], [11], [36], Voronoi diagram (VD) is used for boundary node detection. Briefly speaking, the VD of a node set V is the partition of the euclidean space into polygons, called VPs and denoted by V or(si) for si 2 V such that all the points in V or(si) are closer to si than to any other node in V According to the closeness property of VPs, if some portion of a VP is not covered by nodes inside the VP, it will not be covered by any other node, which implies a coverage hole.Therefore, it is claimed in [9], [11], [36] that each node can locally check whether it is on the coverage boundary under the assumption that VPs can be derived locally. However, it has been shown that, in general, VPs cannot be locally computed [40]. Intuitively, our LVP-based BOND will have smaller communication overhead, or equivalently, smaller energy consumption than the VP-based schemes since LVPs can be locally computed. In what follows, we prove this intuition in a formal way.

Theorem 4. If there exist boundary nodes, the costs of the NEPbased and LVP-based algorithms are always smaller than the cost of the VP-based ones.

5.1.2 Perimeter-Based Schemes

The first realistic localized boundary node detection algorithm is proposed in [16], which is based on the information about the coverage of the perimeter of each node's sensing disk. It can be shown that node si is a boundary node if and only if there exists at least one point v •Disk(si,rs) which is not covered by any sj •

Neig(si) (cf., Fig. 7a). Based on this criterion, an algorithm with the complexity is designed in [16] to locally check whether one node is a boundary node, where k is the number of neighbors.

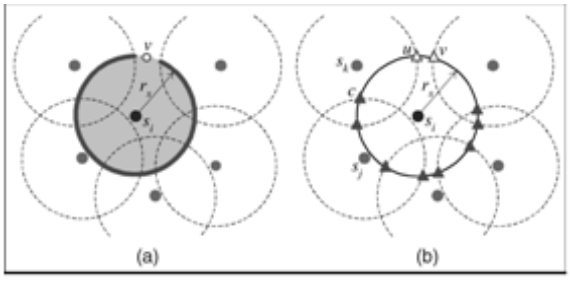

Fig. 7. Perimeter-based boundary node detection approaches.(a) Perimeter coverage checking approach proposed in [16]. The solid curve represents the portion of perimeter of sensing disk covered by neighbor nodes. (b) Crossing coverage checking approach proposed in [13], [42]. Solid and open triangles represent covered and uncovered crossings, respectively.

Our BOND and CROSS can both provide truly localized boundary node detection with operational difference in the neighborhood monitoring phase. In particular, ROSS requires each node to check the positions and statu s of all it neighbors, which is quite inefficient when sensor nodes are densely deployed. This situation becomes worse every time when a node dies, as all its neighbors need recheck the coverage of their perimeters or crossings. In contrast, our BOND-based CIP only has consulting neighbors perform boundary node detection.

5.2 Aggregation-Based Approaches

Aggregation-based approaches are quite different from our BOND in that each node actively communicates with the BS no matter whether it is a boundary node or not. Therefore,we need to compare those schemes to our BOND-based CIP as a whole in this section. In what follows, we classify these approaches into naive ones and spatial ones.

5.2.1 Naive Schemes

The most straightforward scheme requires that each node periodically sends EUPs ("keep-alive" messages) to inform the BS about its existence so that the BS can always learn the connected coverage of the WSN. If the BS does not receive the update information from a particular node in a predetermined time interval, it can infer that this node is dead. This scheme is unlikely to be the optimal one because the death of some nodes does not necessarily imply the change of connected coverage especially when the WSN is densely deployed. In addition, there might be redundant information transmitted to the BS,which means that this scheme is also not energy efficient.

5.2.2 Spatial Aggregation-Based Schemes (SAB)

Since the coverage information is highly spatially correlated,a natural way to improve the energy efficiency of the above naive scheme or its alternative is to perform spatial aggregation at intermediate nodes to reduce redundant transmissions.

Almost all techniques for spatial aggregation require the construction of a routing tree for propagating data from source nodes to the BS [19]. Once the routing tree is established, each node utilizes the routing tree to find a path to the BS.

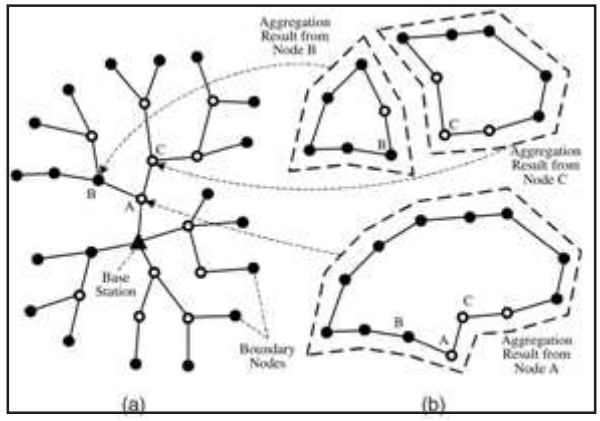

Fig. 11. Illustration of SAB. (a) The routing tree for the spatial aggregation is constructed with the root as the BS. (b) Node A aggregates coverage information by combining polygons from its children B and C. Note that only the solid dots are real boundary

6. EXTENSIONS TO CIP

In this section, we extend our BOND-based CIP by considering location errors and energy depletion, which shows the flexibility of BOND and its ability to deal with some practical considerations.

6.1 Location-Error-Tolerant CIP

So far we have assumed that each node knows its accurate location. Our CIP can also be extended to tolerate bounded location errors. In this section, we assume that the location error (defined as the distance between the actual location of a node and its estimated location) is upper bounded by .We then have the following theorem:

Theorem 5. If the location error is upper bounded by §, and a given node, e.g., si, is an interior node when all

nodes are at their estimated locations and each node uses a sensing range rs -§ node si must be an interior node when all nodes are at their actual locations and each node uses the actual sensing range rs.

6.2 Prediction-Based CIP

Since node death caused by energy depletion is predictable,it is possible to design prediction-based CIP by exploiting the residual energy information of sensor nodes. The challenge here is that the death of some nodes does not necessarily indicate the change of coverage especially when the WSN is densely deployed. Therefore, in order to minimize the information relayed to the BS, we need to detect the nodes whose death caused by energy depletion will affect the coverage.

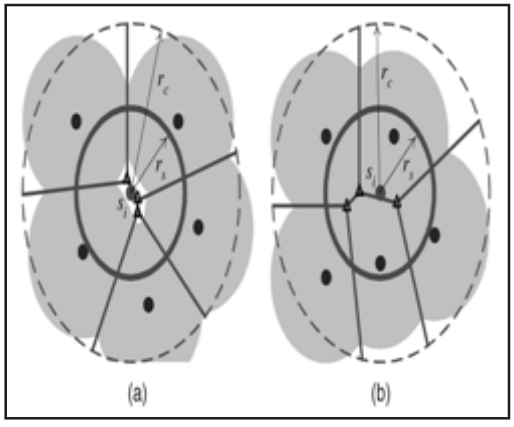

Fig. 13 Voronoi-diagram-based coverage hole prediction

Coverage hole (see Fig. 13a, for example), and node si will report the event that its residual energy is smaller than the threshold to the BS. Otherwise, node si can conclude that its death will not effect the coverage (see Fig. 13b, for example), and thus, does not need to report itself to the BS. Based on the collected residue energy information, the BS can predict where the coverage hole will emerge with high probability.Note that, when the number of healthy neighbors of node si is k, there are elegant algorithms in computational geometry [25] to calculate the Voronoi diagram of HNeig(si) with complexity O(klogk), and there are at most O(k) vertices need to be checked. The polygon operations in BOND can also be reused here. Since only local broadcasts are involved in our scheme, the computational and communication overhead introduced is rather small.

7. CONCLUSION

In this paper, we propose a CIP that allows the BS to get an accurate and in-time measurement of the current connected coverage of the WSN. The CIP is built upon a novel lightweight distributed BOND scheme. Detailed theoretical analysis and simulation studies show that both BOND and CIP are highly effective and efficient. As the future research, we plan to evaluate the performance of BOND and CIP in real sensor platforms. We also intend to further investigate other potential applications of BOND in WSNs such as load balancing, topology control, distributed storage, and network health monitoring.

APPENDIX
NETWORK TOPOLOGIES USED IN PERFORMANCE EVALUATIONS

Consider the situation where sensor nodes are independently and randomly placed in the ROI. Such a random initial deployment is required when individual sensor placement is infeasible and is desirable when a priori knowledge of the ROI and the monitored target is limited or not available. In this case, it is widely accepted in the literature [12] that the locations of sensors can be modelled by a 2D homogeneous SPPP with density ë.

REFERENCES

[1] I. Akyildiz, W. Su, Y. Sankarasubramaniam and E. Cayirci, “Wireless Sensor Networks: A Survey”, Computer Networks, Vol. 38, No.4, Mar. 2002, pp.393-422.

[2] X. Bai, S. Kumar, D. Xuan, Z. Yun and T. Lai, “Deploying Wireless Sensors to Achieve Both Coverage and Connectivity”,

Proc. ACM MobiHoc, May 2006.

[3] X. Bai, C. Zhang, D. Xuan, J. Teng and W. Jia, “Full-Coverage and K-Connectivity (k=14,6) Three Dimensional Networks” , Proc. IEEE INFOCOM, Apr. 2009.

[4] X. Bai, C. Zhang, D. Xuan, J. Teng, and W. Jia, “Low-Connectivity and Full-Coverage Three Dimensional Networks”, Proc. ACM MobiHoc, May 2009.

[5] Y. Bejerano, “Simple and Efficient K-Coverage Verification without Location Information”, Proc. IEEE INFOCOM, Apr. 2008.

[6] B. Bloom, “Spaxe/Time Trade-Offs in Hash Coding with Allowable Errors”, Comm. ACM, Vol.13, No.7, June 1970, pp.422-426.

[7] A. Broder and M. Mitzenmacher, "Network Applications of Bloom Filters: A Survey", Internet Math., Vol.1, No.4, 2005, pp. 485-509.

[8] M. Cagalj, S. Capkun, and J. Hubaux, "Wormhole-Based Anti- Jamming Techniques in Sensor Networks", IEEE Trans. Mobile Computing, Vol.6, No.1, 2006, pp.100-114.

[9] Q. Fang, J. Gao and L. Guibas, "Locating and Bypassing Routing Holes in Sensor Networks", Proc. IEEE INFOCOM, Mar. 2004.

[10] M. Franceschetti, L. Booth, M. Cook, R. Meester and J. Bruck, "Percolation of Multi-Hop Wireless Networks", Technical Report UCB/ERL M03/18, Electrical Engineering and Computer Science Dept., Univ. of California, Berkeley, 2003.

[11] A. Ghosh, "Estimating Coverage Holes and Enhancing Coverage in Mixed Sensor Networks", Proc. Ann. IEEE Int'l Conf. Local Computer Networks (LCN '04), Nov. 2004.

[12] P. Gupta and P.R. Kumar, "Critical Power for Asymptotic Connectivity in Wireless Networks", Stochastic Analysis, Control,Optimization and Applications: A Volume in Honor of W.H. Fleming,Birkhauser, 1998.

[13] P. Hall, "Introduction to the Theory of Coverage Processes", John Wiley Sons, Inc., 1988.

[14] J.M. Hellerstein, W. Hong, S. Madden and K. Stanek, "Beyond Average: Towards Sophisticated Sensing with Queries", Proc.Second Int'l Workshop Information Processing in Sensor Networks (IPSN '03), Mar. 2003.

[15] C. Hsin and M. Liu, "Self-Monitoring of Wireless Sensor Networks", J. Computer Comm., Special Issue On Sensor Networks,Vol.29, No.4, Feb. 2006, pp.462-476.

[16] C.F. Huang and Y.C. Tseng, "The Coverage Problem in a Wireless Sensor Network", Proc. Second ACM Int'l Workshop Wireless Sensor Networks and Applications (WSNA '03), Sept. 2003.ZHANG ET AL.: A COVERAGE INFERENCE PROTOCOL FOR WIRELESS SENSOR NETWORKS 863

[17] S. Kapoor and X. Li, "Proximity Structures for Geometric Graphs,"Algorithms and Data Structures, Springer, July 2003.

[18] H. Karl and A. Willig, "Protocols and Architectures for Wireless Sensor Networks", John Wiley Sons, Inc., 2005.

[19] R. Kumar, M. Wolenetz, B. Agarwalla, J. Shin, P. Hutto, A. Paul and U. Ramachandran, "Fuse: A Framework for Distributed Data Fusion", Proc. First ACM Conf. Embedded Networked Sensor Systems (Sensys '03), Nov. 2003.

[20] S. Kumar, T.H. Lai and A. Arora, "Barrier Coverage with Wireless Sensors", Proc. ACM MobiCom, Aug. 2005.

[21] S. Kumar, T.H. Lai and J. Balogh, "On K-Coverage in a Mostly Sleeping Sensor Network", Proc. ACM MobiCom, Oct. 2004.

[22] M. Leonov, "Polyboolean Library (2004)", http://www.complexa5.ru/polyboolean, 2010.

[23] X. Li, G. Calinescu, P. Wan and Y. Wang, "Localized Delaunay Triangulation with Applications in Wireless Ad Hoc Networks", IEEE Trans. Parallel and Distributed Systems, Vol.14, No.10, 2003, pp.1035-1047.

[24] S. McCanne and S. Floyd, "Network Simulator Version 2," http://www.isi.edu/nsnam/ns, 2010.

[25] A. Okabe, "Spatial Tessellations: Concepts and Applications of Voronoi Diagrams", Wiley, 2000.

[26] S.-J. Park, R. Vedantham, R. Sivakumar, and I.F. Akyildiz, "A Scalable Approach for Reliable Downstream Data Delivery in Wireless Sensor Networks", Proc. ACM MobiHoc, May 2004.

[27] D. Peleg, "Distributed Computing: A Locality-Sensitive Approach", Soc.Industrial and Applied Math. (SIAM), 2000.

[28] M. Penrose, "Random Geometric Graphs", Oxford Univ. Press, 2003.

[29] Y. Sankarasubramaniam, O.B. Akan, and I.F. Akyildiz, "ESRT: Event-to-Sink Reliable Transport in Wireless Sensor Networks", Proc. ACM MobiHoc, June 2003.

[30] S. Chessa and P. Santi, "Comparison Based System-Level Fault Diagnosis in Ad-Hoc Networks", Proc. IEEE 20th Symp. ReliableDistributed Systems (SRDS), Oct. 2001.

An Improved Multi-Period Spraying For Intermittently Connected Networks

C. Poongodi[1] and A.M.Natarajan[2]

[1]Department of Information Technology, Kongu Engineering College, Perundurai, Erode - 638 052, Tamil Nadu

[2]Department of Computer Science and Engineering, Bannari Amman Institute of Technology, Sathyamangalam - 638 401, Erode District, Tamil Nadu

E-mail: amnatarajan2006@yahoo.co.in.

Abstract

In challenging network scenarios like battlefield and disaster recovery scenarios, nodes suffer from frequent network partitions and intermittent connectivity. In these scenarios instantaneous end-to-end path between the sender and receiver will not exist due to link breakdown, less battery or mobility of nodes. To address these challenges in these intermittently connected networks multiple replication strategies are already proposed. The objective of the proposed work is to control the replication of messages while maintaining the same throughput and delay.

Keywords: *Challenged networks, Delay tolerant networks, Intermittently connected networks.*

1. INTRODUCTION

Mobile ad-hoc networks (MANETs) may well complement infrastructure-based wireless networks and allow mobile users to obtain access to interact directly with one another even when they are outside the coverage area of cellular networks or wireless LAN. Similarly, MANETs may enable communication between vehicles, sensors, laptops and other mobile equipment without the need to deploy a fixed infrastructure network. Numerous dedicated routing protocols have been proposed to establish and maintain reachability between communicating nodes in such dynamic environments.

Challenged networks arise from MANETs primarily as a result of various forms of host and router mobility but may also come into being as a result of disconnection due to power management or interference. Examples of such networks include terrestrial mobile networks, exotic media networks, military ad-hoc networks and sensor networks. These challenged networks are characterized by high latency, bandwidth limitations, high error probability, node longevity, or path stability that are substantially worse than is typical of today's TCP/IP based networks [1].

Existing TCP/IP network protocols could not be utilized for these challenged networks since they operate on a principle of providing end-to-end inter-process communication through a concatenation of dissimilar link-layer technologies.

A number of key assumptions are made regarding the overall performance of the underlying links in order to achieve smooth operation: an end-to-end path exists between a data source and its peer, the maximum round-trip time between any node pairs in the network is not excessive, and the end-to-end path loss probability is small. Unfortunately, challenged networks which may violate one or more of the assumptions, are becoming important and may not be well served by the current end-to-end TCP/IP model.

There were numbers of routing protocols proposed for ICN and they are divided into replication based and knowledge based [3]. The proposed routing is replication based but controlled to have smaller number of replications per message.

2. RELATED WORK

For challenged Networks as described above, or called as Intermittently Connected Networks (ICN) which utilizes store-and-forward mechanism is proposed.[1,4]. There were number of routing protocols also proposed. They were based on two strategies which are replication and knowledge [2]. An example for extreme replication strategy is epidemic routing [5]. It is very simple because it requires no knowledge about the network. But the disadvantage is that it requires a large amount of buffer space, bandwidth and power to process large number of copies generated. Therefore in order to minimize the resource utilization quota based protocols are proposed. They limit the number of replicas generated inside a network. Example of quota based routing protocols i.e both knowledge and replication based are Encounter based routing protocols [8], they will spread only limited messages into the network based on the previous contact

or encounter value. Other protocols are spray and focus [7], spray and wait [6], where a finite number of copies generated and sprayed in Spray phase and if the destination is not found in spray phase then in the next phase direct routing or encounter based routing will be followed. Another kind of spraying called multi-period spraying [14] will reduce again the fixed number of copies to some extent. In this, it will initially spray smaller number of copies which was very less than that of the existing spraying schemes. If acknowledgement comes from the destination, then it will stop spraying further. This periodical spraying can be done with two or three periods. But the disadvantage of spraying method is that it will find for optimal distribution strategy for fixed number of copies in spray phase. This is the example for tree based flooding.

Knowledge based forwarding strategies will require some knowledge about the network but they consume fewer resources compared to flooding strategies. In location based routing [12], a node requires location co-ordinates of its own, destination co-ordinates and the co-ordinates of the potential next hops. With these, a node can easily compute the distance function and determine where the message should be sent. There are two main problems in this routing. One is that even if the distance between two nodes is small, there is no guarantee that they will be able to communicate due to any obstruction. Another one is that if a node moves its physical co-ordinates change. If network topology changes then the virtual co-ordinates of a node will change.

Other one forwarding strategy is that Gradient Routing [9]. It assigns a weight to each node that chooses the best custodian to deliver a message. Best custodian is the next node that will have the metric such as the time of last contact between the node and the destination, remaining battery energy, or mobility. The disadvantage is that it can initially take a long time for a good custodian to be found because the metric or weight values initially around a custodian are equally less.

Another approach proposed for ICN is message ferrying [4]. Message ferrying approach is for message forwarding between disconnected networks. In this approach there are two nodes which are Message Ferry (MF) and Regular Node (RN). MF will carry message to disconnected partitions. Regular nodes are devices without need to carry messages but have some assigned task. This MF approach could be utilized for remote village communications, remote area connectivity projects and inter-network connectivity communications where regular connectivity link is weak [11, 20]. Message ferrying scheme in ICN is also studied with the use of multiple ferries [10]. It focused on the ferry route design problem and developed four algorithms to generate ferry routes that meet the traffic demand and minimize the weighted delay.

These algorithms represent different strategies in designing ferry routes.

The proposed system called as multi-hop periodic spraying is another variation in spraying techniques. Since the disadvantage in spraying is whenever the nodes are having constrained mobility, the spraying will spread the copies within a smaller area. Spray and Focus will overcome this disadvantage since in focus phase it will try to make some more copies with the relay nodes which are already met by the destination. But here again the relay nodes should have been encountered by the destination otherwise the copies will not be spread. Therefore, the proposed system is devised to make smaller number of copies like spraying methods. Even the nodes have constrained mobility, it will try to spread the copies to some nodes among the group which have more mobility than other nodes. This makes the copies to be spread fast to the destination and makes the delay to reduce and delivery ratio to be improved.

3. MULTI-HOP MULTIPERIOD SPRAYING

The proposed work explores the problem of efficient routing in intermittently connected mobile networks and describes about Multi-hop periodic Spraying. Our problem setup consists of nodes which are moving inside a bounded area according to a stochastic mobility model. Additionally, we assume that the network is partially disconnected at most times, and that transmissions are faster than node movement. Single-copy routing algorithms proposed in [13] showed that using only one copy per message is often not enough to deliver a message with high reliability and relatively small delay. On the other hand, routing too many copies in parallel, as in the case of epidemic routing or gossiping, can often have disastrous effects on performance. In addition to the very high number of transmissions, flooding-based schemes begin to suffer severely from contention as traffic increases, and their delay increases rapidly. Based on these observations, we have identified the following desirable design goals for a routing protocol in intermittently connected mobile networks:

i. Perform significantly smaller amount of transmissions than multi-copy based routing schemes, under different conditions of ICMN.
ii. Deliver a message faster than all the existing schemes, and exhibit close to optimal delays.
iii. Deliver the majority of the messages generated; Additionally, we would like this protocol to also be:
iv. Highly scalable, in order to maintain the above performance behavior, although changes in node density.
v. Simple but require as little knowledge about the network nodes as possible, in order to help its implementation.

3.2 Algorithm for Multi-hop Periodic Spraying

3.1.1 Source Node Message Forwarding Function

i. If the next node is the destination then deliver the message to the destination and remove this message from its buffer.
ii. Else if next node is a relay node then start spreading the copies of the same message with a relay having good meeting contact.
    - If acknowledgement is received then delete the message from the buffer
    - Else wait for D***t*** time delay and spray some more copies.
iii. Repeat step 2 until the acknowledgement is received or the message *ttl* expires.

3.1.2 Relay Node Message Forwarding Function

i. If the next node is the destination for the buffered message then
    - Deliver the packet to destination
    - Remove the delivered message from its buffer

ii. Else if it has good meeting update than its own value then
    - Exchange the messages to it with the messages from other nodes.

3.1.3 Destination Node Message Acceptance Function

i. If destination is received its own messages

    - Accept the messages and send it to higher layers
    - Flood the acknowledgement to the destination and other nodes to delete that message from the network

4. EVALUATION & PERFORMANCE ANALYSIS

We use simulations to compare the performance of the routing algorithms in different environments. We evaluated the simulations using a discrete event simulator QualNet using ICMN environments [15]. In our evaluations, it is shown that, unlike existing work, our protocol can improve performance for three metrics: total number of replications, minimize average delay and maximize delivery ratios. In all cases, it is found that our protocol significantly outperforms existing protocols, and also performs close to optimal for any kind of node mobility.

This work considers totally four clusters. Each cluster has twenty five nodes which are randomly distributed over an area of 2500m by 2500m. Hence, each group forms a partially disconnected network. In this simulation, all the nodes communicate with one another via the 802.11 links with 2.5 Mbps link bandwidth. Also each node has a buffer size of 200 messages. The traffic is made among some 20 pairs of node and made the simulation to run for 1000 seconds.

To demonstrate the effectiveness of Multi-hop periodic spraying, we performed simulations on the random way point mobility model. To illustrate how the connectivity is made among clusters, due to random mobility and different speeds of a mobile node the clusters are get connected.

Simulation area is kept constant; here CBR type of message is used with a packet size of 512 KB. We evaluate the proposed system against three protocols those are i) Epidemic routing ii) Spray and Focus routing and iii) Multi-period Spraying. In Figure 1, there is a comparison between the delivery ratios of the protocols. In all cases, the number of messages that may coexist within a node's buffer is kept constant.

While looking at the graph of the delivery ratio in Figure 1, we can see that the delivery ratio is increasing for all the protocols while increasing the number of nodes. Even though the Epidemic replicates multiple copies of same message but due to finite buffer size of the nodes results in poor management of buffers. Therefore, number of message drops will make the delivery delay to be low when comparing to other protocols. Spray and Focus will have somewhat higher delivery ratio than the multi-period spray since in the focus phase it forwards the message to the nodes which are already met by the

destination. The multi-hop periodic spray will have improved delivery ratio when nodes are above 40 since it make use of the nodes which are very faster in meeting with other nodes. This makes the messages to be propagated faster with only limited copies itself.

The Figure 2 gives the variations in delivery delay when we change the number of nodes in the scenario. Delay will be very high for Epidemic routing comparatively than other protocols . This is due to the relay nodes which are not really good relays to the destination. The relay nodes which received the copy of the message, will buffer it for a long time since the buffer of all the relay nodes or almost occupied.

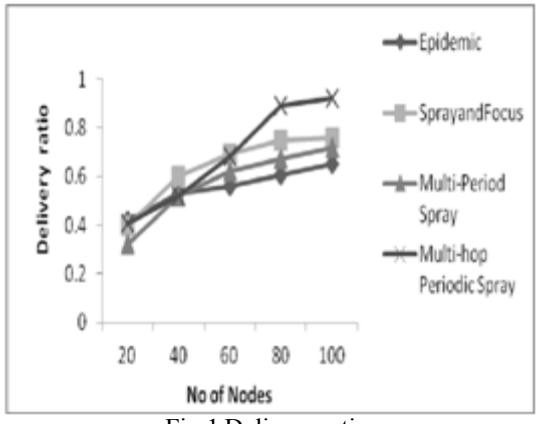

Fig.1 Delivery ratio

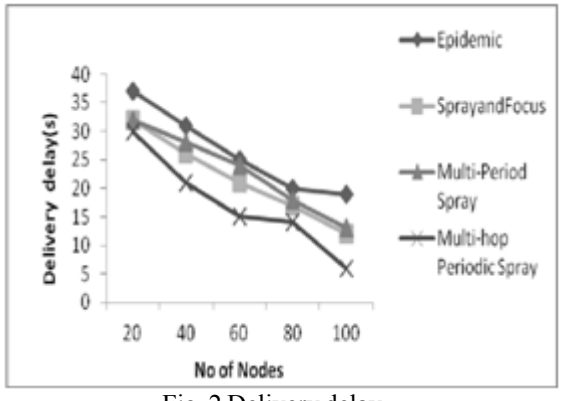

Fig. 2 Delivery delay

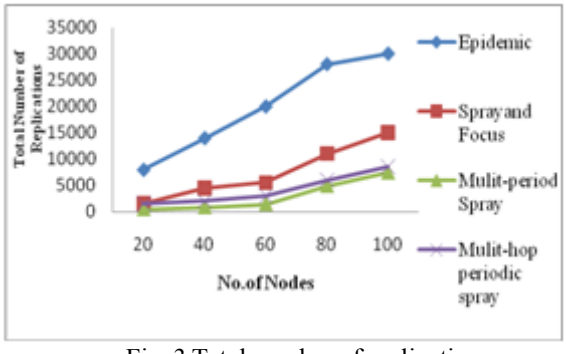

Fig. 3 Total number of replications

The other protocols will have some reduced delay while we increase the number of nodes. Since the number of nodes increases make the nodes to find more number of best relay nodes in case of other spraying methods. The delay in multi-hop periodic spraying is very low since it find more relays with good meeting update. Also the acknowledgement mechanism makes the nodes to delete the messages which are already reached the destination.

Figure 3 gives the total number of duplications of all the data messages. Needless to say duplication is very high for the Epidemic routing rather than for other methods. Since, in Epidemic routing all the node buffers are exhausted soon. But spraying methods will limit the copies to very few and even then it tries to route better to destination. Among all, multi-period spraying will have less number of duplications. Since it sprays in multiple periods, here it is for 3 periods, and also only when the acknowledgement is not received then only the 2 or 3 periods are continued. Mutli-hop period spraying will have somewhat more copies than mutli-period spraying since for a constrained mobility environment multi-period spray may fail. So in that case we need to find more relays to send. Hence, the number of replication is somewhat more in multi-hop periodic spray.

5. CONCLUSION AND FUTURE WORK

In this paper, we develop techniques to allow eventual message delivery in the case where a connected path from source to destination is never available in wireless ad hoc networks. Existing ad hoc routing protocols are unable to deliver packets in the presence of a network partition between source and destination when partition exists for a long time. Therefore multiple replication schemes were introduced. But these multiple replication schemes waste the resources like bandwidth, buffer and battery of the wireless nodes. Since the resource consumption is very essential in wireless nodes, it is a must to go for controlled multiple replication schemes like spraying. Thus, we modified the spraying methods, where message exchanges between two nodes ensure message delivery, reduced delay while at the same time it reduces the resource consumption by limiting the number messages forwarded. The simulation results show that the proposed system outperforms the other controlled replication schemes. As a future work, we are planning to analyze our protocol for energy awareness on relay nodes and then to route. Also the delivery probability of a relay node can be calculated based on region specific or the community based.

REFERRENCES

[1] K. Fall, "A Delay–Tolerant Network Architecture For Challenged Internets," in Proceedings of ACM SIGCOMM, August 2003, pp.27-34.

[2] V. Cerf *et al*., "Delay-Tolerant Network Architecture," IETF RFC 4838, informational, April 2007.

[3] S. Jain, K. Fall and R. Patra, "Routing in a Delay Tolerant Network," in Proceedings of ACM SIGCOMM, ACM Press,Vol. 34, October 2004, pp.145-158.

[4] W. Zhao, M. Ammar and E. Zegura, "A Message Ferrying Approach For Data Delivery in Sparse Mobile Ad Hoc Networks," in Proceedings of ACM MobiHoc, (New York, NY, USA), ACM Press, May 2004, pp. 187-198.

[5] A. Vahdat and D. Becker, "Epidemic Routing For Partiallyconnected Ad Hoc Networks," Tech. Rep. CS-2000-06, Duke University, July 2000.

[6] T. Spyropoulos, K. Psounis and C. S. Raghavendra, "Spray and Wait: An Efficient Routing Scheme For Intermittently Connected Mobile Networks," in Proceedings of the ACM SIGCOMM Workshop on Delay-Tolerant Networking (WDTN'05), August 2005, pp.252-259.

[7] Thrasyvoulos Spyropoulos, Konstantinos Psounis and Cauligi S. Raghavendra, "Spray and Focus: Efficient Mobility-Assisted Routing For Heterogeneous and Correlated Mobility", In Fifth Annual IEEE International Conference on Pervasive Computing and Communications Workshops, 2007.

[8] Samuel Nelson, Mehedi Bakht and Robin Kravets, "Encounter- Based Routing in DTNs", In Proceedings of INFOCOM April 2009.

[9] R.D.Poor, "Gradient Routing In Ad Hoc Networks", MIT Media Laboratory, Unpublished manuscript,http://www.media.mit.edu/pia/Research/ESP/texts/poorieeepaper.pdf, 2000.

[10] W. Zhao, M. Ammar and E. Zegura, "Controlling the Mobility of Multiple Data Transport Ferries in a Delay-Tolerant Network," in Proceedings of IEEE INFOCOM, Vol. 2, April 2005, pp. 1407-1418.

[11] R. C. Shah, S. Roy, S. Jain and W. Brunette, "Data Mules: Modeling a Three-Tier Architecture for Sparse Sensor Networks," in Proceedings of Sensor Network Protocols and Applications, May 2003, pp.30-41.

[12] M. Mauve, A. Widmer and H. Hartenstein, "A Survey on Position-Based Routing in Mobile Ad Hoc Networks," IEEE Network, Vol.15, No. 6, 2001, pp.30-39.

[13] T. Spyropoulos, K. Psounis and C. S. Raghavendra, "Efficient Routing in Intermittently Connected Mobile Networks: The Single copy Case," USC, Tech. Rep. CENG-2005-10, 2005.

[14] Eyuphan Bulut, Zijian Wang and Boleslaw K. Szymanski, "Cost-Effective Multiperiod Spraying For Routing in Delay- Tolerant Networks", In: IEEE/ACM Trans. Netw., Vol. 18, No.5, 2010, pp.1530-1543.

[15] www.scalable-networks.com

Digital Fragile Blind Watermarking Based on Lifting Scheme

V. Kavitha[1], M.Sangeetha[2] and C. Palanisamy[3]
[1]Department of Information Technology, Nandha College of Technology, Erode - 638 052, Tamil Nadu.
[2]Kongu Engineering College, Perundurai, Erode - 638 052, Tamil Nadu
[3]Department of Information Technology, Bannari Amman Institute of Technology, Sathyamangalam - 638 401, Erode Distrct, Tamil Nadu
E-mail: kavithamebit@gmail.com, sangeethcse@gmail.com, cp_samy@yahoo.com

Abstract

This paper introduces an algorithm of digital watermarking based on Discrete Wavelet Transform (DWT) by using lifting scheme. Here the integer wavelet transform based fragile watermarking scheme is presented, according to the characters of human vision and its performance on lossless compression of digital images. In our approach we change a few wavelet coefficients to achieve fragile watermarking. This lifting algorithm hides data into one or more middle bitplane(s) of the integer wavelet transform coefficients in the LH, HL and HH frequency sub bands. It could realize integer wavelet transform, which has wide potential applications. The paper analyzes the wavelet lifting algorithm and approaches of image processing algorithm based on lifting wavelet transform. The lifting wavelet could improve the processing speed and save memory.

Keywords: *DWT- Integer wavelet transformlossless compression.*

1.INTRODUCTION

In this paper we present the basic idea behind the lifting scheme [1], a new construction of biorthogonal wavelets which does not use the Fourier transform. In contrast with earlier papers [Image Denoising Research] [13] we introduce lifting purely from a wavelet transform point of view and only consider the wavelet basis functions in a later stage [2],[5]. We show how lifting leads to a faster, fully in-place implementation of the wavelet transform. Moreover, it can be used in the construction of second generation wavelets, wavelets that are not necessarily translates and dilates of one function. The idea of robust watermarking of images is to embed information data within the image with an insensible form for human visual system but in a way that protects from attacks such as common image processing operations [6]. The goal is to produce an image that looks exactly the same to a human eye but still allows its positive identification in comparison with the owner's key if necessary. The rest of the paper is organized as follows: Section II discusses basic concept of watermarking, LSB, DCT and wavelet transforms. Section III discusses the result analysis based on all the four transform techniques include lifting scheme.

2. BASIC CONCEPT OF WATERMARKING

The increasing amount of applications using digital multimedia technologies has accentuated the need to provide copyright protection to multimedia data. A digital watermark can be described as a visible or preferably invisible identification code that is permanently embedded in the data. It means that it remains present within the data after any decryption process [9]. A general definition can be given: "Hiding of a secret message or information within an ordinary message and the extraction of it at its destination . Complementary to encryption [11], it allows some protection of the data after decryption. By adding watermark, we add a certain degree of protection to the image (or to the information that it contains) even after the decryption process has taken place. The goal is to embed some information in the image without affecting its visual content. The purpose is to forbid any unauthorized use of an image by adding an obvious identification key which removes the image's caommerical value.They can also be used in unauthrozied image's copies detectioneither to prove ownership or to identify a customer [3]. The invisible scheme does not intend to forbid any access to an image but its purpose is to be able to tell if a specified image has been used without the owner's formal consent or if the image has been altered in any way.

2.1 Types of Digital Watermarking

2.1.1 Spatial Domain Method

The spatial domain is the normal image space, in which a change in position in I directly projects to a change in position in space. Distances in I (in pixels) correspond

to real distances (e.g. in meters) in space. This concept is used most often when discussing the frequency with which image values change, that is, over how many pixels does a cycle of periodically repeating intensity variations ccur. One would refer to the number of pixels over which a pattern repeats (its periodicity) in the spatial domain [23]. Here we use Least Significant bit (LSB) method.

2.1.2 Transform Domain Method

The produce of high quality watermarked image is by first transforming the original image into the frequency domain by the use of Fourier, Discrete Cosine Transform (DCT) or Discrete Wavelet transforms (DWT) [5]. With this technique, the marks are not added to the intensities of the image but to the values of its transform coefficients. Then inverse transforming the marked coefficients forms the watermarked image. The use of frequency based transforms allows the direct understanding of the content of the image; therefore, characteristics of the human visual system (HVS) can be taken into account more easily when it is time to decide the intensity and position of the watermarks to be applied to a given image.

2.2 Least Significant Bit

One of the simplest technique in digital watermarking is in spatial domain using the two dimensional array of pixels in the container image to hold hidden data using the least significant bits (LSB) method [23]. The steps to embed watermark image are given below.

2.2.1 Steps of Least Significant bit

i. Convert RGB image to gray scale image.
ii. Make double precision for image.
iii. Shift most significant bits to low significant bits of watermark image.
iv. Make least significant bits of host image to zero
v. Add shifted version (step 3) of watermarked image to modified (step 4) host image.

2.2.2 Limitations of Least Significant Bit Watermarking

This method is comparatively simple, lacks the basic robustness that may be expected in any watermarking, applications. It can survive simple operation such as cropping, any addition of noise. However lossy compression is going to defeat the watermark. An even better attack is to set all the cost of negligible perceptual impact on the cover object. Furthermore, once the algorithm was discovered, it would be very easy for an intermediate party to alter the watermark.

2.3.Discrete Cosine Transform Watermarking

The DCT allows an image to be broken up into different frequency bands, making it much easier to embed watermarking information into the middle frequency bands of an image [5]. The middle frequency bands are chosen such that they have minimized they avoid the most visual important parts of the image (low frequency) without overexposing
themselves to removal through compression and noise attacks [1].

2.3.1 Steps of DCT watermarking

i Transforming from the RGB color of the original image into the formation of Gray color
ii To divide the image into 8 × 8 blocks by JPEG standard.
iii Transforms original 8 x 8 block into a cosinefrequency domain

2.3.2 Extracting Watermarked Image

i. Perform DCT transform on watermarked image and original host image.
ii. Subtract original host image from watermarked image.
iii. Multiply extracted watermark by scaling factor to display.

2.3.3 Advantages

i. DCT domain watermarking is comparatively much better than the spatial domain encoding since DCT domain watermarking can survive against the attacks such as noising, compression, sharpening, and filtering.
ii. It uses JPEG compression method to apply DCT watermarking as a parameter. One may use different parameters related to image processing, and these parameters might provide equal or even stronger robustness against various attacks based on image processing.
iii. Discrete cosine transforms (DCT), where pseudorandom sequences, such as M sequences, are added to the DCT at the middle frequencies as signatures.

2.4 Discrete Wavelet Transform Watermarking

The basic idea in the DWT for a one dimensional signal is the following. A signal is split into two parts, usually high frequencies and low frequencies [20]. The edge components of the signal are largely to the high frequency part. The low frequency part is split again into two parts of high and low frequencies. This process is continued an arbitrary
number of times, which is usually determined by the application at hand.

2.4.1 Steps of DWT Watermarking

i. The first part of the watermarking process is the encoder. The first step is to decompose the image into four frequency bands using first resolutions of Haar wavelets at first level. In second level, decompose image into seven frequency bands using second resolutions of Haar wavelets. At three levels, decompose image into ten frequency bands using third resolutions of Haar wavelets and so on.
ii. The next operation is to add the coefficients of the medium and high frequency bands.
iii. It must be pointed out that the relations (1) and (2), even though they are mathematically different, have the exact same goal which is to put more weight to the watermark added to high value wavelet coefficients.

2.4.2 Advantages

i. The watermarking method has multi resolution characteristics and is hierarchical. It is usually true that the human eyes are not sensitive to the small changes in edges and textures of an image but are very sensitive to the small changes in the smooth parts of an image. With the DWT, the edges and textures are usually to the high frequency sub bands, such as HH, LH, and HL etc. Large frequencies in these bands usually indicate edges in an image.
ii. The watermarking method robust to wavelet transform based image compressions and as well as to other common image distortions, such as additive noise, rescaling/stretching, and half toning. This is advantage over DCT.

3. EXPERIMENTS AND RESULTS

3.1 Steps in Embedding

i. Let R={ $P1$, $P2$,.....Pn} represent the set of all neighboring pixel pairs in one direction and Pi be a single pair for all i=1 to n.
ii. let W = {$W1$,$W2$,.....Wm} represent the watermark data where each {0,1,2,.....,9} Wi are used to represent ASCII characters. The same digits can represent Text or image watermark.

In this above steps are indicating the embedding process for watermarking image. P is represented as each pixel for original image. W is represented as each pixel for key image. The information of low frequency component is an image close to the original image. Most signal information of Original image is in this frequency component. The frequency components of LH, HL and HH respectively, represent the level detail, the upright detail and the diagonal detail of the original image. For testing the performance of this algorithm, the experiments are simulated with the MATLAB [8]. In the following experiments, the gray-level image with size of 256 * to embed watermark.

3.2 IWT Based Watermarking

Table 1PSNR Values of the Embedded Watermarked Image

Transforms	PSNR value in db	Elapsed time in (s)
LSB	1.2212e+005	10.5625
DCT	2.4061e+003	11.6563
DWT	3.1402e+003	10.6563
LWT	33.153037	35.5625

Fig.1 Before watermarking lena image

Fig. 2 IWT Based watermarked Image

Fig.3 IWT based recovered image

The above Table1 shows the different types of transforms embedding and it shows the peak signal to noise ratio (PSNR) and that will take the time for embedding an image. So the above analysis, final result is achieved by integer wavelet transform by using lifting scheme. In addition, the security can be enhanced by incorporating

a private embedding key to code the map associating the embedded bits to the selected wavelet watermarking blocks.

4. EXPERIMENTAL COMPARISON RESULTS

By using the integer wavelet transformation it is avoid the overflow of the data compared with the existing method. The result shows the distortion less watermarked image. The results are presented in Table.1 Indicates the types of transformation like LSB, DCT, DWT, and IWT this compares the results of peak signal to noise ratio value. As a result finally we got good PSNR value in integer wavelet transform. The lifting scheme is a much more effective method to calculate the wavelet transforms than the classical convolution method. The original motivation for the development of the lifting technique was the implementation of second generation wavelets. Second generation wavelets unlike the first generation wavelets do not use the translation and dilation of the same wavelet prototype in different levels. The lifting scheme is a general scheme and is not limited to developing a filter structure for second generation wavelets. It can also be used to build a ladder type structure for first generation wavelet filters.The above result shows the compared different sizes with different images and different wavelet types. In this result shows the cdf2.2 wavelet gives the good PSNR value with Lena image and the size gives the good result for 351kb.

Table 2 Different Wavelets and Size with Lena Image

Size	321kb		40kb		1.67mb	
Wave types	PSNR	M2E	PSNR	M2E	PSNR	M2E
Cdf1.1	28.319	94.995	28.425	92.701	28.310	95.187
Bior2.2	27.796	109.704	27.912	106.810	27.786	109.955
sym5	28.547	90.137	28.656	87.896	28.540	90.276
Bior3.3	27.387	119.606	27.461	116.667	27.347	119.777
Cdf2.2	27.796	109.704	27.912	106.810	27.786	109.955

Table 3 Different images and Sizes with cdf2.2 Wavelet

Image	Lena		Baboon	
Size	PSNR	M2E	PSNR	M2E
351kb	28.319	104.028	29.136	99.105
21kb	27.792	109.704	28.786	104.432
29kb	27.863	108.021	28.767	104.887
32kb	27.363	108.032	28.853	102.802
40kb	27.912	106.810	28.905	101.584
1.67mb	27.777	110.777	28.804	104.734

4. CONCLUSION

Compared with the first-generation wavelet, the lifting scheme could complete the wavelet transform currently without allocating additional memory the algorithm is simple and suitable for parallel processing, which makes the computation faster. In the lifting scheme has to do with the easy invertibility property of lifting. In this paper, we analyze the security of fragile image authentication schemes based on watermarking that can accurately localize modifications. We start with a comparison of PSNR Values and Elapsed time using DWT based algorithm and proposed algorithm. The experiments are carried out using Matlab. In Future work we are going to use the moments for rotation and cropping for watermarked image.

REFERENCE

[1] S.Kurshid Jinna , Dr. L. Ganesan, " Reversible Image Watermarking Using Bit Plane Coding and Lifting Wavelet Transforms", IJCSNS International Journal of Computer Science And Network Security, Vol.9, No.11, November 2009.

[2] Xianting Zenga, Lingdi Ping and Zhuo Li, " Lossless Data Hiding Scheme Using Adjacent Pixel Difference Based On Scan Path", Journal of Multi Media, Vol.4, No.3, JUNE 2009.

[3] Xiaoyun Wu, Junquan Hu, Zhixiong Gu and Jiwu Huang , " A Secure Semi-Fragile Watermarking For Image Authentication Based On Integer Wavelet Transform With Parameters", 2005 Australian Computer Society, Inc, Vol.44.

[4] Sunil Lee, Chang D. Yoo and Ton Kalker, "Reversible Image Watermarking Based On Integer-To-Integer Wavelet Transform," IEEE Trans. Information Forensics and Security, Vol. 2, No.3, Sept. 2007, pp.321-330.

[5] M. Tsai and H. Hung, "DCT and DWT Based Image Watermarking Using Sub Sampling," In Proc. of the 2005 IEEE Fourth Int. Conf. On Machine Learning and Cybernetics, China, 2005, pp. 5308-5313.

[6] Zhao Yuxia and Fan Jingbo, "A Double-Function Digital Watermarking Algorithm Based On Chaotic System And LWT", 2012 International Conference On Medical Physics And Biomedical Engineering.

[7] Min-Jen Tsai, "A Visible Watermarking Algorithm Based On The Content and Contrast Aware (COCOA) Technique National Chiao Tung University, Institute Of Information Management, 2007 Ta-Hsueh Road, Hsin-Chu 300, Taiwan, ROC.

[8] MATLAB Help

[9] C. W. Honsinger, P. Jones, M. Rabbani and J. C. Stoffel, " Lossless Recovery of an Original Image Containing Embedded Data", US Patent Application Docket No: 77102/E D (1999).

[10] S. Walton, "Information Authentication For Slippery New Age", Dr.Dobbs J., Vol. 20, No. 4, Apr. 1995, pp.18-26

[11] B.B. Zhu, M. D. Swanson and A.H. Tewfik, " When Seeing isn't Believing", IEEE Signal Proces. Mag., Vol. 21, No. 2, Mar. 2004, pp.40-49.

[12] M.U. Celik, G. Sharma, E. Saber and A.M. Tekalp, " A Hierarchical Image Authentication Watermark With Improved Localization and Security", In Proc. IEEE Int. Conf. Image Processing, Oct. 2001, Vol. 2, pp.502 505.

[13] W. Sweldens, "The Lifting Scheme: A Custom-Design Construction of Biorthogonal Wavelets", Appl. Comput. Harmon. Anal., Vol. 3, No. 2, 1996, pp. 186 200.

[14] I Dawbechies and W. Sweldens, "Factoring Wavelets Transform In To Lifting Steps", Tech., Rep., Lucent Technologies, Bell Labs., Holmdel, NJ, 1996.

[15] E. Koch And J. Zhao, "Towards Robust and Hidden Image Copyright Labeling", In Proc. IEEE Workshop On Nonlinear Signal and Image Processing, Jun. 1995, pp. 452-455.

[16] C. Deng, X.-B. Gao, D.C. Tao and X.-L, Li, " Digital Watermarking in Image Affine Co- Proc. Int. Conf. Mach. Learn. Cybern., Aug. 2007, Vol. 4, pp. 2125-2130.

[17] C. Deng, X.-B. Gao, D.-C. Tao and X.-L, Li, " Invariant Image Watermarking Based On Local Feature Regions", In Proc. Int. Conf. Cyberworlds, Sep. 2008, pp.6-10.

[18] C. Deng, X.-B. Gao, D.-C. Tao and X.-L, Li, " Geometrically Invariant Watermarking Using Affine Covariant Regions", In Proc. IEEE Int. Conf. Image Process., Oct. 2008, pp. 413-416.

[19] X.Li, "Watermarking In Secure Image Retrieval", Pattern Recognit. Lett., Vol. 24, No. 14, 2003, pp.2431-2434.

[20] D. Wang And P. Lu, " Geometrically Invariant Watermarking Using Fast Correlation Attacks", In Proc. Int. Conf. Intell. Inf. Hiding Multimedia Signal, Dec. 2006, pp. 465-468.

[21] Xue Junxiao and Li Qingbin, Lizhiyong, "A Novel Digital Video Watermarking Algorithm", 2011 International Conference On Advances In Engineering.

[22] Li Song and Gu Qialoum, "A Novel Digital Watermarking Algorithm Based On Wavelet Lifting Scheme And Linear Regression", 2012 International Workshop On Information And Electronics Engineering (IWIEE).

[23] Dharashana Mistry, "Comparison Of Digital Water Marking Methods", IJCSE) International Journal On Computer Science and Engineering, 2010, pp.2905-2909.

Innovation through Knowledge Management for Information Technology Usage in Business Organizations

R. Rajendran[1] and Ranga Rajagopal[2]
[1]Department of Management, Sri Ramakrishna Institute of Technology, Coimbatore - 641 010, Tamil Nadu
[2]Director-operations and CEO of Acenet Technologies India (P) Ltd.

Abstract

Organizations worldwide have adopted Information Systems for effectively managing their businesses. These include Enterprise Resource Planning (ERP), Supply Chain Management (SCM) and Customer Relationship Management (CRM) systems. It is usually found that only the first order effects such as Project scope, Time and Cost are considered for evaluating the project success. To ensure that the project has delivered the intended results, it is our contention that factors such as system use, learning and value have to be considered. Knowledge Management plays a vital role in ensuring the transfer of implicit to explicit knowledge and vice versa. Knowledge through interaction at the departmental and organizational levels grows as a spiral and ensures that organizations transform themselves from being just learning organizations to become knowledge creating organizations. This aspect of innovation by the users ensures that organizations realize the intended business benefits of the information systems that they have adopted. A model has been contributed to moderate the relationship of usage to business value through knowledge transfer.

Keywords: *Business value, Information systems, Knowledge transfer, System usage*

1. INTRODUCTION

Information systems (IS) have become all encompassing and are an integral part of organizations and their business process today. Some among these such as Enterprise Resource Planning (ERP), Supply Chain Management (SCM) and Customer Relationship Management (CRM) systems have matured and deliver substantial business value to their adopting firms. However while a number of organizations have adopted these systems, the level of success is highly varied. This can be attributed to the initiatives taken by them in managing the implementation and post implementation functionality, especially from the user perspective. It is well known that users contribute the most to the success of any information system. Notwithstanding this, the organization needs to provide the requisite eco system to incorporate the necessary interests of the organization, procedures, social interaction norms and processes required to manage the knowledge created through these systems.

Projects success is normally measured based on their first order effects or process based measures. However, the true reflection of project success should be based on their outcome based measures which include use, learning and value. Usage can contribute to efficiency in the case of operational users and to effectiveness in the case of strategic users.. It is noticed that while there has been substantial research in all aspects relating to ERP systems, there is not much work done to understand the role of knowledge management in contributing to business value especially in the context of system usage.

In the following section, literature has been reviewed concerning various variables such as system use, learning and value which are the outcome based measures of ERP implementation. A related model depicting the project success criteria and the relationships between the various constructs is given. A model for knowledge conversion through the "knowledge spiral" is also explained. Adapting this proven concept of knowledge conversion in the ERP context would help in understanding the knowledge management processes being carried out in ERP implementations.

Knowledge is the key differentiator in today's competitive world and can determine the level of benefits organizations derive from their IS investments. Managing this body of knowledge calls for a structured approach. A study was conducted in a large textile manufacturing organization which had implemented ERP and which has been in use for over five years in multiple functions and at various levels. It was here that a phenomenon was observed as to how knowledge was being managed and was enhancing usage of the system thereby contributing to business performance. Based on this study, a model has been evolved which we hope can contribute to the

gap in literature. This model is presented in the next section.

In the concluding section, we have provided a summary of the article with a recommendation on how this study can be developed further. Validating the model in terms of various approaches is also presented. Theoretical works contribute to continuous intellectual renewal and help strike a balance between conceptual and empirical articles. The contribution to the theoretical domain through this conceptual article will add to the existing knowledge base and ongoing research efforts in this area.

2. REVIEW OF LITERATURE

No IT investment is only about technology. However most organizations focus on the implementation of technology and not on the expected benefits. The failure to realize benefits can be attributed to the methods and tools deployed in system usage. By identifying, planning and managing the benefits of technology, organizations can reap the benefits in a reasonable time frame [19].

System usage has received scant theoretical treatment. In the absence of theoretical grounding, studies have arrived at mixed conclusions about the link between system usage and individual performance. Measuring system usage means quantifying it, not evaluating it. Measures will differ between individual usage and collective usage since collective usage at an organization level may not necessarily be the sum of individual usage [7]. The existence of system usage at different levels is acknowledged in IS research. However no concentrated effort has been made in this direction. Studying system usage as a multilevel construct would contribute to understanding it deeper and provide a platform for research. Since studying usage at an individual level can lead to a disjointed view, multilevel studies can highlight the linkages between levels and how these sustain communities [6]. System success through complex feedback loops is a dynamic construct. It is generally believed that system use leads to certain impacts or net benefits. However, if net benefits are not matching with the expectations of the user, he will modify use to achieve greater benefits. When the perceived benefits increase, the commitment to use the system increases. The user's knowledge base is enhanced depending on the extent of use of the system [2]

The use of IT in the primary activities contributes to the value creating potential of the organization. Organizations that use IT with a dual focus, towards both operational effectiveness and strategic advantage derive more value out of their IT investments [30]. The relationship between technology investments and organizational performance is mediated by usage. The actual usage of technology for specific processes and not the investment is the real driver of the impact of IT [5]. The statement, "more use will lead to more business benefits" need not necessarily be true. What is more important is to also consider the nature, quality and appropriateness of the use, Net benefits influence user satisfaction and further use of the IS. Though system usage is the key variable in IS research, this construct has received little scrutiny [4]. The degree of user participation has a positive relationship to system success at different MIS growth stages [13]. Research in technology usage [28], suggests that actual usage and perceived usage are not the same. Usage needs to be tied up with organization performance metrics to ensure it creates the necessary impact. Effective IT expenditure leads to IT assets, effective use of IT assets leads to impacts, impacts and favourable conditions leads to outcome. The central process connecting IT assets to IT impacts raises questions about what constitutes appropriate use, how use differs across different types of IT and how use, skill and appropriate use lead to impacts [26].

Projects need to be measured not only in terms of their first order (or process) measures but also through second order (or outcome) based measures. This is because projects can be successful in terms of either the process measures or outcome measures, or both. Project success also needs to be measured from multiple dimensions and from the perspective of different stakeholders. Benefits realization should be conducted only when business value metrics can be assessed [14]. This relationship between the variables contributing to project success criteria is depicted in Figure 1.

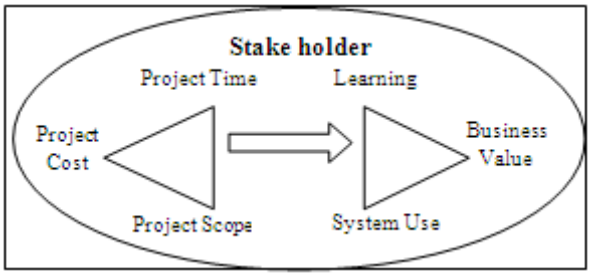

Fig. 1 Project success criteria [14]

An organization's adaptive capability to generate new types of knowledge and to disseminate this through a knowledge structure influences the organization's ability to gain a competitive advantage from its IT investment and usage [10]. Data about where the knowledge resides is as important as the data itself. Hence, a set of expert profiles may have details of the skills, experience and expertise in various areas. IT can be an enabler to increase the reach of the users to other departments to seek expertise since it is believed that the knowledge among the same set of co-workers may be similar. A user may create new knowledge, probably through an insight, and may apply this knowledge leading to additional new knowledge. This knowledge after being applied may be coded into the organizational documents for future reference thereby enabling the creation of explicit knowledge from tacit knowledge. Knowledge management is not a monolithic but a continuous and dynamic process of managing [1]. The knowledge required to make processes work may have become so habitual that those who perform the processes may not be aware of decision steps they go through to do them, and may have trouble explicitly stating how they do what they do.

Tacit knowledge sharing depends on individuals being encouraged to express ideas freely. While the origin of tacit knowledge is the individual, organizations play an important role in amplifying and articulating this tacit knowledge [16]. Tacit knowledge sharing could also be through brainstorming, storytelling, and expressing ideas that are not yet fully formed. Users who find certain parts of the system difficult or cumbersome to use, may even evolve workaround solutions. These workarounds may be very effective in certain situations and may well be converted into explicit form for the benefit of other users. To understand the ways in which information systems can support the management of knowledge in organizations, it is required to consider not only the intended, positive consequences of knowledge and the way it is managed, but also the negative, unintended ones [23]. Ongoing learning includes social interaction with master users. Experimenting and playing with the software includes looking at features and functions of the software actively, creating dummy data sets for trial, anticipating making mistaking and encountering new things while working with the ERP. All these form an integral part of the ongoing learning process which generates tacit knowledge [27]. It is important for the firm to capture as much tacit knowledge as possible from the consultants before they complete and leave the project site. Tacit knowledge sharing with the new user during transition of any user from the department, location or the organization is also very critical. Tacit knowledge sharing during ERP implementation is best when the organization provides an atmosphere conducive for this interaction. Firms that encourage ideas, in spite of whether they are fully formed or are in the "creation' stage, are the ones that derive the maximum benefit from their ERP implementation and KM initiatives [8].

The SECI model proposed by Nonaka provides an analogy of knowledge conversion that can lead to organization learning [15]. The four possible modes of conversion between tacit and explicit knowledge are socialization, externalization, combination and internalization, each unique in its own way. In the concept of socialization, tacit knowledge is converted to new tacit knowledge through everyday interactions among the people (e.g. brainstorming) ; in externalization, new explicit knowledge is created by applying previous tacit knowledge (e.g. verbalization of the best practices in ERP implementation) and; in internalization, new tacit knowledge is created by one's own understanding gained through readings and discussions.

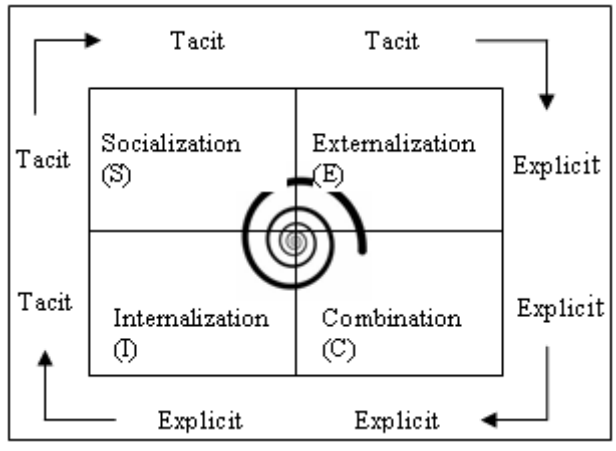

Fig. 2 Nonaka's SECI Model [17]

The combination mode, as the name suggests, refers to the creation of new explicit knowledge from existing explicit knowledge that already exists with the organization. The different modes of knowledge conversion help the organization generate knowledge dynamically through the "upward knowledge spiral". This spiral starts at the individual level and then moves up to the group level and finally to the organizational level, and sometimes even beyond to the inter-organizational level thereby contributing to knowledge creation across the organization [17] (Fig. 2).

The platform structure has been proposed as an extension of the Nonaka SECI model with specific reference to the ERP context [11]. The platform structure comprises of five platforms namely Consulting platform, Co-operative working platform, Individual platform, Knowledge transfer platform and Organization KM platform. While the individual platform provides technology support and enables users to convert tacit knowledge to explicit knowledge, the co-operative platform consists of the communications and document management module. The knowledge transfer platform facilitates transfer of knowledge from the individual to the organization and vice-versa. The organization platform provides support for all the KM activities of the organization. The consulting platform includes transferring the implicit and explicit knowledge of the consultants to the project team and to provide user training, which is mostly done through the "Train the Trainer" concept [11]. These 5 platforms can act as formative constructs in aiding knowledge transfer.

Though the origin of new knowledge is the individual, in the knowledge based view, a firm is viewed as an entity creating knowledge. The capability to create and put to use the knowledge thus created is what sustains and provides the firm its competitive advantage. This knowledge is that which helps the firm to innovate new processes/procedures and more efficient/effective ways of working. Knowledge integration is a continuously evolving process which includes construction and articulation of knowledge and interacting with members of the organization to share these beliefs. There exists an empirically tested positive relationship between KM competence and enterprise systems success [25]. Knowledge creation, transfer, retention and application are the four types of knowledge processes. The potential of creating innovations is enhanced through the knowledge creation process. In spite of knowledge creation being expensive, owing to factors such as employee attrition/mobility and the necessity to innovate to be ahead of competition, organizations are forced to ensure effectiveness of knowledge creation to deliver better business performance and success. Knowledge transfer ensures better efficiency in ERP usage for the operational and tactical users and contributes towards enhancing the effectiveness in the case of strategic users thereby contributing to business performance.

Successful transfer of best practices comes from a personal and organizational willingness to learn. It calls for an innate sense of curiosity and a deep desire and respect to learn from others. Learning and transfer of knowledge is an interactive, ongoing process and cannot depend on a body of knowledge which is static. Users are constantly exploring, improvising, inventing and learning something new every day. The key is to convert this tacit knowledge to explicit knowledge for the benefit of other users in the organization [18]. The diversity of knowledge across the enterprise among various business units needs to be integrated. It is essential to have standardization and transparency of knowledge throughout the organization. Knowledge is also embedded in legacy systems since users tend to compare and make sense of the change. Knowledge is embedded in external systems such as those of suppliers, contractors etc, making integration of knowledge a challenge. Post implementation, knowledge integration is enabled by structural integration through inter personal and group based relations.

The third generation of KM has suggested some interventions. Some such ways to constantly revive key knowledge are communities of practice, debriefing processes, storytelling or narratives. One of the new areas in knowledge management is how to handle things that cannot or will not be codified [24]. Prior knowledge could also include knowledge about the recent scientific and technological developments. The ability to recognize this, assimilate it and apply it is what can be called absorptive capacity. Exploiting knowledge thus for the benefit of the organization demonstrates the innovative capabilities of the individual and the organization since the absorptive capacity of the organization is the reflection of what is possessed by individual members [3]. The progress of KM initiatives in a firm can be better understood by exploring the barriers to knowledge flow. It is found that the main factors contributing to this include technophobia, lack of trust in the system, lack of authority to access/ modify knowledge documents and lack of systematic knowledge documentation [12].

Interaction between post implementation maintenance and the mechanism of knowledge management has a positive effect on business performance. It is also found that if the knowledge gained through ERP usage is effectively stored but not shared with other organization members, it cannot increase the influence of knowledge management on business performance [31]. Knowledge dissemination from the consultants to users where the former possess thorough knowledge about the ERP and the latter, their specific domain falls under this category of innovations. Source credibility, shared understanding, absorptive capacity, communication competence and motivation are some of the key factors that influence transfer of knowledge [9].

It is only through enterprise wide innovation that any organization can respond to changes in its environment. Business innovation now increasingly depends on IS. It is also through IS innovations that many new technologies are effectively integrated with the organization strategy and processes. ERP implementations belong to Type III innovations which are knowledge intensive and involve transfer of knowledge among participants whose structure is asymmetric [29]. The success of IS innovation depends on the partnership between the IS department and other users since in many cases, these functional users are the source of the innovation.

3. PROPOSED MODEL

Case study, as a research strategy is particularly suited to situations where the research question needs detailed understanding of the organization process because of the rich data that can be collected. The model has been evolved based on phenomenon that was observed as part of a case study conducted at a leading textile company which has implemented ERP across multiple functions and has been in use for over 5 years [22]. The triangulation method of data collection [33] was adopted wherein personal interviews were conducted, documents were reviewed and the work done by the users was observed.

Once a phenomenon is observed, it evolves from the idea generation to the justification stages. This discovery is what is contributed as a conceptual work. It is hence necessary to encourage theoretical work to ensure that a vibrant environment for knowledge development is sustained. Not sustaining the efforts for conceptual work will weaken the theoretical core of any discipline [32].

3.1 Case Study

The case study was conducted in a privately held Export Oriented Unit (hereafter referred to as "THE COMPANY") involved in the manufacture and export of textile products and is recognized as one of the leading brands in the world in its category [21]. THE COMPANY started its operations in the year 1993 and subsequently expanded its operations by adding three additional plants in the vicinity in the years 2003, 2005 and 2006 respectively. It also added a new Unit at a new location about 30 km away in the year 2009. THE COMPANY's production capacity is 1200 tones of terry products per month and it had an annual sales turnover of INR 2800 million (2010-2011). THE COMPANY has a workforce of 2170 employees consisting of 470 management staff and 1700 workers working in 3 shifts.

3.2 A Strategic Vision

THE COMPANY has taken a strategic management approach to modernizing its internal information flow by embarking on a computerization drive in the year 1997 through the usage of Tally for accounts, a PPC system for materials planning and a punch card based payroll and HR system for personnel management.

In the year 2003 the same practices were implemented in another Unit. THE COMPANY understood the need of an integrated system and went in for an ERP system in the year 2004. In spite of early failures in implementation the company persisted with the implementation and succeeded in the year 2005. The vendor of the ERP system responsible for implementing the system quit the project in September 2005 without completing the project. This did not deter the company. The information systems department of the company took up the project and completed it successfully. In the year 2009, when the new unit started functioning, the system was introduced from the date of commencement of operations.

3.3 Implementing Change

THE COMPANY's vision of implementing continuous change for the better is evident from the interest and purpose the top management has shown in modernizing the MIS structure of the company. The need to create a learning organization is evident. There are pockets of resistance to change which the organization seems to have addressed fairly well. The 1st and 2nd kickoff's which failed during the year 2004 shows the

resistance from the employees and possibly even the management staff. Training and development is an ongoing process in an organization which aims to continuously develop for the better. At THE COMPANY, with specific reference to ERP implementation, DEOs (Data Entry Operators) have been recruited and trained initially and whenever a new person joins, he/she too is trained. This environment of training and learning had motivated the data entry head to learn other aspects about ERP. The organization had given permission to use the Test Server without restriction for learning and training. This encouraged employees to learn. Even the data entry operators learnt and used shortcuts effectively based on self-learning. Training of staff in other departments including Purchase and Finance was done on a regular basis.

3.4 Effective Knowledge Capturing - Challenges

Knowledge transfer from the consultants deputed by the vendors involved in the implementation of the ERP system was not sufficient, as they did not have the required domain expertise. Hence, they were not able to provide the required confidence to the actual users. But the prior experience of the Finance manager in implementing information systems in four different earlier instances had helped in successful implementation when the consultants had left the project incomplete.

Knowledge capturing and storing has been a problem area in various departments since the documentation procedure during the various stages of implementation, though completed by the vendor, had been insufficient. The user manuals for the ERP system have been developed by the initiative of the department members themselves in some departments in order to address this insufficiency. In few other departments, the employees are open to the suggestion of creating user manuals. In some departments, the department heads do not seem to acknowledge and accept the importance of creating user manuals for their departments.

This is an impediment to the knowledge creation and captures process and needs to be addressed in order to ensure effective knowledge transfer. Otherwise, the successful and continuous functioning of the ERP system without being dependant on the tacit knowledge of certain key individuals may be a problem in case these individuals leave the organization. This reluctance of experienced individuals in giving away their control of a domain by transferring their tacit knowledge has to be addressed delicately by the top management.

Based on this case study, a model has been developed. In this model, system usage is taken as the Independent variable which in the case of operational users leads to efficiency and in the case of strategic users' leads to effectiveness. It would be appropriate to consider usage from a multi level perspective across various business functions to study usage of the system from a diverse range of perspectives. As understood form the case, knowledge transfer is what can lead to enhanced usage of the system. Knowledge transfer hence acts as a moderating variable in this model. The Nonaka SECI model suggests how knowledge can be converted from tacit to explicit form and vice versa at various stages during and after implementation. This leads to the creation of organization usable knowledge through the upward knowledge spiral. This would in turn drive better usage of the system thereby contributing to enhancing the business value which is the dependant variable.

In the model shown, system usage is depicted as a reflective construct since it is manifested in the form of usage across multiple functions at various levels. The relationship between constructs and measurement items is often ignored by researchers while taking substantial efforts justifying the link between constructs. It is necessary to understand the various choices available before analyzing and specifying a certain construct in a model. Designating a construct as being reflective or formative without a clear understanding may be quite elusive. Misspecification of formative constructs can lead to potential errors and can affect theory development. It could even restrict researchers from testing theory meaningfully owing to improper results [20].

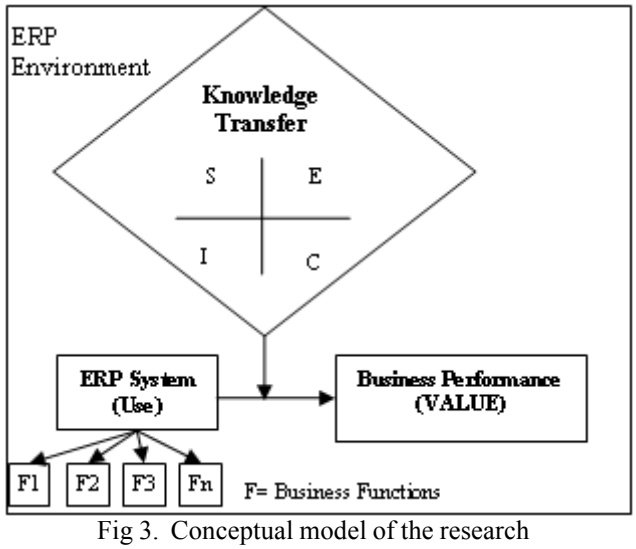

Fig 3. Conceptual model of the research

4. CONCLUSION

The article presents the process based measures and outcome based measures in IS projects. Having studied various references to these measures in literature, it comes to light that the true reflection of the success of IS projects is due to the second order effects which are the outcome based measures. It is also noticed that there has not been adequate research in establishing how knowledge management can act as a true catalyst to translate the IT investment through system usage into business value for the adopting organization. It is this gap in literature that has been addressed here. The case study that was conducted was an eye opener on how organizations which have successfully deployed IS systems and are deriving substantial value have been going about their knowledge management process. It is also observed both through literature and the case study that the true reflection of usage can be got only when it is observed and studied from the perspective of users across multi levels. It is found that use of the system is what drives people to experiment and learn more about the system, thereby aiding in generating abundant tacit knowledge which is then shared with other users in the organization through a structured KM process. The knowledge spiral is what has been instrumental in contributing to the firm becoming a 'knowledge creating" organization. Based on these inputs, a model has been proposed. This model has to be further tested through case replication logic to be conducted at a few more business organizations. Moreover, the model can also be empirically tested to validate the findings. It would be of interest, in future, to build on this research and find how operational users derive efficiency and strategic users derive effectiveness from their IS usage through effective knowledge management procedures. This would ensure that the firm, in the long term, transforms itself from than being just a learning organization into a knowledge creating organization thereby enhancing business value.

REFERENCES

[1] M. Alavi and D.E.Leidner, "Knowledge Management and Knowledge Management Systems: Conceptual Foundations and Research Issues". MIS Q Vol.25, No.1, 2001, pp.107-136.

[2] T.D.Clark, M.C. Jones and C.P. Armstrong, "The Dynamic Structure of Management Support Systems: Theory Development, Research Focus and Direction", MIS Q Vol.31, No.3, 2007, pp.579-615.

[3] W.M. Cohen and D.A. Levinthal, "Absorptive Capacity: A New Perspective on Learning & Innovation", Admin. Sci. Q. Vol.35, No.1, 1990, pp.128-150.

[4] WH.DeLone and ER.McLean, "The DeLone and McLean Model of Information Systems Success: A Ten-year Review", J Manage Inf. Syst. Vol.19, No.4, 2003, pp.9-30.

[5] S. Devaraj and R. Kohli, "Performance Impacts of Information Technology: is Actual Usage the Missing Link", Manage Sci. Vol.49, No.3, 2003, pp.273-289.

[6] A.B.Jones and MJ. Gallivan, "Towards a Deeper Understanding of System Usage in Organisations: A Multilevel Perspective", MIS Q Vol.31, No.4, 2007, pp.657-678.

[7] A.B.Jones and DW. Straub, "Reconceptualising System Usage: An Approach and Empirical Test", Inf Syst Res. Vol.17, No.3, 2006, pp.228-246.

[8] MC. Jones, "Knowledge Sharing During ERP Implementation: A Multi-site Case Study", lnf Resources Manage J. Vol.18, No.2, 2005, pp.1-23.

[9] DG. Ko, LJ.Kirsch and WR.King, "Antecedents of Knowledge Transfer from Consultants to Clients in Enterprise Systems Implementations", MIS Q Vol.29, No.1, 2005, pp.59-85.

[10] Z. Lee and J.Lee, "ERP Implementation Case Study from a Knowledge Transfer Perspective", J Inf Technol. Vol.15, 2000, pp.281-288.

[11] Y.Li, XW. Liao and HZ.Lei, "A Knowledge Management System for ERP Implementation", Syst Res and Behavioral Sci. Vol.23, No.2, 2006, pp.157-168.

[12] C. Lin, J C. Wu and DC.Yen, "Exploring Barriers to Knowledge Flow at Different Knowledge Management Maturity Stages", Inf & Manage . Vol.49, 2012, pp.10-23.

[13] H. Lu and J. Wang, "The Relationships Between Management Styles, User Participation, and System Success Over MIS Growth Stages", Inf and Manage. Vol.32, No.4, 1997, pp.203-213.

[14] RR.Nelson, "Project Retrospectives: Evaluating Project Success, Failure, and Everything in Between", MIS Q Executive, Vol.4, No.3, 2005, pp.361-372.

[15] I. Nonaka, "The Knowledge Creating Company", Harvard Bus Rev., Nov-Dec 1991, 2005, pp.96-104.

[16] I. Nonaka, "A Dynamic Theory of Organizational Knowledge Creation", Organ Sci, Vol.5, No.1, 1994, pp.14-37.

[17] I. Nonaka, P.Byosiere, C.C.Borucki and N. Konno , "Organizational Knowledge Creation Theory: A First Comprehensive Test", International Bus Rev. Vol.3, No.4, 1994, pp.337-351.

[18] C. O'Dell and C.J. Grayson, "If Only We Knew What We Know: Identification and Transfer of Internal Best Practices", California Manage Rev. Vol.40, No.3, 1998, pp.154-174.

[19] J. Peppard and J.Ward, "Unlocking Sustained Business Value from IT Investments", California Manage Rev Berkeley, Vol.48, No.1, 2005, pp.52-70.

[20] S. Petter, D. Straub and A. Rai, "Specifying Formative Constructs in Information Systems Research", MIS Q, Vol.31, No.4, 2007, pp.623-656.

[21] R. Rajendran and R.Rajagopal, "Knowledge Management in an ERP Environment: The Case of STPL", Proc 2nd Int Case Conf IMT Nagpur Case Res Soc of India, Goa, India, 2011.

[22] R. Rajendran and R.Rajagopal, "Why are Business Performance Benefits not being Realized in ERP Systems Usage in Spite of Implementation Success", Proc Int. Conf. on IT Sys & Mgt IIM Kozhikode, India, 2011, pp.359-367.

[23] U. Schultze and DE. Leidner, "Studying Knowledge Management in Information Systems Research: Discourses and Theoretical Assumptions", MIS Q Vol.26, No.3, 2002, pp.213-243.

[24] P. Schutt, "The Post Nonaka Knowledge Management", J of Universal Comp Sci. Vol. 9, No.6, 2003, pp.451-462.

[25] D. Sedera and G.G.Gable, "Knowledge Management Competence for Enterprise System Success", J of Strategic Inf Syst., Vol.19, No.4, 2010, pp.296-306.

[26] CM. Soh and L. Markus, "How IT Creates Business Value: A Process Theory Synthesis", Proc Int Conf Inform Syst, 1995, pp.29-41.

[27] VK.Spitler, "Learning to Use IT in the Workplace: Mechanisms and Masters", J Organ End User Computing, Vol.17, No.2, 2005, pp.1-25.

[28] D. Straub, M.Limayem and EK.Evaristo EK, "Measuring System Usage: Implications for IS Theory Testing", Manage Sci , Vol.41, No.8, 1995, pp.1328-1342.

[29] E B. Swanson, "Information Systems Innovation Among Organizations" Manage Sci 40(9): 1069-1090, 1994

[30] PP.Tallon, "Does IT Pay to Focus? An Analysis of IT Business Value Under Single and Multi-focused Business Strategies", J Strategic Inf Syst, Vol.16, No.3, 2007, pp.278-300.

[31] M.Tsai, E Y.Li, K.Lee and W. Tung, "Beyond ERP Implementation: The Moderating Effect of Knowledge Management on Business Performance", Total Quality Mgt & Bus Excellence, Vol.22, No.2, 2011.pp.131-144.

[32] MS. Yadav, "The Decline of Conceptual Articles and Implications for Knowledge Development", J of Marketing, Vol.74, January 2010, pp.1-19.

[33] R.K.Yin, "Case Study Research: Design and Methods" (2nd ed., 1st ed., 1984; rev.ed., 1989). Thousand Oaks, CA: Sage Publications, 1994.

Preparation of Gelatin (Typeaprotein) From Sun Dried Fish (Tilapia – Oreochromis Mossambicus) Skin

A. Logeswari, M. Thirumarimurugan and T. Kannadasan
Department of Chemical Engineering, Coimbatore Institute of Technology, Coimbatore - 641 014, Tamil Nadu.
E-mail: kannadasan@cit.edu.in

Abstract

Sun-drying was carried out to dry fish skins (Tilapia – Oreochromis mossambicus) and to obtain gelatin from the skins. The fish skins were pretreated using 0.05 M acetic acid followed by extraction at 80^{0}C for 2 h. The gelatin obtained was confirmed by Ninhydrins test. Gelatins from dried fish skins (Tilapia – Oreochromis mossambicus) had higher crude protein, lower ash content and lower crude lipid. Drying of fish skin led to decreased viscosity, increased gel strength, and no significant effect on melting point. Gelatin from dried skins showed a higher turbidity and darker appearance. It was observed that drying did not interfere with amino acid composition.This study showed that sun-drying seems to be a prospective method for preservation of fish skins.

Keywords: *Extraction, Fish gelatin, Seawater fish, Skin, Sun-drying.*

1. INTRODUCTION

Gelatin, an extracted protein from animal collagen, has several functions for food, pharmaceutical, medical, cosmetic and photographic industries. The major gelatin in the world is derived from pigskin and bovine hide. Bovine spongiform encephalopathy (BSE) becomes an issue in consuming products from cow (Baziwane and He, 2003; Gudmundsson, 2002). Therefore, find inane alternative to the mammalian gelatins which is acceptable to these religious groups and overcoming food safety issues is in urgent need. Gelatin from fish is the potential alternative to mammalian gelatins.

The extraction and characterization of gelatin properties from several fish skins like megrim, cod, tuna, yellow fin tuna, Nile perch and tilapia. Fish gelatin is now commercially available and it has been used for several applications in place of mammalian gelatins. The source of fish skin in sea is abundantly available. As the marine country with a large number of coastal areas, it affords various species of seawater fishes. The by-products of these fishes are usually processed into animal feed. In fact, these materials are potential sources of collagen that further can be converted into gelatin. [11]

Fresh fish skin is commonly utilized as a source material for gelatin production. However, fresh fish skin is highly susceptible to deterioration, when compared to mammal sources which are more stable and easily preserved. Moreover, after degutting and filleting of fish, skins are often kept together with the rest of by-products, being subject to rapid enzymatic and microbial damage. This problem urges the need of seeking methods for preservation. The best method to preserve fish skins by freezing. However, gelatin extracted from frozen fish skin per formed a bit lower functional properties, especially molecular distribution and rheological characteristics. Also, this method seems costly in terms of energy consumption and machinery installation [11].

Another method to preserve fish skin is by drying. Drying has been used for longtime to stabilize fishery products. Sun-drying is the oldest, conventional and traditional technique to preserve agricultural and fishery products therefore it can stabilize them from deterioration. Drying of the materials reduces transportation, storage and distribution costs compared to freezing similarly; drying could be an alternative method to stabilize fish skin before further processing in gelatin manufacturing[12].

Air drying method has been studied to preserve skins of Dover sole fish and channel catfish. The gelatin extracted from Dover sole fish was reported to have gel strength 140-170Bloom, was similar to that of extracted from the fresh skin. In addition, gelatin from dried channel catfish skin exhibited higher gel strength, similar gelling and melting point compared to those of extracted from fresh fish skin. This study was aimed to investigate the gelatins properties extracted from fresh and sun-dried skins of seawater fish. The gelatins were analyzed for the yield, proximate composition, functional properties, and amino acids composition. [12]

2. OBJECTIVE

The main objective of this project is preparation of gelatin from sun dried fish skins in an eco-friendly manner. The goal is to prepare the gelatin commercially low cost and wealth from waste.

3. MATERIALS AND METHODS

3.1 Materials and Equipments Required

The main materials used for this project

i. Tilapia – Oreochromis mossambicus fish skin (50kg)
ii. Water (4litres)
iii. 0.05M acetic acid (2litres)

Equipments used for this project

i. Oven
ii. Filter paper – layer cloth
iii. Cabinet drier

3.2 Experimental Procedure for Manufacture of Gelatin

Gelatin extraction employed type A method using acid solution in accordance to Montero and Gómez-Guillén (2000) with a slight modification. Dried fish skins were treated specifically before extraction process.[11]

Fig.1 Fresh fish skin

3.2.1. STEP 1

They were initially rehydrated by dipping in water with the ratio of skin and water 1:4 (w/v) for4 h. This pretreatment was done to create favorable condition for extraction process, as similar condition in the fresh skins [1].

Fig.2 Rehydrated fish skin (the ratio of skin and water 1:4 (w/v) for 4h)

3.2.2. STEP 2

The skin was treated in hot water for about 1 min, and cleaned from remaining fat and other impurities [1].

Fig. 3 Treated fish skin in hot water

3.2.3. STEP 3

The skins were cut into small pieces, and dipped in 0.05 M acetic acid solution with the ratio of fish skin and acid solution was 1:4 (w/v) at Ambient temperature for 10 h. After that, the skin was rinsed with abundant tap water until neutral condition [1].

Fig.4 Treated fish skin in 0.05 M acetic acid solution ambient temperature for 10 h.

3.2.4. STEP 4

Gelatin extraction was conducted by putting the fish skins in distilled water at 1:3 (w/v) ratios and heated up to 80^0C for 2 h [1].

Fig. 5 Treated fish skin with acetic acid and heated upto 80^0C for 2hr.

3.2.5. STEP 5

The gelatin liquor was then filtered through a filter paper-layered cloth to obtain gelatin filtrate [1].

Fig. 6 Gelatin filtrate

3.2.6. STEP 6

The filtrate was put on the pan, and dried in a cabinet drier at 55^0C for 48 h to obtain gelatin sheets. The sheets were ground to result in gelatin granules. The gelatin granules were packed in a plastic, and kept in a refrigeration temperature until used for analysis [1].

Fig.7 Cabinet drier

Fig. 8 Filtrate (after drying)

Fig. 9 Protein powder

3.3 Confirmatory Tests For Proteins

i. The Bicinchronic acid assay test.
ii. Biuret reagent tests for proteins and polypeptides.
iii. Bradford protein assay test.
iv. The Phadebas Amylase Test determines alpha-amylase activity.
v The Carbylamines reaction tests for primary amines.

vi The Van Slyke determination tests for specific amino acids.
vii Ninhydrins reagent test.

Among the above given tests ninhydrins reagent test for proteins holds good due to its easy availability, lab usage and economic. The ninhydrins test is described as follows:

3.3.1 Ninhydrins Reagent Test [13]

i. Take 3ml of sample solution in a clean test tube.
ii. Add two to three drops of ninhydrins reagent.
iii. Mix the solution thoroughly and boil it.
iv. Cool it down to room temperature.
v. If the sample turns bluish color, it will indicate the presence of protein.((Baziwane and He, 2003; Gudmundsson, 2002).

3.4 Explanation

Initially 3ml of the protein sample solution is taken in a clean test tube. Then add two to three drops of ninhydrins reagent to the sample solution taken in the test tube. Mix the entire solution thoroughly and boil it [13].

Fig. 10 Boiling of protein sample with ninhydrins reagent

It is then followed by cooling process where the solution is to be cooled down to room temperature. After sometime the sample solution turns bluish color indicating the presence of proteins which is shown in fig 12[12].

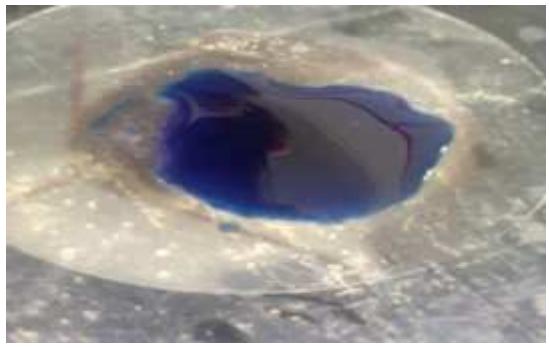

Fig.11 Test sample

3.3.2 Sample Gelatin Powder

Fig 12.Sample gelatin powder

4. RESULTS AND DISCUSSIONS

4.1. Calculation for %Yield

Yield was expressed in a percentage (%),calculated by weighing the resulted gelatin granules divided by the weight of fish skin in dry basis (db.),after considering the moisture content of each condition[1].

Weight of fresh fish skin = 50g
% of protein in fresh fish skin = 17.61%
Weight of protein in fresh fish skin = .1761*50 = 8.805g
Weight of gelatin powder obtained = 10g
% of protein in gelatin powder = 85.4%
Weight of protein in gelatin powder = 10*.854 = 8.54g
% yield = (weight of protein in gelatin)
(Weight of protein in fresh fish skin)
= 8.54/8.805
= .961*100
% yield = 96.1%

4.2 Composition of Fresh Fish Skin and Gelatin Powder

Fresh fish skin and the sample powder composition were determined in the ALPHA laboratory by using various tests.

Fresh Fish Skin	% Composition	Protein Powder	% Composition
Moisture	74.52	Moisture	3.17
Fat	2.73	Fat	1.24
Ash	5.13	Ash	9.85
Protein	17.61	Protein	85.4

5. CONCLUSION

The optimization of dry skin rehydration need to be investigated accordingly to obtain the optimum yield as close to those of extracted from fresh skins. Sun-drying on fish skins has advantages for preservation compared to freezing since the dried skins are able to stand at room temperature for longer time and the weight is largely decreased, which leads to reduction in transportation, distribution and energy cost.

6. SCOPE FOR FUTURE WORK

In this method we have done the extraction of gelatin from seawater fish species Tilapia. The scope for future work is that gelatin can also be extracted from other types of seawater fishes like yellow fin tuna and brown stingray and the properties of gelatin extracted from all these fishes can be compared. In case of humid days, the atmospheric temperature may not be adequate, so another alternative has to be found out for drying the fish skin.

APPENDIX

Weight of fresh fish skin = 50g
% of protein in fresh fish skin = 17.61%
Weight of protein in fresh fish skin = .1761*50 = 8.805g
Weight of gelatin powder obtained = 10g
% of protein in gelatin powder = 85.4%
Weight of protein in gelatin powder = 10*.854 = 8.54g

$$\% \text{ yield} = \frac{\text{(weight of protein in gelatin)}}{\text{(weight of protein in fresh fish skin)}}$$

$$= \frac{8.54}{8.805}$$

$$= .961*100$$

$$\% \text{ yield} = 96.1\%$$

REFERENCES

[1] D.Baziwane and Q.He, "Gelatine: The Paramount Food Additives ", Food Reviews International, BSI (British Standard Institution),1975.Methods for sampling and testing gelatine (physical and chemical Methods). London: BSI, 2003, Vol.19, No.4, pp.423-435.

[2] S.M.Cho, Y.S.GU and S.B. Kim, "Extracting Optimization and Physical Properties of Yellow Fin Tuna (*Thunnus Albacares*) Skin Gelatine Compared To Mammalian Gelatines'. Food Hydrocolloids, 2005, Vol.19, pp.221- 229.

[3] C.S.Cheow, M.S.Norizah, Z.Y.Kyaw and N.K. Howell, "Preparation and Characterisation of Gelatine From the Skins of Sin Croaker (*Johnius Dussumieri*) and Shortfin Scad (*Decapterus Acrosoma*)", Food Chemistry, 2007, Vol.101, pp.386-391.

[4] M.D.Fernandez Diaz, P. Montero and M.C. Gómez-Guillén, "Effect of Freezing Fish Skins On Molecular and Rheological Properties of Extracted Gelatine", Food Hydrocolloids, 2003, Vol.17, pp.281-286.

[5] M. C.Gómez-Guillén, J.Turner, M.D. Fernandez Diaz, N.Elmo,M. A.Lizarbe and P. Montero, "Structural and Physical Properties of Gelatine Extracted From Different Marine Species: A Comparative Study", Food Hydrocolloids, 2002, Vol.16, No.1, pp.25-34.

[6] M.Gudmundsson, "Rheological properties of fish gelatine", Journal of Food Science, 2002, Vol.67, No.6, pp.2172-2176.

[7] B. Jamaal and K.G. Harbinger, "Properties of Gelatin From Skins of Fish-black Tilapia (*Oreochromis Mossambicus*) And Red Tilapia (*Oreochromis Militia*)", Food Chemistry, 2002, Vol.77, pp.81-84.

[8] H.Liu, D.Li and S. Guo, "Rheological Properties of Channel Catfish (*Ictalurus Punctual*) Gelatine From Fish Skins Preserved By Different Methods", LWT Food Science and Technology, Moeljanto.1992. Pengawetan dan pengolahan hasilperikanan. Jakarta: Penebar Swadaya, 2008, Vol.41, pp. 1425-1430.

[9] P.Montero and M.C.Gómez-Guillén, "Extracting Conditions for Megrim (*Lepidorhombus Boscii*) Skin Collagen Affect Functional Properties of the

Resultant Gelatin", Journal of Food Science, 2000, Vol.65, pp.434-438.

[10] J.H.Muyonga, C.G.B.Cole and K.G. Duodu, "Extraction And Physio-chemical Characterisation of Nile Perch (*Lates Niloticus*) Skin And Bone Gelatin", Food Hydrocolloids, 2004, Vol.18, pp.581-592.

[11] M. C.Gómez-Guillén, J. Turnay, M.D. Fernández-Díaz, N.Ulmo, M. A.Lizarbe and P. Montero, "Structural And Physical Properties Of Gelatin Extracted From Different Marine Species: A Comparative Study", Food Hydrocolloids, 2002, Vol.16, No.1, pp.25-34.

[12] M.Gudmundsson, "Rheological properties of fish gelatins.Journal of Food Science, 2002, Vol.67, No.6, pp.2172–2176. B.Jamilah, and K.G. .Harvinder, "Properties Of Gelatins From Skins of Fish-black Tilapia (*Oreochromis Mossambicus*) and Red Tilapia (*Oreochromis Nilotica*)", Food Chemistry, 2002, Vol.77, pp.81-84.

Experimental Studies on a Dual Fuel Diesel Engine

Abhishek Sharma[1], V. Meda[2] and S. Murugan[3]
[1,2&3]Department of Mechanical Engineering, National Institute of Technology, Rourkela, Orissa, India
E-mail: abhisharma1998@gmail.com, recmurugan@yahoo.co.in

Abstract

Gaseous fuels such as LPG, CNG, hydrogen; acetylene and producer gas are considered as potential alternative fuels for the existing petroleum fuels for IC engines. They offer potential reduction in particulate emission and increased thermal efficiency in comparison with diesel operation when they are used in dual fuel mode. In the present study, experiments have been conducted to find the effective distance at which acetylene can be inducted in a single cylinder, four stroke, air cooled, direct injection, diesel engine developing power of 4.4kW at 1500 rpm. Acetylene with a minimum flow rate of 2lpm was inducted at four different locations 24cm, 40cm, 56cm and 70cm from the intake manifold of the engine.Experimental results showed thatacetylene inducted at 56cm gave a better performance and lower emissions in comparison with the induction of acetylene at 24cm, 40cm and70cm at full load.

Keywords: *Acetylene,Diesel engine, Dual fuel operation, Emission, Performance*

1. INTRODUCTION

The enormous growth of the world's population in the last few decades, technical developments and increase in standard of living in the developed nations resulted in twin crisis; fossil fuel depletion and environmental pollution. Therefore, there was a serious thought arised throughout the world to search for suitable alternative fuels for internal combustionengines. Fuels which are renewable, clean burning and produced easily are of more interest. In recent years many research works have been carriedout on the utilization of biogas, liquefied petroleum gas (LPG), natural gas, hydrogen as alternative fuels in spark ignition (SI) engines. As they have high self-ignition temperatures,they cannot be as fuel used directly in compression ignition (CI) engines. These engines however can be made to use the gaseous fuels on dual fuel mode. In this mode, a gaseous fuel called primary fuel is inducted along with intake air into the cylinder and compressed, but does not auto-ignite due to its very high self-ignition temperature. Ignition of homogeneous mixture of air and gas is achieved, by injection of small quantity of diesel called pilot fuel near the end of the compression stroke. The pilot diesel fuel auto-ignites first and acts as a deliberate source of ignition for the primary fuel–air mixture. The combustion of the gaseous fuel occurs by the flame initiation by auto-ignition of diesel pilot injection at unspecified location in the combustion chamber. This ignition source can develop into propagation flame, similar to SI engine combustion. Thus, dual fuel engine combines the features of both SI and CI (compression ignition) engine in a complex manner [1].

Some researchers studied the use of acetylene in diesel engine with different induction techniques,such as manifold induction,manifold injection, port injection etc.Karim [2] did an extensive research to understand the nature of the combustion process in the dual fuel mode in CI engines. He used variety of gases like methane, ethane, propane, butane, hydrogen, ethylene, and acetylene as primary fuel. He proved that the performance of dual fuel engines, irrespective of the type of gaseous fuel employed, is better at medium and high loads. However, it has been reported that at low outputs the efficiency is slightly inferior to the diesel engine. Researchers have stressed the need to control the quantity of both pilot and gaseous fuel depending on load conditions for better performance.

B.B.Sahoo *et al* [3] reviewed few workson performance, combustion and emission characteristics of dual-fuel engines which use natural gas, biogas, producer gas, methane, liquefied petroleum gas, propane, etc. as gaseous fuel. Different engine operating and design parameters, namely, load, speed, pilot fuel injection timing, pilot fuel mass, compression ratio, inlet manifold conditions, and type of gaseous fuel, that play an important role in the performance of dual-fuel diesel engines were considered for the review. There was a minor reduction in power output and higher BSFC for the engines. Lower peak cylinder pressure was noticed for a dual-fuel engine compared to the normal diesel engine at a given load condition, which is encouraging since no danger exists for the engine structure. The rate of pressure rise increased with increase in load and was

always higher than that of diesel fuel case. Combustion duration was found to be longer for dual fuel operation compared to diesel operation at low load. Lower NO_x and drastic decreased in soot emissions with all gaseous fuels. But, at all load conditions, CO and HC emissions were considerably higher compared tothat diesel operation. With respect to the engine speed, the thermal efficiency improves with increasing engine speed. Maximum combustion pressure was slightly higher than the diesel fuel level at constant engine speed. There was an improvement in thermal efficiency and torque output noticed by increasing the amount of pilot fuel. Early knocking was observed with increase in the amount of pilot fuel at high loads. Increasing the pilot fuel and reducing primary fuel reduced the knocking phenomena. By increasing the amount of pilot fuel, higher NO_x and reductions in CO and UBHC were noticed.

Wulff *et al* [4] studied the behavior of diesel engine by sending acetylene as primary fuel and diesel as pilot fuel in dual fuel mode at different power outputs and different speeds. Positive results like reduction in NO_x, HC and CO emissions were achieved in comparisons with diesel fuel operation in the same engine. G.Nagarajan and T.Lakshamanan [5] conducted experiments on a diesel engine aspirated acetylene along with air at different flow rates without dual fuel mode. They carriedout the experiments on a single cylinder, air cooled, direct injection (DI), diesel engine designed to develop the rated power output of 4.4 kW at 1500 rpm under variable load conditions. Acetylene aspiration results came with a lower thermal efficiency reduced smoke, HC and CO emissions, compared to that of baseline diesel operation. With acetylene induction, due to the high combustion rates the NO emission significantly increased. The peak cylinder pressure and maximum rate of pressure rise also increased in the dual fuel mode of operation due to the higher flame speed. It was concluded that the induction of acetylene could significantly reduce smoke, CO and HC emissions with a small penalty on efficiency. T.Lakshamanan *et al* [6] conducted experiments to study the performance and emission characteristics of DI diesel engine in dual fuel mode of operation by aspirating acetylene gas at constant 3lpm in the inlet manifold for various loads with diesel as an ignition source. The brake thermal efficiency in the dual fuel mode was found to be lower than that of diesel operation at full load, as a result of continuous induction of acetylene in the intake.

The present research work is aimed to determine the optimum length at which acetylene can be inducted in the intake manifold of a single cylinder, four stroke, air cooled, direct injection, diesel engine developing power output of 4.4kW at 1500 rpm running on a dual fuel mode. Acetylene gas with a flow rate of 2lpm was inducted at different locations viz., 24cm, 40cm, 56cm and 70cm away from the manifold of the intake.The performance and emmision parameters of the engine were evaluated,analysed,compared with diesel fuel operation and presented in this paper.

2. PROPERTIES OF ACETYLENE GAS

Table 1 gives the comparison of physical and combustion properties of acetylene, with other gaseous fuels. The properties of diesel, the pilot fuel were showed in Table 2.

Acetylene gas has low density, high auto ignition temperature and very little ignition energy which are closer to that of hydrogen. The calorific value of acetylene gas is more than that of diesel fuel and sufficient flammability limits. Therefore the acetylene gas can be used as an alternative fuel for diesel engine

3. EXPERIMENTAL ENGINE SETUP

Technical specifications of the engine are given in Table 3 andschematic diagram of experimental arrangement is shownin Figure 1.

Acetylene gas at 2lpm was continuously inducted in the intake pipe at a constant flow rate for all loads. This 2lpm was taken as constant flow rate, because the flow meter used in the study had least value of measurement of 2lpm. Different locations viz., 24cm, 40cm, 56cm and 70cm were chosen based on the standard pipe lengths available in the market that were fitted . These locations were away from the intake manifold of the engine at which the constant flow of acetylene was inducted and diesel injected conventionally in the cylinder.The arrangement for acetylene induction is shown in Figure2.

The acetylene gasenters in to the combustion chamber along with intake air in the suction stroke. In the compression stroke, the air and acetylene gas gets mixed and compressed. At the end of compression stroke diesel was injected conventionally by the injector that was controlled by the governor.

Table 1Comparison of Physical and Combustion Properties of C_2H_2, H_2 and Biogas, CNG, Producer Gas

Properties	Acetylene	Hydrogen	CNG	Biogas	Producer Gas	LPG
Composition	C_2H_2	H_2	Major CH_4 86.4-90%;	Major CH_4 57%	CO, CO_2 CH_4, H_2	C_4H_{10}, 70% C_3H_8- 30%
Density, kg/m^3(At 1 atm & 20 °C)	1.092	0.08	0.72	1.2	1.287	2.26
Auto Ignition temp, K	598	845	723	923	1023	678-723
Flammability Limits ,Volume %	2.5-8.1	4-74.5	5.3-15	7.5-14	17-70	2.25-9.6
Lower Calorific Value,MJ/kg	48.2	120	45.8	17	5	45.7
Ignition Energy ,MJ	0.019	0.02	0.28	-	-	-
Adiabatic Flame Temperature, K	2500	2400	2214	2184	1800	2243
Flame Speed, m/s	1.5	3.5	0.38	.25	.50	.38

Table 2 Physical and Combustion Properties of Diesel

Properties	Diesel
Formula	$C_8 - C_{20}$
Density, kg/m^3(At 1 atm& 20 °C)	840
Auto Ignition Temp, K	527
Boling Point, °C	180-330
Cetane Number	52-55
Stoichiometric Air Fuel Ratio, kg/kg	14.5
Flammability Limits, Volume %	0.6-5.5
Lower Calorific Value, kJ/kg	42,500

Table 3 Engine Specifications

Make/Model	Kirloskar TAF 1
Brake Power, kW	4.4
Rated Speed, rpm	1500
Bore, mm	87.5
Stroke ,mm	110
Piston Type	Bowl-in-piston
Compression Ratio	17.5:1
Nozzle Opening Pressure, Bar	200
Injection Timing,°CA	23
Injection Type	Pump-line-nozzle Injection System
Nozzle Type	Multi hole
No. of Holes	3

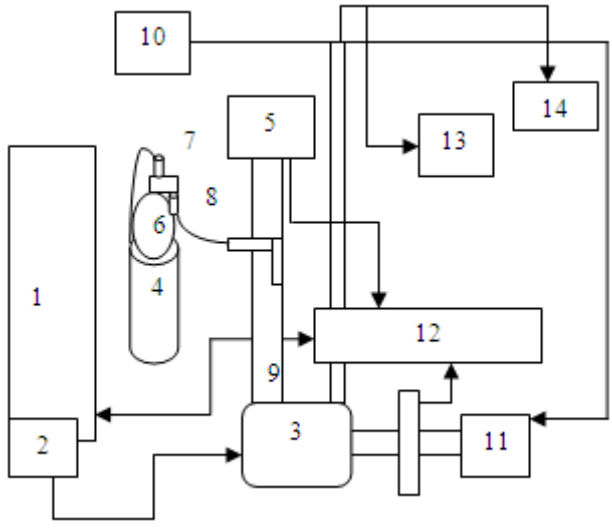

1. Data Acquisition System
2. Fuel Tank
3. Engine
4. Acetylene Cylinder
5. Air Box
6. Pressure Regulator
7. Flow Meter
8. Flash Back Arrestor
9. Intake Pipe
10. Electric Load Cell
11. Electric Dynamometer
12. Data Receive Unit
13. Smoke Meter
14. Exhaust Gas Analyzer

Fig. 1 Schematic diagram of experimental setup

In the dual fuel mode, the combustion reaction starts with pilot fuel and continues with primary fuel. In this work acetylene as a primary fuel for the engine and diesel as a pilot fuel. Acetylene gas has higher calorific value than that of diesel and it compensates some of the energy by diesel. So, there was a reduction noticed in diesel consumption. Diesel acts as pilot fuel to initiate

the combustion reaction at the end of the compression stroke of the diesel engine. The details of instruments used in the investigation are given in Table 4.

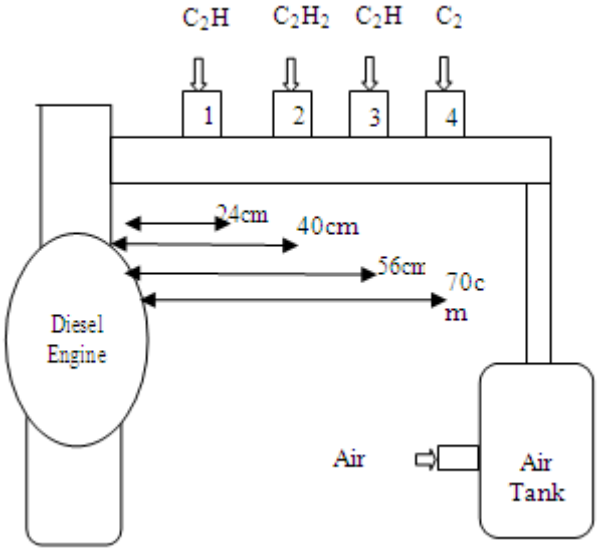

Fig. 2 Acetylene gas inductions at different locations

4. PERFORMANCE PARAMETERS

Performance parameters such as brake thermal efficiency, Brake specific energyconsumption (BSEC) and exhaust gas temperatures in dual fuel mode are compared with diesel and discussed below.

4.1 Brake Thermal Efficiency

Figure 3 portrays the variation of brake thermal efficiency with load for acetylene induction at different locations and diesel.

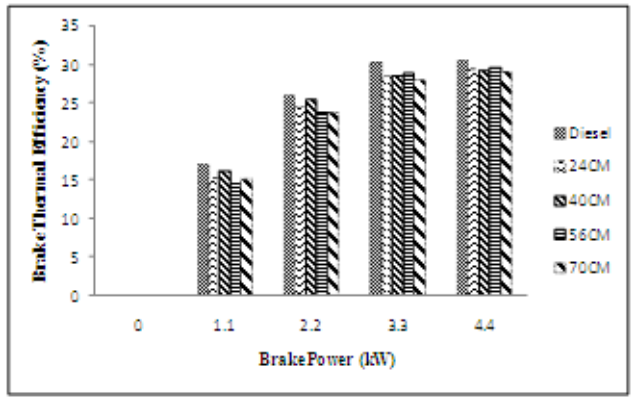

Fig.3 Variation of brake thermal efficiency with brake power

Table 4 Ranges, Accuracy and Uncertainty of the Instruments

Sl. No.	Instrument	Range	Accuracy	Uncertainty
1	Load Indicator	250-6000W	±10W	0.2
2	Temperature Indicator	0-900	±1 °C	0.1
3	Burette	1-30cc	±0.2 cc	1.0
4	Speed Sensor	0-10,000 rpm	±10rpm	0.1
5	Exhaust Gas Analyser	NO-0-5000 ppm	±50ppm	1
		HC-0-20000 ppm	±10ppm	0.5
		CO-0-10%	0.03%	1
6	Smoke Meter	0-100%	±1 %	1
7	Pressure Transducer	0-110bar	±0.1bar	0.15
8	Crank Angle Encoder	0-720	±0.2°	0.5

It can be observed from the figure that for acetylene induction and diesel the brake thermal efficiency increases with increase in load. It can also be observed that the brake thermal efficiency of acetylene induction is higher than that of diesel at full load at 70 cm. Higher thermal efficiency is result of better mixing of acetylene with the combustible mixture in the time availableformixing. The brake thermal efficiency decreases while acetylene is inducted as supplementary fuel. The brake thermal efficiency marginallydecreases with acetylene induction of 2lpm irrespective of length due to high combustion rate and fast energy release [3]. As the induction distance increases away from engine to 24cm, 40cm, 56cm the brake thermal efficiency increases up to 56cm then it decreases at 70cm. The reason may be due to the time for mixing of gas and air increases and diesel may be unable to mix properly with air alone. The thermal efficiency of the engine was

28.54%, 29.30%, 29.62% and 29.06% at full load, when acetylene was inducted at 24cm, 40cm, 56cm and 70cm respectively of full load.

4.2 Exhaust Gas Temperature (EGT)

Figure 4 shows the variation the between exhaust gas temperature and brake power. The exhaust gas temperature increases with acetylene induction in comparison with diesel operation throughout the load specimen. This may be due to more energy input with acetylene gas. The EGT varies from 120°C to 366°C for diesel operation from no load to full load respectively. There is no much deviation observed in the exhaust gas temperature from no load to full load for induction of acetylene at different locations, except for the acetylene induction at 56cm away from the engine intake manifold. The exhaust gas temperature reaches to 385°C while gas was inducted at 56cm away from the engine. The increase in exhaust gas temperature while inducting acetylene gas may be due to some of the heat released by the combustible mixture that later part of the even expansion stroke.

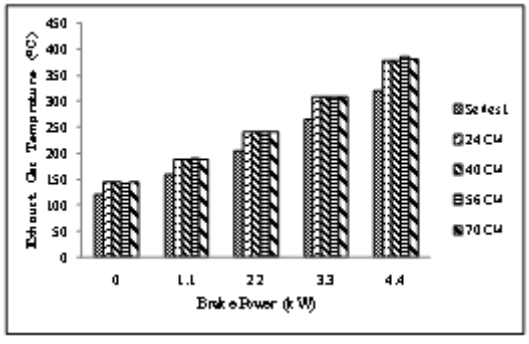

Fig.4 Variation of exhaust gas temperature with brake power

4.3 Brake Specific Energy Consumption(BSEC)

The variation of brake specific energy consumption with brake powerfor the all locations for acetylene induction is depicted in Figure 5. Induction of acetylene provides more energy share compared to that of diesel and hence the brake specific energy consumption decreases. The BSEC for diesel is in the range of 21.8MJ/kWh to 11.7MJ/kWh from no load to full load respectively. When the location of acetylene induction is at56cm and 70cmaway from the engine the energy consumption is more compared to that of diesel operation. BSFC for acetylene induction at 24, 40, 56, and 70cm is in between 23.51 to 12.18MJ/kWh, 22.05to12.18MJ/kWh, 24.62 to 12.14MJ/kWh and 23.88 to 12.38MJ/kWh respectively from no load to full load condition.

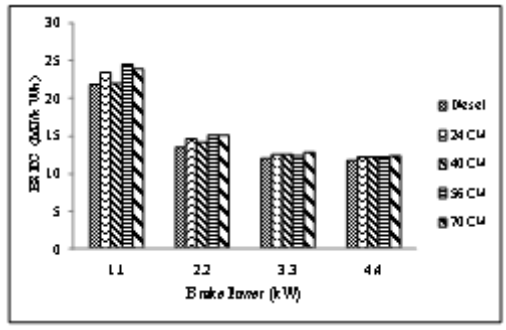

Fig.5 Variation of brake specific energy consumption with brake power

5. EMISSION PARAMETERS

Emissions such as carbon monoxide, unburnt hydrocarbon and nitric oxide that exhausted from the acetylene dual fueled engine are compared with that of diesel operation and discussed in this section.

5.1 Carbon Monoxide (CO) Emission

Figure 6 shows that the CO emission values are higher for acetylene induction of 2lpm at all locationstested exceptfor induction length of 56cm.

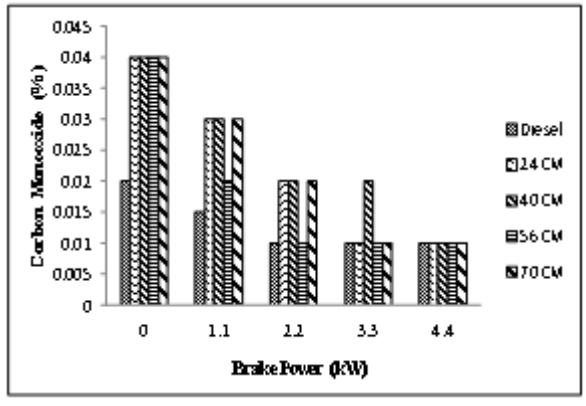

Fig. 6 Variation of carbon monoxide with brake power

Carbon monoxide present in the exhaust gas is due to unavailability of oxygen during the combustion process. Poor mixingmay also be the reasonfor CO emissions [27] .The carbon monoxide values for diesel are in range of 0.02% to 0.01% at no load to full load. Some amount of acetylene gas replacing the air in the intake pipe that leads to insufficient of air for proper combustion and fuel becomes rich mixture. This may be the reason for more CO emissions while using acetylene gas as fuel. But, at full load the values of CO are closer to diesel

operation. It can also be found that at low loads, the acetylene induction results in more CO emissions due to improper mixing and availability of oxygen at some places in the combustion chamber. The CO values are same for all induction lengths and it is same for diesel operation at full load.

5.2 Unburnt Hydrocarbon (UHC) Emission

Figure 7 shows the variation of UHC emissions for different induction lengths of acetylene and for diesel. Because of non-homogeneity of the fuel air mixture some local spots in the combustion chamber will be too lean to combust properly. Other spots may be too rich, without enough oxygen to burn all the fuel. With under mixing some fuel particles in fuel rich zone never react due to lack of oxygen. Bythe induction of acetylene at 2lpm, there was a little replacement of intake air by acetylene which might cause low volumetric efficiency and lead to improper mixing of fuel [27]. The UHC emissions for diesel range from 22ppm to 14ppm from no load to full load respectively. The UHC emission at full load is13ppm,12ppm,12ppm and 16ppm of acetylene induction at 24cm,40cm,56cm and 70cm respectively. It shows that, when acetylene induction was 56cmaway from the engine manifold, gave less UHC in comparison with other induction lengths and diesel operation also.

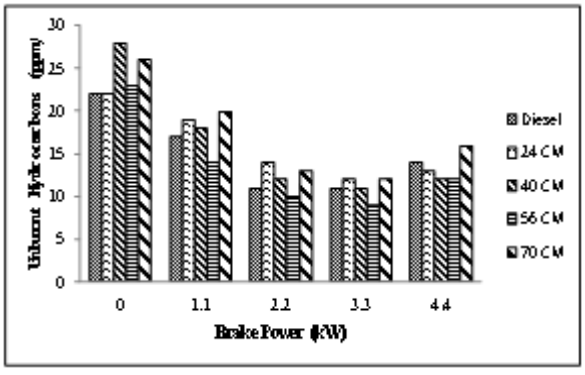

Fig.7 Variation of unburnt hydrocarbons with brake power

5.3 Nitricoxide (NO) Emission

Figure 8 shows the values of NO emissions for acetylene and diesel operation. Nitric oxide emissions are resulted by attaining very high temperatures and oxygen availability in the combustion chamber [27]. The NO emission for diesel is 502ppm at full load. For acetylene induction of 2lpm, the values are 560ppm, 533ppm, 518ppm and 520ppm at full load for 24cm, 40cm, 56cm and 70cm away from intake manifold of the engine respectively.

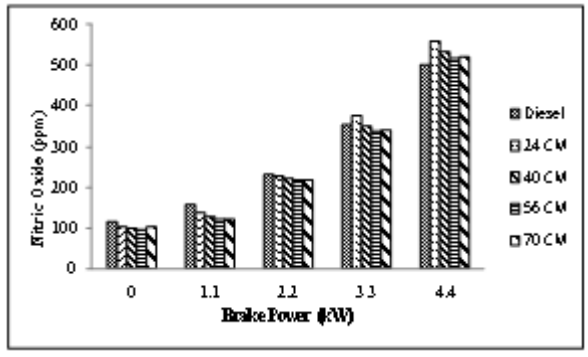

Fig.8 Variation of nitric oxide with brake power

As the induction distance increases away from the engine the NO emissions decreases up to induction of acetylene at 56cm and further marginally increases. The increase in NO emissions is due to increase in temperature and in cylinder pressure, compared to that of diesel operation [15].

6. CONCLUSIONS

The performance and emission of a single cylinder, four stroke, and air-cooled DI diesel engine of 4.4 kW running on dual fuel mode were evaluated, when acetylene at 2lpm was inducted along with air at 24cm, 40cm, 56cm and 70cm from the intake manifold. The results were also compared with diesel operation. The conclusions of the investigation are summarized and given below.

i. The brake thermal efficiency increases with increasing the induction distance from 24cm to 56cm at full load. The brake thermal efficiency of dual fuel engine at flow rate of 2lpm inducted at 56cm is 29.54% which is higher than the induction of acetylene at other locations.
ii. By inducting of acetylene gas at 2lpm, the diesel consumption is reduced by about 6 % to the normal diesel operation.
iii. The CO values increase with acetylene induction different locations tested than diesel operation. But, the CO values for induction of acetylene at 56cm are less than that of induction at other locations.
iv. The UHC values increase with inducting acetylene gas and decreases with induction length. While acetylene was inducted at 56cm, the UHC emissions are less compared to diesel operation and induction of acetylene at other locations.
v. NO emissions increase while inducting acetylene gas. By increasing the induction length away from the engine the NO emissions decrease and less for acetylene induction at 56cm.

vi. Based on the performance and emission parameters, the location of induction at 56cm is optimized.

REFERENCES

[1] S.Swaminathan, J.M.Mallikarjuna and A.Ramesh, "Effect of Charge Temperature And Exhaust Gas Re-Circulation on Combustion and Emission Characteristics of Acetylene Fuelled Hcci Engine", Fuel, 2010, Vol.89, pp.515-521.

[2] G.A. Karim, "The Knock In Dual-Fuel Engine", N.P.W. Moore ProcInstnMechEngrs, 1966-67, Vol.181, pp.453-466.

[3] B.B.Sahoo and N.Sahoo"Effect of Engine Parameters and Type of Gaseous Fuel On the Performance of Dual-Fuel Gas Diesel Engine- A Critical Review", *et al*. Renewable and Sustainable Energy Reviews, 2009, Vol.13, pp.1151-1184.

[4] Wulff *et al*, "Dual Fuel Composition Including Acetylene for Use with Diesel and Other Internal Combustion Engines", Patent No: US 6,287,351 B1, Patent Date: Sep11, 2001.

[5] T.Lakshmanan and G.Nagarajan,"Experimental Investigation on Dual Fuel Operation of Acetylene in a Di Diesel Engine", Fuel Processing Technology, 2010, Vol.91, pp.496-503.

[6] T.Lakshmanan and G.Nagarajan, "Performance and Emission of Acetylene-Aspirated Diesel Engine", Jordan Journal Of Mechanical And Industrial Engineering, June 2009, Vol.3, No.2.

[7] T.Lakshmanan and G.Nagarajan, "Study on Using Acetylene In Dual Fuel Mode With Exhaust Gas Recirculation", Energy, 2011, Vol.36, pp.3547-3553.

[8] John W.H.Price, "An Acetylene Cylinder Explosion: A Most Probable Cause Analysis" , Engineering Failure Analysis, 2006, Vol.13, pp.705-715

[9] T.Lakshmanan and G.Nagarajan, "Experimental Investigation of Port Injection of Acetylene In Di Diesel Engine In Dual Fuel Mode", Fuel 2011, Vol.90, pp.2571–2577.

[10] G.A.Rao and A.V.S.Raju, "Performance Evaluation of A Dual Fuel Engine(Diesel+LPG)", *et al*. Indian Journal of Science and Technology, March 2010, Vol.1, No.3.

[11] K.Sudheesh and K.M.Mallikarjuna, "Effect of Cooling Water Flow Direction on Performance of an Acetylene Fuelled HCCI Engine", Indian Journal of Engineering And Material Sciences, Apr, 2010, Vol.17, pp.79-85.

[12] Okjoo Park, Peter S.Veloo, "Combustion Characteristics of Alternative Gaseous Fuels", *et al*. Proceedings of Combustion Institute, 2010.

[13] Mohamed Y.E.Selim, "Sensitivity of Dual Fuel Engine Combustion and Knocking Limits to Gaseous Fuel Composition", Energy Conversion and Management, 2004, Vol.45, pp.411-425.

[14] Mohamed Y.E.Selim, "Effect of Engine Parameters and Gaseous Fuel Type on the Cyclic Variability of Dual Fuel Engines", Fuel, 2005, Vol.84, pp.961-971.

[15] T.Lakshmanan and G.Nagarajan, "Experimental Investigation of Timed Manifold Injection of Acetylene in Direct Injection Diesel Engine In Dual Fuel Mode", Energy, 2010, Vol.35, pp.3172-3178.

[16] H.E. Saleh," Effect Of Variation In LPG Composition On Emissions And Performance in a Dual Fuel Diesel Engine", Fuel, 2008, Vol.87, pp. 3031–3039.

[17] L.M. Das,"Hydrogen Engine Research And Development (R&D) Programs in Indian Institute of Technology (IIT)", Int. J. Hydrogen Energy, Vol. 27, 2002, 953-965.

[18] M. SenthilKumar,"Use Of Hydrogen To Enhance The Performance Of a Vegetable Oil Fuelled Compression Ignition Engine", International Journal of Hydrogen Energy, 28 (2003) 1143–1154.

[19] Stanislaw Szwaja, Karol Grab-Rogalinski,"Hydrogen Combustion In A Compression Ignition Engine",International journal of hydrogen energy, 34 (2009) 4413–4421.

[20] C.M. White_, R.R. Steeper, A.E. Lutz, "The Hydrogen-Fueled Internal Combustion Engine: A Technical Review", International Journal of Hydrogen Energy, 31 (2006) 1292 – 1305.

[21] MurariMohon Roy, Eiji Tomita, Nobuyuki Kawahara, Yuji Harada, Atsushi Sakane,"Performance And Emission Comparison of a Supercharged Dual-Fuel Engine Fueled By Producer Gases With Varying Hydrogen Content", International Journal Of Hydrogen Energy, 2009, Vol.34, pp.7811-7822.

[22] M.A. Escalante Soberanis and A.M. Fernandez, "A Review on the Technical Adaptations for Internal Combustion Engines to Operate With Gas/ Hydrogen Mixtures", International Journal of Hydrogen Energy, 2009, pp.1-7.

[23] L.M.Das, "Fuel Induction Techniques for a Hydrogen Operated Engine", International Journal Hydrogen Energy, 1990, Vol 15, No.11, pp.833-842.

[24] V Edwin Geo ,"Studies On Dual Fuel Operation Of Rubber Seed Oil and Its Bio Diesel With Hydrogen as Inducted Fuel", *et.al*, International Journal Hydrogen Energy. 2008, Vol.33, pp.6357-6367.

[25] N.R.Banapurmath, "Experimental Investigations of a Four-Stroke Single Cylinder Direct Injection Diesel Engine Operated On Dual Fuel Mode With Producer Gas As Inducted Fuel And Honge Oil And Its Methyl Ester(Home) As Injected Fuels", *et al*, Renewable Energy, 2008, Vol. 33, pp.2007-2018.

[26] K.Purushotham, "Performance, Combustion and Emission Characteristics of Compression Ignition Engine Operating on Neat Orange Oil", *et.al,* Renewable energy, 2009, Vol.34, pp.242–245.

[27] V. Ganesan, "Internal Combustion Engine. 3rd ed",Singapore, McGraw Hill Book Company; 2007.

[28] J.B. Heywood, "Internal Combustion Engine Fundamentals", Singapore: McGraw Hill Book Company; 1998.

[29] R.K.Rajput, "Thermal Engineering", Seventh Edition, Laxmi Publication, 2009.

[30] Website-http://encyclopedia.airliquid.com

A 3D Smart Actuator for Robotic Eyes Industrial Applications Using A Flexural Vibration Ring Transducer

M. Shafik[1], B. Nyathi[2] and S. Fekkai[3]
[1]School of Technology, University of Derby, UK, [2]Associate Lecturer, University of Derby, UK
[3]Pera Innovation Ltd, UK.
E-mail: uk.linkedin.com/pub/mahmoud-shafik/7/237/60

Abstract

This paper presents a 3D piezoelectric ultrasonic actuator using a single Flexural Vibration Ring Transducer. The actuator consists of three main parts, the rotor, the stator and the housing unit. The stator is a piezoelectric transducer ring made of PZT S42 material. Three steel rods and a magnet were designed to support the rotor. The rotor is a sphere of metal size of 28mm that rests on the stator intersecting at the tips of the steel rods and the magnet. The housing unit is made of Perspex, a transparent thermoplastic material. Longitudinal and bending vibration modes, of oscillating structures are superimposed in the actuator, generating elliptical micro motions at the driving tips. Pressing the rotor against the stator tips the micro motions are converted into a 3D rotational motion via the friction between the tips of the three rods and the rotor. The actuator structures, working principles, design and finite element analysis are discussed in this paper. A prototype of the actuator was fabricated and its characteristics measured. Experimental tests show typical speed of movement equal to 35 revolutions per minute, a resolution of less than 5ìm and maximum load of 3.5 Newton.

Keywords*: Mechatronics, Piezo-actuator industrial applications, Ultrasonic motor, 3D Ultrasonic motor*

1.INTRODUCTION

Ultrasonic motors (USM) principles of operations are based mainly on the concept of driving the rotor by a mechanical vibration force generated on the stator (Lead Zirconate Titanate (PZT) Transducer) via piezoelectric effect. USM can be classified into two main categories based on the PZT working mode, bonded type motors [1-5] and bolt-clamped type motors [6-8]. USM have compact size, high force density, and simple mechanical structure, slow speed without additional gear or spindle, high torque, non-magnetic operation, freedom for constructional design, very low inertia, fast dynamic time responses, direct drive, fine position resolution, miniaturization and noiseless operation. These criteria gave them the potential to be used in a number of industrial applications [9-17]. Demanding and careful examination for these applications reveals that there are apparent teething issues. The first is in regard to the dynamic response of the actuator and its transfer function. While a piezo-ceramic element, typically PZT, expands in direct proportion to the magnitude of the applied voltage, the USM on the other hand accumulates those displacements over time. Therefore the transfer function of the motor, relating to the magnitude of the driving signal to the displacement is an integrator [14, 17-18] and this shows a delay in the dynamic response of the USM, but it is not nearly significant as that in an electromagnetic servomotor. The second issue is that because motion is generated through a friction force therefore it has a dead band. Often USM does not move until the input signal is greater than 10% of the maximum allowed voltage to overcome the friction, such a dead band limits the ability of USM to accelerate quickly [1, 17-18].

2. STRUCTURE OF THE PROPOSED USM

Fig. 1 shows the actuator structure. It has three main parts, which are the stator, the rotor and the housing unit. The stator is a PZT transducer ring, made of PZT S42 material. Three titanium rods and a magnet were designed to support the rotor. The rotor is a sphere of Aluminum of size 28mm that rests on the stator intersecting at the tips of the rods. The structure is housed by Perspex, a transparent thermoplastic material. The working principle is based on creating elliptical motions of surface points generated by superposition of longitudinal and bending vibration modes of oscillating structures. By pressing the rotor against the driving tips of the stator, the micro motions are converted into a 3D rotary motion, through the friction between parts of the motor. However, to create a strong second bending vibration mode, the polarisation direction of the

piezoelectric vibrator is perpendicular to the titanium rods; the piezoelectric ceramic vibrator was arranged as shown in Fig. 2. The longitudinal and bending vibration modes are coupled by asymmetry of the piezoelectric ceramic vibrator [4, 14, 16]. The vibration energy across the PZT ring causes the titanium rods, A, B and C to have elliptical micro motion causing the rotor to move in 3D. The rotor movement is caused by the sequential frictional force generated at the tip of each rod.

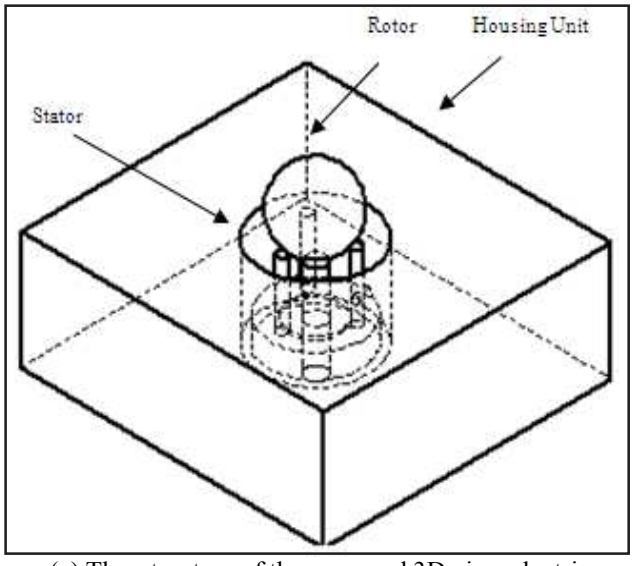

(a) The structure of the proposed 3D piezoelectric ultrasonic motor aluminum ball

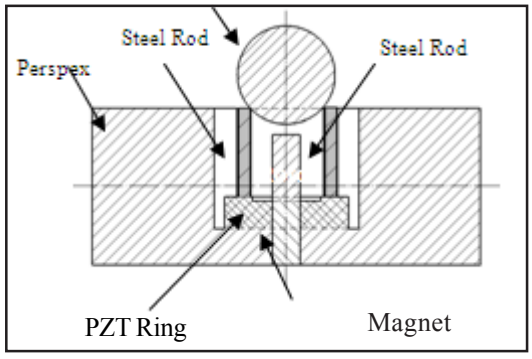

(b) Side section view of the proposed 3D piezoelectric ultrasonic motor

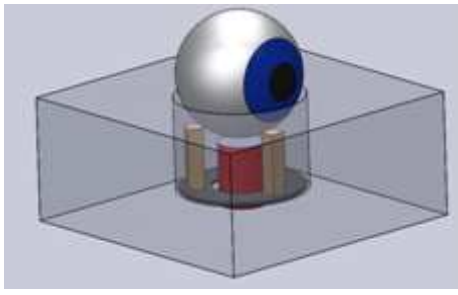

(c) 3D Sold modelling of the actuator for use as a robotic eyes

Fig.1 Structure of the proposed 3D piezoelectric ultrasonic actuator

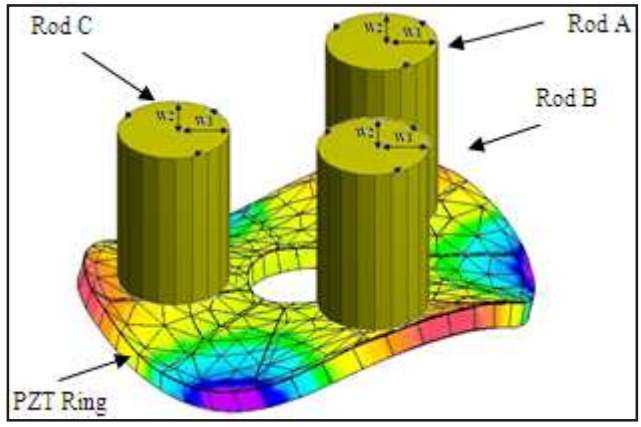

Fig. 2 Configuration of the proposed USM stator and principles used to generate 3D motion

The following equations (1) and (2) represent the vibrations of the displacement in the parallel and perpendicular direction of the travelling wave generated by the flexural vibration ring transducer, respectively.

$$X_A = W_1 \cos(2\pi f_1 t + \alpha) \quad (1)$$

$$Y_A = W_2 \cos(2\pi f_1 t + \alpha) \quad (2)$$

Where X_A and Y_A is the possible displacement in parallel and perpendicular direction, respectively. W_1 and W_2 are the maximum vibration amplitudes in the horizontal and vertical directions respectively, f_1 is the resonant frequency, and t is the time.

3. USM ACTUATOR WORKING PRINCIPLE

The proposed actuator is designed using standing wave vibrations, which has a fixed wave length. The concept is to utilise two modes of vibrations as shown in Fig. 2 to obtain the desired motion of the piezoelectric element longitudinal and transverse (bending) vibrations, one vibration produces a normal force while the other vibration generates thrust force, which is perpendicular to the normal force, resulting in an elliptical trajectory of micro motion at a number of the rig surface, by attaching three perpendicular rods, with 120 degree separation angle, to the piezoelectric ceramic ring surface (stator). The micro elliptical motion transferred to the rods tips is converted into a 3D rotational motion based on the friction between the tips and the Aluminum sphere. As the combination of modes of vibrations create a friction based driving force between the stator and the rotor at the contact tips, a movement in bidirectional i.e. forward or backward direction is created depending on the

methodology used to excite the piezoelectric ceramic transducer to generate the modes of vibrations.

4. DESIGN AND ANALYSIS OF THE PROPOSED USM

USM's have many complex non-linear characteristics. Commonly two methods of analysis can be used to simulate and model such types of motors [2, 4, 6, 12-13, 16]. These methods are the Analytical Analysis and the Finite Element Analysis (FEA) methods. FEA has been used in the proposed 3D actuator design process to investigate the material modes of vibration (transverse and bending modes), actuator structure and obtain the actuator technical operating parameters.

Samples of the data used in the proposed actuator modelling are illustrated in tables 1 and 2. The solid structure is divided into small portions named finite elements; an approximate solution for each finite element is generated. A summation of all the approximate solutions of the finite elements is obtained. The finite element analysis of proposed 3D UDM structure has been carried out. The ring has been defined as made of piezoelectric Ceramic S42 and the three rods have been selected as made of titanium material. ANSYS CAE software has been used in this simulation.

As stated in Table 2, the piezoelectric charge constant D_{31} rated as -155 is the working mode of the piezoelectric ring used to excite the bending vibrations of the ring. The D_{31} mode has a lower electromagnetic coupling efficiency compared to the D_{33} (320).

Figure 3 shows the FEA variations of the displacement of the PZT Transducer ring against exciting frequency, for the proposed USM structure. This shows the natural frequency of the proposed structure equal to 39.7 KHz. The natural frequency indicates the dynamic response of the USM and in this case it is on the order of microseconds. This can be calculated roughly as Q times the vibration period. Where Q is the quality factor of the motor, which can be determined using [13-14]:

$$Q = \frac{R_m}{\sqrt{\frac{L}{C_\Sigma}}} \qquad (3)$$

Where R_m is the equivalent resistor of the vibrating transducer at a fixed operating frequency, L is the inductance of the LC-driving circuit and C_Σ is the total capacitance which is not constant and depends on the vibrating transducer internal capacitance, cable internal capacitance and LC-driving circuit capacitance.

Table 1Pzt-s42 Piezo-ceramic Material, Titanium Solid Rods Material, and the Aluminum Ball Material Used in the Proposed USM

Material	*Coefficient (Unit)*	*Value*
PZT-S42	Relative permittivity (Ωm)	1450
	Dissipation Constant (%)	0.4
	Mechanical Quality factor	600
	Density (g/cm^3)	7.6
Titanium Rod	Poisson's ratio	0.32
	Young's Modulus of elasticity (Gpa)	116
	Density (g/m^3)	16.69
Aluminum Ball	Poisson's ratio	0.3
	Young's Modulus of elasticity (Gpa)	70
	Density (g/m^3)	2.7

Table 2 Transformation of E-coefficient to D-coefficient for Piezo-ceramic Material Used in USM Modeling

Material	*Coefficient*	*Value (m/v)*
Piezo-ceramics	D_{31} x10^{-12}	-150
	D_{33} x10^{-12}	320

Figure 4 shows the dynamic model of the proposed USM motor. The dimensions of the stator (PZT Transducer) for such actuator are mainly based on the vibration modes, capacitance ratio, and direction of vibratory displacement obtained using FEA [17, 19, 21-22]. The vibration modes at drawn operating frequency are shown in Figures 5 and 6.

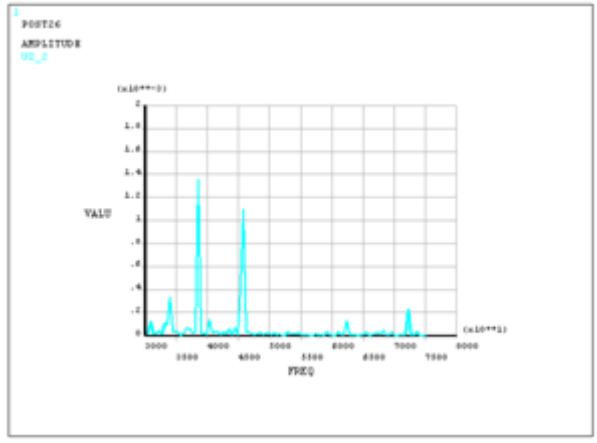

Fig.3 The variations of the PZT vibration ring transducer displacement vs. frequency

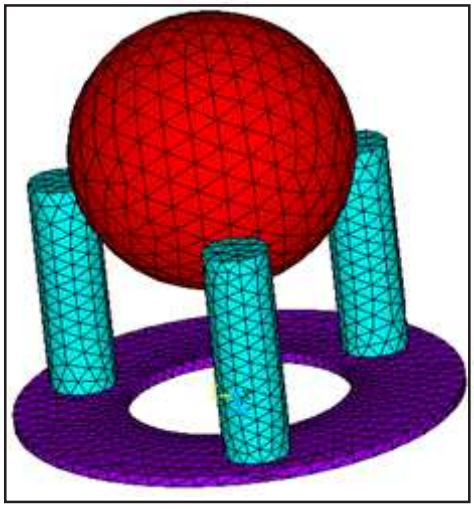

Fig. 4 The FEA dynamic model for the proposed 3D USM motor

4. EXPERIMENTS

A prototype of the USM was fabricated to test and validate the actuator simulation and design principles. The parts of the developed prototype were integrated successfully into the housing of the actuator and a series of experimental tests were carried out to examine the potential characteristics of the developed prototype. Figure 7 shows the fabricated prototype.

The arrangement shown in figures 8 and 9 has been used to test and measure the actuator main characteristics. A piezoelectric driver was used to provide the piezo-ceramic vibrating transducer ring with the alternative driving voltage. A function generator was used to provide various shapes of signal including sinusoidal, saw-tooth and square wave. A display unit, which consists of a digital oscilloscope and PC computer, was used to trace the signal and determine the actuator operating parameters.

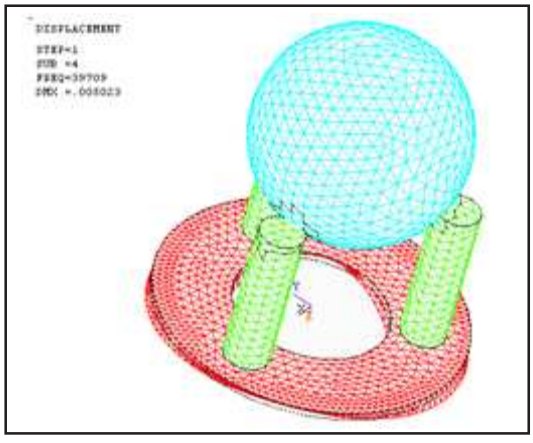

Fig.5 3D USM FEA model at drawn frequency of 39.709 kHz [transverse bending vibration mode]

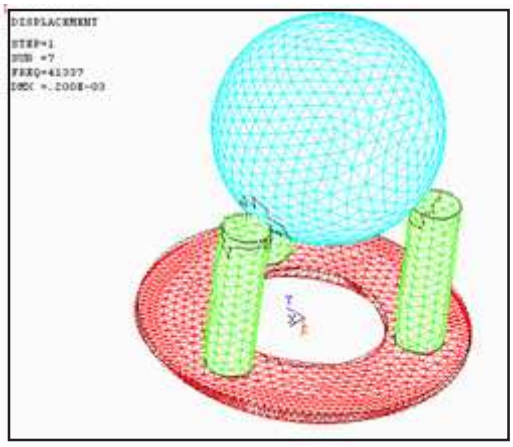

Fig. 6 3D USM FEA model at drawn frequency of 39.709 kHz [transverse bending vibration mode]

A measurement of the operating parameters is carried out using the same arrangement used in the modelling of the actuator as shown in Figure 2. The PZT ring transducer is connected to a single phase AC power source with a wide range of amplitude and frequency. A switching unit has been used to regulate the AC input power to the PZT ring transducer. Then a measurement for both the amplitude and frequency of the AC input signal is carried out. A sine wave input signal for the piezo driver is obtained from the signal generator with the frequency set to 100 kHz range to obtain the appropriate frequencies. The input signal is monitored using the digital oscilloscope and the current is monitored using a digital Multimeter.

A gain of-25-amplification factor was obtained by making the load range of the piezo driver model 603 low. The high voltage output is connected to the positive side of the piezoelectric ring (stator) and the ground of the piezo driver is connected to the negative. The input signal from the signal generator is monitored on the oscilloscope. Voltage ranges of 1V -5V are selected. The voltage was increased in 1V intervals by adjusting the amplitude of the signal generator. The frequency of the input signal is adjusted on the signal generator, by gradually increasing it in 3-5 kHz intervals. The voltage and frequency is increased until the resonance frequency of the piezoelectric ring is reached. This is noted by a series of hissing sound from the ring. The voltage is kept constant, and the frequency is adjusted at 1-2 kHz intervals until a trajectory is obtained. The trajectory is controlled by varying the frequency on the signal generator until a 3D rotational motion is obtained. Then the relation between the driving voltage and current has been obtained and is shown in Figure10.

Fig. 7 Fabricated Prototype of the proposed 3D USM using a single piezo-ceramic flexural vibrating ring transducer

The rotor movement started when the voltage reached 45V and the frequency reached 39.53 KHz. A constant voltage has been chosen of 100VAC, varying the frequency up and down between 38 kHz to 42 kHz, the movement trajectory of the rotor was moving in 3D. The frequency of USM driver has been altered incrementally. The speed of the actuator has been measured for each increment.

It was noticed during this process that the speed of the actuator increases as the frequency of the actuator driver increased. The relation between the speed of movement, voltage and frequency has been determined. Figures 11 and 12 show this relation.

This shows the possibility to control the developed prototype precisely, as the rotor movement was responding precisely to the changes of the voltage and frequency.

Figure 13 shows the variations of the speed of movement against the increase of the load attached incrementally to the sphere.

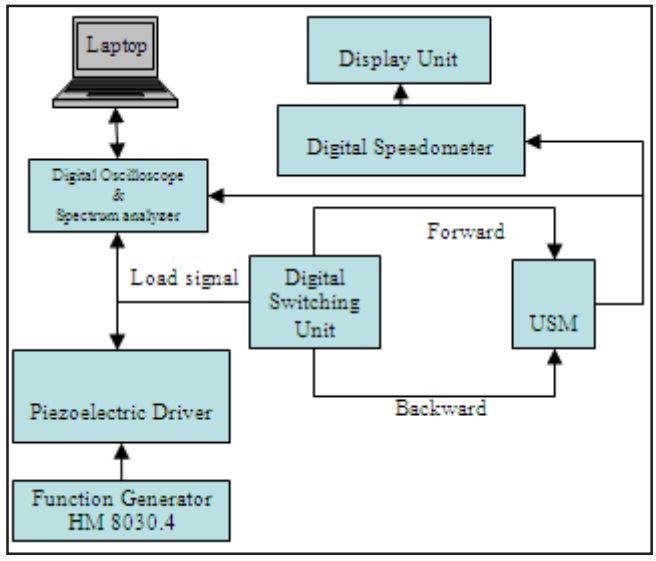

Fig. 8 Block diagram of the test rig used to measure the characteristics of the fabricated 3D USM prototype

Fig.9 Practical test rig used to measure the characteristics of the fabricated 3D USM prototype

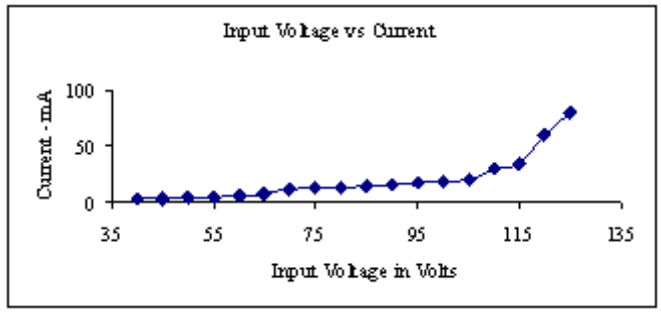

Fig.10 The variation of the current vs. input voltage for the fabricated 3D USM prototype

The power was calculated as the operating parameters were found. Current is equal to 50 mA and voltage is equal to 100 volt. This shows that the overall power to drive such USM is low.

The resolution of the rotor was measured and was found less than 5 micrometer, at nominal operating parameters of voltage of 100VAC, current of 50 mA and frequency of 39.53 KHz.

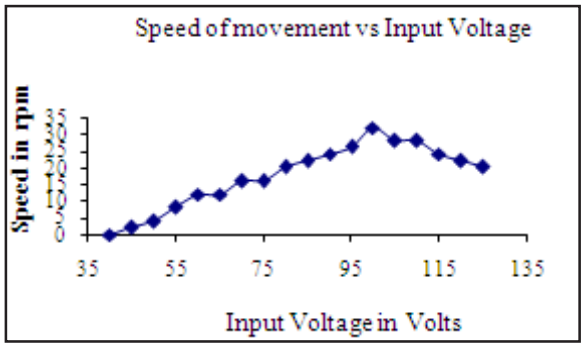

Fig. 11 The variation of the speed of movement vs. input voltage for the fabricated 3D USM prototype

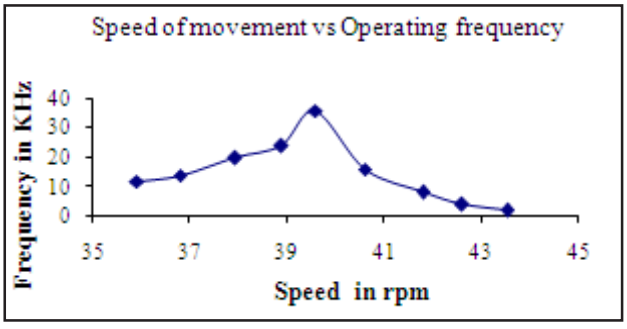

Fig. 12 The variation of the speed of movement vs. the applied frequency for the fabricated 3D USM

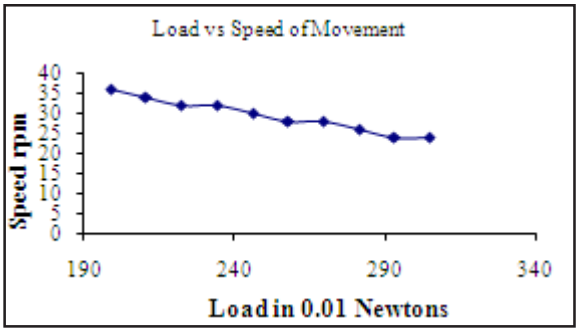

Fig.13 The variation of the speed of movement vs. load for the fabricated 3D USM prototype

5. CONCLUSIONS

A 3D piezoelectric ultrasonic actuator using a single flexural vibration ring transducer has been developed and presented in this paper. The actuator structures, working principles, design and finite element analysis are discussed. A prototype of the actuator was fabricated and its characteristics measured. Experimental tests showed that the operating parameters of the fabricated prototype are: frequency equal to 39.53 KHz, voltage: 100 volt and current: 50 m-amperes and this has demonstrated a close agreement with FEA. The prototype typical speed of movement is equal to 35 revolutions per minute, a resolution of less than 5ìm and maximum load of 3.5-Newton.

REFERENCES

[1] Chunsheng Zhao, "Ultrasonic Motors: Technologies and Applications", Science Press, New York, 2011.

[2] S. Lin, "An Improved Cymbal Transducer with Combined Piezoelectric Ceramic Ring and Metal Ring", Elservier, China, Sensors and Actuators A: Physical Vol.16, 2010, pp.226-276.

[3] D. Engleke, B. Oehme and J. Strackeljan, "A Novel Drive Option for Piezoelectric Ultrasonic Transducers", Hindawi Publishing Corp, Modelling and Simulation in Engineering, Vol.1, 2011, ID 910876, pp.1-6.

[4] J.S. Park, S.T. Kim and J.W. Kim, "Ultrasonic Linear Motor Using L1-B4 Mode and its Analysis", Jpn. J. Appl. Phys. Vol.44 (1A), 2005, pp.412-416.

[5] Yu. G. Martynenko, I.V. Merkuryev and V.V. Podalkov. "Control of Nonlinear Vibrations of Vibrating Ring Microgyroscope", Mechanics of Solids. Vol.43, No. 3, 2008, pp.379-390.

[6] J. Jiamei and Z. Chunsheng, "A Novel Traveling Wave Ultrasonic Motor Using a Bar Shaped Transducer", J.Wuham University of Technology, 2008.

[7] C.H. Yun, T. Ishii, K. Nakamura, S. Ueha and K. Akashi, "A High Power Ultrasonic Linear Motor Using a Longitudinal and Bending Hybrid Bolt-Clamped Langevin Type Transducer", Jpn. J. Appl. Phys., Vol.40, 2001, pp.3773-3776.

[8] F. Zhang, W.S. Chen, J.K. Liu and Z.S. Wang, "Bidirectional Linear Ultrasonic Motor Using Longitudinal Vibrating Transducers", IEEE Trans. Ultrason. Ferroelectr. Freq. Control., Vol.52, No.1, 2005, pp.134-138.

[9] S.J. Shi and W.S. Chen, "A Bidirectional Standing Wave Ultrasonic Linear Motor Based On Langevin Bending Transducer", Ferroelectronics, Vol.35, 2008, pp.102–110.

[10] M. Shafik, J. A. G. Knight and H. Abdalla, "Development Of A New Generation Of Electrical Discharge Texturing System Using An Ultrasonic Motor", 13th International Symposium for Electromachining, ISEM, Spain, May 9th to 11th, , 2001.

[11] M. Shafik, J. A. G. Knight and H. Abdalla, "An Investigation Into Electro Discharge Machining System Applications Using an Ultrasonic Motor", Proceeding of ESM'-2002 International Conference, Belfast, August 28th to 31st, 2002.

[12] M. Shafik and J. A. G. Knight, "Computer Simulation and Modeling of an Ultrasonic Motor Using a Single Flexural Vibrating Bar", Proceeding of ESM'2002 International Conference, Germany, June 3rd to 5th, 2002.

[13] M. Shafik, "Computer Aided Analysis and Design of a New Servo Control Feed Drive for EDM using Piezoelectric USM", PhD Thesis, De Montfort University, Leicester, UK, 2003.

[14] M. Shafik, E. M. Shehab and H. S. Abdalla, "A Linear Piezoelectric Ultrasonic Motor Using a Single Flexural Vibrating Transducer for Electro Discharge System Industrial Applications", Int. J. Adv. Manuf. Technol., 2009, Vol.45, pp.287-299.

[15] He SY *et al*. "Standing Wave Bi-Directional Linearly Moving Ultrasonic Motor", IEEE trans. On Ultrasonic's ferr. and Freq. Control, Vol. 45, No.5, 1998.

[16] J. Satonobu and J. R. Friend, "Travelling Wave Excitation in a Flexural Vibration Ring by Using a Torsional-Flexural Composite Transducer", IEEE Tran on Ultrasonics, Ferroelectrics and Frequency Control, Vol. 48, No. 4, 2001.

[17] H. Tobias and Jorg Wallaschek, "Survey of the Present State of the Art of Piezoelectric Linear Motors", Ultrasonics, Vol.38, 2000, pp.37-40.

[18] Woo Seok Hwang and Hyun Chul Park. "Finite Element Modelling Piezoelectric Sensors and Actuators", AIAAJ, Vol. 31, No. 5, 1993.

[19] Yingxiang Liu, Weishan Chen, Junkao Liu and Shengjun Shi, "A Cylindrical Standing Wave Ultrasonic Motor Using Bending Vibration Transducer", Ultrasonics, Vol.51, 2011, pp.527-531.

[20] S. Ben-Yaakov, *et al*, "A Resonant Driver for a Piezoelectric Motor", Power Conversion and intelligent Motor Conference, June 1999, pp. 173-178.

[21] S. Ueha and Y. Tomikawa, "Ultrasonic Motors Theory and Applications", Clarendon press, Oxford, London, UK, 1993.

[22] Jacob Tal, "Servomotors Take Piezoceramic Transducers for a Ride", Machine Design (ISSN 0024-9114), Penton Media, Inc., USA, 1999.

Speed Estimation of Induction Motor Using Extreme Learning Machine Algorithm

R.Subasri[1] and A.M.Natarajan[2]

[1]Department of Electronics and Instrumentation Engineering, Kongu Engineering College, Perundurai, Erode - 638 052, Tamil Nadu

[2]Department of Computer Science and Engineering, Bannari Amman Institute of Technology, Sathyamangalam - 638 401, Erode Distrcit, Tamil Nadu

E-mail: soamisuba@kongu.ac.in,amnatarajan2006@yahoo.co.in

Abstract

This paper proposes a new method for estimating the speed of an induction motor using neural network. The neural network is trained to follow the relationship between the stator currents, stator voltage and rotor speed. The performance of neural network is analyzed with simulated data from Matlab and also with real time data acquired by interfacing LabVIEW with induction motor. The induction motor is modeled using feed forward neural structure with Extreme Learning Machine (ELM) algorithm and its performance is compared with back propagation algorithm in estimating the speed. The results demonstrate that the proposed neural model of induction motor trained with ELM algorithm can replace the speed sensor used in the closed loop speed control.

Keywords: *ELM, Induction motor, LabVIEW, Matlab, Neural network, Speed estimation.*

1. INTRODUCTION

Traditionally a high performance control of induction motors must require measured data of real time speed as a feedback signal. In order to overcome the disadvantages of speed sensors, such as encoders, resolvers, etc., sensor-less speed control methods of induction motor using the estimated speed instead of the measured speed have been proposed [2], [4], [7]. Many approach such as Model Reference Adaptive System (MRAS) methods, Extended Kalman Filter Algorithms (EKFA), etc. have been implemented to achieve more accurate and robust speed estimation performance [3], [5], [8], [9], [10], [11].

An induction motor is highly coupled, non-linear dynamic plant, and its parameters vary with time and operating conditions. Therefore, it is very difficult to obtain good performance for an entire speed range and transient states using previous methods. Recently, the use of neural networks to identify and control nonlinear dynamic systems has been proposed [15], because they can approximate a wide range non-linear function to any desired degree of accuracy. They have the advantages of extremely fast parallel computation, immunity from input harmonic ripples, and fault tolerance characteristics. Since 1990's, there have been some investigation into the application of artificial neural network to power electronics and DC drives, including speed estimation.

The application of neural networks for induction motor in estimating the speed of induction motor was reported [1], [12], [16], [17]. In most of the papers, the dynamic model of induction motor is based on, either current model or voltage model for speed estimation. To improve accuracy in speed estimation, the relationship between stator currents and speed is modeled using neural network at various load conditions [17].But the drawback is, the variation in stator voltage is not considered.

Recently, a new neural algorithm referred to as Extreme Learning Machine (ELM) is proposed for optimizing the neural parameters [5], [13], [18]. Different from traditional learning algorithms, the proposed learning algorithm will converge to smallest training error and also has good generalization capability. Also this algorithm is extremely faster in training compared to traditional algorithm namely back propagation.

This paper deals with the modeling of induction motor using feed forward neural network architecture trained by Extreme Learning Machine algorithm. The squirrel-cage induction motor under test is modeled with the help of Matlab-Simulink and the transient speed response of the motor for different load conditions is considered. Also the motor is interfaced with LabVIEW to retrieve real time data under various load conditions. The three phase stator currents, stator voltage and the corresponding speed are used as training data for the feed forward neural network and the performance of network is

compared by using two learning algorithms, namely back propagation and ELM. Here the voltage variations are simulated by adding 3rd and 5th harmonics in stator voltage. This paper is organized as follows. Extreme Learning Machine Algorithm is discussed in section II. Section III, discusses speed estimation by neural network with the simulated data generated using Matlab –Simulink model of induction motor and also real time data retrieved by interfacing induction motor with LabVIEW software. In Section IV results are discussed and conclusion follows in section V.

2. EXTREME LEARNING MACHINE ALGORITHM

Many neural network learning algorithms, based on gradient descent techniques are proposed over the past two decades. Among them back propagation is most popular and widely used in various applications such as classification, function approximation, etc. But these algorithms have the limitations such as over fitting, local minima and time consuming. new learning theory called ELM is proposed [18] to overcome these limitations. In ELM, parameters of hidden nodes are not updated during training but selected randomly. Moreover the output weights of the network can be analytically determined through simple generalized inverse operation of the hidden layer output matrices.

According to the ELM theory, a feed forward neural network with single hidden layer with N hidden neurons and activation function $g(x)$ can be modeled, for a given N arbitrary distinct samples (x_i, t_i), where $x_i = [x_{i1}, x_{i2}, \ldots. x_{in}]^T \varepsilon R^n$ and $t_i = [t_{i1}, t_{i2}, \ldots\ldots. t_{im}]^T \varepsilon R^m$, as

$$\sum_{i=1}^{N}\beta_i g_i(x_j)=\sum_{i=1}^{N}\beta_i g(w_i.x_j+b_i)=o_j \quad ,j=1\ldots N, \ldots..(1)$$

Where $w_i = [w_{i1}, w_{i2}, \ldots\ldots. w_{in}]^T$ is the weight vector connecting the i^{th} hidden node and the input nodes, $\beta_i = [\beta_{i1}, \beta_{i2}, \ldots\ldots. \beta_{im}]^T$ is the weight vector connecting the i^{th} hidden node and the output nodes, and b_i is the threshold of the i^{th} hidden node. $w_i.x_j$ denotes the inner product of w_i and x_j. The above N equations can also be written compactly in matrix form as $H\beta=T$.

The three step training algorithm is as follows:

Step 1: Randomly assign input weight w_i and bias b_i, i = 1… N

Step 2: Calculate the hidden layer output matrix H.

Step 3: Calculate the output weight β;$\beta= H^{\dagger} T$ where $H^{\dagger}$ is the Moore-Penrose generalized inverse of hidden layer output matrix H [18].

The ELM algorithm has many special features such as extremely fast learning speed, much simpler, better generalization performance, etc. As this ELM is more suitable in applications which require fast prediction and response capability, its performance is verified for estimating the speed of induction motor, in any speed control applications.

3. SPEED ESTIMATION USING NEURAL NETWORKS

3.1 Data Generation using Matlab Simulink Model

The block diagram representation of three phase squirrel-cage induction motor used for simulation using Matlab-Simulink is shown in Figure 1. The motor is made to run under sudden load torque variations for the time duration of 0 to 1 sec. From 0 to 0.2 sec, the load torque is maintained at 2 N-m and from 0.2 to 0.4 sec; the load torque is changed to 4 N-m. Similarly the motor is simulated with varying load torque as 0, 2,4,8,12,15 N-m for the duration of 1 sec in step of 0.2 sec and the corresponding transient response of three phase stator currents, stator voltage and speed are retrieved for training the neural network. For testing the network, the load variation is simulated as 0, 1, 5, 7, 11, 15 N-m for the same time duration of 0 to 1 sec in step of 0.2 sec.

3.2 Real Time Data Generation using LABVIEW

The laboratory model consists of a three phase induction motor, current to voltage converter, data acquisition (DAQ) card, proximity sensor and the specifications of three phase induction motor are 5HP, 415V, 4.5A, and 1470 rpm. The NI USB-6008 is programmed using LabVIEW to retrieve the stator voltage, stator currents and speed of the induction motor. The maximum DC current that can be allowed by the DAQ card is 500mA. If rectified stator currents within the permissible level are given as input to the DAQ card, it will introduce higher noise level. To overcome this, the stator currents are converted into equivalent voltage signals. The voltage level generally accepted by DAQ 6009 is -10V to +10V DC. Hence, the three phase stator currents of the squirrel cage induction motor are given to a current to voltage converter.

The output of current to voltage converter is interfaced with LabVIEW through DAQ card. Proximity sensor is used for speed measurement. The output of the proximity sensor as pulses which is given to the LabVIEW as voltage pulse signals and the corresponding speed values are displayed in the front panel of the LabVIEW program.

The LabVIEW block diagram developed for retrieving real time data is shown in Figure 2. The pulse measurement block provides the facility to analyze the duty cycle, pulse duration and the time period of the speed signal of induction motor. For the accurate measurement of the speed of the motor, the duty cycle along with the pulse duration is used. The filter block is used to remove any noise in the sensor signal. The resolution of the data to be stored can be specified by the user. The type of sampling that is used is one sample on demand. The maximum sampling rate of the DAQ 6009 is 8000 samples per second. When all the eight channels are used, the sampling is evenly divided between the channels allowing a maximum of 1000 samples per channel. The amplitude of the voltage signal from the converter is in the range of 0-5V. The three voltage signals from converters in each phase are sampled by the DAQ.

4. RESULTS AND DISCUSSION

The input variables selected are three phase stator currents, stator voltage of any one phase and output variable is speed of induction motor. Hence the selected feed forward neural architecture has four input neurons and one output neuron. A single hidden layer with 60 neurons is used and the learning rate parameter is 0.001.The network parameters get converged in 70 epochs. To highlight the effect of load torque variations clearly, the response curve for the simulated data is highlighted for the time period from 0.5 sec to 1 sec. The neural predicted speed using BPN algorithm for the simulated data is compared with the original speed in Figure 3 and the corresponding error curve is shown in Figure 4. The error range is -50 to 50 rpm.

The same neural network is trained using extreme learning machine algorithm. The training time using ELM is 40 sec compared to back propagation algorithm which takes 8 mintues though the number of hidden neurons used in extreme learning machine is 680. The performance of neural network using ELM algorithm is shown in Figure 5 and it is evident that the neural network with ELM algorithm accurately predicts the actual speed and the error range is very less between -0.2 to +0.4 and it is shown in Figure 6. The selected feed forward neural network is also trained with the real time data using the two neural algorithms.

The motor is made to run under various load torque conditions and the sampled values of stator voltage, three phase stator currents and the rotor speed are saved in excel sheet . Out of 245 samples retreived, 200 samples are used for training and remaining 45 samples are used for testing.The neural predicted speed using back propagation algorithm is shown in Figure 7 and the error in prediction is between -40 rpm to +40 rpm as in Figure 8. The performance of the neural network using ELM algorithm is good in predicting the speed compared to BPN algorithm,which is shown in Figure 9. The error range is between -5 rpm to 7 rpm for ELM as in Figure10.

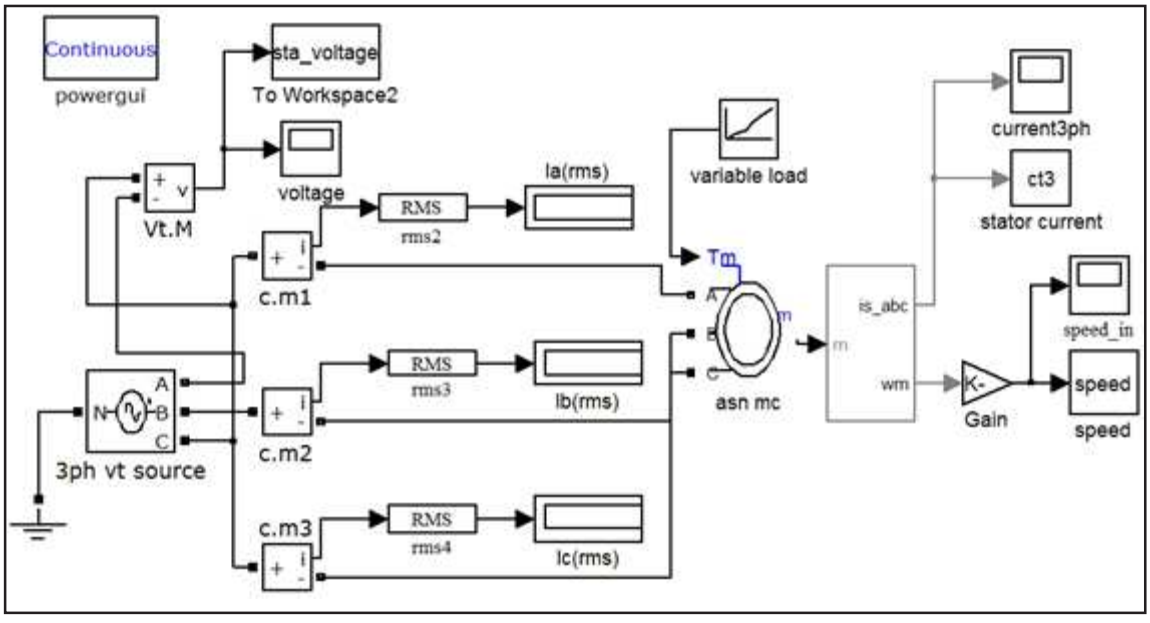

Fig.1 Simulink model of three phase induction motor

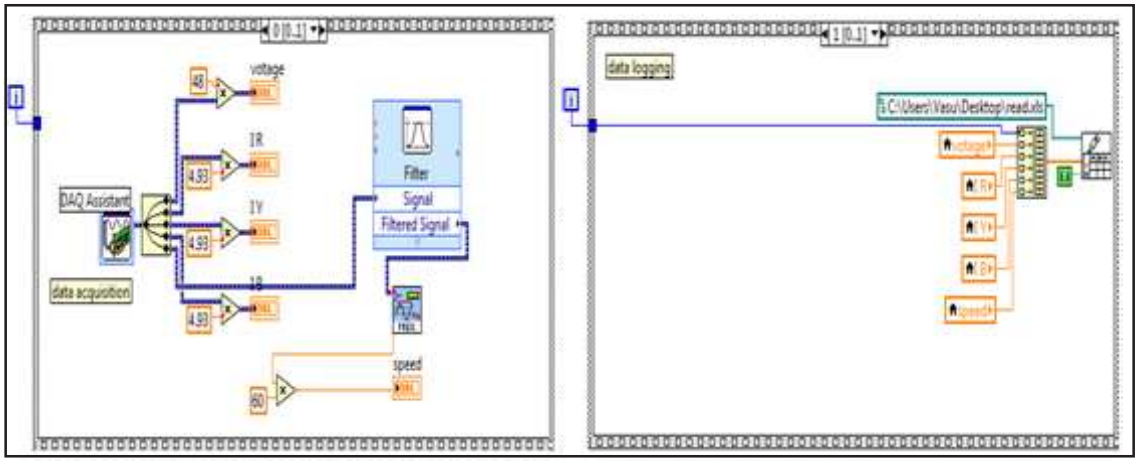

Fig. 2 LabVIEW program for acquiring current and speed signals

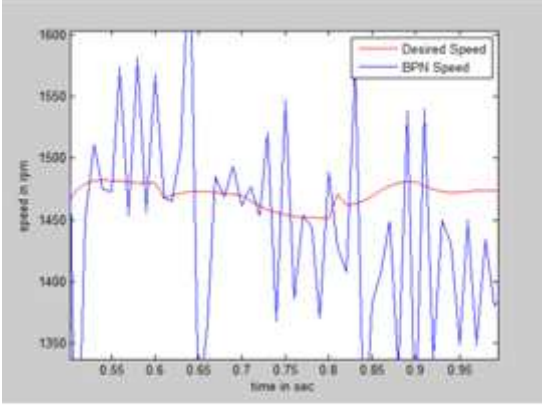

Fig.3 Speed estimated by BPN algorithm for simulated data

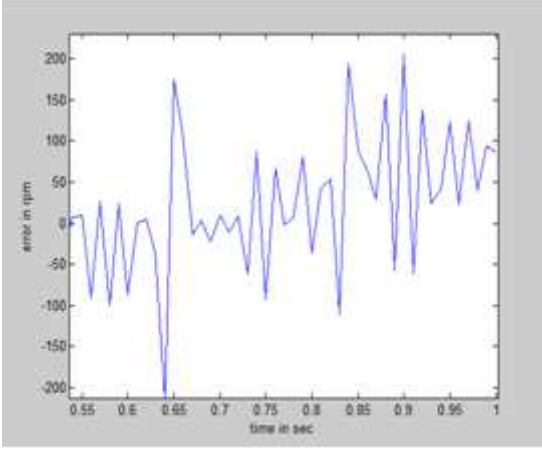

Fig.4 Error in speed estimation by BPN algorithm for simulated data

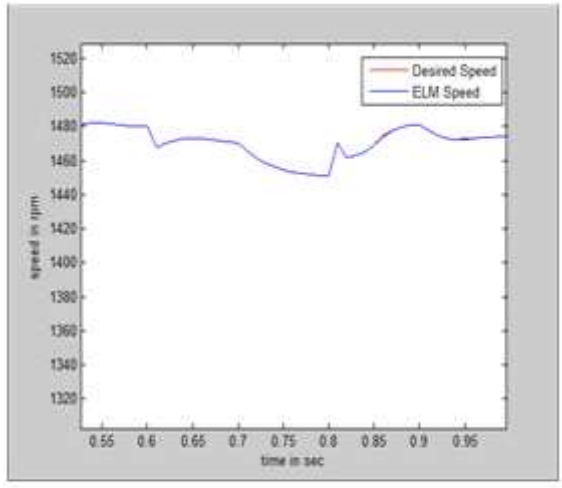

Fig. 5 Speed estimated by ELM algorithm for simulated data

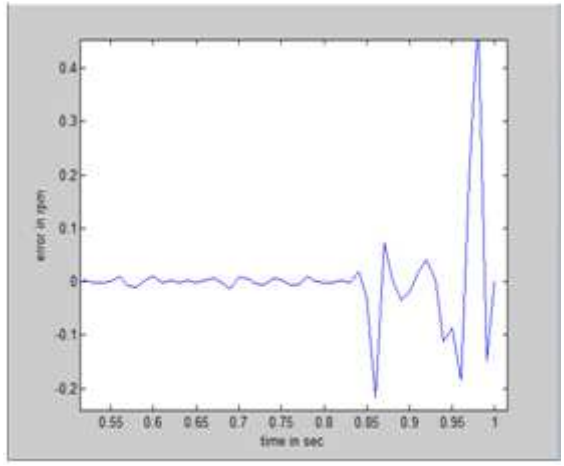

Fig. 6 Error in speed estimation by ELM algorithm for simulated data

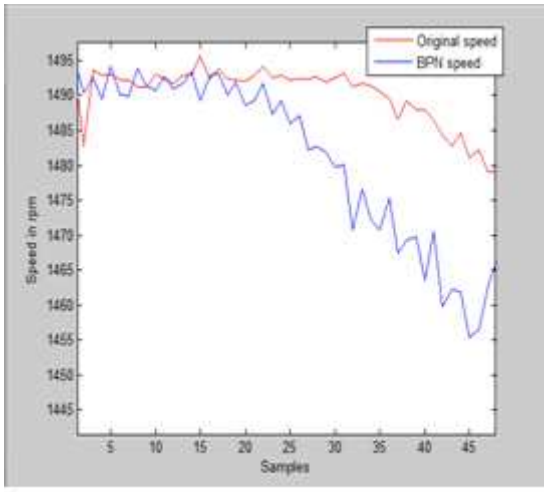

Fig. 7 Speed estimated by BPN algorithm for real time data

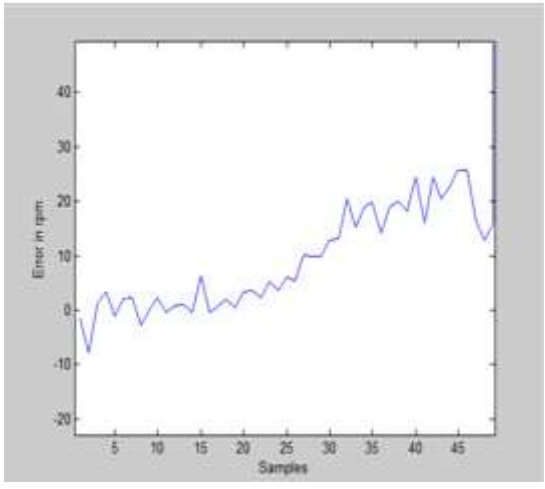

Fig. 8 Error in speed estimation by BPN algorithm for real time data

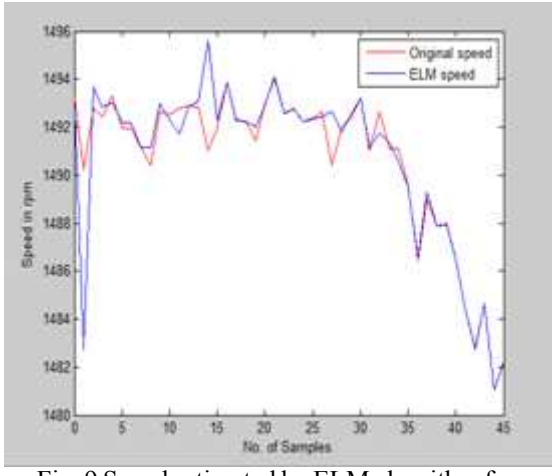

Fig. 9 Speed estimated by ELM algorithm for real time data

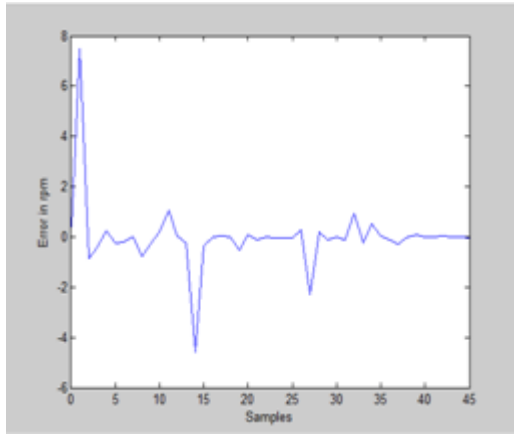

Fig.10 Error in speed estimation by ELM algorithm for real time data

5. CONCLUSION

In order to improve the performance of sensorless motor control , a new speed estimation technique is proposed based on neural network modeling.The selected feed forward neural structure considers the stator voltage with harmonic effects,three phase stator currents and speed as inputs and output to model the induction motor for speed estimation. The training data are retrieved using real time data acquisition using LABVIEW and simulated model of induction motor using Matlab. Also, from the result, it is evident that the proposed ELM algorithm has better generalization performance than the back propagation algorithm. The ELM tends to reach the solutions straightforward without several issues such as local minima, improper learning rate and over fitting, etc. Modelling by means of data collection over a wide range of speed improves the accuracy, reduces the complexity, increases the immunity to noise, and fewer controllers are needed. The results obtained here have demonstrated that the proposed neural model of induction motor with ELM algorithm can sufficiently capture all the system dynamics over the desired operating range.

REFERENCES

[1] I. Ben-brahim and t. Kudor, "Implementation of an Induction Motor Speed Estimator Using Neural Network", proceedings in ipec, 1995, pp.52-57.

[2] B.k. Bose, "Modern Power Electronics and AC Drives", 5th ed. Pearson Education, Singapore, 2005.

[3] Q.Gao, G.asher and H.Umida, "Consideration About Problems And Solutions of Speed Estimation Method and Parameter Tuning for Speed

Sensorless Vector Control Of Induction Motor Drive", IEEE Trans.Ind.Appl., 2002, Vol.38, No.5, pp.1282-1289.

[4] J.Holz, "Sensor Less Control of Induction Motor Drives", Proc. IEEE, 2002, Vol.90, No.8, pp.1359-394.

[5] Huang Yanwei, Wu Dengguo, "Nonlinear Internal Model Control with Inverse Model Based on Extreme Learning Machine", School Of Electric Engineering and Automation, Fuzhou University, Fuzhou, China, 2011.

[6] Y.R. Kim, S.K.Sul and M.H. Park, "Speed Sensorless Vector Control of an Induction Motor Using an Extended Kalman Filter", In Conf. Rec. IEEE-IAS Annu. Meeting, 1992, pp.594-599.

[7] B.Krishnan, "Electric Motor Drives, Modeling, Analysis and Control", 1st ed.Pearson Education, Singapore, 2001.

[8] J. Maes and J.A. Melkebeek, "Speed-Sensor less Direct Torque Control Of Induction Motors Using An Adaptive Flux Observer", IEEE Trans. Ind. Appl., 2000, Vol. 36, No.3, pp.778-785.

[9] D.P.Marcetic and S.N.Vukosavic, "Speed-Sensor Less AC Drives with the Rotor Time Constant Parameter Update", IEEE Trans. Ind. Electron, 2007, Vol.54, No.5, pp.2618-2625.

[10] S.Mohamed Zaky, M. Mahmoud Khater, S. Shokry Shoalla, and Hussian A. Yasin, "Wide-Speed-Range Estimation With Online Parameter Identification Schemes Of Sensorless Induction Motor Drives", IEEE Transactions on Industrial Electronics, 2009, Vol.56, No.5.

[11] A.B. Proca and A. Keyhani, "Sliding-Mode Flux Observer With Online Rotor Parameter Estimation For Induction Motors", IEEE Trans.Ind.Electron, 2007, Vol.54, No.2, pp.716-723.

[12] Seong-hwan Kim , Tae-sik Park, Ji-yoon Yoo and Gwi-tae Park, "Speed Sensorless Vector Control Of An Induction Motor Using Neural Network Speed Estimation", IEEE Transactions on Industrial Electronics, 2001, Vol.48, No.3.

[13] Yoan Miche, Antti Sorjamaa, Patrick Bas, Olli Simula, Christian Jutten and Amaury Lendasse, "Optimally Pruned Extreme Learning Machine", IEEE Transactions On Neural Networks, 2010, Vol.21, No.1, pp.158-162.

[14] M.S, Zaky, M, Khaterm, M.Yasin, S.S. Shokralla and A.E.L. Sabbe, "Speed-Sensorless Position and Speed Control of Induction Motor Drives", Eng.Res.J, 2007, Vol. 30, No.4, pp.433-444.

[15] K.S. Narendra and K.Parthasarathy, "Identification and Control of Dynamical Systems Using Neural Network", IEEE Transaction 1:4-27.doi:10.1109/72.80202, 1990.

[16] DFodor, J.P.Six and D.Diana, "Neural Network Applied for Induction Motor Speed Sensorless Estimation", Proceedings of the International Symposium. IEEE Press, 1995, doi:10.1109/isie.1995.496623, pp-181-186.

[17] Hui.Deng, Jing Yang, Dianguo Xu, "Sensorless Speed Estimation for Induction Motor Based on Neural Network", Proceedings of 6th World Congress on Intelligent Control and Automation, 2006.

[18] Guang-bin Huang_, Qin-yu Zhu, Chee-kheong Siew, "Extreme Learning Machine: Theory and Applications", Neurocomputing, 2006, Vol.70, pp.489-501.

Gene Selection Methods for Cancer Classification: A Review

C.Gunavathi[1] and K.Premalatha[2]
[1]Department of Computer Science and Engineering, K.S.Rangasamy College of Technology,
Tiruchengode - 637 215, Tamil Nadu.
[2]Department of Computer Science and Engineering, Bannari Amman Institute of Technology,
Sathyamangalam - 638 401, Erode District, Tamil Nadu.
E-mail: gunavathic@ksrct.ac.in

Abstract

Microarray data classification is a challenging task because of its huge dimension and the small sample sizes. Cancer classification is a major line of research in bioinformatics. A significant trend in bioinformatics is identifying genes or group of genes that differentiate different cancer types. Thus, in order to analyze gene expression profiles correctly, gene selection method is essential for the classification process, and there is a need for an effective gene extraction method that is necessary for eliminating irrelevant genes and decreasing the classification error rate. Data mining algorithms are widely used to classify gene expression data, in which prediction of disease plays a vital role. This paper aims to present a review about different gene selection methods used for cancer classification.

Keywords: *Cancer Classification, Gene Selection.*

1. INTRODUCTION

1.1. Microarray Gene Expression Data

A DNA micro array is a gathering of microscopic DNA spots attached to a solid surface. These arrays are used by many researchers and scientists to measure the expression levels of thousands of genes at the same time. They generate large datasets with expression values for thousands of genes but not more than a few dozens of samples [3]. The raw microarray data are images that are transformed into gene expression matrices. The rows in the matrix correspond to genes, and the columns represent samples or experimental conditions. The numbers in each cell denote the expression level of particular gene in a particular sample or condition. Expression levels can be absolute or relative. They are used to simultaneously monitor and study the expression levels of thousands of genes, relationship between genes, their functions and classifying genes or samples.

The microarray technology enables a researcher to analyze the expression of thousands of genes in a single experiment and provides quantitative measurements of the differential expression of these genes. The gene expression matrix can be studied either by comparing expression profiles of genes under different experimental conditions or by comparing expression profiles of samples. If two rows are similar, we can infer that the respective genes are co-regulated and possibly functionally related. By comparing samples, we can find which genes are differentially expressed.Each column contains the results obtained from a single array in a particular condition and is called a profile of that condition. Each row vector is an expression pattern of a particular gene across all the condition.

Recent advances in microarray technology allow scientists to measure the expression levels of thousands of genes simultaneously and determine whether those genes are active, hyperactive, or silent in normal or cancerous tissues.

1.2. Cancer Disease

Cancer is actually a group of many related diseases that all have to do with cells. Cells are the very small units that make up all living things, including the human body. There are billions of cells in each person's body. Cancer happens when cells that are not grow normal and spread very fast. Normal body cells grow and divide and know to stop growing. Over time, they also die. Unlike these normal cells, cancer cells just continue to grow and divide out of control and don't die when they are supposed to.

Cancer cells usually group or clump together to form tumors. A growing tumor becomes a lump of cancer cells that can destroy the normal cells around the tumor and damage the body's healthy tissues. This can make someone very sick. Sometimes cancer cells break away from the original tumor and travel to other areas of the

body, where they keep growing and can go on to form new tumors. This is how cancer spreads. The spread of a tumor to a new place in the body is called metastasis.

So, Cancer is featured by an irregular, unmanageable growth that may demolish and attack neighboring healthy body tissues or somewhere else in the body. Gene expression profiling by microarray method has been emerged as an efficient technique for classification and diagnostic prediction of cancer nodules.

1.3. Cancer Prediction and Classification

Cancer classification or prediction refers to the process of constructing a model on the microarray dataset and then distinguishing one type of samples from other types with this induced model. The expression level of genes holds the solutions to overcome basic drawbacks related to the prevention and treatment of cancer.

Supervised learning, also known as class prediction, is the search for a gene expression signature that predicts class (phenotype) membership. The basic methodology for class prediction is to start with two data sets, a training set and test set; training data set is used to build a classifier (class predictor) based on the chosen classification method; and test data set is used to test the classifier.

1.4 Preprocessing

An objective of gene expression Microarray data preprocessing is to select a small set of genes which can be used to improve the accuracy and efficiency of classification from a high dimensional gene expression dataset [6] . For example, normally a gene expression Microarray dataset contains less than 100 examples, but has tens of thousands of genes (attributes). High dimensionality may cause significant problems in Microarray data analysis. To tackle this problem, the need to reduce dimensionality was soon recognized and the use of feature selection techniques has become customary [2]. An equally important reason to decrease dimensionality is to help biologist to identify the underlying mechanism that relates gene expression to diseases. Reasons for the need of gene selection methods are,

i. Irrelevant and noise genes decrease the quality of classification. Gene expression Microarray data often contain a great deal of noise which is caused by human errors, malfunctions and missing values. In addition, not all genes in a dataset are informative for classification. Using irrelevant and noise genes for classification only causes a greater risk of decreasing the accuracy of classification. The noise and irrelevant genes should be removed from Microarray data before classification takes place.
ii. The huge number of genes causes great computational complexity in building classifiers. A Microarray dataset contains large number of genes. This high dimensionality makes many classification algorithms inapplicable or inefficient.

2. FEATURE OR GENE SELECTION METHODS

Gene selection methods can be classified into two categories. If gene selection is carried out independently from the classification procedure, the methods belong to the filter approach. Otherwise, it is said to follow a wrapper (hybrid) approach. Filter method uses the measures like Distance (the degree of separation between classes), Consistency (find the minimum number of features that can distinguish classes) and Correlation (measures the ability to predict one variable from another).

2.1 t-Statistic

t-Statistic is used to find the difference between two sample means measured in terms of standard error of those means [2]. By using this we can find the t-statistic value for normal and tumor samples.

$$d = \frac{\bar{X}_1 - \bar{X}_2}{\sqrt{\frac{{s_1}^2}{n_1} + \frac{{s_2}^2}{n_2}}}$$

where numerator gives the difference between means. The denominator gives the ratio between variance and sample size.

2.2 Minimum Redundancy-Maximum Relevance (MRMR)

MRMR proposed by Ding and Peng selects features by minimizing redundancy among them with maximal relevance [1]. MRMR uses mutual information criterion as a measures of relevance for discrete datasets whereas F-statistic between the genes and the class variable is considered as the score of maximum relevance for the continuous variables.

2.3 Relief-F

Relief-F has been introduced as an extension to Relief algorithm for dealing with noisy, incomplete and multi-class datasets. It assigns a ‘‘relevance’’ weight to each feature. Randomly, a sample instance (R) is selected from m sample instances and the relevance values are updated based on the difference between the selected instance (R) and the nearest instances of the same (H) (called nearest hit) and different class (M(C)) (called nearest miss of class C). It gives more weight to features that discriminate the instance from neighbors of different classes. The weights are updated by considering average contribution of nearest misses M(c). The average contribution also takes into account of prior probability of each class.

The key idea of Relief is to estimate the relevance of features according to how well their values distinguish among the instances of the same and different classes that are near each other (Yu and Liu, 2003). Original algorithm was extended by Kononenko (Kononenko, 1994) so that it can deal with multi-class problems and missing values. Later it was further improved by Robnik–Sikonja and Kononenko (Sikonja and Kononenko, 1997) so that it is suitable for noisy data and can also be used for regression problems. ReliefF is claimed (Stiglic et al., 2008) to behave well when few attributes are selected.

2.4 Gene Ranking -ANOVA p-values

Analysis of Variance (ANOVA) is a technique, which is frequently used in the analysis of microarray data, e.g. to assess the significance of treatment effects, and to select interesting genes based on P-values. [5]. The ANOVA test is known to be robust and assumes that all sample populations are normally distributed with equal variance and all observations are mutually independent. The one-way ANOVA performs an analysis on comparing two or more groups (classes) for each gene and returns a single p-value that is significant if one or more groups are different from others. The most significantly varying genes have the smallest p-values.

Of all the information presented in the ANOVA table, if the p value for the F- ratio is less than the critical value, then the effect is said to be significant. The very small p-value indicates that differences between the column means are highly significant. The probability of the F-value arising from two identical distributions gives us a measure of the significance of the between-sample variation as compared to the within-sample variation. Small p-values indicate a low probability of the between-sample variation being due to sampling of the within-sample distribution, small p-values indicate interesting genes.

2.5 ERGS (Effective Range based Gene Selection) Algorithm

ERGS algorithm does not require any search strategy for feature subset generation unlike most of the popular feature selection algorithm. It does not require iterative process for feature subset evaluation criterion as the case of many existing feature selection algorithm. It works under the principle that a feature should be given more weight if decision boundaries among classes are very far away from each other i.e. classes can easily be distinguished [1]. The decision boundaries of the classes are obtained by statistically defined effective range.

3. DATASETS

The following are the different sample Gene Expression data sets used for cancer classification.

3.1 All _Aml

ALL_AML data consists of 72 samples. The samples consist of two types of leukaemia, 25 samples of acute myeloblastic leukaemia (AML) and 47 samples of acute lymphoblastic leukaemia (ALL). The samples are taken from 63 bone marrow samples and 9 peripheral blood samples. There are 7192 genes in the dataset.

3.2 Colon Tumor

Colon dataset consists of 62 samples of colon epithelial cells from colon-cancer patients. The samples consist of tumor biopsies collected from tumors, and normal biopsies collected from healthy part of the colons of the same patient. The number of genes in the dataset is 2000.

3.3 Diffuse Large B-cell Lymphoma (DLBCL)

DLBCL is an aggressive malignancy of mature B-lymphocytes. DLBCL dataset contains 96 samples of 4026 genes. The samples are categorized into two molecularly distinct forms of DLBCL i.e. ’germinal centre B-like DLBCL’ and ‘activated B-like DLBCL’.

3.4 Lung Cancer

Lung dataset contains 181 tissue samples described by 12,533 genes and categorized into 2 classes namely, malignant pleural mesothelioma (MPM) and adenocarcinoma (ADCA). The 181 samples include 31 MPM and 150 ADCA.

3.5 Mixed-Lineage Leukaemia (MLL)

MLL dataset contains 72 samples of 12,582 genes. The samples consist of three types of leukaemia, 24 samples of acute lymphoblastic leukaemia (ALL), 20 samples of Mixed-Lineage Leukaemia (MLL), and 28 samples of acute myeloblastic leukaemia (AML).

3.6 Prostate

Prostate cancer dataset contains 102 samples of 12,600 genes and categorized into two classes. The dataset contains gene expression patterns from 52 tumor and 50 normal prostate samples.

3.7 Ovarian Cancer

It consists of 32 samples, 15 of which are ovary biopsies of ovarian carcinomas, 13 of which are biopsies of normal ovaries and 4 samples belong to other tissues. 28 of the samples are labeled.

4. CONCLUSION

In this paper the basics of Micro array Gene Expression Data and different feature selection methods used are discussed. From the huge volume of data, informative Genes are selected by using feature selection methods. These feature selection methods are very useful in cancer classification. It helps the biologists in diagnosing the disease.

REFERENCES

[1] B. Chandra and M. Gupta, "An Efficient Statistical Feature Selection Approach for Classification of Gene Expression Data" Journal of Biomedical Informatics, 2011, Vol. 44, pp.529-535.

[2] Saeys *et al.,* "A Review of Feature Selection Techniques In Bioinformatics", Journal of Bioinformatics, 2007, Vol. 23, No.19, pp.2507-2517.

[3] K. Yendrapalli, R. Basnet, S. Mukkamala and A. H. Sung, "Gene Selection for Tumor Classification Using Microarray Gene Expression Data", Proceedings of the World Congress on Engineering, 2007, Vol.1.

[4] TR. Golub *et al.*, "Molecular Classification of Cancer: Class Discovery And Class Prediction by Gene Expression Monitoring", Science, 1999, pp.286:531–7.

[5] Lei Yu, Yue Han and Michael E. Berens, "Stable Gene Selection from Microarray Data via Sample Weighting", IEEE/ACM Transactions on Computational Biology and Bioinformatics, January/ February, 2012, Vol. 9, No. 1.

[6] Mallika Rangasamy, Saravanan Venketraman, "An Efficient Statistical Model Based Classification Algorithm for Classifying Cancer Gene Expression Data with Minimal Gene Subsets", International Journal of Cyber Society and Education, December 2009, Vol. 2, No. 2, pp.51-66.

[7] Yishi Zhang and Zigang Zhang, " Feature Subset Selection with Cumulate Conditional Mutual Information Minimization", Expert Systems with Applications, 2012, Vol.39, pp.6078–6088.

[8] Alexander Statnikov, Constantin F. Aliferis, Ioannis Tsamardinos, Douglas Hardin and Shawn Levy, " A Comprehensive Evaluation Of Multicategory Classification Methods For Microarray Gene Expression Cancer Diagnosis", Journal of Bioinformatics, 2005, Vol. 21, No. 5, pp. 631-643.

[9] Saras Saraswathi, Suresh Sundaram, Narasimhan Sundararajan, Michael Zimmermann, and Marit Nilsen-Hamilton, " ICGA-PSO-ELM Approach for Accurate Multiclass Cancer Classification Resulting in Reduced Gene Sets in Which Genes Encoding Secreted Proteins Are Highly Represented", IEEE/ ACM Transactions on Computational Biology and Bioinformatics, March/April 2011, Vol.8, No.2.

[10] J. Carlos, *et al.,* "Microarray Gene Expression Classification With Few Genes: Criteria To Combine Attribute Selection And Classification Methods" Elsevier Expert Systems with Applications, 2012, Vol.39, pp.7270-7280.

[11] F. Model, P. Adorj´an, A. Olek, and C. Piepenbrock, "Feature Selection for DNA Methylation Based Cancer Classification", Bioinformatics, 2001,Vol.17, pp. 157-164.

[12] M. Dash and H. Liu, "Feature Selection for Classification", Intell. Data Anal., 1997, Vol. 1, No. 3, pp.131–156.

[13] I. Guyon and A. Elisseeff, "An Introduction to Variable And Feature Selection," J. Mach. Learn. *Res.*, 2003, Vol.3, pp. 1157-1182.

Technology And Financial Inclusion

S. Padmavathy[1], T. Dheepa[2] and J. Ashok[3]
[1&2]Department of Management Studies, Kongu Engineering College, Perundurai, Erode - 638 052, Tamil Nadu
[3]KMC Constructions, VEE Technologies, AKR Parcel Services (P) Ltd., Sagoserve.

Abstract

This paper discusses the different technological innovations by banking industry for the financial inclusion of unbanked. India is a country where many people are in unorganized sectors. People having a bank account are less in number. GoI and RBI are making efforts to increase the number of non-customer group as customers of bank. With the advent of Information and Communication Technologies (ICTs), the problem of financial exclusion is getting solved.

Keywords: *Information and Communication Technology, Financial Inclusion, Financial Exclusio.*

1. INTRODUCTION

Financial exclusion is a phenomenon which is restricted to rural areas where accessibility is limited and the population density is substantially lower. However, in recent days the phenomenon has also been observed in urban areas where some segment of the populace remains financially excluded in spite of the existence of bank branches. This exclusion is due to constraints such as access timings, and income potential. On a global basis, 62% of population living in Asia, Africa, and the Middle East and other developing countries are financially excluded. In India and China only one third of the population participates in the formal banking sector. The extent of financial exclusion is very high in India. For example, only 55 percent of the population have deposit account and 9 percent have credit accounts with banks. India has the145 million highest numbers of households excluded from Banking. The NSSO survey- 59th round states that 51.40% of farmer households are financially excluded from both formal/informal sources (459 lakh out of 893 lakh). Of the total farmer households, 73% of farmer households have no access to formal sources of credit.

Dr.K.C.Chakrabarty, Deputy Governor, RBI says, "Financial inclusion, thus, has become an issue of worldwide concern, relevant equally in economies of the under-developed, developing and developed nations. Building an inclusive financial sector has gained growing global recognition bringing to the fore the need for development strategies that touch all lives, instead of a select few."

Financial Inclusion becomes the greater concern for Government. To enhance investments, the role of ICT is much essential in today's scenario. The Information Communication Technology (ICT) is aimed at promoting financial inclusion, kindle the transfer of research and technology in financial inclusion, increase the technological interest and the capacity of financial service providers/ users and encourage an environment of innovation and cooperation among stakeholders (Dr.K.C.Chakrabarty). The GoI, Reserve Bank of India (RBI) and NABARD with an intention to increase the Financial Inclusion a Rs. 500 crore corpus to be contributed in a ratio of 40:40:20.

2. ROLE OF INFORMATION TECHNOLOGY IN FINANCIAL INCLUSION

Technology and financial inclusion are the popular coinage in banking parleys in the country. Technology is a great enabler for continued and inclusive growth. Banks have been quick to realise and adopt technology in a big way. In day-to-day banking in India the visible benefits of IT are quite well known. Today, the 'Anywhere Banking' and 'Anytime Banking' through core banking system, 24/7/365 delivery channels like Automated Teller Machines (ATMs), and Net and Mobile Banking, etc., are becoming an integral part of today's banking services. With the intervention of IT, the structure has enabled efficient, accurate and timely management of the increased transaction volume that comes with a larger customer base.

With the initiatives of RBI the technology driven system helps the unbanked in various way. The inclusion of unbanked would be made possible by reducing transaction cost while dealing with poor, developing institutions to act as intermediaries between existing

institutions and the excluded, building a platform for tackling the issues and supportive legal environment.

3. TECHNOLOGIES SUPPORTING FINANCIAL INCLUSION

Financial inclusion has become a mandate for all banks and targets are created as part of their Financial Inclusion Plan that has to be approved by RBI. As a result, the Banks have signed Business Corespondance agreements with various telecom providers like Airtel, Vodafone, etc and technology solutions providers like TCS, Oxigen, etc and financial payment systems like A Little World-ALW, Eko, FINO, etc are to deliver financial services. NABARD supported MYRADA to develop NABYUKTI, a software to generate simplified MIS for promoting and linking SHGs with banks. Ekgaon technologies offer software for accounting and MIS in case of SHG-based financial intermediation. Integra offers iMFAST [integra Mobile Financial Applications Secure Terminal], which is a portable teller machine that performs simple banking functions in rural areas.

3.1 Mobile Based Banking

Telecommunications has taken the world to a new phase in managing communication and data irrespective of a person's location. The global economy is abuzz with the increasing use of handheld and mobile devices for the purposes like data transfer, information exchange, and service delivery. In today's scenario, the banking and payments industry is foreseeing a similar excitement with the analysts predicting that mobile banking is going to be the next big revenue generator.

Table1Showing the Number of People Having Bank Account and Mobile Phones

World-Total Population	6.9 billion	100%
World-People Having Bank Account	2.1 billion	30.43 %
World-People Having Mobile Phones	5.2 billion	75.36 %
India-Total Population	1.21 billion	100%
India-People Having Bank Account	200 million	16.52 %
India-People Having Mobile Phones	811 million	68%

Source: The Hindu dtd: July 10, 2011

While banks are experimenting with numerous ways of servicing customers, the mobile market was growing with unprecedented penetration across all customer segments.

The Indian banking industry looks set to move into a new phase leveraging the mobile industry and its growing outreach, especially among the rural population. It is expected that the mobile connections would reach to 200 million by 2012, up from the current 90 million. Thus, the mobile devices are used for payment and banking services, which could be the best suited model for branchless banking in India. In India alone the total number of people having mobile phones by 2011 was 5.2 billion as against 4 billion in 2008. The number of mobile subscribers has grown over 4.5 times within a period of three years. India is adding more subscribers per month than any other country. This typical trend is not only isolated to India but in reality, it has made a drastic change in almost all developing economies like Africa, Latin America, and Asia. Some of the successful implementation of mobile-led financial inclusion are,

3.2 m-Pesa Model in Africa

A mobile-based money transfer service launched in Africa in a venture between Vodafone and Safaricom. In this model, to make payments, transfer money and redeem the cash, customers can use a wallet on their mobile phone. The servicing of these customers is through the network of airtime resellers.

The m-Pesa model offers several features such as:
- Withdraw and deposit cash
- Utility bill payment
- Money transfer

The m-Pesa model is quite popular in many countries of Africa, such as Kenya, Tanzania, and South Africa. A recent study also suggests that more than 10 percent of Kenya's GDP now pass through the mobile channel.

3.3 Community Banking in Standard Bank

The community banking division of Standard Bank leverages MTNs MobileMoney solution. This product allows the client account to be linked to a SIM card. The customers can then transact on these accounts through an agent or a community banker who is a partner of Standard Bank. This solution allows customers to perform transactions such as:
- Purchase transactions
- Money transfers
- Account Enquiries

These transactions can be performed directly on the customer mobile phone or through the agent mobile phone. The customer money is reflected as information

on a wallet on the SIM card which can then be used to perform the various transactions.

3.4 Grameen Village Phone in Bangladesh

In Bangladesh, the Grameen Foundation launched its much acclaimed Microfinance program. The key objective of the program was to provide wide-spread access to loans to the unbanked women of Bangladesh. In this model, the beneficiary can procure a mobile phone from Grameen Phone with some pre-paid credit. The mobile phone can then be a source of income for the beneficiary as people in the village can use this phone to make telephone calls.

3.5 ATM Based Banking

Micro ATMs: Deploy low cost ATMs with minimum basic features like cash withdrawal, balance enquiry where rural people frequently visit. It is the most convenient and cost effective method of financial inclusion.

Biometric ATMs: For the convenience of illiterate and semi-illiterate customers, biometric ATMs are to be deployed. This system uses the thumb impression of the card holders which will be scanned and transferred to the central server. ATM dispenses cash and other services only after verifying the impression with the available finger print in the bank database.

Mobile ATMs: ATMs are designed in such a way that a van would move to the pre-determined places for easy banking of unbanked. It is also accessible to biometric card holders. Bank transactions like opening an account, cash withdrawal would be effectively used during the visits to the rural areas.

3.6 Handheld Devices

A compact and portable device, easy to carry in field and ideal for a rural/semi-urban scenario. It can function on the field on any means of connectivity that is available in the country like GSM/GPRS, CDMA and the telephone line. It support various financial/non-financial transactions in offline mode in field such as, deposit, withdrawal, account transfer, standing instruction, new product request & alerts.

Simputer (Simple Computer or Simple Inexpensive Multi-lingual Computer): A low cost portable palmtop which breaks the literacy barrier through natural user interface. It supports multi-lingual text and speech output. It has a personalized smart card facility facilitating community-sharing with no user limitation.

SIM Toolkit: Using a SIM Toolkit, mobile operators can load m-banking applications into the customer's mobile SIM card. It ensures availability of application as and when customer buys a new SIM card. Since the operator is closely associated with the mobile banking project and hence the task of delivery of service is easy

Mobile Application Development Platforms: These technologies describe various programming languages using which applications can be developed for mobile phones. These applications along with customer's data reside on the mobile phone. It is operator independent and highly user interface. The development skill set is widely present for GPRS. It has a high ability to design and deliver better features.

3.7 Smart Cards

State Governments are taking higher initiatives in Pension payments for senior citizens and disbursal under Rural Employment Generation Program through smart cards linked bank accounts. It provides biometric authentication, which helps in reducing frauds and ensure identity of customers. Such cards can also hold all transaction details on the card. In order to popularize smart cards, all agriculture short term loans and payment of social security schemes are to be dispensed through Smart Cards.

3.8 Aadhaar Project

Government of India established Unique Identification Authority of India (UIDAI) with an objective to issue a unique identification number known as Aadhaar to all Indian residents with intent to eliminate duplicate/fake identities and to put hassle-free, cost effective verification/authentication system in place thereby to save considerable resources of various user departments as well as beneficiaries at large. UID project gives a big push to the government's financial inclusion agenda and also provides the strong foundation to deliver better services and paves the way to improve the operational efficiency of the system. All Public Sector Banks are acting as Registrars to undertake enrollment and authenticated services to their clientele and also other residents using technology embedded outsourced model.

Tie-up with Post Offices Modernization of Post Offices is in full swing and now they are well connected. Banks may make use of the presence of the post offices to extend banking services to the persons of unbanked areas. Smart Cards with bio-metric features will be delivered to them. The customer has to produce the Smart Card at post office for remitting cash or for withdrawal.

E-Seva Centers: Banks may enter agreement with the respective state governments for sharing of resources, so that our rural/semi-urban customers can undertake financial transactions (Cash Deposit/Withdrawals) at these centres, which will be updated at Banks' server every day.

3.9 T-Banking

The presence of Television in all households is the order of the day and now it has become one of the most cost effective modes to disseminate information across the country. Banks may explore the possibility of making use of cable network to extend banking services to remote rural areas and this can be used as non-branch service delivery channel.

In the above backdrop, Banks need to revisit their approach towards low value accounts of vast neglected population and adopt "High Volume – Low Margin – High Profit" business model backed by technology. This strategy enables to bring more customers in to bank's fold since this segment provides ample opportunities to improve business/profit on account of cost effective solutions.

4. CHALLENGES AHEAD

The penetration of the technology based delivery channel, while very popular, has its own share of issues which are affecting its growth. These issues primarily affect the security paradigm, customer experience, and data sanity of the financial transactions.

The key issues are as mentioned below:

i. Biometric authentication is currently available in a limited set of mobile phones. This poses an issue, as many financial inclusion programs rely on biometric authentication as the primary mode of customer authentication.

ii. Mobile phones are good for limited data entry. However, complex transactions such as customer registration, service requests cannot be offered very easily. This limits the facilities which can be provided.

iii. The user experience in case of self service can be an issue, as mobile phones provide a very simplistic user interface. Also, many of the self service models are not very intuitive and require customer education.

iv. The SMS mode of operation, the most widely used mode of communication in mobile led financial inclusion, is not very secure and this poses a new challenge to be overcome.

v. In terms of regulatory aspects, AML, KYC, etc. norms should have inclusive parameters for rural banking.

vi. Due to high delivery costs, legacy systems and inflexible procedure the physical and banking infrastructure are underutilized.

vii. Information asymmetry due to non- availability of credit history of rural customers, willful defaulting and unclear Government policies .

5. CONCLUSION

Even though a multitude of operational issues are quoted as reasons for lagging behind in financial inclusion targets, it could be resolved if banks begin to look at financial inclusion as a business opportunity and a service to the down trodden rather than an obligation and to fulfill their corporate social responsibility (CSR). It needs to be realized that technology per se is not an end in itself. Technology helps to the reform process and acts as a ladder to achieve the ultimate goal of providing financial services to the financially excluded. It is important that technology should be leveraged by Indian banks by providing affordable and cost-effective banking services to the masses through multi-delivery channels. The challenge now lies in taking greater advantage of new technologies and effective implementation of the same to expand the coverage of the banking and financial system. Thus, technology based solutions would go a long way for achieving greater financial inclusion.

REFERENCES

[1] NSSO-59th Round Report, An Analysis by DESACS, RBI, New Delhi, 2011.

[2] Analyze the Obstacles to Financial Inclusion-A Report by UN Department of Economic and Social Affairs (DESA) and the UN Capital Development Fund (UNCDF), 2010.

[3] Financial Inclusion - http://rbidocs.rbi.org.in/rdocs/Speeches/PDFs/FIC060911DG.pdf. Delivering Financial Inclusion Services to Rural Citizens through

the Common Service Centers An Evaluation of State Implementation Models -http://www.mit.gov.in/sites/upload_files/dit/files/Financial_Inclusion_through_CSCs_28_02_2011.pdf
[4] Major role of technology in financial inclusion - http://www.thehindu.com/business/Industry/article2216563.ece
[5] Financial Inclusion: Role of Information Technology - http://www.iims-bitesys.in/index.php?option=com_content&view=article&id=32:-financial-inclusion-role-of-information-technology&catid=10
[6] The Evolving Role of Technology in Financial Services - http://www.statestreet.com/vision/technology/pdf/TheEvolvingRoleTech.pdf.
[7] http://www.nabard.org/departments/crr_fid.asp
[8] What is Financial Inclusion-http://www.chillibreeze.com/articles_various/Indian-Finance.asp

"Automated Postal Machine (APM) - An Unique Innovative System to Automate Speed Post Service"

K.Elamvazhuthi
Department of Management Studies, Jayam College of Engineering and Technology, Dharmapuri - 636 813, Tamil Nadu

Abstract

Postal Service is one of the steady revenue generating business of the Central Government. The network is well established throughout the nooks and corners of India. Speed Postal service is a unique service of Department of Posts started in the year August 1986 generating revenue of Rs 5500 crores yearly. The department employs over 5, 20,000 people across the country. There are 290 speed posts offices linking 1200 towns in India. There are 73 countries covered under the International Speed Post. The major limitations in the present system are that the Speed Postal Service is available only for limited durations say from 10 am to till 8pm in district GPOs and lesser hours of operations in other rural Post offices and a customer has to spend minimum 10-15 minutes in front of the counter to send a Speed post. To solve the problem and to make the service available for 24 hours, an unique Innovative System to automate Speed Post Service- ***Automated Postal Machine (APM)*** *is proposed for implementation.*

The APM is a complex system comprising different modules for operation and functioning and they are a Machine similar to Automated Teller Machine or its modified version to suit the requirements, Machine similar to Baggage scanner used in Airports, Barcode generator and Printer, Envelope collecting container, Electronic weighing scale to measure the weights of the envelopes, Modified Currency Vending machine, Appropriate DBMS software for effective implementation and commercialization. The proposed advantages of APM are Speed post service is made available 24 hours like an ATM machine, Fully automated, Increased revenue for the department, Eliminates manual work and error, Eliminates the waiting time for the public, Improved customer satisfaction as the sender and the receiver is notified in advance regarding the parcel booking. The limitations of the system are that it's a new concept, first of its kind in the world such automation is introduced in the postal department. It will take more time for the public to accept the machine.

Keyword: *Automated Postal Machine (APM),Vending Machine.*

1. INTRODUCTION

The world is moving towards hi-tech in various fields and the customers' needs and expectations are changing now and then. Now it is the period of customers' delightment rather than customer satisfaction. The common publics have become more literate and they are very conscious of time and money. Their expectations towards the service rendered are increasing manifold. Customer retention is of paramount important in the current scenario of cut-throat competitions.

Speed postal service is a value added service offered to the public and has successfully completed quarter century. In spite of hectic competitions existing now through the private courier services, the speed postal services has found a worldwide acceptance as the most reliable and safe service for sending and receiving documents within the country and or to other countries world over.

Around 1200 towns in India are linked through 290 speed posts offices and there are more than 5,20,000 people working day and night to provide the services. The network is well established in India and worldwide covering more than 73 countries.

2. PROBLEM DEFINITION

In the present speed postal service system, the following problems are faced by the public:

i. The waiting time spent to send one document is minimum 10 to 15 minutes.
ii. The service is available only for limited hours in a day.
iii. The service is not available on Sundays and on government holidays.

iv. One has to log into the speed post website to ascertain the delivery of the documents which is practically not possible for all those who do not have the facilities.

3. MAIN OBJECTIVES OF THE NEW AUTOMATED POSTAL MACHINE (APM) SYSTEM

To eliminate the various practical problems faced by the public in using the speed postal service, an Unique Innovative System.

4. UNIQUENESS OF THE SYSTEM

It is the first of its kind in the world to provide a value added service to the common public through automated speed postal service machine. There are various automatic vending machines available in the world to site few examples are: newspaper vending machine, vending machines for stamps, cigarettes, instant noodles, rice, books, beverages, chocolates are predominantly found in Australia, US, Japan, Italy, Spain, UK and in Europe.

5. CONCEPT OF AUTOMATED POSTAL MACHINE (APM)

A robust machine similar to ATM (Automated Teller Machine) is fabricated. The person who wants to send a document can operate the system without any other persons' support. The APM has a touch screen monitor, inbuilt keyboard, baggage scanner, barcode generator cum printer, electronic weighing scale and currency vending machine.

6. SEQUENCE OF OPERATION OF APM

Step 1: The user / speed post parcel booking person enters the A/C room of the APM machine.
Step 2: He / She touches the APM screen. It gets activated. The system asks the user to enter number from 10 to 99 to confirm the physical presence of the user. The number entered is displayed in the screen.
Step 3: The system then displays the message as "please keep the parcel on the pan"
Step 4: The user keeps the parcel in the pan linked to the electronic weighing balance which is not visible to the naked eye.
Step 5: The machine first scans for the document for its originality and for the presence of any unauthorized material in the parcel.
Step 6: The screen displays immediately the weight of the parcel and the screen shows the columns in the screen for entering the"from and to" address of the parcel.
Step 7: Once the destination is entered and known to the system, the system then calculates the speed post tariff depending upon the weight and the distance and it is displayed.
Step 8: The currency note is fed into the system and it gives the balance changes just like a currency-coin vending machine.
Step 9: After the payment is accepted, the system then displays a message to confirm the address entered. Once it is clicked "yes", it automatically generates a bar code and it is printed on the envelope. The barcode contains all the relevant details about the document.
Step 10: The system generates a receipt for the sender as the proof of registering the speed post.
Step 11: The system displays a message to drop the parcel into the machine containing a box which is under locked condition and which is opened at regular intervals by postal department personnel.
Step 12: Immediately, the APM machine generates a sms to the sender and as well as the receiver of the document / parcel.
Step 13: Then the machine is ready for the next user.

Daily after every 3 to 4 hours, the representative from the Postal department collect the parcels and process it for further operations in the normal regular methods. The system is connected or linked to the main server of the post office and the number of bookings done at any point of time can be viewed in the system. Once the document is delivered to the addressee, a delivery confirmation report is sent through an sms to the sender. Also it is possible to track the movement of the parcel in transit through web as it is being done now.

Schematic Diagram of ATM and APM

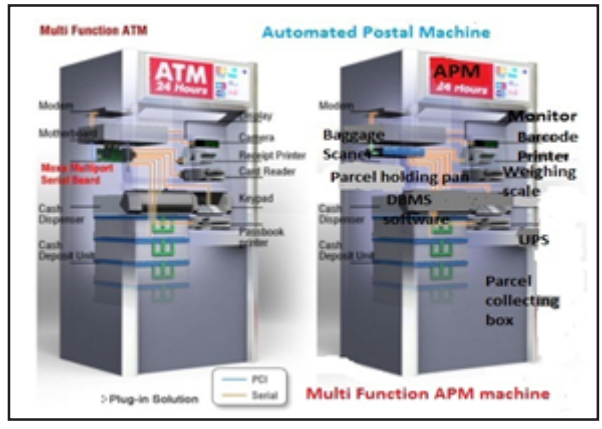

7. APPROXIMATE BUDGET FOR MAKING ONE APM

i. Modified ATM machine = Rs 5,00,000 /-
ii. Inbuilt baggage scanner = Rs 50,000/-
iii. Barcode Generator cum printer = Rs 50,000/-
iv. Electronic weighing scale = Rs 50,000/-
v. Currency vending machine = Rs 2,00,000/
vi. DBMS software = Rs 1,00,000/
vii. UPS = Rs 50,000/-
viii. A/C cabin with suitable lightings= Rs 1,25,000/-
Total = Rs 11,25,000/-
(Rupees Eleven Lakhs Twenty Five Thousands only)

8. FUNCTIONS OF INDIVIDUAL COMPONENTS OF APM

8.1. Touch Screen Keyboard Monitor

i. The monitor gets activated the moment the user touches the screen
ii. The keyboard keys are shown on the monitor
iii. The "From & To" address columns are programmed in the system and it is displayed on the screen.
iv. If the addresses are not entered properly for example, in case the Pin code, destination town and the mobile number is not there means, the system will not accept the parcel and will be processed further.

8.2. Baggage Scanner

i. Scanning the document / parcel is the first activity of the system to detect for any hazardous chemicals, explosives, dangerous weapons like pistol, knife and also for all the prohibited items listed out by the postal department which cannot be sent by post within the country and or to outside the country.
ii. Using the X- ray mechanism, the parcel is scanned and the report is displayed in the screen.
iii. If the parcel is normal, the screen displays the report as "okay" and shows the columns for entering the addresses.
iv. If the document is found to contain any unwanted banned items, it rejects the parcel.

8.3 Electronic Weighing Scale

i. The parcel holding platform is linked to the weighing scale.
ii. As soon as the parcel is kept on the platform, it measures the weight and it is displayed on the screen.
iii. The system immediately displays the address columns for entering the details.
iv. Once "to address" is known to the system, it calculates the speed post tariff considering the weight of the parcel and the distance.
v. If the destination is outside India, then it calculates the tariff separately.
vi. Minimum and maximum weight of the parcel is fixed as 100 Gms to 5000 Gms. If a parcel is found having more than the specified weights, the system will reject the document and it could be send only by the manual mode.

8.4 Currency Vending Machine

i. The machine is installed inside the APM to collect the speed post tariff amount and give the change to the person automatically.
ii. Once the currency is inserted in to the machine, it checks for the genuineness and originality of the currency note.
iii. If it is a fake note, it rejects it and the whole transaction is terminated immediately as a precautionary measure.
iv. The tariff charges can be fixed in multiples of Rs 5/= and the machine can be designed to accept the currency denominations of Rs 5, Rs 10, Rs 20, Rs 50, Rs 100, Rs 500 and Rs 1000/=
v. The machine is designed robustly such that the remaining balance is dispersed accurately just like "Coin Vending Machine' installed by Banks at some of the busiest bus stands and railway stations.

8.5 Barcode Generator cum Printer

i. The Barcode is the easiest and reliable system for traceability of a product or a document.
ii. Once the address details are entered in the system, it is fed into the Barcode generator and it generates the barcode in the real time and the printer is designed such that the code is printed or sprayed on the envelope or parcel or document.
iii. The same code is used in the receiving Post offices where the details are displayed on the screen the moment it is scanned and through which the delivery confirmation report is generated and the message is conveyed through the SMS to the sender and also the receiver.
iv. It is authentic proof to show that the parcel has been delivered to correct addressee and not to the unknown persons.

8.6 Data Based Management System (DBMS) Software

i. The software is designed such that all the details entered in the APM are saved in the server of Head Post offices and the data can be accessed from the beneficiary post offices also from any part of the world.
ii. If there is more number of APMs installed in a particular locality, then all the APMs are labeled with proper identification and the details are stored separately in the system. This will be convenient to know from which APM machine a particular parcel has been booked in case of any problems.
iii. The system generates the list of documents booked at any point of time and it can be used for further processing.
iv. The system is designed such that at any point of time, the post offices which are linked to the server of APM will be able to know, how many parcels are booked from the town under which the particular post office is having the control and how many parcels are due to be received to the post office. And when the parcels are received by the regular mode by postal van, they can countercheck the quantity received.
v. All the data can be stored for a minimum period of two weeks after the delivery of the parcel and or as per the normal regular practice of the department.

9. PLAN OF ACTION FOR IMPLEMENTATION

i. Approval for making few APMs to be sought from the Department of Postal Service, Government of India.
ii. An ATM machine manufacturer to be approached for modifying it to APM machine incorporating all the components.
iii. For trial purpose, few APMs to be installed in the head post offices of Delhi, Chennai, Mumbai, Bangalore and Kolkata. We can install it in the metro towns where maximum numbers of speed posts are made every day.
iv. The practical problems in the usability of APM could be studied for 6 to 12 months and can be decided for installing in more number of post offices.
v. It can also be tried to install few APMs in IT park campuses in Delhi, Chennai & Bangalore where there are more learned knowledge professionals.

10. ADVANTAGES OF APM

i. Speed post service is made 24 hours like an ATM machine available for 7 days a week and 365 days in a year.
ii. Fully automated. Increased revenue for the department.
iii. Eliminates manual work and error.
iv. Eliminates the waiting time for the public.
v. Improved customer satisfaction as the sender and the receiver is notified in advance regarding the parcel booking.

11. LIMITATIONS OF APM

i. It is a new concept, first time in the world such automation is introduced in the postal department. Will take more time for the public to accept the machine.
ii. It's a complex machine, might take more time, money and effort to fabricate it and commercialize the same.

REFERENCE

[1] Guidelines: https://sites.google.com/site/automated teller machine/.

Optimization of Machining Parameters of WEDM Process Based On the Taguchi Method

R.Kalidas[1], S.Boopathi[2], K.Sivakumar[3] and P.Mohankumar[4]
Department of Mechanical Engineering, Bannari Amman Institute of Technology, Sathyamangalam – 638 401, Erode District, Tamil Nadu
E-mail: sivakumark@bitsathy.ac.in

Abstract

WEDM is a widely recognized unconventional material cutting process used to manufacture components with complex shapes and profiles of hard materials. In this thermal erosion process, there is no physical contact between the wire tool and work materials. Wire electrical discharge machining (WEDM) is getting more tasks in fields like dies, punches, aero and many more. It is the very difficult task to get optimum process parameters for higher cutting efficiency; accuracy is becoming a predominant factor nowadays. In this paper, EN31 is taken for study. The design of experiments (DOE) is done in Taguchi L27 orthogonal array (OA). Rough machining with WEDM gives poor surface finish and has micro cracks and pores. Finish machining gives better surface finish (Ra) but with very poor machining speed (MRR). Hence achieving higher MRR and minimizing the Ra is the objective which is done by Taguchi method.

Keywords: *DOE, MRR, orthogonal array, Ra, Taguchi method, WEDM.*

1. INTRODUCTION

In this paper, the Optimization of the electrical discharge machining process with multiple performance characteristics has been investigated to illustrate this approach. Wire Electrical discharge machining (WEDM) has been used effectively in the machining of hard, high-strength, and temperature resistant materials. The Taguchi method can optimize performance characteristics through the settings of process parameters and reduce the sensitivity of the system performance to sources of variation. As a result, the Taguchi method has become a powerful tool in the design of experiment methods however; most published Taguchi applications to date have been concerned with the optimization of a single performance characteristic.

Handling the more demanding multiple performance characteristics are still an interesting research problem. Material is removed by means of rapid and repetitive spark discharges across the gap between the tool and the work piece. In wire electrical discharge machining, it is important to select machining parameters for achieving optimal machining performance .Usually, the desired machining parameters are determined based on experience or handbook values. However, this does not ensure that the selected machining parameters result in optimal or near optimal machining performance for that particular wire electrical discharge machine and environment. To solve this task in the present study, the Taguchi method is used as an efficient approach to determine the optimal machining parameters in the wire electrical discharge machining process. J.L. Lin *et al* [1] the application of the Taguchi method with fuzzy logic for optimizing the electrical discharge machining process with multiple performance characteristics has been reported. The machining parameters (the work piece polarity, pulse-on time, duty factor, and open discharge voltage, discharge current and dielectric fluid) are optimized with considerations of the multiple performance characteristics (electrode wear ratio and material removal rate). Nihat Tosun *et al* [2] find on the effect and optimization of machining parameters on the notch and material removal rate (MRR) in wire electrical discharge machining (WEDM) operations.

The experimental studies were conducted under varying pulse duration, open circuit voltage, wire speed and discharge flushing pressure. The settings of machining parameters were determined by using Taguchi experimental design method. Can Cogun [3] the settings of machining parameters were determined by using Taguchi experimental design method. The level of importance of the machining parameters on the kerf and the MRR is determined by using ANOVA. The highly effective parameters on both the kerf and the MRR were found as open circuit voltage and pulse duration, whereas wire speed and dielectric flushing pressure were less

effective factors. Amar Patnaik *et al* [4] Introducing zinc coated copper as electrode tool with the process parameters of Discharge current, Pulse duration, Pulse frequency, Wire speed, Wire tension, Dielectric flow rate. By using factors, maximization of MRR and minimization of surface roughness is done in WEDM process using Taguchi method. Tanimura *et al* [5] projected new EDM process using water mist, which requires no tank for the working fluid. They also pointed out that the mist-EDM/WEDM enables non-electrolytic machining even when electrically conductive water is used as the working liquid. Fu-chen Chen *et al* [6] Research is based on fuzzy logic analysis coupled with Taguchi methods to optimize the precision and accuracy of the high-speed electrical discharge machining (EDM) process, pulse time, duty cycle, peak value of discharge current as the most important parameters, powder concentration, powder size are found to have relatively weaker impacts on the process design of the high speed EDM. The most important factors affecting the precision and accuracy of the high-speed EDM process have been identified as pulse time, duty cycle, and peak value of discharge current. Dry EDM has many advantages such as, extremely low tool wear ratio, higher precision, smaller heat affected zone. The experimental studies were conducted under varying pulse duration, open circuit voltage, wire speed and dielectric flushing pressure. H.Singh *et al* [7] analyze the effects of various input process parameters like pulse on time, pulse off time, gap voltage, peak current , wire feed and wire tension have been investigated and impact on MRR is obtained. Finally they reported MRR increase with increase in pulse on time and peak current. MRR Decrease with increase in pulse off time and servo voltage. Wire feed and wire tension has no effect on MRR. A.K.M. Nurul Amin *et al* [8] Conducting experiments on cutting of Tungsten Carbide ceramic using electro-discharge machining (EDM) with a graphite electrode by using Taguchi methodology. The Taguchi method is used to formulate the experimental layout, to analyze the effect of each parameter on the machining characteristics, and to predict the optimal choice for each EDM parameter such as peak current, voltage, pulse duration and interval time. It is found that these parameters have a significant influence on machining characteristic such as metal removal rate (MRR), electrode wear rate (EWR) and surface roughness (SR) the peak current significantly affects the EWR and SR, while, the pulse duration mainly affects the MRR. Taguchi method has been used to determine the main effects, significant factors and optimum machining condition to the performance of EDM. Kuo-Wei Lin *et al* [9] conduct test Wire Electrical Discharge Machining (WEDM) of magnesium alloy parts via the Taguchi method-based Gray analysis was conducted, they considered Multiple quality characteristics required include material removal rate and surface roughness following WEDM. This work machines magnesium alloy parts under controlled machine parameter settings, and measures the above quality characteristics. The optimized machine parameter settings clearly improve quality characteristics of the machined work piece compared to quality levels achieved for initial machine parameter settings. The complex interactions in WEDM involve wire feed rate, pulse-on time, pulse-off time, no load voltage, servo voltage, and wire tension. Kamal Jangra *et al* [10] Investigated on Influence of taper angle, peak current, pulse-on time, pulse-off time, wire tension and dielectric flow rate are investigated for material removal rate (MRR) and surface roughness (SR) during intricate machining of a carbide block. In order to optimize MRR and SR simultaneously, grey relational analysis (GRA) is employed along with Taguchi method. WC-Co composite is studied, grey relational analysis (GRA) is employed along with Taguchi method, the percentage error between experimental values and predicted results are less than 4% for both machining characteristics.

Table 1 Parameters of the Setting

Control Factors	Symbols	Fixed Parameters	
Applied Voltage	Factor A	Wire	Molybdenum Wire
Pulse Width	Factor B	Shape	Rectangular Product
Pulse Interval	Factor C	Location of Work Piece on Work Table	At The Centre of The Table
Speed	Factor D	Thickness of Work Piece	8 mm
		Stability	Servo Control
		Height of Work Piece	50 mm
		Wire Type	Molybdenum, Diameter 0.20 mm

2. EXPERIMENTAL DATA COLLECTION

This section describes the experimental setup, explains the method of conducting experiments, and Design of experiment based on Taguchi method.

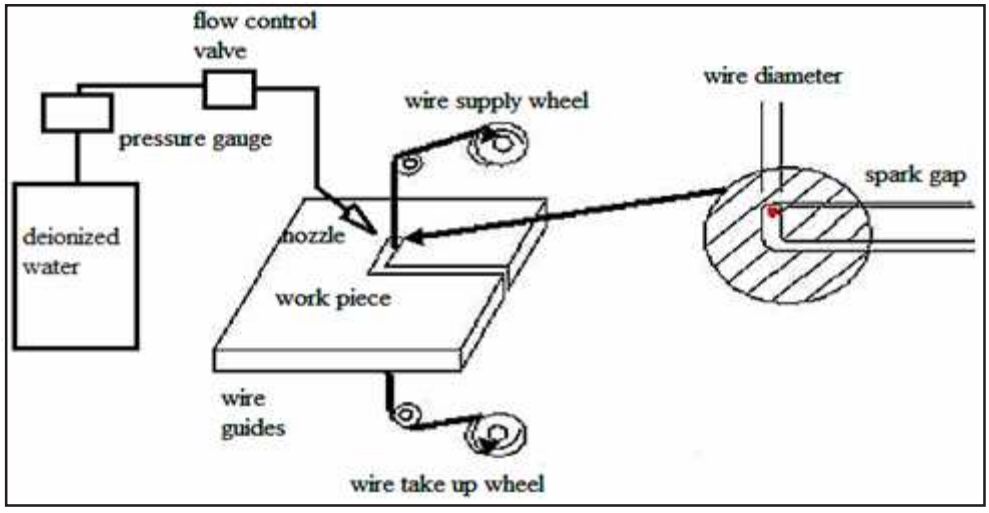

Fig.1 Design of experiment based on taguchi method

2.1. Experimental Set Up

Experiments were conducted on ST CNC-E3 (MCJ) wire cut EDM machine. It was made by Steer Corporation this machine is numerically controlled wire EDM machine. The X and Y axis of the table movement can be controlled by using servo controller. In X axis the table will move at a distance of 300mm and in Y axis the table will move at a distance of 250mm. According to the convention of normal polarity, the work-piece is connected to the positive terminal of the source and the tool is attached to the negative terminal of the source.Figure 1 shows that arrangement of wire cut EDM machine the experimental data based on the DOE were collected to study the effect of various machining parameters of the EDM process. These studies had been undertaken to investigate the effect of applied voltage, discharge current, pulse width, pulse interval on the Metal removal rate and surface roughness.

Table 2 Levels for Various Control Factors

Level				
Control factors	**I**	**II**	**III**	**Units**
A. Applied voltage	75	90	105	Volts
B. Pulse width	3	4	5	µs
C. Pulse interval	20	25	30	µs
D. Speed	250	500	750	Rpm

2.2. Experimental Procedure

The experiments were conducted on EN 31 alloy steel material having composition of (1.00% C, 0.50% Mn, 1.40% Cr, and 0.20% Si.) as a work specimen. The work piece is in the form of rectangle plate having dimensions of $100mm \times 50mm \times 8mm$. Work piece had been machined using molybdenum wire is used as a tool having diameter of 0.20mm and de-ionized water as a dielectric fluid. Each sample had been machined for a length of 4mm. machining time were measured using a stop watch. After machining to calculate the MRR and Ra values were measured using Mitutoyo SJ.201P surface tester. Meter has a stylus stroke of 350µm, Resolution of 0.01 µm, minimum cut-off of 0.25mm and 2µm stylus radius was used. The measurement length was set to 3mm.

The WEDM process consists of three operations, a roughing operation, a finishing operation, and a surface finishing operation. Usually, performance of various types of cutting operations is judged by different measures. In case of finish cutting operation, the surface finish is of primary importance whereas both metal removal rate and surface finish are of primary importance for rough cutting operation. Dimensional accuracy is highly dependent on cutting width. This means that the rough cutting operation is more challenging because three goals must be satisfied simultaneously. Therefore, the rough cutting phase is investigated in the present approach considering two performance goals like MRR and Ra. The experiment is carried out on ST CNC-E3 (MCJ) wire cut EDM machine, the input parameters to be chosen from a limited set of possible values. The values of input parameters, which are of interest in the rough cut with finishing phase, are recorded. To evaluate the

effects of machining parameters on performance characteristics (MRR, and Ra) and to identify the performance characteristics under the optimal machining parameters, a special designed experimental procedure is required.In this study, the Taguchi method, a powerful tool for parameter design of the performance characteristics was used to determine optimal machining parameters for maximization of MRR and minimization of Ra in WEDM.

Table 3 Experimental Design Using L_{27} Orthogonal Array

Expt. No	A	B	C	D	MRR (mm^3/min)	S/N (db)	Ra (mμ)	S/N (db)
1	1	1	1	1	3.315	10.4	3.32	-10.42
2	1	1	2	2	4.975	13.93	3.31	-10.39
3	1	1	3	3	2.66	8.5	3.13	-9.91
4	2	2	1	2	7.88	17.94	3.64	-11.22
5	2	2	2	3	7.2	17.15	3.42	-10.68
6	2	2	3	1	3.81	11.61	3.42	-10.68
7	3	3	1	3	11.4	21.13	3.65	-11.24
8	3	3	2	1	6.93	16.81	3.59	-11.1
9	3	3	3	2	5.64	15.03	3.75	-11.48
10	2	3	1	2	7.13	17.06	3.5	-10.88
11	2	3	2	3	7.14	17.07	3.41	-10.65
12	2	3	3	1	7.02	16.93	3.71	-11.38
13	3	1	1	3	6.96	16.86	3.37	-10.55
14	3	1	2	1	4	12.04	3.56	-11.02
15	3	1	3	2	4.58	13.21	3.46	-10.78
16	1	2	1	1	4.52	13.11	3.32	-10.42
17	1	2	2	2	2.25	7.07	3.42	-10.68
18	1	2	3	3	6.13	15.74	3.34	-10.47
19	3	2	1	3	7.99	18.06	3.45	-10.75
20	3	2	2	1	5.66	15.06	3.46	-10.78
21	3	2	3	2	4.89	13.8	3.46	-10.78
22	1	3	1	1	4.18	12.42	3.49	-10.85
23	1	3	2	2	6.08	15.68	3.63	-11.19
24	1	3	3	3	5.69	15.1	3.31	-10.39
25	2	1	1	3	3.89	11.8	3.32	-10.42
26	2	1	2	2	5.87	15.37	3.2	-10.1
27	2	1	3	1	3.65	11.26	3.24	-10.21

3. RESULTS AND DISCUSSION

Figures 2, 3 show graphically the effect of the four control factors on MRR, Ra respectively. The analysis was made using the popular software specifically used for design of experiment applications known as MINITAB 16.

The S/N ratio response table and response graphs are shown for S/N ratio for MRR in Table 3 and Fig. 2, respectively. Similarly, response table and response graphs are shown for S/N ratio for Ra in Table 3 and Figure 3, respectively. Analysis of the result leads to the conclusion that factors at level A3, B3, C1, D3 gives maximum MRR. Although factors C factor is not show significant effect on material removal rate and surface finish as shown in Figure 2 Factor C is having least significance effect for improving MRR. Similarly, it is recommended to use the factors at level A3, B3, C1, D2 for minimization of Ra as shown in Figure 3. Factors C and D have least contribution for minimization of R_a

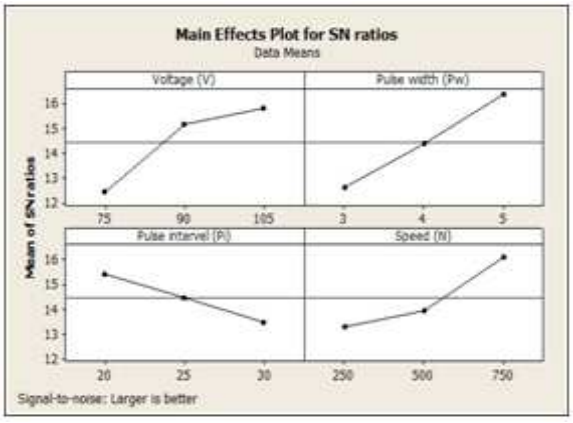

Fig.2 Effect of control factors on MRR

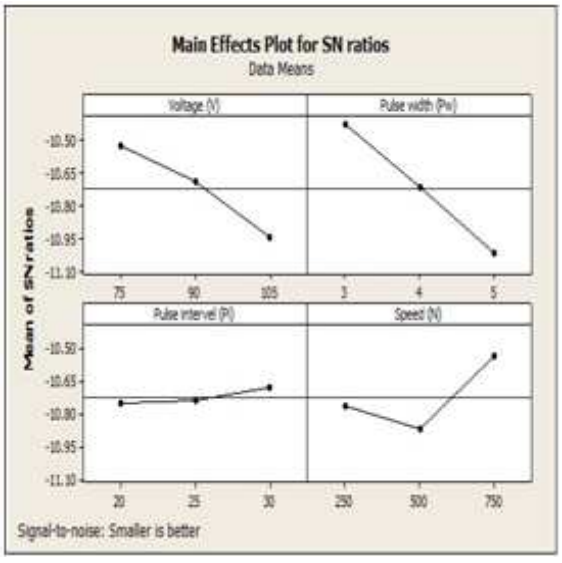

Fig.3 Effect of control factors on Ra

4. CONFIRMATION TEST

The optimal combination of machining parameters has been determined in the previous analysis. However, the final step is to predict and verify the improvement of the observed values through the use of the optimal combination level of machining parameters. The estimated S/N ratio for MRR and Ra are shown in table 4&5.

Table 4 S/N ratio Response Table for MRR

Level	A	B	C	D
level 1	12.44	12.6	15.42	13.3
level 2	15.14	14.4	14.47	13.95
Level 3	15.78	16.36	13.47	16.11
Delta	3.34	3.76	1.95	2.82
Rank	2	1	4	3

Table 5 S/N Ratio Response Table for Ra

Level	A	B	C	D
Level 1	-10.53	-10.43	-10.75	-10.77
Level 2	-10.69	-10.72	-10.74	-10.87
Level 3	-10.95	-11.02	-10.68	-10.53
Delta	0.42	0.6	0.08	0.34
Rank	2	1	4	3

The predicted and experimental value comparison for MRR and Ra from the optimal values by Minitab16 is shown in tables 6&7.

Table 6 Results of the Confirmation Experiment for MRR

	Optimal Machining Parameter	
	Prediction	Experimental
Level	$A_3B_3C_1D_3$	$A_3B_3C_1D_3$
MRR(mm3/min)	9.57367	9.611

Table 7 Results of the Confirmation Experiment for Ra

	Optimal Machining Parameter	
	Prediction	Experimental
Level	A3B3C1D2	$A_3B_3C_1D_2$
Ra(μm)	3.15556	3.12

5. CONCLUSION

In this article, an attempt was made to determine the significant machining parameters for performance measures like MRR and Ra separately in the WEDM process. Factors like Voltage, Pulse width and Speed have been found to play a significant role for MRR and surface roughness. Taguchi's method is used to obtain optimum parameters combination for maximization of MRR and minimization of Ra. The conformation experiments were conducted to evaluate the result predicted from Taguchi Optimization.

REFERENCES

[1] J.L. Lin, K.S. Wang, B.H. Yan and Y.S. Tarng, "Optimization of the Electrical Discharge Machining Process Based on the Taguchi Method with Fuzzy Logic", Journal of Materials Processing Technology, Vol.102, 2000, pp.48-55.

[2] Nihat Tosun C. Cogun and H. Pihtili, "A Study On Kerfs And Material Removal Rate In Wire

Electrical Discharge Machining Based On Taguchi Method", Journal of Materials Processing Technology, Vol.152, 2004, pp.316-322.

[3] Can Cogun, "A Study on Kerf and Material Removal Rate in Wire Electrical Discharge Machining Based on Taguchi Method", Journal of Materials Processing Technology, 2004.

[4] S. S. Mahapatra, Amar Patnaik, "Optimization of Wire Electrical Discharge Machining (WEDM) Process Parameters Using Taguchi Method", International Journal of Advanced Manufacturing Technology, 2006.

[5] Tanimura, "Taguchi and Gauss Elimination Method: A Dual Response Approach for Parametric Optimization of CNC Wire Cut EDM Of PRAlSiCMMC", A. International Journal of Advanced Manufacturing Technology, Vol.28, 2006, pp.67-75.

[6] Yih-fong Tzeng and Fu-chen Chen, "Multi-Objective Optimisation of High-Speed Electrical Discharge Machining Process Using A Taguchi Fuzzy-Based Approach", Materials and Design, Vol.28, 2007, pp.1159-1168.

[7] H. Singh and R. Garg, "Effects of Process Parameters on Material Removal Rate in WEDM", Journal of Achievements in Material and Manufacturing Engineering, Vol.32, 2009.

[8] Mohd Amri Lajis, H.C.D. Mohd Radzi and A.K.M. Nurul Amin, "The Implementation of Taguchi Method on EDM Process of Tungsten Carbide", European Journal of Scientific Research, ISSN 1450-216X, Vol.26 No.4, 2009, pp.609-617.

[9] Kuo-Wei Lin and Che-Chung Wang, "Optimizing Multiple Quality Characteristics of Wire Electrical Discharge Machining via Taguchi Method-based Gray analysis for Magnesium Alloy", Journal of C.C.I.T., Vol.39, No.1, May 2010.

[10] Kamal Jangra, Sandeep Grover and Aman Aggarwal, "Simultaneous Optimization of Material Removal Rate and Surface Roughness for WEDM of WCCO Composite Using Grey Relational Analysis Along With Taguchi Method", International Journal of Industrial Engineering Computations, Vol.2, 2011, pp.479-490.

Poly (Ethyleneglycol Dimethacrylate) Grafted Chitosan Nanoparticles: Synthesis and Evaluation as a Carrier for Controlled Drug Delivery

K. Subramanian[1], V. Vijayakumar[2] and M. S. Kavitha[3]

[1,2&3] Department of Biotechnology, Bannari Amman Institute of Technology, Sathyamangalam- 638 401, Erode District, Tamil Nadu

Abstract

Natural polymers such as chitosan, gelatin, starch, carboxy methyl cellulose, guar gum etc., are widely used as drug carrier due to their biocompatibility, biodegradability, and non-toxicity. But these natural polymers are lacking required mechanical properties to achieve controlled delivery of drugs. Among these polymers chitosan occupies a leadingrole for various medical applications. But this polymer is brittle with low swellability. In the present study chitosan has been chosen as a candidate and chemically modified through radical grafting of poly (ethyleneglycol methacrylate) (PEGDMA) as a bifunctional macromonomer having polyether as flexible spacer.The percentage grafting was>97%. The synthesized graft copolymer was converted into nanoparticle of size 50-200nm as characterized by SEM and Zeta potential analysis. Increased grafting increased the amorphous character and swell ability of chitosan. The nanoparticles were loaded with theophylline a drug used in asthma therapy and its in-vitro release characteristic was investigated spectrophotometrically. The release rate enhanced with increased grafting level. The cytotoxicity study of the grafted chitosan using NIH 3T3 cells revealed a good cell viability implying its biocompatibility. The results demonstrated that the PEGDMA grafted chitosan nanoparticle can be used as a promising carrier for controlled and sustained release of theophylline.

Keywords: *Chitosan nanoparticles, Controlled release, FT-IR, Poly (ethylene glycol dimethacryalate), Zeta potential analyser, SEM, XRD.*

1. INTRODUCTION

Polymers are the choice materials as drug carriers in controlled release of drugs for therapeutic applications. Natural polymers are increasingly being used as carriers in recent years in drug delivery due to their inherent biodegradability, biocompatibility ad non-toxicity. Among these natural polymers chitosan a biopolymer derived from chitin, the second most abundantnaturalcarbohydratebiopolymer after cellulose, is finding increasing applications in medical field such as drug delivery[1], wound dressing[2], tissue engineering etc., due to its biocompatibilityand antimicrobial[3] properties. But its poor physical properties suchashigh brittleness and poor solubility [4] require improvementto widen its medical applications particularly in drug delivery, as a carrier matrix. Many chemical and biochemical routeshave been reported to modify chitosan to improve the aforesaid properties. Among these grafting [5] of chitosanusing synthetic vinyl monomers is one of the widely employed method to incorporate desirable propertiesinto chitosan without sacrificing its aforementioned properties.In this context poly (ethyleneglycol dimethacrylate) (PEGDMA) has been selected as a co-monomer/crosslinker in thepresentwork to graft chitosan since EGDMA is known to be a biocompatible difunctional monomer because of the hydrophilic and biocompatible nature of its polyether moiety [5]. Moreover, increasing interest being focussed on the use of polymer nanoparticle as drug carrier due to advantages such as targeted delivery without overdosing,enhanced solubility and transfection ability[6]etc. Nanoparticles are expected to be adsorbed as intact form in the gastrointestinal tract after oral administration [7]. They are able to protect drugs from degradation, to improve permeation and/or penetration of the drugs across mucosal surface and also to control the release of the encapsulated or adsorbed drug. Hence, inthepresent investigation the main effort is to synthesis PEGDMA grafted chitosannanoparticle, its characterization and evaluation as a tunable drug carrier for*invitro* release studies in simulated biofluids taking theophylline, as a model drug. In the present study the macromonomer, PEGDMAwas chosen for grafting on the ground that it will notdisplay any cell toxicity and hemolytic activity [8] and possesses good resistance toward penetration of microbes. Moreover introduction of polyether moiety of PEGDMA through grafting on chitosan may impart flexibility to the copolymer.

2. EXPERIMETAL

2.1 Materials

Chitosan (CTS, low density, 80–85% deacetylated, inherent viscosity 12.2 dL/g in 0.1 M HOAc at 30°C) was purchased from Kerala State Co-operative Federation for Fisheries Development Ltd and used after purification by reprecipitation. Sodium tripolyphosphate (TPP), poly(ethyleneglycol dimethacrylate) (PEGDMA) (Sigma–Aldrich) was purified by column chromatography on activated basic alumina just before use. Trypsin, ethylenediamine tetraacetic acid(EDTA) acetone (SRL Mumbai) monosodium dihydrogen phosphate, disodium hydrogen phosphate, sodium chloride, hydrochloric acid, nitric acid, stannous chloride, acetic acid, 2- methoxy ethanol(Rankem), ceric ammonium nitrate, citric acid (Qualigens fine chemicals). Theophylline, glycine, pyrogallaol, ninhydrin (Himedia). The murine embryonic fibroblasts cell line (NIH 3T3) (NCCS, Pune) Dulbecco's Modified Eagles Medium, fetal bovine serum (FBS). Simulated gastrict fluid (SGF) and simulated intestinal fluid (SIF) were prepared according to US pharmacopeia.

2.2 Synthesis of PEGDMA Grafted Chitosan(chitosan-g-PEGDMA)

Chitosan(2gm) was taken in a three necked round bottom flask equipped with mechnical stirrer, nitrogen inlet and thermometer and immersed in 1% (v/v) acetic acid(50 ml) at room temperature for 4 h. The solution was heated to 70° C under nitrogen purging in a preheated water bath. The initiator, ceric ammonium nitrate(0.05M) solution was added to reaction mixture and stirred for 5 minutes under nitrogen. Then predetermined amount of PEGDMA (ranged from 0.00177M to 0.0177M) was added to the reaction mixture and stirring continued for 5h. After this the reaction mixture was quenched by adding ice cold acetone to precipitate the graft polymer. Then it was filtered out and dried under vaccum at 60°C for 24h. The dried graft copolymer thus obtained was powdered and purified by soxhlet extraction using 1:1 (v/v) methanol-acetone mixed solvent and dried. The purified graft copolymer thus obtained was seived through 150 micron mesh and stored in HDPE vials for further use. Grafting yield (%) was calculated using the equation.

$$\text{Grafting yield}(\%) = \frac{\text{weight of the graft copolymer}}{\text{weight of the chitosan + weight of PEGDMA}} \times 100$$

2.3 Preparation of Chitosan-*g*-PEGDMA Nanoparticles

Chitosan-*g*-PEGDMAnano particles were prepared according to the ionotropic gelationprocess [9-11]. Nanoparticles were obtained upon the addition of a TPP aqueous solution (1 mg/ml) to a chitosan solution in 1% acetic acid (2 mg/ml) and stirred (400 rpm)using a magnetic stirrer at room temperature. The chitosan-*g*-PEGDMA nanoparticles will be formed as a result of the interaction between the negatively charged groups of TPP and the positively charged amino groups of chitosan. Then it was solicited at 20 KHz for 30 minutes by keeping it in a low temperature (15-20°C) water bath using the sonicator, Sonics VCX 130, Vibracell. The synthesised chitosan-*g*-PEGDMA nanoparticle was freeze dried.

2.4 Swelling Studies

Swelling studies were performed in water and simulated bio fluids (SGF and SIF) at 37°C by keeping a known weight (60 mg) of grafted copolymer in a stainless steel (SS) cylindrical mesh (30 mm die; 50 mm height) immersed in 20 ml of water or SGF or SIF taken in a 25 ml beaker and allowed to swell. The weights of the swelled copolymers at predetermined time intervals were calculated after wiping the mesh containing the swelled polymer with a tissue paper. Then, the average degree of swelling (= $(W_t–W_0)/W_0$, where W_t and W_0 are the weights of the polymer after and before swelling) for the triplicate experiments is plotted against time.The degree of swelling was calculated bythe expression.

$$\%\ \text{Degree of swelling} = \frac{\text{Weight of swollen polymer} - \text{Weight of dry polymer}}{\text{Weight of dry polymer}} \times 100$$

2.5 Characterization

2.5.1 FT-IR Spectra

FT-IR spectra of chitosan and chitosan-graft-PEGDMA were recorded on Kerr pellet for the spectral range 400– 4000 cm^{-1} using ABB Bookmen MB 3000 spectrophometer by accumulating 48 scans at a resolution of 4cm^{-1} .

2.5.2 X-Ray Diffractogram

X-Ray diffractogram was recorded on Shimadzu XRD-6000 diffractometer with Cu Ká radiation operated at 40kV voltage and 30 mA current for the 2è values 5-45°at a scan speed of10° per minute 5 to 100°

2.5.3 Determination of Particle Size

Sample for particle size analysis was prepared by dispersing 10 mg of grafted chitosan in 50 ml of water

by sonication using the solicitor (Sonics VCX 130, Vibracell) at Hz. Measurements of average particle size of the grafted copolymer nano-particles was measured on the Zeta potential analyser, Zetasizer nano ZS90 (Malvern Instruments) equipped with a dynamic light scattering and laser Doppler microelectrophoresis devices. The particle size was measured for 15 min at 25 °C with a 90° scattering angle. The cumulative curve was used to present the mean hydrodynamic diameter. The measurements of zeta-potential were made using the aqueous flow cell in the automatic mode at 25 °C. The measurement of the average particle size was automatically repeated for three times based on the ZetasizerZS90 internal setting and the zeta-potential of the prepared nano-particle was examined for five times.

2.5.4 Scanning Electron Microscopy

The morphological features of nanoparticles (gold coated) were analysed using a scanning electron microscope (JEOL 6390) operating at an accelerating voltage of 20 kV for the magnification range 4000 X-7500X.

2.6 Biodegradability

The biodegradability of grafted copolymer was studied by immersing aknown amount of polymer in 50 ml of SGF and SIF at 37°C. The amount of polymer recovered through precipitation employing ice cold acetone as non-solvent from the dispersion was determined gravimetrically for different known intervals of time over a period of 12 days.

2.7 Cytotoxicity

The monolayer cells grown from the murine embryonic fibroblasts cell line (NIH 3T3) were detached with trypsin-ethylenediamine tetraacetic acid (EDTA) to make single cell suspensions and viable cells were counted using a hemo cytometer and diluted with medium containing 5% FBS to give final density of $1x10^5$ cells/ml. One hundred microlitres per well of cell suspension were seeded into 96-well plates at plating density of 10,000 cells/well and incubated to allow for cell attachment at 37°Cin 5% CO_2, 95% air and 100% relative humidity. After 24h the cells were treated with serial concentrations of the test samples. They were initially dispersed in serum free medium and an aliquot of the sample solution was diluted to twice the desired final maximum test concentration with serum free medium. Additional four serial dilutions were made to provide a total of five sample concentrations. Aliquots of 100 µl of these different sample dilutions were added to the appropriate wells already containing 100 µl of medium, resulting in the required final sample concentrations. Following sample addition, the plates were incubated for an additional 48 h at 37°Cin 5% CO_2, 95% air and 100% relative humidity. The medium containing without samples were served as control and triplicate was maintained for all concentrations [12, 13].

2.8 MTT Assay

MTT is a yellow water soluble tetrazolium salt. A mitochondrial enzyme in living cells, succinate-dehydrogenase, cleaves the tetrazolium ring, converting the MTT to an insoluble purple formazan. Therefore,the amount of formazan produced is directly proportional to the number of viable cells.After 48h of incubation, 15µl of MTT (5mg/ml) in phosphate buffered saline (PBS) was added to each well and incubated at 37°C for 4h. The medium with MTT was then flicked off and the formed formazan crystals were solubilized in 100µl of DMSO and then its absorbance at 570 nm [14] is measured using micro plate reader. The percentage cell viability was then calculated with respect to control as follows [12, 13]

% Cell viability = [A] Test / [A]control x 100

2.9 Drug Loading

0.2gm of chitosan-g-PEGDMA was dispersed in 10ml of deionized water and to this 0.01gm of theophylline solutionin 5ml of distilled water was added with vigorous stirring and stirring continued for 30 min. Then it was centrifuged at 15,000 rpm for 30 min. The supernatant was removed and the amount of drug present in it was determined by measuring its absorbance at 270nm [15]. The entrapment efficiency (E.E %) of the drug in the graft copolymer was calculated using the expression.

$$E.E\ \% = \frac{[\text{Theophylline}]\ \text{taken} - [\text{Theophylline}]\ \text{free}}{[\text{Theophylline}]\ \text{taken}} \times 100$$

where $[\text{Theophylline}]_{total}$ and $[\text{Theophylline}]_{free}$ were the total drug taken and free drug in the supernatant.

The drug loaded graft copolymer thus obtained was used for drug release studies.

2.10 In Vitro Drug Release

In vitro release of theophylline was performed inPBS (pH 7.4).The drug loaded grafted chitosan polymer

nanoparticles were suspended in 10.0 ml of PBS at37 ± 0.2°C in a thermostated water bath shaker agitated at 50 rpm. At known definite intervals of time, it was centrifuged at 10,000 rpm for 10 min and 33µl of the resulting supernatant was taken and its drug content was estimated spectrophotometric ally at 270 nm after appropriate dilution. During each withdrawal an equal Vol. of thermo stated fresh fluid was added to maintain the Vol.constant. The % drug release was determined using the equation

$$\text{Release \%} = \frac{\text{Amount of drug released}}{\text{Drug loaded in nanoparticle}} \times 100$$

3. RESULTS AND DISCUSSION

3.1 Grafting Yeild

The grafting yeild in terms of percentage for the synthesized grafted chitosans namely,CTS-1, CTS-2 , CTS-3, CTS-4, CTS-5 and CTS-6 were 97.5, 93.5,91.5, 87.5,85and 83.5 respectively for typical feed compositions (Table1).

Table 1 %Grafting* at Various Feed Composition

Graft Copolymer Code	Chitosan (g)	Initiator(g)(CAN)	PEGDMA (g)	% of Grafting
CTS-1	2	0.275	1	97.5
CTS-2	2	0.275	0.5	93.5
CTS-3	2	0.275	0.3	91.5
CTS-4	2	0.275	0.2	87.5
CTS-5	2	0.275	0.1	85.0
CTS-6	2	0.275	0.075	83.5

* Volume of reaction mixture: 50 ml

3.2 Swelling Studies

The swelling profiles for the grafted copolymers, CTS-1, CTS-2 , CTS-3, CTS-4, CTS-5 and CTS-6 in water,SGFand SIF are shown in Figures 1,2 and 3 respectively.The time required for equilibrium swelling for these samples were around 40h. Analysis of the swelling profile indicated that with the increased concentration of PEGDMA in the grafting feed decreased the swelling rate. This implies that the swellability can be fine-tuned by varying the concentration of PEGDMA in the feed. Percentage degree of present swelling was maximumin distilled water, followed by SGF and SIF.

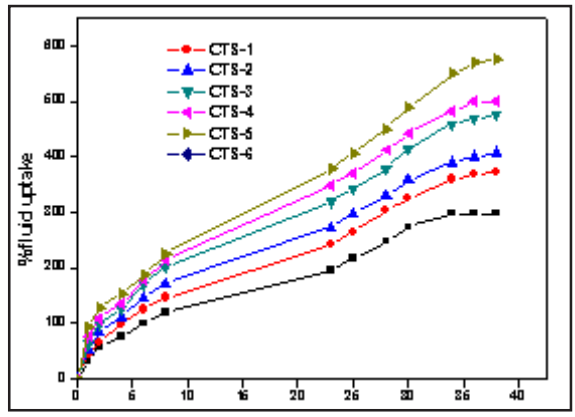

Fig.1 Swelling profile of CTS-1, CTS-2, CTS-3, CTS-4, CTS-5, and CTS-6in distilled water at 37°C

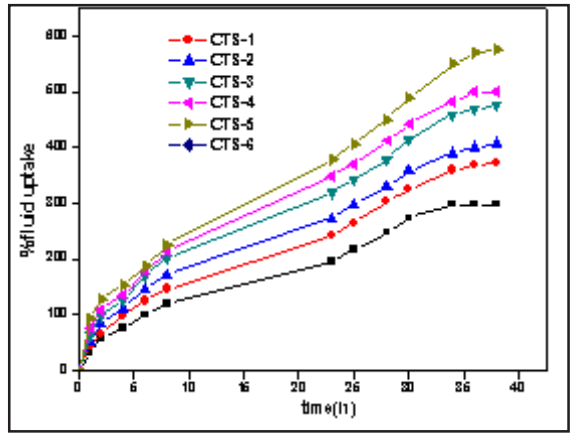

Fig.2 Swelling profile of CTS-1, CTS-2, CTS-3, CTS-4, CTS-5, and CTS-6 in SGF at 37°C

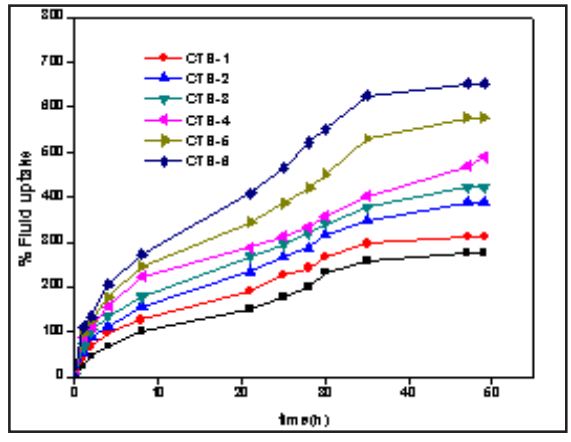

Fig.3 Swelling profile of CTS-1, CTS-2, CTS-3, CTS-4, CTS-5, and CTS-6 in SIF at 37°C

3.3 Characterization

3.3.1 FT-IR Spectra

FT-IR spectra of precipitated chitosan CTS, CTS-1, and CTS-5 are shown in the Figure 4, 5 and 6 respectively.

The absorption peak at 1728 cm^{-1} in CTS-1, CTS-4 and CTS-5 is attributed to ester carbonyl of PEGDMA grafted on chitosan [5].This peak is absent in precipitated chitosan (Figure 4). This confirmed the grafting of PEGDMA on chitosan.

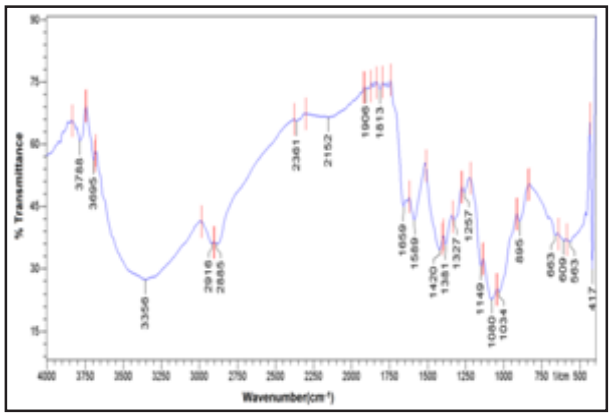

Fig. 4 FTIR spectrum of precipitated chitosan (CTS)

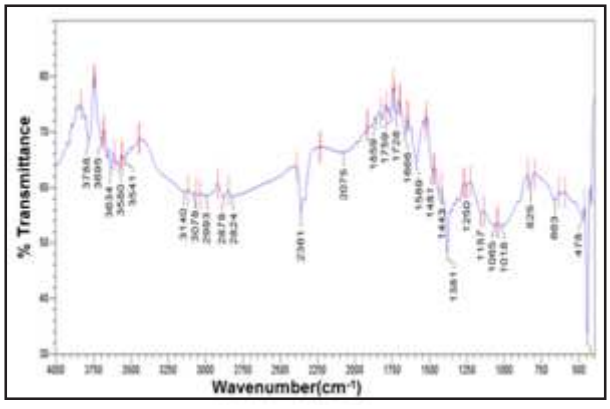

Fig. 5 FTIR spectrum of grafted chitosan, CTS-1

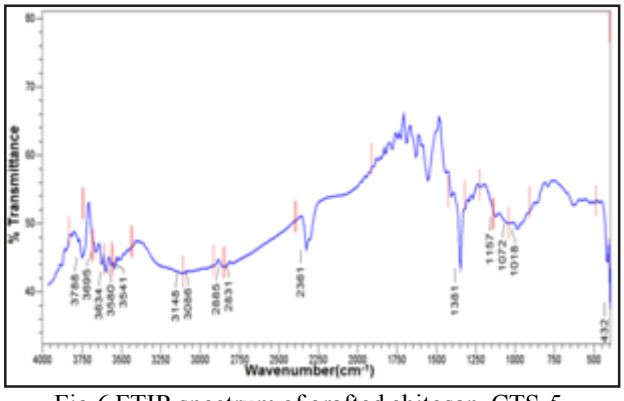

Fig.6 FTIR spectrum of grafted chitosan, CTS-5

3.3.2 X-Ray Diffractogram (XRD)

XRD patterns of chitosan and grafted chitosan (CTS-2) (Figure 7) revealed a broad peak around 22° (2è) indicating that both the polymers are predominantly amorphous in nature and the diffraction angle is not much altered by grafting. The decreased intensity of XRD peak around 22° after grafting implied the enhanced amorphouscharacter of grafted chitosan.Introduction of substituents into polysaccharide structures may disrupt the crystalline structure of chitosan, especially by the loss of the hydrogen bonding. Hence there was anincrease of amorphous character of grafted chitosan.

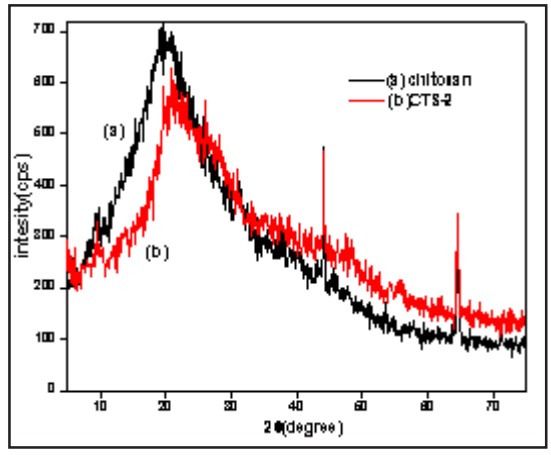

Fig.7 X- Ray diffractograms of chitosan and CTS-2

3.3.3 Particle Size and Particle Size Distribution

The particle size distributions in graftedchitosansCTS-1 and CTS-2 determined by zeta potential analyser were given in Figures8, 9 &10respectively. Average particle size for CTS-1 before and after sonication were 325nm and 161nm respectively implying that sonication brings down the particle size.

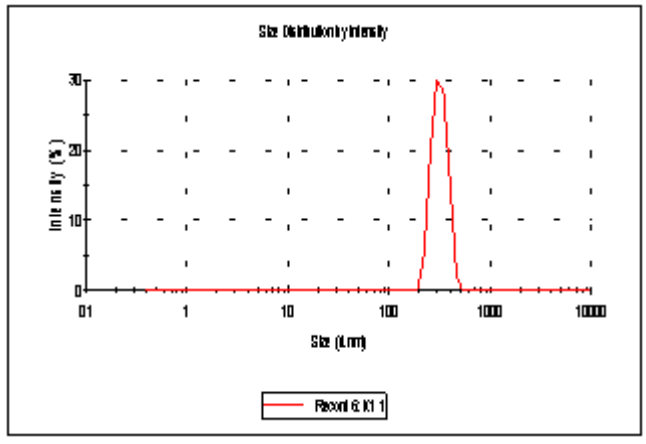

Fig. 8 Particle size distributions in CTS-1

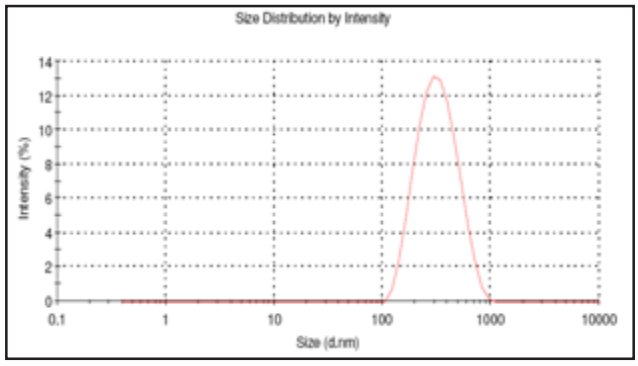

Fig. 9 Particle size distributions in CTS-2

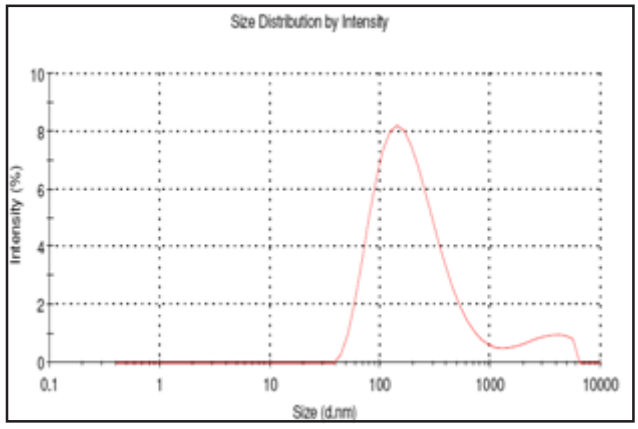

Fig.10 Particle size distributions in CTS-1 after sonication

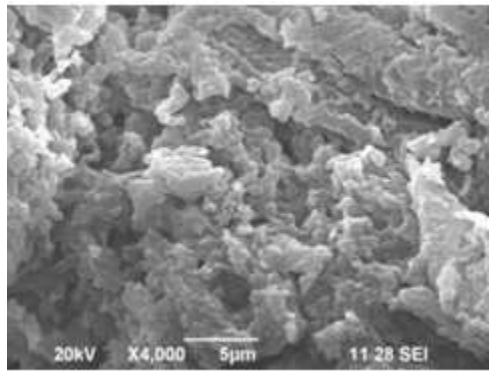

Fig. 11 Micrograph of the grafted chitosan CTS-2

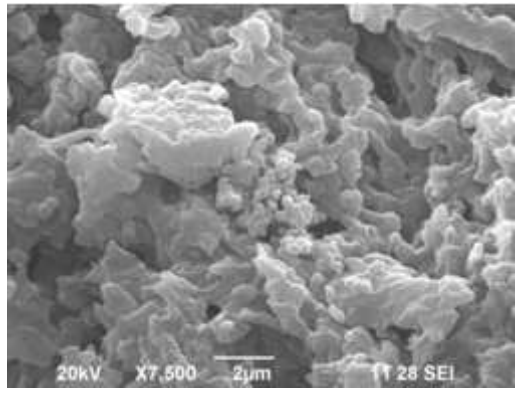

Fig.12 Micrograph of the grafted chitosan CTS-2

3.3.4 Analysis of Free Amino Group

The amino group present in pure chitosan and grafted chitosan moles of free amino groups utilised for grafting in different grafted chitosan polymers CTS-1, CTS-2, CTS-3 and CTS-4 are given in Table 2.

Table 2 Free Amino Groups per Gram of Polymer

Polymer Samples	Moles of Free Amino Groups(10^{-3})
CTS-1	0.00001995
CTS-2	0.000159
CTS-3	0.00132
CTS-4	0.000933
CTS-5	0.00003

3.3.5 SEM Micrograph

The surface morphology and the size of chitosan – grafted nanoparticles were also analysed using SEM. Typical SEM micrographs of CTS-2 are shown in the Figures11 and 12. The average particle size was in around 152nm. The surface morphology also reveals that the particle sizes were not uniform and were heterogeneous.

3.3.6 Biodegradationstudies

The degradability of grafted chitosan CTS-1 in SIF is shown in the form of profile (Figure 13) obtained by plotting weight of recoveredpolymer from SIF at different intervals of time. The weight of insoluble polymer recovered from SIF after 12 days was nil indicating confirmingthe high degradability of the polymer in SIF.

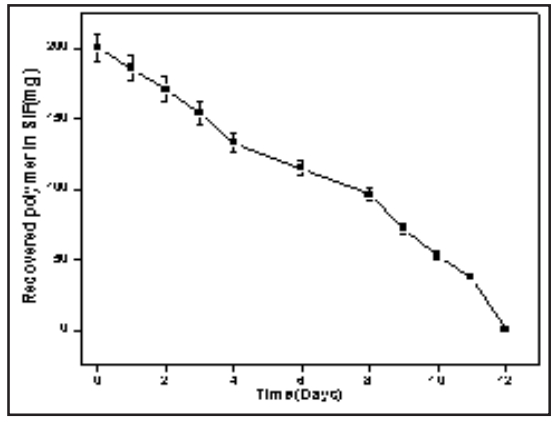

Fig.13 Degradation of CTS-1 in SIF at 37°C

3.3.7 Cytotoxicity

Typical microscopic images of the NIH 3T3 cellproliferation on chitosan and graftedchitosan (CTS-2) are shown in Figures 14&15. The cell viability for the different grafted chitosan is given in the form of histogram. The imagesand the histogram revealed that the cells are viable on the grafted chitosan indicating the biocompatibility of grafted chitosan.

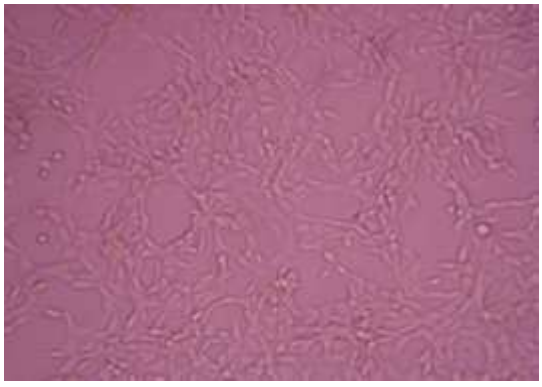

Fig.14 Microscopic image of NIH 3T3 cell proliferation on chitosan

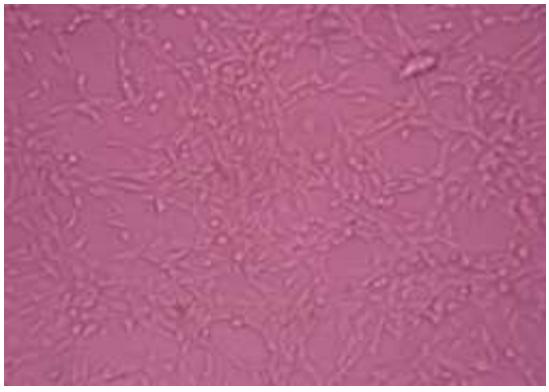

Fig.15 Microcopic image of NIH 3T3 cell proliferation on CTS-2

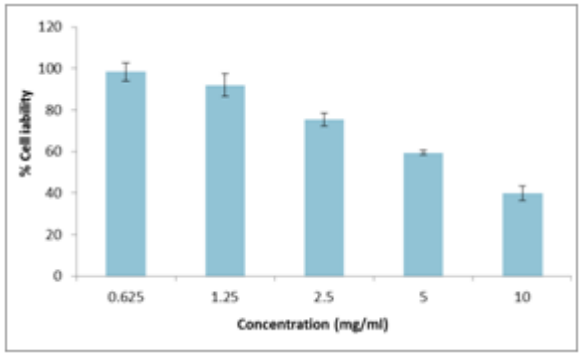

Fig.16 % viability of NIH 3T3 cells on grafted chitosan CTS-2 nano particles

3.4 Drug Loading

Amount of drug loaded into the polymers CTS-1, CTS-2, CTS-3, CTS4, CTS5 and CTS-6are displayed in histogram (Figure17). Drug loading was maximum for polymer (CTS-1).Increasing the level of PEGDMA in the feed and hence in the polymer, increased the extent of drug loading and this may be attributed to the more interaction through the grafted PEGDMA moiety through swelling and more entrapment by increased cross-linking.

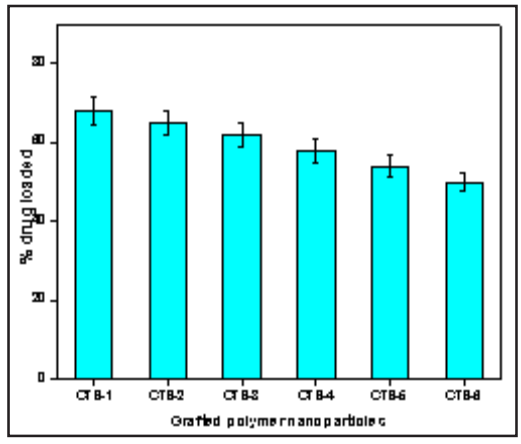

Fig.17 % drug loaded in the grafted chitosan

3.5 In Vitro Drug Release

Typical theophylline release profiles in SIF using nanoparticle grafted chitosan copolymers as a carrier are displayed in Figure 18. Analysis of the profile indicates that there is no significant difference in the drug release rate for the initial two hours. After 5 hours the release rates were highly composition dependent. That is the rates of drug release increased with the increase in the concentration of PEGDMA. This may be attributed to the greater swellability of the matrix in SIF with the increased concentration of PEGDMA.

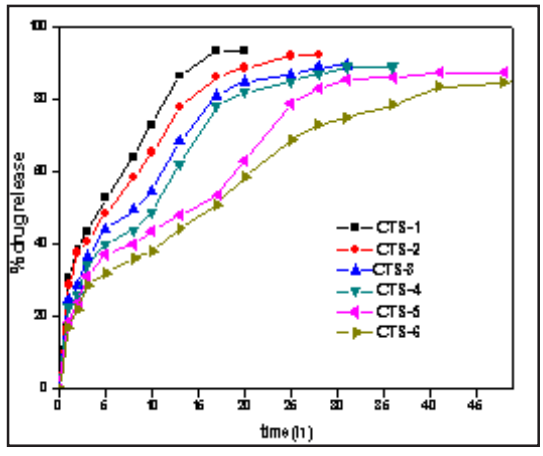

Fig. 18 Drug release profile in PBS

Typical theophylline release profiles using nanoparticle grafted chitosan copolymeras a carrier are displayed in Figure18.Analysis of the profiles indicated that thedrug release rate was very slow. For theinitial release time of two hours, increasing the concentration of PEGDMA in the grafting feed decreased the drug release rate. For instance graft copolymers synthesised using 1.0gm (CTS-1) and 0.075gm (CTS-6) of PEGDM released 93.5 and 60% of drug respectively after 24h. Hence it is very clear by controlling the content of PEGDMA in graft copolymer, drug release rate and characteristics canbe controlled.

4. CONCLUSION

PEGDMA grafted chitosan nanoparticles were prepared and used as a carrier for controlled release of theophylline. The percentage grafting achieved was greater than 97.5% for the given experimental conditions. The size of the nanoparticle was in the range 50-200nm and particle size distribution was heterogeneous as indicated by SEM micrograph. But the particle size distribution determined by the zeta potential method was narrow. Grafting enhanced the amorphousphase of the polymer. Drug release rate and features were highly dependent on the concentration of PEGDMA. Drug release rate decreasedwith the increased PEGDMA demonstrating that controlled release of drug can be achieved by fine tuning the extent of graftingwith PEGDMA. The grafted chitosan is biodegradable and biocompatible. The cytotoxicity of the grafted chitosantested using NIH 3T3 cells revealed the grafted polymer is biocompatible.

REFERENCES

[1] JH.Park, G.Saravanakumar, K Kim and IC.Kwon, "Targeted Delivery of Low Molecular Drugs Using Chitosan and Its Derivatives", Advanced Drug Delivery Reviews, Vol.62, No.1, 31 January, 2010, pp.28-41.

[2] R. Jayakumar, M.Prabaharan, PT. Sudheesh Kumar, SV.Nair and H. Tamura, "Biomaterials Based on Chitin and Chitosan in Wound Dressing Applications", Biotechnology Advances, Vol. 29, No.3, May–June 2011, pp.322-337.

[3] M.Kong, XC.Chen, K. Xing and HJ.Park, "Antimicrobial Properties of Chitosan and Mode of Action: A State of the Art Review" International Journal of Food Microbiology, Vol. 144, No.1, 15 November 2010. pp.51-63.

[4] R.Ravindra, KR. Krovvidi and AA. Khan, "Solubility Parameter of Chitin and Chitosan", Carbohydrate Polymers, Vol. 36, No.2-3, July 1998, pp.121-127.

[5] T. Adali and E. Yilmaz, "Synthesis, Characterization And Biocompatibility Studies On Chitosan-Graft-Poly (EGDMA)", Carbohydrate Polymers, Vol. 77, No.1, 22 May 2009, pp.136-141.

[6] H. Nolte, C.Schilde and A.Kwade, "Determination of Particle Size Distributions And The Degree of Dispersion in Nano Composites", Composites Science and Technology, Vol. 72, No.9, 21 May 2012, pp. 948–958.

[7] Y.Wu, W.Yang, C.Wang, J.Hu and S. Fu, "Chitosan Nanoparticles as a Novel Delivery System for Ammonium Glycyrrhizinate", International Journal of Pharmaceutics, Vol. 295, No.1-2, 13 May 2005, pp.235-245.

[8] SN. Dobiæ, JM. Filipoviæ and SL.Tomiæ, "Synthesis And Characterization of Poly (2-Hydroxyethyl Methacrylate/Itaconic Acid/Poly (Ethylene Glycol) Dimethacrylate) Hydrogels", Chemical Engineering Journal, Vol. 179, 1 January 2012, pp.372-380.

[9] S. Shiraishi, T. Imai and M. Otagiri, "Controlled Release of Indomethacin by Chitosan-Polyelectrolyte Complex: Optimization and *In Vivo/ In Vitro*evaluation", Journal of Controlled Release, Vol. 25, No.3, June 1993, pp.217-225.

[10] XZ. Shu and KJ. Zhu, "A Novel Approach to Prepare Tripolyphosphate/Chitosan Complex Beads for Controlled Release Drug Delivery", International Journal of Pharmaceutics, Vol. 201, No.1, 15 May 2000, pp.51-58.

[11] Q.Gan, T .Wang, C.Cochrane and P. McCarron, "Modulation of Surface Charge, Particle Size and Morphological Properties of Chitosan–Tpp Nanoparticles Intended for Gene Delivery", Colloids and Surfaces B: Biointerfaces, Vol. 44, No.2-3, August 2005, pp. 65-73.

[12] T. Mosmann, "Rapid Colorimetric Assay for Cellular Growth and Survival: Application to Proliferation and Cytotoxicity Assays", Journal of Immunological Methods, Vol. 65, 1983, pp.55-63.

[13] A. Monks, D. Scudiero, P. Skehan, R.Shoemaker, K. Paull, D.Vistica, C.Hose, J.Langley, P.Cronise, AV.Wolff, MG. Goodrich, H. Campbell, J. Mayo and M.Boyd, "Feasibility of a High-Flux Anticancer Drug Screen Using a Diverse Panel of Cultured Human Tumor Cell Lines", Journal of the National Cancer Institute, Vol.83, 1991, pp.757-766.

[14] JA. Plumb, R. Milroy and SB.Kaye, "Effects of The Ph Dependence of 3-(4,5-Dimethylthiazol-2-Yl)-2,5-Diphenyl- Tetrazolium Bromide-Formazan Absorption On Chemosensitivity Determined By A Novel Tetrazolium-Based Assay", Cancer Research. Vol. 49, No.16, Aug 15, 1989, pp.4435-4440.

[15] KB. Sloan, HD. Beall, HE. Taylor, JJ. Getz, R.Villaneuva, R.Nipper and K.Smith, "Transdermal Delivery of Theophylline From Alcohol Vehicles", International Journal of Pharmaceutics, Vol. 171, No.2, 15 September 1998, pp.185-193.

An Experimental Investigation on the Properties of Self-curing Concrete

G.S.Rampradheep[1] and N.Arunachalam[2]
[1]Department of Civil Engineering, Kongu Engineering College, Perundurai, Erode - 638 052, Tamil Nadu
[2]Department of Civil Engineering, Bannari Amman Institute of Technology, Sathyamangalam - 638 401, Erode Distrcit, Tamil Nadu
E-mail: gsramcivil34@gmail.com, drnarunachalam@yahoo.co.in.

Abstract

The aim of this investigation is to study the use of water-soluble Polyethylene Glycol as self-curing agent. The function of self-curing agent is to reduce the water evaporation from concrete, and hence they increase the water retention capacity of concrete compared to the conventionally cured concrete. The use of self-curing admixtures is very important from the point of view that saving of water is a necessity everyday (each one cubic metre of concrete requires 3m^3 of water in a construction, most of which is used for curing). In this study, compressive strength and split tensile strength of concrete containing self-curing agent is investigated and compared with those of conventionally cured concrete. It is experimentally found by the authors that concrete cast with Polyethylene Glycol as self-curing agent is stronger than that obtained by sprinkler curing as well as by immersion curing.

Keywords: *Immersion curing, Polyethylene Glycol, Self-curing concrete, Sprinkler curing, Water retention.*

1. INTRODUCTION

Curing of concrete is maintaining satisfactory moisture content in concrete during its early ages in order to develop the desired properties. Curing of concrete plays a major role in developing the concrete microstructure and pore structure, and hence improves its durability and performance. However, good curing is not always practical in many cases due to the non availability of good quality water. Several investigators are anxious to identify suitable self-curing agent. Therefore, the methods of using self-curing agents have attracted several researchers. The function of self-curing agents is to reduce the water evaporation from concrete, and, thereby, they increase the water retention capacity of the concrete compared to the conventionally cured concrete. It has been found that water-soluble polymers(Polyethylene Glycol) can be used as self-curing agents in concrete (1). In the new millennium, concrete incorporating self-curing agents will represent a new trend in the concrete construction.

2. ADVANTAGES OF SELF-CURING CONCRETE

i. Water resources are becoming valuable every day. Each one cubic metre of concrete requires about 3m^3 of water for construction, most of which is used for curing. Self-curing concrete will not require water for curing.
ii. Helps to reduce the cost of labourers needed for curing the concrete.
iii. Holds good when there is a problem of occurrence of water scarcity.
iv. Holds good in the place of large buildings and in complicated areas where curing process is difficult and costly.

3. EXPERIMENTAL PROGRAM

3.1 Material

The materials that have been used in this study are Portland Pozzolana Cement of brand name "SANKAR", conforming to IS:1489 (PT 1):1991 , fine aggregate obtained from Karur River bed and tested as per IS:383-1970 and angular coarse aggregates of maximum size 20mm and tested as per IS:383-1970. Table 1 shows the concrete mix used in this investigation. Two concrete mixes have been adopted with the same w/c ratio. One mix included the self-curing agent and the other mix was without self-curing agent. The slump value and compacting factor value based on workability tests for conventional concrete and self-curing concrete are given in Table 2. The self-curing agent used in this study was water-soluble polymers (i.e; Polyethylene Glycol) conforming to molecular weight 400. The dosage of self-curing agent was kept at 0.3% of cement by weight

Table 1(a) Concrete Mixes Involving Self Curing Agent for One Cube of Size 150 Mm

Grade of Concrete	Cement (kg)	Sand (kg)	Coarse Aggregate (kg)	w/c	PEG (ml)
M20	2.2	3.14	7.47	1.18	6.5
M30	2.9	2.89	7.27	1.17	9
M40	3.7	3	6.5	1.16	11

Table 1(b) Concrete Mixes Involving Self Curing AgentFor one Cylinder

Grade of Concrete	Cement (kg)	Sand (kg)	Coarse Aggregate (kg)	w/c	PEG (ml)
M20	1.4	2	4.76	750	4.2
M30	1.85	1.84	4.63	750	5.55
M40	2.36	1.91	4.14	744	7.08

Table 2 Slump and Compacting Factor Tests Results

Grade of Concrete	Designation	w/c	Slump (mm)	Compacting Factor
M_{20}	Conventional concrete	0.5	130	0.94
	Self-curing concrete	0.5	180	0.97
M_{30}	Conventional concrete	0.43	75	0.92
	Self-curing concrete	0.43	90	0.94
M_{40}	Conventional concrete	0.36	15	0.85
	Self-curing concrete	0.36	25	0.9

4. SLUMP CONE TEST

Fig.1 Workability tests

5. COMPRESSION AND SPLIT TENSION TESTS

Cubes of size 150mm and cylinder of size 150mm diameter and 300mm height of both conventional and self-curing concretes were cast. Each layer was compacted with 25 blows using steel tamping rod of 16mm diameter and 600mm length. For conventional concrete involving immersion curing, the specimens were allowed to get cured 24 hour after their casting. For conventional concrete involving sprinkler curing, water was sprinkled on the cubes and cylinders periodically. Self-cured specimens were kept as such without the application of any external curing after their removal from moulds.

The strength related tests were carried out for hardened conventional concrete and self-cured concrete at the age of 3 days, 7 days and 28 days to ascertain the strength related properties such as cube compressive strength, cylinder compressive strength and cylinder split tensile strength.

Fig. 2 Non – Destructive test (Rebound Hammer) on cylinder

Fig. 3 Split tensile test on a cylinder

Fig. 4 Compression tests for cubes

6. DURABILITY TEST (WATER SORPTIVITY TEST)

Water sorptivity test was carried out for measuring rate of absorption of water. The specimens used were cylinders of size 50mm diameter and 100mm height of both conventional and self-curing concrete. The specimens were oven dried at 110 ±5°C for 24 hours and then the specimens were left to cool in dry condition during the following 24 hours. The test was carried out by allowing one circular surface of the specimen to be in contact with water at 5mm depth as per ASTM C 1585 – O4e1 as shown in Figure 5.

The remaining portion of the specimen(other than 5mm) was coated with high quality water proofer (High Bond Polymers) in order to create unidirectional flow pattern through the concrete specimen.

The water sorptivity (by capillary suction) tests were carried out for hardened conventional concrete and self-cured concrete at the age of 28 days to ascertain the amount of absorption of water at the specified period of 30 min, 60 min, 90 min, 120 min, 150 min and 180 min and the water sorptivity could be found by the formula, W/(A x “t) = k where, W = weight of water absorbed, A = cross sectional area of specimen, t = time in mins, k = sorptivity coefficient.

Fig. 5 Water sorptivity test

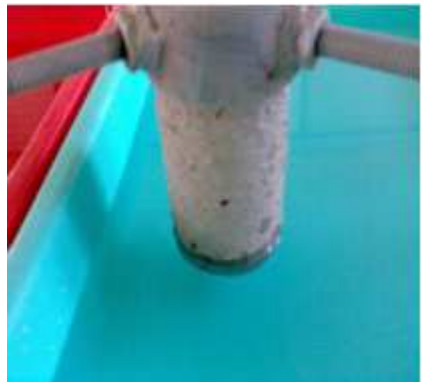

Fig. 6 Depth of penetration of specimen

7. TEST RESULTS AND DISCUSSION

The compressive strength of cube, compressive strength of cylinder, split tensile strength of cylinder and sorptivity test for cylinder are given in the Fig.7-15.

The results show that there is increase in compressive strength in the case of self-cured concrete specimens when compared to other concrete specimens. The 3, 7 and 28 days cube and cylinder compressive strengths of specimens cured under different conditions are shown in Fig. 7 to 9. From these figures, it is clear that self-

cured concrete gives more compressive strength based on NDT (Rebound Hammer) compared with cubes and cylinders subjected to the other two types of curing. The 3, 7 and 28 days compressive strengths of cubes cured under different types of conditions is shown in Fig.10. From these figures, it is clear that self-cured concrete gives more compressive strength, obtained by HEICO compression Testing machine compared to the other two types of curing. The 3, 7 and 28 days Split Tensile strengths of specimens for cylinders cured under different types of curing is shown in Figure11. From these figures, it is clear that self-cured concrete gives more Split Tensile strength compared to the other two types of curing. The results for water absorption and water sorptivity for the self-curing and conventional concrete at the age of 28 days is shown in Fig.12-15. From these figures, it is clear that there is a decrease in the value of amount of water absorption and water sorptivity as decrease in the w/c ratio. The results conveys that in all these grades of concrete the amount of absorption of water and water sorptivity for self-cured concrete is found to be lesser than that of fully cured and sprinkler cured concrete specimens showing that the amount of pores is in self cured concrete is less compared to the other two types.

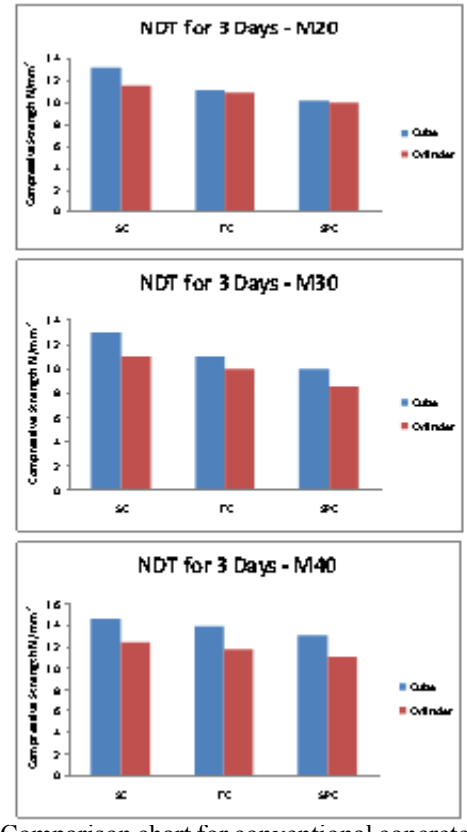

Fig. 7. Comparison chart for conventional concrete (Fully cured / Sprinkler cured) with Self – cured concrete for 3 days using NDT Test (Schmidt Rebound Hammer)

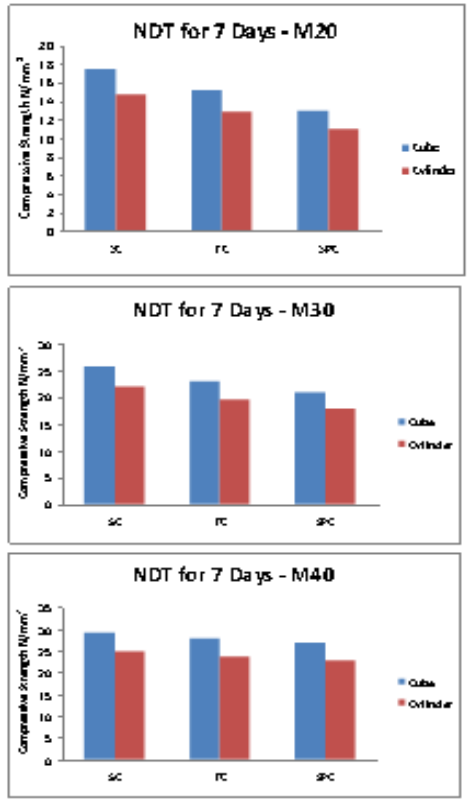

Fig. 8 Comparison chart for conventional concrete (Fully cured / Sprinkler cured) with Self – cured concrete for 7 days using NDT Test (Schmidt Rebound Hammer

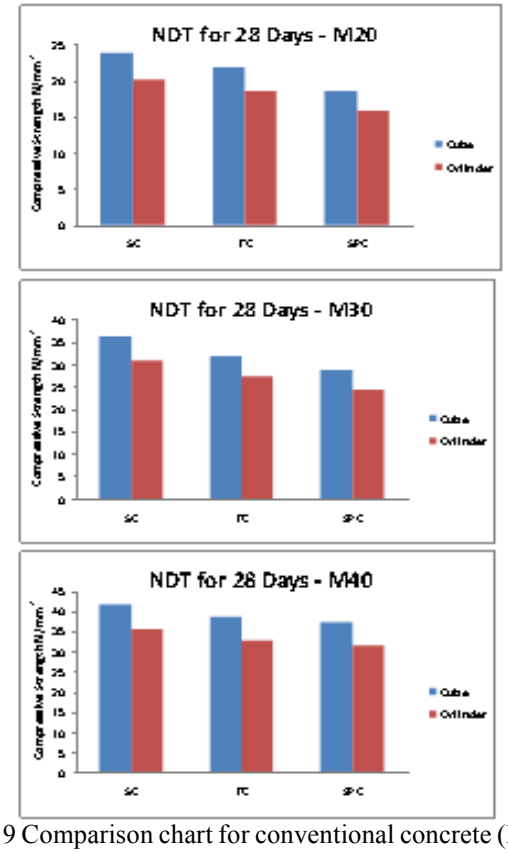

Fig. 9 Comparison chart for conventional concrete (Fully cured / Sprinkler cured) with Self – cured concrete for 28 days using NDT Test (Schmidt Rebound

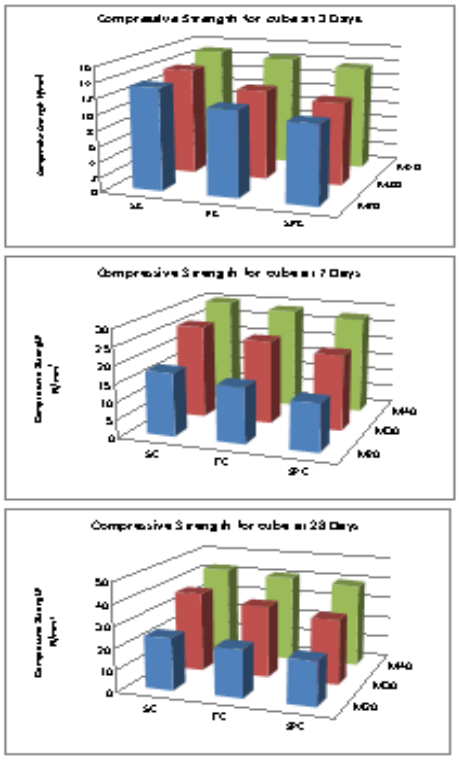

Fig. 10 Comparison chart for conventional concrete (Fully cured / Sprinkler cured) with Self – cured concrete for cubes at 3 days, 7 days and 28 days using Compression Testing Machine

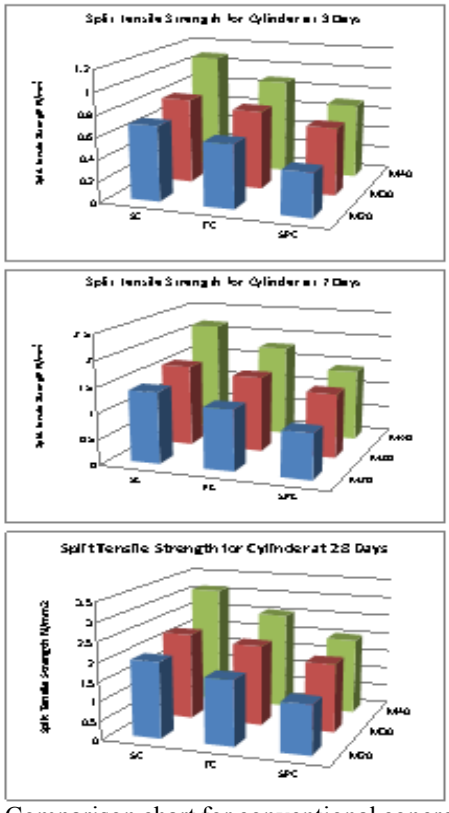

Fig. 11. Comparison chart for conventional concrete (Fully cured / Sprinkler cured) with Self – cured concrete for cubes at 3 days, 7 days and 28 days using Compression Testing Machine

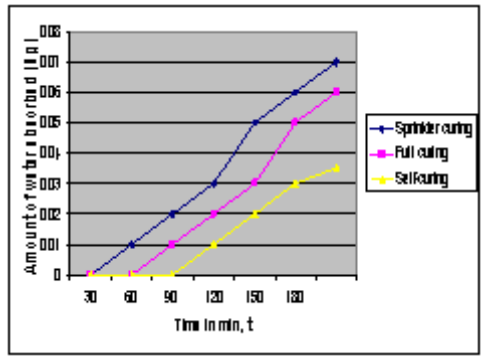

Fig.12 Water absorption for M_{30}

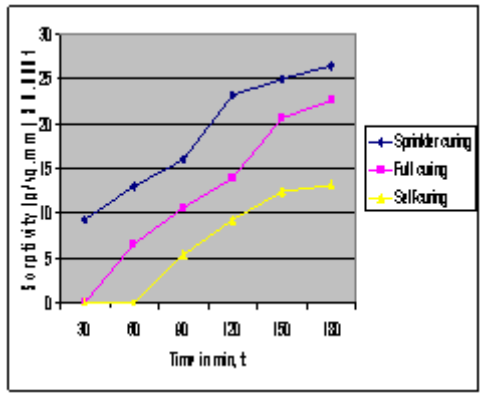

Fig.13 Water sorptivity for M_{30}

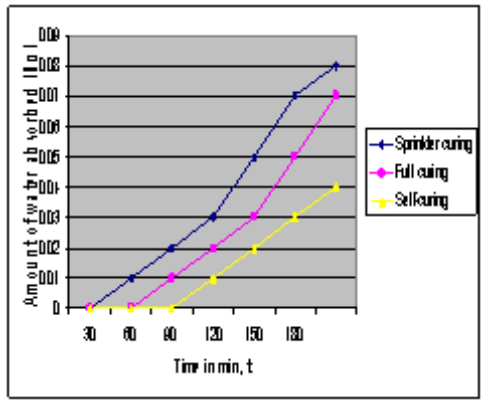

Fig.14 Water Absorption for M_{40}

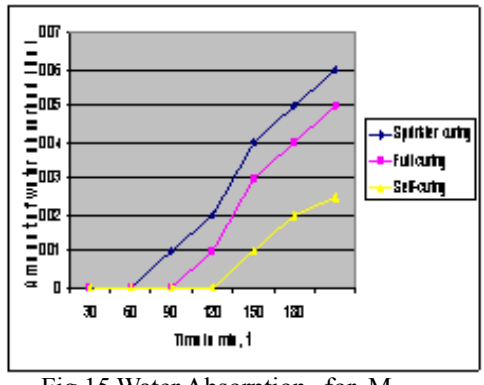

Fig.15 Water Absorption for M_{40}

8. CONCLUSIONS

The following could be concluded from the results obtained through this experimental investigation:

i. The compressive strength of cubes and cylinders by NDT (Rebound Hammer) for self-cured concrete is higher than that of conventional concrete cured by full curing and sprinkler curing.

ii. The compressive strength of cubes and cylinders by HEICO compression Testing machine for self-cured concrete is higher than of concrete cured by full curing and sprinkler curing.

iii. The cylinder split tensile strength self-cured concrete is higher than that of conventional concrete cured by full curing and sprinkler curing.

iv. Self-cured concrete is found to have less water absorption and water sorptivity values compared with concrete cured by the other methods.

v. Self-cured concrete thus has less amount of pores.

REFERENCES

[1] ASTM C 1585 – O4e1 "Standard Test method for measurement of Rate of Water Absorption by Hydraulic Cement Concretes".

[2] R.K.Dhir, P.C. Hewlett, J. S.Lota and T.D Dyet, "Investigation Into The Feasibility Of Formulating 'Self Cure' Concrete", Materials and Structures, Vol.27, 1994, pp.606-615.

[3] IS 456:2000 (Clause 13.5) "Specifications for Curing of Concrete".

[4] IS 10262:1982 "Indian Standard Recommended method of M_{20} Concrete Mix Design".

[5] Mix Proportioning of Internal Curing, by Dale P.Batz Building and Fire Research Laboratory, National Institutes of standard and Technology, Gaithersberg, MD 20899 U.S.A. M.S. Shetty, Concrete Technology: Theory and Practice Fifth Edition.

[6] Protected Paste Volume in Concrete Extension To Internal Curing Using Saturated Light Weight Fine Aggregate by D.P.Bentz, K.A.Snydar (Building and fire research laboratory, National Institute of Standards and Technology, Gaithersburg, Received 26 April 1999; accepted 8 August 1999).

[7] Self-Curing Concrete : Water Retention, Hydration And Moisture Transport by A.S. DIEB, R.K.Dhir, P.C.Hewlett and T.D.Dyert – Magazine of Concrete Research, 1998, No.1, March., 85 – 90.

[8] Study of Sorptivity of Self-Compacting Concrete with Mineral Additives by Luiz Antonio Pereira de Oliveira.

Low Power And Low Area Analog Multiplier Using MIFGMOS

K. Duraisamy[1] and U. Ragavendran[2]
[1]Department of Computer Science and Engineering, K.S.Rangasamy College of Technology,
Tiruchengode - 630 215, Tamil Nadu
[2]Anna University of Technology, Coimbatore - 641 047, Tamil Nadu
E-mail: deanac@ksrct.ac.in, ragasivaka@gmail.com

Abstract

A novel 4- quadrant analog multiplier using floating gate MOS (FGMOS) transistors operating in saturation region are implemented. Floating gate MOSFETs are being utilized in a number of new and existing analog applications. These devices are not only useful for designing memory elements but also we can implement circuit elements. The main advantage in FGMOS is that the drain current is proportional to square of the weighted sum of input signals. By using conventional transistors we obtain only few hundred mill volts range of the supply voltage and when we go for square law devices we obtain up to 50%. So in order to get 100% range of the supply voltage we go for FGMOS. This can be obtained by the control voltage applied at the gate of the FGMOS. This simulation is done with the SPICE tools.

Keywords: *MOSFET circuits, MOS logic circuits, MOS integrated circuits, VLSI.*

1. INTRODUCTION

Four quadrant analog multipliers are important building blocks neural networks, fuzzy controllers, wireless communications and electronic systems such as voltage controlled oscillators and filters, modulation and demodulation circuits, adaptive filters, automatic gain control, frequency mixers etc. They can be used for waveform generation and modulation, and power measurements. Other typical applications also include the implementation of dividers and square-rooters, through feedback configuration, etc. Several techniques of implementing four-quadrant analog multipliers, using MOS technology, have been reported. They are the variable transconductance technique (modified Gilbert cell) [1]-[3], the voltage-controlled transconductance technique, which employs MOS transistors operating in the triode region [4]-[6], the bias feedback technique [7], techniques based on square-law characteristics of MOS transistors operating in the saturation region, implementing either the quarter-square identity [8]-[10] or other algebraic identity [11]-[12], and the technique based on linear transconductors [13]-[15]. The Gilbert six transistors cell (GSTC), using the variable transconductance technique, is very popular in bipolar technology since its output current has a linear relationship with the tail current source which allows the nonlinear relationship with the input signals, *Vx* and *Vy,* to be compensated simply by an appropriate pre-distortion circuit. However, the output current of a MOS transistor multiplier, based on the modified GSTC, has a nonlinear relationship with the tail current source and makes compensation by a pre-distortion circuit very difficult [2] This limits the linear input range of the multiplier to only a few hundred mill volts [l]. On the other hand most of the square-law based multipliers reported so far have input signal range limited to about 50% of the supply voltage.

In this paper, a novel four-quadrant analog multiplier using floating-gate MOS (FGMOS) transistors operating in the saturation region is presented. The drain current is proportional to the square of the weighted sum of the input signals. This square law characteristic of the FGMOS transistor is used to implement the quarter square identity by utilizing only six FGMOS transistors. The main features of this remarkably simple multiplier circuit configuration are the large input signal range equal to 100% of the supply voltage, nonlinearity of 0.0078% and THD of maximum 2.74% (while the inputs are at their maximum values) Rest of the paper is organized as follows. In Section II, the basic structure of the FGMOS transistor is described. The principle of operation of the FGMOS four-quadrant analog FGMOS multiplier are presented in Section III and. Simulation results of the proposed circuit are shown in section IV followed by conclusion in section V.

2. THE FGMOS TRANSISTOR

The basic structure of the MFMOS transistor is shown in Figure 1(a), (also known as the “neuron MOS”

by Shibata and Ohmi [19]). It consists of a -channel MOS transistor with a floating gate (first polysilicon layer) over the channel and in some cases extending over to the field oxide area.

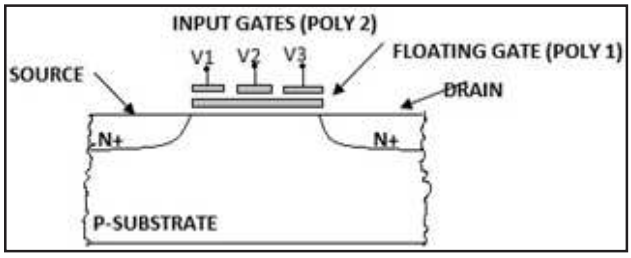

Fig.1(a)

An array of control gates (multiple input gates) are formed by the second polysilicon layer over the floating-gate. The capacitive coupling between the multiple input gates and floating-gate and the channel is shown in Fig. 1(b) while Fig. 1(c) is the symbolic representation of such a device.

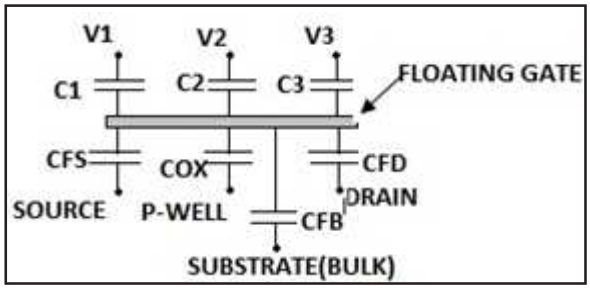

Fig. 1(b)

MOS model for the same technology with the equation that relates V_{FG} to V_i, V_d, V_S, C_i, C_{GD}, C_{GS} and C_{GB}. This equation can be obtained by applying the charge conservation law to the floating node (FG). If there is an infinite resistance between the FG and all the surrounding layers, there will be no leakage current between them, and so, the FG will be perfectly isolated. Under this assumption the voltage at the FG is given by

$$\left[V_{FG} = \sum_{i=1}^{N} (C_1 / C_T) V_1 + (C_{GS} / C_T) V_S + (C_{GD} / C_T) V_D + (Q_{FG} / C_T)\right] \quad (1)$$

Where term C_T refers to the total capacitance seen by the FG and is given by

$$C_T = C_{FD} + C_{FS} + C_{FB} + \sum_{i=1}^{N} C_i \quad (2)$$

The equations modelling the large signal behaviour of the FGMOS can now be obtained by replacing Vgs in the equations describing the large signal behaviour of the MOS transistor, with the expression describing the voltage between the FG and source which can be obtained by referring V_{FG} to the source terminal rather

$$I_d = 0.5k \left(\sum W_i V_i + W_b V_b - W_S V_S - W_T V_T^*\right)^2 \quad (3)$$

Where the capacitive coupling ratios,

$$W_i = (C / C_T),$$
$$W_B = (C_{BB} / C_T),$$
$$W_S = [1 - (2/3)(C_{FS} / C_T) - (2/3)(C_{OX} / C_T)] \quad (4)$$
$$W_T = 1 - (2/3)(C_{OX} / C_T)$$

Where V_T^* is the threshold voltage seen from the floating-gate, $K = \mu_n C_{OX}\left(\frac{W}{L}\right)$ is the trans-conductance parameter, μ_n is the electron mobility, and L is the channel length. C_T is the total capacitance associated with the floating gate Eq(4) shows that the FGMOS transistor drain current in saturation is proportional to the square of the weighted sum of the input signals, where the weight of each input signal is determined by the capacitive coupling ratio of the input.

3. EXISTING FOLDED COMS – MULTIPLIER

Figure 4.a shows the conventional multiplier circuit based on the folded CMOS Gilbert Cell while Figure 4.b shows the proposed floating gate multiplier circuit which is based on the topology given in [2], employing FGMOS differential pairs instead of conventional pairs to improve the circuit behaviour. M1a, M1b transistors form one differential pair where as M2a, M2b form the other. They are cross connected by connecting the drains of the transistors M1a, M2a and M1b, M2b together. A differential input VX is applied to the cross connected differential pairs while the other differential input VY is applied to the differential pair formed by M3a and M3b. M3a and M3b transistors form tail transistors for the two differential pairs. The bias currents (ISS1, ISS2, and ISS3) are provided as tail currents to the differential pairs.

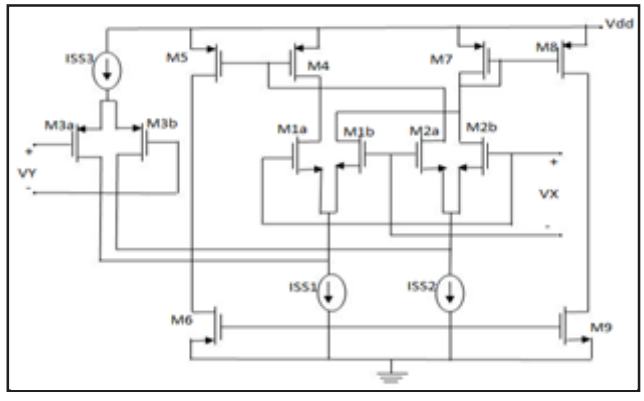

Fig. 2 Conventional multiplier

3.1 Simulation Results

The proposed circuit (Figure 3) was simulated using MCNC 1.25um CMOS Process. The supply voltage is V_{DD}=5V, VGC is set to 0.5v The tail currents are I_{SS1}=I_{SS2}=350 ìA I_{SS3}=100 ìA. The input capacitor value is taken C_i=4pF while the C_{FGD} and C_{FGS} values are calculated as 59.24f and 0.5540p, respectively. The dimension for cross connected differential pair transistors M1a, M1b, M2a and M2b is W / L = 2.5 ìm / 250 nm, for M3a and M3b is W / L = 2.5 ìm / 250 nm.

For conventional multiplier, when the linear input range is limited to the 50% of the supply voltage range. Simulation results at input range less than 50% of supply voltage is shown in Figure 2(a)

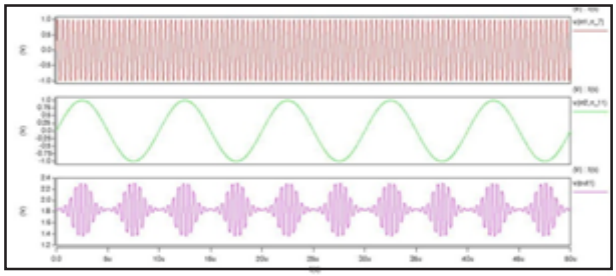

Fig.2 (a)

For conventional multiplier, when the linear input range is limited to the 50% of the supply voltage range. Simulation results at input range equal to the supply voltage is shown in Figure 2(b)

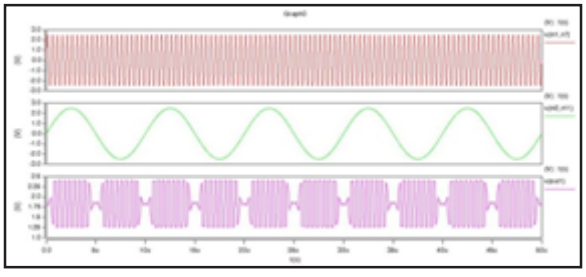

Fig.2 (b)

For conventional multiplier, when the linear input range is limited to the 50% of the supply voltage range. Simulation results at input range greater than the supply voltage is shown in Figure 2(c).

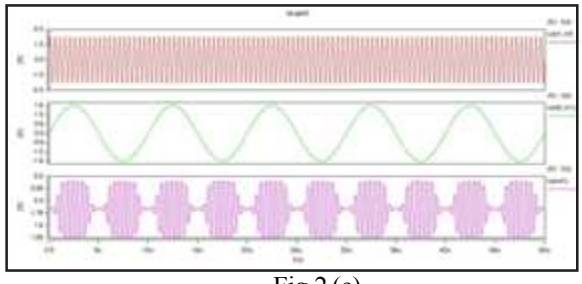

Fig.2 (c)

4. PROPOSED FGMOS TRANSISTOR-MULTIPLIER

Each transistor in differential pairs has two inputs which are applied through two equal sized capacitors, Ci. The differential signals of the inputs are applied to one of the floating gates in the differential pairs. VX and VY act as input signals while VGC as a control voltage to the floating gates. Since the voltage at the gate is less than the input voltage the differential pair transistors can work in saturation even when large signals are applied. This leads to increase the input dynamic swing

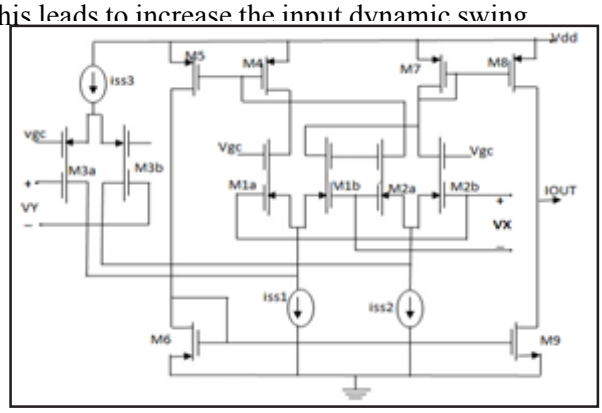

Fig. 3 Proposed multiplier

4.1 Simulation Results

For proposed multiplier, large input signal range equal to 100% of the supply voltage. Simulation results at input range less than 50% of supply voltage is shown in Figure 3(a).

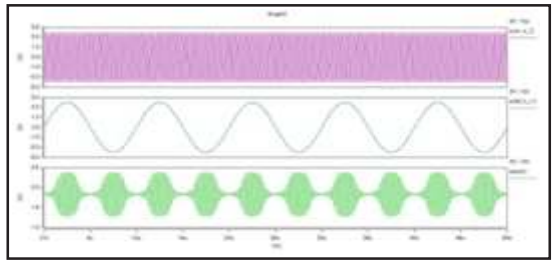

Fig.3 (a)

For proposed multiplier, when the input signal range is equal to 100% of the supply voltage. Simulation results at input equal to the supply voltage is shown in Figure 3(b).

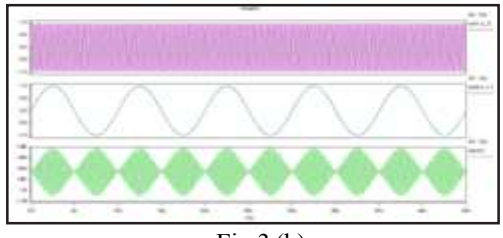

Fig.3 (b)

For proposed multiplier, when the input signal range is equal to 100% of the supply voltage. Simulation results at input greater than the supply voltage is shown in Figure 3(c).

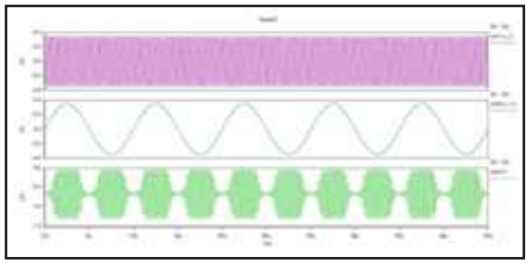

Fig.3(c).

5. POWER ANALYSIS

For conventional multiplier, when the linear input range is limited to the 50% of the supply voltage range

i. VVy1 from time 1e-009 to 5e-00
ii. Average power consumed -> 4.441178e-012 watts
iii. Max power 1.094650e-008 at time 4.56687e-006
iv. Min power 1.976560e-021 at time 5e-005.

For proposed multiplier, when the input signal range is equal to 100% of the supply voltage range

i. VV1 from time 1e-009 to 5e-005
ii. Average power consumed -> 1.250723e-008 watts
iii. Max power 1.516830e-004 at time 2.52469e-006
iv. Min power 4.881126e-017 at time 5e-005

6. CONCLUSION

A novel FGMOS four quadrant multiplier has been designed and simulated. It is based on the square law dependence of the drain current on the weighted sum of the input signals. The circuit configuration is remarkably simple. It has a large input voltage range equalling the supply voltage. The measured nonlinearity and total harmonic distortion are 0.0078 % and 2.74% under full scale input conditions, respectively. with low power consumption for high power input range.

REFERENCES

[1] S. I. Liu and Y. S. Hwang, "CMOS Four-quadrant Multiplier Using Bias Feedback Techniques", IEEE J. Solid- State Circuits, Vol. 29, No.6, June, 1994, pp.750-752.

[2] J. Pena-Fino1 and J. A. Connelly, "A MOS Four Quadrant Analog Multiplier Using The Quarter-square Technique", IEEE J. Solid-State Circuits, Vol. SC-22, No.6, December, 1987, pp.1064-1073.

[3] H. G. Song and C. K. Kim, "A MOS Four-quadrant Analog Multiplier Using Simple Two-input Squaring Circuits With Source Followers", IEEE J. Solid-State Circuits, Vol.25, No.3, June 1990, pp.841-848.

[4] C. W. Kim and S. B. Park, "Design And Implementation of a New Four Quadrant MOS Analog Multiplier", Analog Integrated Circuits and Signal Processing, Vol.2, 1992, pp.95-103.

[5] N. Saxena and J. J. Clark, "A Four-quadrant CMOS Analog Multiplier for Analog Neural Network," IEEE J. Solid- State Circuits, Vol.29, No.6, June 1994, pp.746-749.

[6] K. Bult and H. Wallinga, "A CMOS Four-quadrant Analog Multiplier", IEEE J. Solid-State Circuits, Vol.SC-21, No.3, June 1986, pp.430-435.

[7] S. L. Wong, N. Kalyansundaram, and C. A. T. Salama, "Wide Dynamic Range Four-quadrant CMOS Analog Multiplier Using Linearized Transconductance", IEEE J. Solid-State Circuits, Vol.SC-21, No.6, 1986, pp.1120-1122.

[8] Z. Wang, "A CMOS Four-quadrant Analog Multiplier With Single-ended Voltage Output And Improved Temperature Performance," IEEE J. Solid-State Circuits, Vol.26, No.9, 1991, pp. 1293-1301.

[9] S. R. S. Garimella, J. Ramirez-Angulo, A. Lopez-Martin and R. G. Carvajal, "Design of Highly Linear Multipliers using Floating Gate Transistors and/or Source Degeneration Resistor", IEEE International Symposium on Circuits and Systems, 2008, pp.1492-1495.

[10] S.S. Jamuar, S. Sharma and S.S.Rajput, "Analog Signal processing Using FGMOS Based Structures: A Tutorial," J. Of Active and Passive Electronic Devices, Vol.3, 2008, pp.109-124.

A Novel Approach for Segmentation of Pectoral Muscle on Medio-lateral Oblique View Mammograms

B. Nagarajan[1] and W. Jai Singh[2]

[1]Department of Computer Applications, Bannari Amman Institute of Technology, Sathyamangalam - 638 401, Erode Distrcit, Tamil Nadu

[2]Department of Master of Computer Applications, Park College of Engineering and Technology, Coimbatore - 641 659, Tamil Nadu

Abstract

Mammography is one of the best methods for early detection of breast abnormalities. When mammograms are analyzed by using computer, the pectoral muscle should preferably be excluded from processing intended for the breast tissue. It also represents a predominant density region in most Medio-Lateral Oblique (MLO) views of mammograms; its inclusion can affect the results of intensity based image processing methods in the detection of breast cancer. In this paper, a novel approach is developed to automatically segment the pectoral muscle on MLO view mammograms. The proposed method is applied to different categories of mammograms which are available in Mammographic Image Analysis Society (MIAS) database. The region of pectoral muscle is segmented and the results are proven effective when compared to existing method.

Keywords: *Automatic segmentation, Iterative Threshold, Mammogram, Morphology, Pectoral Muscle, Polyline.*

1. INTRODUCTION

Breast cancer is the most common cancer disease among women. Mammography is the best technique of choice to detect breast cancer and it is based on the difference in absorption of X-rays between the various tissue components of the breast such as fat, tumor tissue, and calcifications. The projection of the breast on mammogram can be made from different angles. The two most common projections are Medio-Lateral Oblique and Cranio-Caudal view. The advantage of the medio-lateral oblique projection is that almost the whole breast is visible, often including lymph nodes. Part of the pectoral muscle will be shown in upper part of the image. With the MLO view, the pectoral (chest) muscle should be depicted obliquely from above and visible down to the level of the nipple or further down.

The pectoral muscle represents a predominant density region in most MLO views of mammograms and can affect the results of image processing methods [1]. Pectoral muscle appears almost at the same density as the dense tissues in the image. Therefore, segmentation of pectoral muscle is important in order to limit the search for the breast abnormalities only to the breast cancer which is the region of interest. The detection and segmentation of pectoral muscle is studied of many authors.

Ferrari *et.al.*[1] have developed multiresolution technique using Gabor wavelets to identify and segment the pectoral muscle region. Sze Man kwok et. al. [2] developed new adaptive algorithms called Straight Line Estimation and cliff detection to segment the pectoral muscle region in Mediolateral Oblique view (MLO) mammogram. It uses knowledge about the position and shape of the pectoral muscle. Non-linear Diffusion filtering which is an edge preserving smoother used by Mirzaalian *et. al.* [3] to segment the pectoral muscle. Yuji Hatanaka *et.al.*[4] used statistical features like average pixel value, standard deviation and coefficient of correlation to segment pectoral muscle region in digitized mammogram. Weidong *et. al.* [5] have developed an algorithm called hough transform and polyline fitting to fit the boundary of the pectoral muscle, and an elastic thread algorithm was used to extract the pectoral muscle. Mario mustra *et.al.* [6] have segmented the pectoral muscle region by using bit depth reduction and wavelet decomposition. Ramachandran chandrasekhar *et. al.* [7] have developed a method based on the observed behavior of the pattern of intensities on the mammogram adjacent on the skin air interface to locate the nipple on mammograms. Punam K. Saha *et. al.* [8] described and validated an automatic and reproducible method to segment dense tissue regions from fat within breasts from mammograms using scale-based fuzzy connectivity methods. Chandrasekhar and Yattikiouzel [9] have developed a method new range

based neighborhood operator for extracting edge and texture information from mammogram. Wei-Ying Ma, and B. S. Manjunath [10] have detected the boundary and image segmentation by using Edge-flow technique. This scheme utilizes a predictive coding model to identify the direction of change in color and texture at each image location at a given scale, and constructs an edge flow vector.

In the proposed approach, pectoral muscle segmentation in MLO view is accomplished. At the first stage, all digitized mammograms are oriented and region of interest is defined. Second, Iterative threshold method is applied to get the binary image. Third, median filter and morphological techniques are applied to remove the impulse noise and to reconstruct the shapes of the pectoral muscle respectively. Fourth, polynomial fitting and moving average filter is applied to smooth pectoral muscle region border. Finally, the pectoral muscle region is segmented by tracking the background pixels. The experimental results show that the pectoral muscle region can be accurately segmented in MLO view mammograms.

The organization of the rest of this paper is as follows. The data acquisition is illustrated in section II. Orientation of mammogram and defining of region of interest is described in Section III. In Section IV, a novel approach is presented. In Section V, Straight Line Estimation is described. The experimental results and conclusions are given in Section VI and VII respectively.

2. DATA ACQUISITION

At present, CAD schemes are frequently evaluated with a database generated by the investigator(s), which may contain different proportions of subtle cases and obvious cases. As a consequence, it is not possible to perform meaningful comparisons of different schemes. A common database is an important step toward achieving the consistency in performance comparison and the objective testing of algorithms. The Mammographic Image Analysis Society (MIAS), which is an organization of United Kingdom research groups is interested in the understanding of mammograms and has produced a digital mammography database which we have chosen to use in our research. An original MIAS mammogram mdb058 and mdb120 with pectoral muscle region is shown in Figure 1 (a) and Figure 1(b).

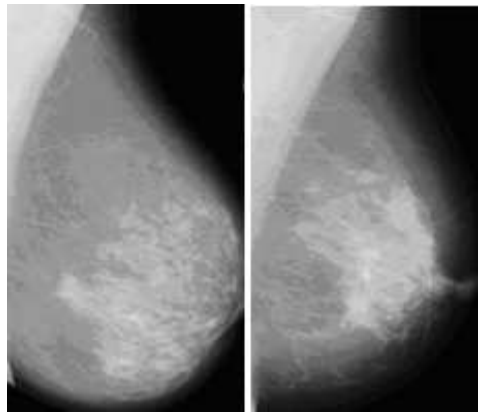

1 (a) 1 (b)

Fig.1 (a) and 1(b) – Original MIAS database mammogram (mdb058, mdb120) with pectoral muscle region

3. ORIENTATION AND NOTATION

In our segmentation algorithm, all digitized mammograms are oriented so that the nipple faces the right, i.e., all the right breast images are mirrored vertically. Therefore, all input images are always upright with the pectoral muscle at the top left corner. Fig. 2(a) shows the right breast image (mdb099) and fig. 2(b) shows the resulting image after orientation. The intensity of the image is denoted by I(x,y) in the range [0,Imax]. The origin of the coordinate system is at the top left corner of the image, where x is defined to be the row number and y to be the column number of the image.

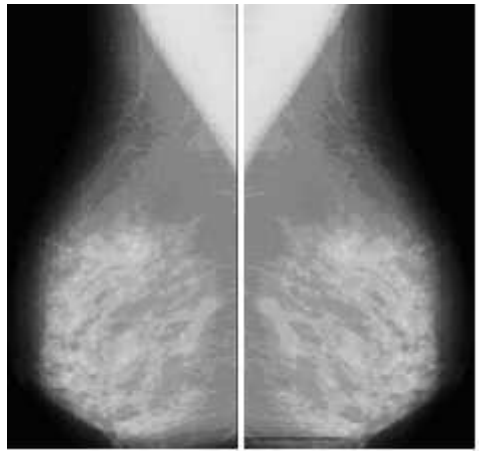

2 (a) 2 (b)

Fig. 2(a) Original right breast image (mdb099). Fig. 2(b) Resulting image after orientation

3.1 Defining Region of Interest

The pectoral muscle is located at the top left corner of the image; the top left quarter of the image is taken to be the Initial Region of Interest (IROI). The IROI is

defined by using (1). Fig. 3(a) and 3(b) shows the Initial ROI of mammogram (mdb058 and mdb120) taken from the MIAS database.

$$IROI = \left\{ (x,y) : 0 \le x < \frac{\#of\ rows}{2} and 0 \le y < \frac{\#of\ columns}{2} \right\} \quad (1)$$

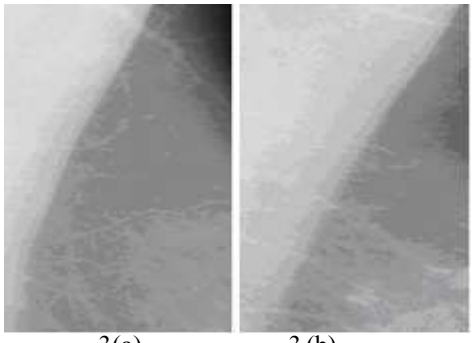

3(a) 3 (b)

Fig. 3(a) and 3(b) – Pectoral and non-pectoral regions in the Initial ROI image taken from MIAS database (mdb058 and mdb120)

4. NOVEL ALGORITHM FOR SEGMENTATION OF PECTORAL MUSCLE

Image segmentation remains as one of the major challenges in image analysis. Iterative threshold method is useful to segment the image. Hence in this paper, Iterative threshold with mathematical morphological techniques is proposed to segment the pectoral muscle region in MLO view mammograms. The main idea for this step is to approximate the ideal threshold value that should be used in order to remove all pectoral muscle and yield to better output. Mathematical morphology is a powerful tool for image shape analysis. The implementation of the proposed algorithm is as follows.

Step 1: The Initial ROI image IROI(x,y) is a 2D gray level image and contains N pixels with gray levels 1 to G. The initial threshold T is the mean intensity for the whole image. Fig. 4(a) shows the original MIAS mammogram (mdb099). Fig. 4(b) shows the Initial ROI image.

$$T = \frac{\sum_{i=1}^{m}\sum_{j=1}^{n} IROI(x_i, y_j)}{N} \quad (2)$$

Step 2: The image is segmented into object and background pixels as described above, creating two sets:

i. $G1 = \{IROI(x,y) : IROI(x,y) > T\}$ (Object pixels) (3)

ii. $G2 = \{IROI(x,y) : IROI(x,y) \le T\}$ (Background pixels) (4)

Note: IROI(x,y) is the value of the pixel located in the x^{th} row and y^{th} column.

Step 3: The mean value of object and background is calculated by using the following equations.

$$\overline{G1} = \frac{\sum_{i=1}^{m}\sum_{j=1}^{n} G1(x_i, y_j)}{N} \quad (5)$$

$$\overline{G2} = \frac{\sum_{i=1}^{m}\sum_{j=1}^{n} G2(x_i, y_j)}{N} \quad (6)$$

Here N is the number of pixels in the set G1 and G2 respectively.

Step 4: A new threshold value is created as the mid-point of $\overline{G1}$ and $\overline{G2}$.

$$T = \frac{(\overline{G1} + \overline{G2})}{2} \quad (7)$$

Step 5: Now, using the new threshold value computed in step four, go back to step two and keeps repeating until the new threshold matches the one before it. (i.e., until convergence has been reached)

Step 6: The IROI image is converted into Binary Image (BI) based on optimal threshold value.

Step 7: The impulse noise on the binary image is removed by applying a 5x5 median filter.

Step 8: Mathematical morphology is a powerful tool for image shape analysis. Binary morphological operators are employed to reconstruct the shapes of the pectoral muscle region and remove the isolated pixels. The basic binary morphological operators such as dilation and erosion are defined as follows.

Dilation:

$$A \oplus B = \left\{ x \mid (\hat{B})_x \cap A \ne \phi \right\} \quad (8)$$

Erosion:

$$A \ominus B = \{ x \mid (B)_x \subseteq A \} \quad (9)$$

Where A is a Binary Image (BI) and B is a small image called structure element. In our experiments, a 2x2 square structure element is employed.

Step 9: The horizontal line of the binary image is scanned from left to right, and the first background pixel on each scan line is selected. The x and y coordinates of all the selected pixels stored in vector S1(x) and S2(y) that represents the pectoral edge crisscross curve.

Step 10: Find the coefficients of a polynomial p(S1) of degree n that fits the data, p(S1(i)) to S2(i), in a least

squares sense. The result p is a row vector of length n+1 containing the polynomial coefficients in descending powers.

Step 11: Smooth the detected curve by using moving average filter. This curve is called the pectoral edge.

Step 12: The pixels from left corner to pectoral edge are called the pectoral muscle region. The pectoral region is converted to black from the original mammogram image to remove the pectoral muscle from the breast region [Fig. 4(f)]. The resulting image R(x,y) defined as

$$R(x,y) = \begin{cases} 0 & \text{if } BI(x,y) \neq 0 \text{ (upto pectoral edge)} \\ IROI(x,y) & \text{otherwise} \end{cases} \quad (10)$$

Where, m and n are number of rows and number of columns of binary image.

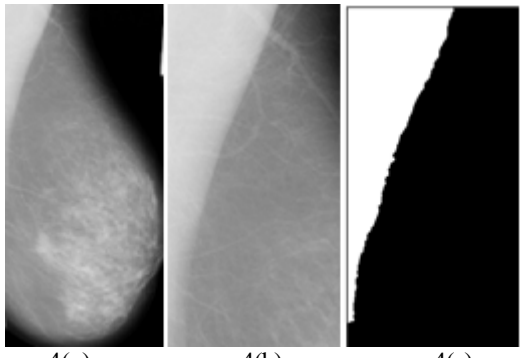

4(a) 4(b) 4(c)

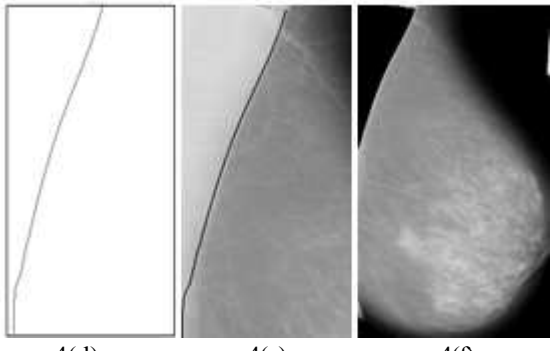

4(d) 4(e) 4(f)

Fig. 4 Illustration of proposed algorithm. (a) Original MIAS mammogram (mdb099). (b) Initial ROI image (c) Image after applying median filter and morphological operators. (d) smoothed pectoral muscle region. (e) pectoral muscle segmentation in IROI. (f) Resulting image after segmentation of pectoral muscle region.

5. STRAIGHT LINE ESTIMATION

Sze Man Kwok[2] et. al., have developed a new adaptive algorithm to automatically extract the pectoral muscle on digitized mammograms. This algorithm is based on iterative threshold selection and straight line fitting with a gradient test. It uses knowledge about the position and shape of the pectoral on mediolateral oblique views. The pectoral edge is estimated by a straight line which is validated for correctness of location and orientation. Figure 5 shows the illustration of straight line estimation.

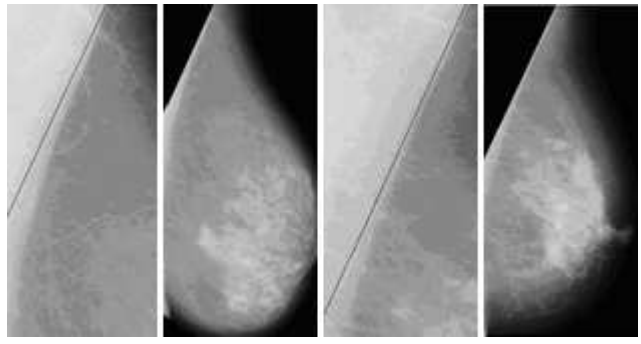

5(a) 5(b) 5(c) 5 (d)

Fig.5 Straight Line Estimation. 5(a) and 5(c) - straight line approximation to the pectoral edge. 5(b) and 5(d) Resulting image - Segmentation of pectoral muscle

6. EXPERIMENTAL SETUP AND RESULTS

We have made an attempt through the new approach to segment the Pectoral Muscle region in MLO mammograms. The experiments were conducted on digitized mammograms with a spatial resolution of 200 ìm from the MIAS database, comprising tumor cases amounting to 114 images and 50 randomly selected non tumor cases. The test database comprised 19 speculated masses, 23 circumscribed masses, 14 ill-defined masses, 24 cases having Lesions, 15 cases with asymmetry, 19 cases with architectural distortion, and 50 normal cases. The proposed system was developed by using MATLAB 7.0.

The purpose of the segmentation is to localize the pectoral margin with sufficient accuracy; the "pectoral triangle" has been segmented on mediolateral oblique mammograms. The proposed novel approach and straight line estimation was implemented in 164 MIAS mammogram images. The results obtained from the proposed and existing method were evaluated by radiologists experienced in mammography analysis. The original and resulting images were simultaneously presented on a computer monitor for subjective assessment. By visual comparison, the radiologists assigned one of the four ranking options to the segmentation results. According to the radiologist rating, out of the 164 cases that were analyzed, 52 and 63 were categorized as either excellent or good for straight line estimation, 74 and 65 for proposed method respectively as listed in table 1. The numbers of straight line

estimation and proposed method for pectoral muscle segmentation images accepted by the radiologist are listed in table 2. It shows that radiologist rated 115 (70%) images out of 164 cases as acceptable using Straight line estimation and 139 (84%) images for proposed method.

Table 1 Radiologist Evaluation for Proposed and Existing Methods

Radiologist Rating	Straight Line Estimation		Proposed Method	
	Number of Images	%	Number of Images	%
Excellent	52	31	74	45
Good	63	38	65	39
Average	31	18	16	9.7
Poor	18	10	9	5.4

Table 2 Number of Segmentation Accepted By the Radiologist

Radiologist Decision	Straight Line Estimation		Proposed Method	
	Number of Images	%	Number of Images	%
Acceptable	115	70	139	84
Not Acceptable	49	30	25	16

In an adequate mammogram, the pectoral muscle should be visible down to the level of the nipple. In some cases, the muscle may appear on the mammogram as very small, very large, with internal edges of different edges strengths, obscured by tapes of different thickness. Some examples of results of segmentation process are shown in Fig. 6. The result shows, irrespective of the size and thickness of the pectoral muscle, it has been segmented accurately in different MLO mammograms.

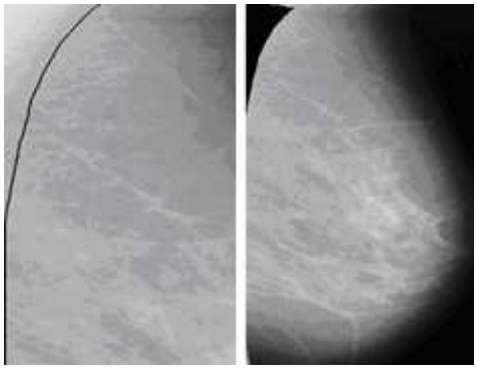

6(a) mdb024

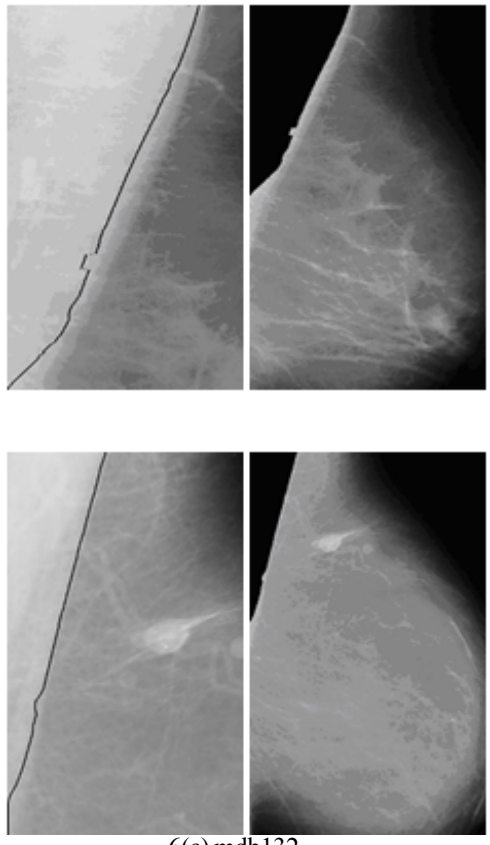

6(c) mdb132

Fig. 6 Segmentation results using Proposed Method on MLO mammograms from the MIAS database

7. CONCLUSION

We have described a new algorithm to locate and segment the pectoral muscle automatically on MLO mammograms. The algorithm was adaptive to large variations in appearance of the pectoral muscle and margin. The algorithm remained effective when parts of the pectoral edge were obscured by superimposed glandular tissue or artifacts. The method was tested out on the 164 digitized mammograms of the MIAS database and mammographic radiologist assessed the segmentation results. With the new segmentation results, we find that the proposed systems are capable of segmenting the pectoral muscle on MLO mammograms at low false positive rates.

REFERENCES

[1] R.J.Ferrari, R.M.Rangayyan, J. E. L. Desautels, R. A. Borges and A. F. Frere, "Automatic Identification of the Pectoral Muscle in Mammograms", IEEE Trans. on Medical Imaging, Vol.23, No.2, February 2004, pp. 232-245.

[2] Sze Man Kwok, Ramachandran Chandrasekhar, Yianni Attikiouzel, and Mary T. Rickard, "Automatic Pectoral Muscle Segmentation on Mediolateral Oblique View Mammograms", IEEE Trans. on Medical Imaging, Vol. 23, No.9, September 2004, pp.1129-1140.

[3] H. Mirzaalian, M.R. Ahmadzadeh and S. Sadri, "Pectoral Muscle Segmentation on Digital Mammograms by Nonlinear Diffusion Filtering", IEEE Pacific Rim Conference on Communications, Computers and Signal Processing, September 2007, pp.581-584.

[4] Yuji Hatanaka, Takeshi Hara, Hiroshi Fujita, Satoshi Kasai, Tokiko Endo, and Takuji Iwase, "Development of an Automated Method for Detecting Mammographic Masses with a Partial Loss of Region", IEEE Trans. on Medical Imaging, Vol.20, No.12, December 2001, pp.1209-1214.

[5] Weidong Xu, Lihua Li and Wei Liu, "A Novel Pectoral Muscle Segmentation Algorithm Based on Polyline Fitting and Elastic Thread Approaching", ICBBE 2007, pp.837-840.

[6] Mario Mustra, Jelena Bozek and Mislav Grgic, "Breast Border Extraction and Pectoral Muscle Detection using Wavelet Decomposition", IEEE EUROCON 2009, pp.1428-1435.

[7] Ramachandran Chandrasekhar, and Yianni Attikiouzel, "A Simple Method for Automatically Locating the Nipple on Mammograms", IEEE Transactions on Medical Imaging, Vol.16, No.5, October 1997, pp.483-494.

[8] K.SahaPunam , K.Udupa Jayaram , Emily F. Conant, Dev P. Chakraborty and Daniel Sullivan, "Breast Tissue Density Quantification Via Digitized Mammograms", IEEE Trans. on Medical Imaging, Vol.20, No.8, August 2001, pp.792-803.

[9] R. Chandrasekhar and Yattikiouzel, "New Range-Based Neighbourhood Operator for Extracting Edge and Texture Information from Mammograms for Subsequent Image Segmentation and Analysis", IEE Proc.-Sci. M Eas. Technol., Vol.147, No.6, November 2000, pp.408-413.

[10] Wei-Ying Ma and B. S. Manjunath, "Edgeflow: A Technique for Boundary Detection and Image Segmentation", IEEE Trans. on Image Processing, Vol.9, No.8, August 2000, pp.1375-1388.

Structural Parameter Optimization of Woven Fabrics Using Simulated Annealing

Subhasis Das, Anindya Ghosh and Debamalya Banerjee
[1&2]Government College of Engineering & Textile Technology, Berhampore - 742 101, India
Department of Production Engineering, Jadavpur University, Kolkata - 700 032, India

Abstract

This paper proposes a new approach to design woven fabrics with desired quahty and low manufacturing cost by optimizing the structural parameters such as count, crimp and thread spacing of warp (longitudinal) and weft (transverse) yams in fabric. To fulfill this goal, we endeavor to devise a searching mechanism based on Simulated Annealing (SA) algorithm for efficiently finding the appropriate combination of the parameters. SA is a kind of stochastic method and is well known for its feature of effective escaping from local minimum trap. It is an established fact that fabric areal density is directly proportional to the fabric production cost for a given range of yam counts. In this work an attempt has been made to select the optimum parameters of plain woven 100% cotton fabrics using SA by minimizing the fabric areal density in order to achieve desired fabric quality. The result shows that the SA is a useful non-traditional optimization technique for engineering design of fabrics which posses low production cost as well as desired physical and mechanical properties.

Keywords: *Areal density, Cotton fabrics,Fabric engineering,Simulated Annealing,Structural parameters.*

1. INTRODUCTION

It is always a cherished goal sought by every fabric manufacturer to produce fabrics with minimum cost and optimum quality. Optimization of structural parameters of fabrics stands for minimization of production cost such that different fabric parameters such as cover, tensile modulus, shear modulus, bending rigidity and crimp balance both in warp (longitudinal) and weft (transverse) directions are retained within the desired levels. The intricate relationship of fabric structural parameters with its physical and mechanical properties makes it too complex to solve this optimization problem by means of traditional technique. Recently the scientific community has been able to solve a big variety of complex engineering optimization problems with the advent of non-traditional optimization techniques such as genetic algorithm (GA), simulated annealing (SA), particle swarm optimization (PSO) etc. SA has successfully been applied to many engineering optimization problems. Corana et al. [1] first compares SA to conventional algorithms on four econometric models. Simulated annealing has been used successfully in computer and circuit design [2], pollution control [3], a special case of 0-1 programming [4], neural networks [5], reconstruction of pollycrystalline structures [6] and image processing [7]. Both Vanderbilt et al. [8] and Bohachevsky et al. [9] have modified simulated annealing for continuous variable problems.

In this work an attempt has been made to design engineered fabrics using SA. The excellent searching capacity of SA facilitates to select the best combinations of structural parameters to obtain fabrics with desired quality with low manufacturing cost. It is essential to have an appropriate areal density or GSM of fabric for a good quality as well as economic production. If the GSM of a fabric is too low, it will obviously be too sparse to have the required quality. Yet, higher GSM of fabric increases its manufacturing cost due to the more consumption of yams. Therefore, it is necessary to maintain a particular range of yam count while optimization of fabric cost by minimizing GSM. Three different range of yam counts are considered in this work for theproduction of light, medium and heavy weight fabrics, respectively.

Over the years. Leaf and his colleagues, in particular, produced useful equations that express tensile moduli [10], shear modulus [11], and bending moduli [12] for plain woven fabrics with reasonably high accuracy. These equations are used in this work for mechanical property considerations. The considered physical properties are fabric weight and the cover factor, since they are well-defined and frequently referred to in practice. The crimp balance equation is also taken into account, since its specification indicates the fully relaxed state of a fabric.

1.1 An Overview of Simmulated Annealing

The simulated annealing (SA) is a stochastic strategy for selecting the minimal configuration of states of a system. It was first put forward by Metropolis and successfully applied to the optimization problems by Kirkpatrick [13]. The SA resembles the cooling process

of molten metals through annealing. The SA algorithm is quite simple as depicted in Figure 1.

The SA procedure simulates the process of slow cooling of molten metal to achieve the minimum function value in a minimization problem. The cooling phenomenon is simulated by controlling a temperature-like parameter introduced with the concept of Boltzmann probability distribution. According to the Boltzmann probability distribution, a system in thermal equilibrium at a temperature *T* has its energy distributed probabilistically according to *PiE) = exp* (*-E/kT),* where *k* is the Boltzmann constant. This expression suggests that a system at high temperature has almost uniform probability of being at any energy state, but at low temperature it has a small probability of being at high energy state. Thus, by controlling the temperature *T* and assuming that the search process follows the Boltzmann probability distribution, the convergence of an algorithm can be controlled. Metropolis *et al.* [14] suggested one way to implement the Boltzmann Probability in simulated thermodynamic systems. The same can also be used in the function minimization context. Let us say, at any instant the current point is x^^^ and the function value at that point is *Eit)=fix^^^).* Using this Metropolis algorithm, we can say that the probability of the next point being at x^^^^^ depends on the difference in the function values at these two points or on Ai? = *E(t+l) - E(t)* and is calculated using the Boltzmann Probability distribution: *P{E* (f+1)) = min [1, exp *(-AE/kT)]* (1)

If *AE* < 0, this probability is one and the point x^^^^^ is always accepted. In the function minimization context, this makes sense because if the function value at /'^'^ IS better than that at x^^\ the point x^*^^^^ must be accepted. This interesting situation happens when AE > 0, which implies that the function value at x^^^^^ is worse than that at x^^\ According to many traditional algorithms, the point x^^^^^ must not be chosen in this situation. But according to the Metropolis algorithm, there is some finite probability of selecting the point x^^^^^ even though it is worse than the point *x'-^* However this probability is not the same in all situations. This probability depends on the relative magnitude of the *AE* and *T* values. If the parameter *T* is large, this probability is more or less high for points with largely disparate function values. Thus, any point is almost acceptable for large value of *T.* On the other hand, if the parameter *T* is small, the probability of accepting an arbiter point is small. Thus, for small values of *T,* the points with only small deviation in function value are accepted.

SA is a point-by-point method. The algorithm begins with an initial point and a high temperature *T. A* second point is created at random in the vicinity of the initial point and the difference in the function values *(AE)* at these two points is calculated. If the second point has a smaller function value, the point is accepted; otherwise the point is accepted with probability exp *(-AE/kT).* This completes one iteration of the SA procedure. In the next generation, another point is created at random in the neighborhood of the current point and the Metropolis algorithm is used to accept or reject the point. In order to simulate the thermal equilibrium at every temperature, a number of points *(n)* are usually tested at a particular temperature, before reducing the temperature at a fixed cooling rate. The algorithm is terminated when a sufficiently small temperature *(Tmm)* is obtained or a small enough change in function values is found.

2. METHODS

The areal density or GSM (g/m^) of a fabric made from a given range of yam counts such as finer, medium and coarser is directly proportional to the cost of its production. Three different range of counts for warp and weft yams i.e. fine (10 to 24 tex), medium (30 to 50 tex) and coarse (60 to 100 tex) made from 100% cotton fibres are considered in this study for the production of light, medium and heavy weight fabrics, respectively. SA was used to minimize the fabric areal density *(W)* such that different fabric parameters such as cover *(K),* tensile modulus *(Ej* and *E2),* shear modulus (G), flexural rigidity (5; and *B2)* and crimp balance, (shown in Equations 2 - 9), are retained within the desired levels. The areal density of the fabric. Equation 2 is used as objective function. The inequality constraint equations are formulated for fabric cover, tensile modulli, shear modulus, flexural rigidity and an equality constraint equation is formulated for crimp balance. All these mechanical and physical properties are used as constraints in the optimization process. Table 1 shows the lower and upper bounds of inequality constraints for three types of fabrics. The search space for the weaving parameters determining the physical and mechanical properties of different fabrics is given in Table 2.When a value range is specified for each of these properties, it actually define a feasible region for the optimization. As a result, a solution can only be found within this feasible region, so that the engineered fabric meets the property requirements. The rigid thread model of fabric structure having plain weave is considered in this study. A penalty function method is used to handle the inequality and equality constrains [15].

The optimum solution of SA is obtained with the values of 1000 and 0.9 for *T* and *Tmm,* respectively. Maximum number of iteration at a particular temperature was set to 30. The optimized parameters of fabrics to be produced are obtained using SA by means of MATLAB (version 7.7) coding on a 2.6 GHz. PC.

Table 1Boundary of the Constraints for Different Types of Fabrics

Fabric Properties	Light weight Fabric (Using Fine Yarns)		Medium Weight Fabrics (Using Medium Count Yarns)		Heavy Weight Fabrics (Using Coarse Yarns)	
	Lower Bound	Upper Bound	Lower Bound	Upper Bound	Lower Bound	Upper Bound
K	0.6	0.72	0.6	0.72	0.6	0.72
E1, mN/mm	1000	2500	2000	3500	3500	5500
E2, mN/mm	1000	2500	2000	3500	3500	5500
G, mN/mm	50	150	100	250	200	350
Bi, mN mm	3	12	6	15	12	20
B2, mN mm	3	12	6	15	12	20

Table 2 Search Space for the Fabric Parameters

Fabric Properties	Light weight Fabric (Using Fine Yarns)		Medium Weight Fabrics (Using Medium Count Yarns)		Heavy Weight Fabrics (Using Coarse Yarns)	
	Lowe r	Upper Bound	Lower Bound	Upper Bound	Lower Bound	Upper Bound
Ti, tex	10	24	30	50	60	100
72, tex	10	24	30	50	60	100
ci, fraction	0.03	0.15	0.03	0.15	0.03	0.15
C2, fraction	0.03	0.15	0.03	0.15	0.03	0.15
pi, mm	0.20	0.40	0.45	0.80	0.50	0.85
P2,mm	0.20	0.40	0.45	0.80	0.50	0.85

Table 3 Optimum Values of Fabric Parameters

Fabric Properties	Light weight Fabric (Using Fine Yarns)	Medium Weight Fabrics (Using Medium Count Yarns)	Heavy Weight Fabrics (Using Coarse Yarns)
Ti, tex	13	33	70
72, tex	13	33	73
ci, fraction	0.102	0.122	0.122
C2, fraction	0.104	0.127	0.096
pi, mm	0.391	0.632	0.761
P2,mm	0.391	0.635	0.787

Fabric Properties	Light weight Fabric (Using Fine Yarns)	Medium Weight Fabrics (Using Medium Count Yarns)	Heavy Weight Fabrics (Using Coarse Yarns)
K	0.57	0.57	0.65
E1, mN/mm	1894	2151	3542
E2, mN/mm	1828	2022	4556
G, mN/mm	149.6	197.4	336.5
Bi, mN mm	3.0	6.0	12.2
B2, mN mm	3.0	6.0	12.0
W, g/m^	73.8	116.2	205.4

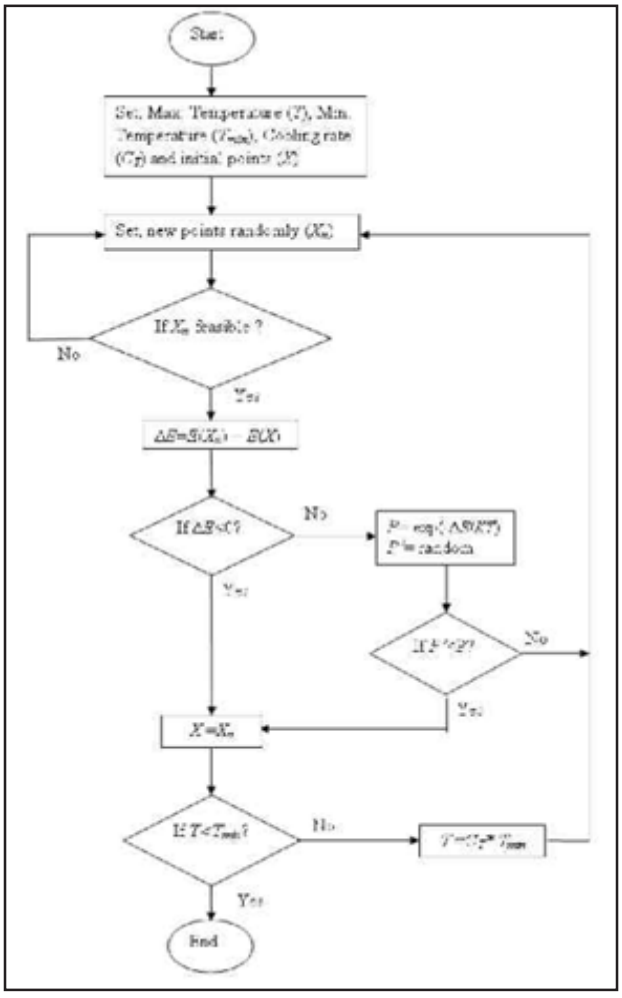

Fig.1Flowchart of SA algorithm

$$W = \frac{T_1(1+c_1)}{P_1} + \frac{T_2(1+c_2)}{P_2} \quad (2)$$

$$K = \frac{d_1}{P_1} + \frac{d_2}{P_2} - \frac{d_1 d_2}{P_1 P_2} \quad (3)$$

$$E_1 = \frac{12 p_2 \beta_1}{p_1 (l_1 - D\phi_1)^3 \sin^2 \theta_1} \times \left[1 + \frac{\beta_2 (l_1 - D\phi_1)^3 \cos^2 \theta_1}{\beta_1 (l_2 - D\phi_2)^3 \cos^2 \theta_2} \right] \quad (4)$$

$$E_2 = \frac{12 p_1 \beta_2}{p_2 (l_2 - D\phi_2)^3 \sin^2 \theta_2} \times \left[1 + \frac{\beta_1 (l_2 - D\phi_2)^3 \cos^2 \theta_2}{\beta_2 (l_1 - D\phi_1)^3 \cos^2 \theta_1} \right] \quad (5)$$

$$G = 12 \left\{ \frac{p_1 (l_1 - D\phi_1)^3}{\beta_1 p_2} + \frac{p_2 (l_2 - D\phi_2)^3}{\beta_2 p_1} \right\}^{-1} \quad (6)$$

$$B_1 = \frac{\beta_1 p_2}{p_1 (l_1 - D\phi_1)} \quad (7)$$

$$B_2 = \frac{\beta_2 p_1}{p_2 (l_2 - D\phi_2)} \quad (8)$$

At relaxed state of a fabric, the intemal forces acting vertically on the warp and weft threads due to the resistance of bending are balanced if the following equation is satisfied [16].

$$\frac{\beta_1 \sin \theta_1}{p_2^2} = \frac{\beta_2 \sin \theta_2}{p_1^2} \quad (9)$$

Equation 9 has predominant influence on the balance of crimp and therefore known as crimp balance equation. The relationship between angle of contact (^) and weave angle *(9)* are shown in the following equation [11].

$$\phi = \sin^{-1}(2 \sin \theta - \frac{p}{D}) \quad (10)$$

A penalty function method is used to handle the constraints. A bracket penalty operator is used to handle the inequality constraints whereas the equality constraint was handled by a parabolic penalty operator [15]. The inclusion of constraint changes the objective function/ (S^^ to the following penalty.

$$P(X,R) = f(X) + \Omega\{R, g(X)\} \quad (11)$$

$$\Omega = R(g(X))^2 \quad (12)$$

where a bracket operator *(c^'i* is defined as *{a} = c:,* when *a* is negative and zero, otherwise.

3. RESULTS AND DISCUSSION

The optimum values of the fabric structural parameters obtained by solving the optimization problem of Equations 2-9 for different fabrics are summarized in Table 3. The physical and mechanical properties of fabrics were predicted from the obtained parameters of Table 3 using the Equations 3-10. Table 4 depicts the predicted values of the physical and mechanical properties of three different fabrics. It is evident from the Table 4 that the predicted properties of fabrics are lying within the desirable limits for all three fabrics. The optimized fabric parameters given in Table 3 also satisfy the Equation 9. This ensures the balance of inter yam forces in the fabric which in tum effects the balance of warp and weft crimp. The obtained values of fabric GSM with the optimized parameters using SA are 73.8, 116.2 and 205.4 g/m^ for light, medium and heavy weight fabrics, respectively.

4. CONCLUSION

This paper demonstrates a new approach for engineering design of woven fabrics. It is found that SA is a useful non-traditional optimization technique for engineering design of plain woven 100% cotton fabrics

which posses low production cost as well as desired physical and mechanical properties. SA is an excellent algorithm which allow fabric designer to obtain the best combinations of weaving parameters during manufacturing, considering costs. SA is a very powerful technique of optimization and it can be useful for engineering design of all kind of fabrics.

REFERENCES

[1] A. Corana, M.Marchesi, C.Martini and S. Ridella, "Minimizing Multimodal Functions of Continuous Variables with the Simulated Annealing Algorithm", ACM Transactions on Mathematical Software, Vol.13, 1987, pp.262-280.

[2] D.F.Wong, H.W. Leong and C.L.Liu, "Simulated Annealing for VLSI Design", Kluwer Academic Publishers, Boston, 1988.

[3] D. Derwent, "A Better Way to Control Pollution", Nature, Vol. 331, 1988, pp.575-578.

[4] A. Drexl, "A Simulated Annealing Approach to the Multiconstraint Zero-One Knapsack Problem", Computing, Vol.40, 1988, pp.1-8.

[5] D. Wasserman Philip and T. Schwartz, "Neural Networks, Part 2: What Are They and Why Is Everybody So Interested in Them Now?" IEEE Expert Spring, 1988, pp.10-15.

[6] H. Telly, M.Liebling and A. Mocellin, "Reconstruction of Polycrystalline Structures: A New Application of Combinatorial Optimization", Computing Vol.38, 1987, pp.1-11.

[7] P. Camevali, L.Coletti and S. Patamello, "Image Processing by Simulated Annealing", IBM Joumal of Research and Development, Vol.29, 1985, pp.569-79.

[8] D.Vanderbih and G.L. Seven, "A Monte Carlo Simulated Annealing Approach to Optimization over Continuous Variables", Joumal of Computational Physics, Vol.56, 1984, pp.259-271.

[9] I. O. Bohachevsky, E.J. Mark and L. Stein Myron, "Generalized Simulated Annealing for Function Optimization", Technometrics, Vol.28, 1986, pp.209-217.

[10] G A.V. Leaf and K. H. Kandil, "The Initial Load-extension Behaviour of Plain-woven Fabrics", Joumal Textile Institute Vol.71, 1980, pp.1-7.

[11] G A.V. Leaf and A. M. F.Sheta, "The Initial Shear Modulus of Plain-woven Fabrics", Joumal Textile Institute, Vol.75, 1984, pp.157-163.

[12] G A.V. Leaf , Y. Chen and X.Chen, "The Initial Bending Behaviour of Plain Woven Fabrics", Journal Textile Institute, Vol.84, 1993, pp.419-428.

[13] S. Kirkpatrick, C.D. Gelatt and M.P. Vecchi, "Optimization by Simulated Annealing", Science, Vol.220, No.4598, 1983, pp.671-680.

[14] N.Metropolis, A.Rosenbluth, M.Rosenbluth, A. Teller and E.Teller, "Equation of State Calculations by Fast Computing Machines", Journal of Chemical Physics, Vol.21, 1953, pp.1087-1092.

[15] K. Deb, "Optimization for Engineering Design: Algorithms and Examples", Prentice Hall, New Delhi, 2005.

[16] F. T.Peirce, "The Geometry of Cloth Structure", Journal of the Textile Institute, Vol.28, No.3, 1937, pp.T45 -T112.

Indian Journal of Engineering, Science, and Technology
ISSN: 0973-6255
Volume 6 Number 1&2 **January - December 2012**

CONTENTS

S.No.	Title	Page.No.
1	**Economic Analysis of 10kw Roof-mounted Grid Connected Photovoltaic System** R.Vijay Kumar, Yuva Raju Anand and R. Rudramoorthy	01
2	**Experimental Research on Improving the Concrete Property by Using Nanosilica Flyash** Yuvaraj Shanmuga Sundaram, Dinesh Nagarajan, Karthic Ramachandran and SatishBabu	09
3	**Zernike Feature based Pattern Retrieval Using Artificial Neural Network** R. Parivallal, B. Nagarajan and R. Sathish Kumar	15
4	**Awareness of Natural UV Protection Finish on Garments among Chennai People** Habeebuniss	19
5	**A Coverage Inference Protocol for Wireless Sensor Networks** Yuguang Fang and P. Dineshkumar	24
6	**An Improved Multi-Period Spraying for Intermittently Connected Networks** C. Poongodi and A.M.Natarajan	33
7	**Digital Fragile Blind Watermarking Based on Lifting Scheme** V. Kavitha, M.Sangeetha and C. Palanisamy	38
8	**Innovation through Knowledge Management for Information Technology Usage in Business Organizations** R. Rajendran and Ranga Rajagopal	43
9	**Preparation of Gelatin (Typeaprotein) From Sun Dried Fish (Tilapia – Oreochromis Mossambicus) Skin** Logeswari, M. Thirumarimurugan and T. Kannadasan	51
10	**Experimental Studies on a Dual Fuel Diesel Engine** Abhishek Sharma, V. Meda and S. Murugan	57
11	**A 3D Smart Actuator for Robotic Eyes Industrial Applications Using A Flexural Vibration Ring Transducer** M. Shafik, B. Nyathi and S. Fekkai	65
12	**Speed Estimation of Induction Motor Using Extreme Learning Machine Algorithm** R.Subasri and A.M.Natarajan	72

S.No.	Title	Page.No.
13	**Gene Selection Methods for Cancer Classification: A Review** C.Gunavathi and K.Premalatha	78
14	**Technology And Financial Inclusion** S. Padmavathy, T. Dheepa and J. Ashok	82
15	**"Automated Postal Machine (APM) - An Unique Innovative System to Automate Speed Post Service"** K.Elamvazhuthi	87
16	**Optimization of Machining Parameters of WEDM Process Based On the Taguchi Method** R.Kalidas, S.Boopathi, K.Sivakumar and P.Mohankumar	91
17	**Poly (Ethyleneglycol Dimethacrylate) Grafted Chitosan Nanoparticles: Synthesis and Evaluation as a Carrier for Controlled Drug Delivery** K. Subramanian, V. Vijayakumar and M. S. Kavitha	97
18	**An Experimental Investigation on the Properties of Self-curing Concrete** G.S.Rampradheep and N.Arunachalam	106
19	**Low Power And Low Area Analog Multiplier Using MIFGMOS** K.Duraisamy and U.Ragavendran	112
20	**A Novel Approach For Segmentation Of Pectoral Muscle On Medio-lateral Oblique View Mammograms** B. Nagarajan and W. Jai Singh	116
21	**Structural Parameter Optimization of Woven Fabrics Using Simulated Annealing** Subhasis Das, Anindya Ghosh and Debamalya Banerjee	122

Indian Journal of Engineering, Science, and Technology (IJEST)

(ISSN: 0973-6255)
(A half-yearly refereed research journal)

Information for Authors

1. All papers should be addressed to The Editor-in-Chief, Indian Journal of Engineering, Science, and Technology (IJEST), Bannari Amman Institute of Technology, Sathyamangalam - 638 401, Erode District, Tamil Nadu, India.
2. Two copies of manuscript along with soft copy are to be sent.
3. A CD-ROM containing the text, figures and tables should separately be sent along with the hard copies.
4. Submission of a manuscript implies that : (i) The work described has not been published before; (ii) It is not under consideration for publication elsewhere.
5. Manuscript will be reviewed by experts in the corresponding research area, and their recommendations will be communicated to the authors.

Guidelines for submission

Manuscript Formats

The manuscript should be about 8 pages in length, typed in double space with Times New Roman font, size 12, Double column on A4 size paper with one inch margin on all sides and should include 75-200 words abstract, 5-10 relevant key words, and a short (50-100 words) biography statement. The pages should be consecutively numbered, starting with the title page and through the text, references, tables, figure and legends. The title should be brief, specific and amenable to indexing. The article should include an abstract, introduction, body of paper containing headings, sub-headings, illustrations and conclusions.

References

A numbered list of references must be provided at the end of the paper. The list should be arranged in the order of citation in text, not in alphabetical order. List only one reference per reference number. Each reference number should be enclosed by square brackets.

In text, citations of references may be given simply as "[1]". Similarly, it is not necessary to mention the authors of a reference unless the mention is relevant to the text.

Example

[1] M.Demic, "Optimization of Characteristics of the Elasto-Damping Elements of Cars from the Aspect of Comfort and Handling", International Journal of Vehicle Design, Vol.13, No.1, 1992, pp. 29-46.

[2] S.A.Austin, "The Vibration Damping Effect of an Electro-Rheological Fluid", ASME Journal of Vibration and Acoustics, Vol.115, No.1, 1993, pp. 136-140.

SUBSCRIPTION

The annual subscription for IJEST is Rs.600/- which includes postal charges. To subscribe for IJEST a Demand Draft may be sent in favour of IJEST, payable at Sathyamangalam and addressed to IJEST. Subscription order form can be downloaded from the following link http:// www.bitsathy.ac.in./ ijest.html.

For subscription / further details please contact:

IJEST
Bannari Amman Institute of Technology
Sathyamangalam - 638 401, Erode District, Tamil Nadu Ph: 04295 - 226340 - 44
Fax: 04295 - 226666 E-mail: ijest@bitsathy.ac.in Web:www.bitsathy.ac.in

Indian Journal of Engineering, Science, and Technology

Volume 6, Number 1&2, January - December 2012

CONTENTS

Economic Analysis of 10kw Roof-mounted Grid Connected Photovoltaic System 01
R.Vijay Kumar, Yuva Raju Anand and R. Rudramoorthy
Experimental Research on Improving the Concrete Property by Using Nanosilica Flyash 09
Yuvaraj Shanmuga Sundaram, Dinesh Nagarajan, Karthic Ramachandran and SatishBabu
Zernike Feature based Pattern Retrieval Using Artificial Neural Network 15
R. Parivallal, B. Nagarajan and R. Sathish Kumar
Awareness of Natural UV Protection Finish on Garments among Chennai People 19
Habeebuniss
A Coverage Inference Protocol for Wireless Sensor Networks 24
Yuguang Fang and P. Dineshkumar
An Improved Multi-Period Spraying for Intermittently Connected Networks 34
C. Poongodi and A.M.Natarajan
Digital Fragile Blind Watermarking Based on Lifting Scheme 38
V. Kavitha, M.Sangeetha and C. Palanisamy
Innovation through Knowledge Management for Information Technology Usage in Business Organizations 43
R. Rajendran and Ranga Rajagopal
Preparation of Gelatin (Typeaprotein) From Sun Dried Fish (Tilapia – Oreochromis Mossambicus) Skin 51
Logeswari, M. Thirumarimurugan and T. Kannadasan
Experimental Studies on a Dual Fuel Diesel Engine 57
Abhishek Sharma, V. Meda and S. Murugan
A 3D Smart Actuator for Robotic Eyes Industrial Applications Using A Flexural Vibration Ring Transducer 65
M. Shafik, B. Nyathi and S. Fekkai
Speed Estimation of Induction Motor Using Extreme Learning Machine Algorithm 72
R.Subasri and A.M.Natarajan
Gene Selection Methods for Cancer Classification: A Review 78
C.Gunavathi and K.Premalatha
Technology And Financial Inclusion 82
S. Padmavathy, T. Dheepa and J. Ashok
"Automated Postal Machine (APM) - An Unique Innovative System to Automate Speed Post Service" 87
K.Elamvazhuthi
Optimization of Machining Parameters of WEDM Process Based On the Taguchi Method 91
R.Kalidas, S.Boopathi, K.Sivakumar and P.Mohankumar
Poly (Ethyleneglycol Dimethacrylate) Grafted Chitosan Nanoparticles: Synthesis and Evaluation as a Carrier for Controlled Drug Delivery 97
K. Subramanian, V. Vijayakumar and M. S. Kavitha
An Experimental Investigation on the Properties of Self-curing Concrete 106
G.S.Rampradheep and N.Arunachalam
Low Power And Low Area Analog Multiplier Using MIFGMOS 112
K.Duraisamy and U.Ragavendran
A Novel Approach For Segmentation Of Pectoral Muscle On Medio-lateral Oblique View Mammograms 116
B. Nagarajan and W. Jai Singh
Structural Parameter Optimization of Woven Fabrics Using Simulated Annealing 122
Subhasis Das, Anindya Ghosh and Debamalya Banerjee